

N 71-15291

NASA CR 111696

INVESTIGATION OF SPACE STORABLE PROPELLANT ACQUISITION DEVICES

FINAL REPORT

VOLUME I - EVALUATION

OCTOBER 1970

This work was performed for the Jet Propulsion Laboratory,
California Institute of Technology, as sponsored by the
National Aeronautics and Space Administration under Contract
NAS7-754.

MARTIN MARIETTA

DENVER DIVISION

CASL FILE
COPY

MCR-70-171 (Vol I)


INVESTIGATION OF SPACE STORABLE
PROPELLANT ACQUISITION DEVICES

FINAL REPORT

VOLUME I
EVALUATION

October 1970

Approved



Howard L. Paynter
Program Manager

This work was performed for the Jet Propulsion Laboratory, California Institute of Technology, as sponsored by the National Aeronautics and Space Administration under Contract NAS7-754.

MARTIN MARIETTA CORPORATION
P.O. Box 179
Denver, Colorado 80201

FOREWORD

This report is submitted in accordance with Article II, Paragraph D, of Contract NAS7-754 dated 24 July 1969. This is Volume I of two volumes. This volume covers the period from 24 July 1969 to 15 April 1970. The second volume will cover the period from April 1970 to November 1970.

Information on the compatibility of both metals and nonmetals with nitrogen tetroxide, oxygen difluoride, diborane, monomethylhydrazine, and nitrated hydrazine propellants was compiled to aid in evaluating and selecting materials for the propulsion subsystems of interest. This information is included in two separate reports, published during the July 1969 to April 1970 period (Ref III-54 and III-55).

The following Martin Marietta personnel made technical contributions to this study: Thomas J. Cassidy, Glenn F. Holle, James R. Tegart, Preston E. Uney, Dennis E. Gilmore, Daniel L. Balzer, G. Robert Page and David N. Gorman. Task Leaders were: Dale A. Fester, Thomas R. Barksdale, and John E. Anderson.

The work is being administered under the technical direction of Mr. Robert Lem of the Jet Propulsion Laboratory. Mr. Howard L. Paynter, Subsystems Technology Section Chief, Propulsion Research Department, is the Martin Marietta Program Manager.

CONTENTS

	<u>Page</u>
Foreword	ii
Contents	iii
Summary	xi
Symbols	xiii thru xvi
I. Introduction	I-1 thru I-3
II. Program Objectives, Mission Criteria and Study Guidelines	II-1
A. Program Objectives	II-1
B. Mission Criteria	II-1
C. Study Guidelines	II-12 thru II-14
III. Candidate Propellant Acquisition Concepts	III-1
A. Dielectrophoretic Systems	III-1
B. Polymeric Bladders and Diaphragms	III-9
C. Metallic Bladders and Diaphragms	III-33
D. Bellows	III-53
E. Surface Tension Systems	III-66
F. External Settling	III-77
G. Capillary/Bellows	III-87
H. Start Tanks	III-92 and III-93
IV. Pressurization System	IV-1
A. Pressurization Subsystem Mass	IV-2
B. Effects of Pressurization Subsystem on Acquisition Devices	IV-36
C. Effects of Two versus Four Propellant Tanks on Pressurization System	IV-39 and IV-40

V.	Tank Design and Packaging	V-1
	A. Propellant Tank Packaging Considerations	V-2
	B. Tank Material Evaluation	V-8
	C. Propellant Tank Design and Weight Analysis	V-14 thru V-22
VI.	Evaluation and System Selection	VI-1
	A. Propellant Tank Subsystem	VI-2
	B. Propellant Acquisition Subsystem	VI-11
	C. Pressurization Subsystem	VI-31
	D. Selected Propulsion Subsystems	VI-35 thru VI-39
VII.	Influences of Possible Changes in Mission Criteria	VII-1
	A. Propellant Change Effects	VII-1
	B. Propellant Tank Design Considerations	VII-5
	C. Propulsion Duty Cycle Effects	VII-9
	D. Pressurization System Effects	VII-10
	E. Sterilization Effects	VII-11 and VII-12
VIII.	Conclusions and Recommendations	VIII-1
	A. Conclusions	VIII-1
	B. Recommendations	VIII-3
IX.	References	IX-1 thru IX-15
Appendix --	Capillary/Bellows Feasibility Test Program	A-1 thru A-21

Figure

I-1	Study Approach for the First Phase of the Program	I-2
II-1	Propulsion System Envelope, Missions A ₁ and A ₂	II-2
II-2	Propulsion System Envelope, Mission B	II-3
II-3	Baseline Propulsion System Schematic for Mission A ₁	II-8
II-4	Baseline Propulsion System Schematic for Mission A ₂	II-9
II-5	Baseline Propulsion System Schematic for Mission B	II-11
III-1	Dielectrophoretic System	III-2
III-2	Expanding Polymeric Bladder System for Mission A ₁	III-11
III-3	Collapsing Polymeric Bladder System	III-13
III-4	Polymeric Diaphragm System	III-16
III-5	Expulsion Characteristics of Polymeric Bladders and Diaphragms	III-19
III-6	Ring-Reinforced Diaphragm, Spherical Tank Assembly	III-34
III-7	Design Changes to Provide Higher Cycle Life	III-35
III-8	Ring-Reinforced Diaphragm, Conospheroid Tank Assembly	III-35
III-9	Convolutd Diaphragm Design	III-37
III-10	Telephragm Expulsion Action	III-39
III-11	Bonded Rolling Diaphragm System Geometry	III-40
III-12	Typical Expulsion Cycle for a Transverse Collapsing Bladder	III-42
III-13	Improved Cycle Life Diaphragm Tank Assembly	III-47
III-14	Operating Pressure Differential for Bladders and Diaphragms as a Function of Expulsion Efficiency	III-48

III-15	Bellows in Compression	III-56
III-16	Bellows in Tension	III-56
III-17	Effect of L/D Ratio and Pitch/Span Ratio on Weight of Welded-Leaf Bellows	III-58
III-18	Welded-Leaf Bellows Cycle Life as a Function of Pitch/Span Ratio	III-59
III-19	Typical Capillary Concepts	III-67
III-20	Liquid/Gas Interface Shape	III-68
III-21	Propellant Settling	III-78
III-22	Settling Rocket System Schematic	III-83
III-23	Capillary/Bellows System	III-87
III-24	Operation of the Capillary/Bellows Expulsion Device	III-88
III-25	Propellant Start Tank Schematic	III-92
IV-1	Total Helium Usage for Mission A ₁	IV-8
IV-2	Total Nitrogen Usage for Mission A ₁	IV-9
IV-3	Mission A ₁ Vaporized Oxygen Difluoride	IV-10
IV-4	Pressure and Temperature Histories for Mission A ₁ Oxygen Difluoride Tank	IV-11
IV-5	Pressure and Temperature Histories for Mission A ₁ Diborane Tank	IV-12
IV-6	Mission A ₁ Pressurization Subsystem Mass	IV-18
IV-7	Mission A ₂ Pressurization Subsystem Mass	IV-22
IV-8	Mission B Tank Pressure History Using Helium Pressurant	IV-25
IV-9	Propulsion System Schematic for Mariner '71	IV-28
V-1	Baseline, Two Spherical-Tank System	V-3
V-2	Baseline, Two Cylindrical-Tank System	V-3
V-3	Baseline, Four Spherical-Tank System	V-3
V-4	Baseline, Four Cylindrical-Tank System	V-3
V-5	Two Conospheroid-Tank System	V-4
V-6	Four Conospheroid-Tank System	V-4

V-7	Special Two-Cylinder Tank System	V-4
V-8	Special Four-Cylinder Tank System	V-4
V-9	Four Spherical-Tank Arrangement, 50% Volume Increase	V-6
V-10	Mission B Baseline Spherical-Tank System . . .	V-6
V-11	Mission B Baseline Cylindrical-Tank System . .	V-6
V-12	Mission B Spherical Tank with 50% Volume Increase	V-6
V-13	Mission B Cylindrical Tank with 50% Volume Increase	V-7
V-14	Mission B Conospheroid Tank with L/D of 1.6	V-7
V-15	Mission B Conospheroid Tank with L/D of 2.43	V-7
V-16	Mission B Special Cylindrical Tank	V-7
V-17	Definition of Geometric Terms for Conospheroid	V-16
V-18	Statistical Factor for the Design of Spherical Shells to Prevent Buckling in Compression . .	V-19
VI-1	Propellant Tank Subsystem Evaluation	VI-2
VI-2	Evaluation of Propellant Acquisition Concepts	VI-12
VI-3	Pressurization System Evaluation	VI-32
VI-4	Revised Propulsion System Schematic for Mission A ₁	VI-37
VI-5	Revised Propulsion System Schematic for Mission A ₂	VI-38
VI-6	Operational Sequence for Explosively-Actuated Isolation Valve Packages, Missions A ₁ and A ₂	VI-39
VII-1	Cylindrical Tank Arrangement for a Total Impulse of 10 ⁶ lb _f -sec	VII-6
VII-2	Comparison of Series and Parallel Tank Arrangements	VII-7

Table

II-1	Propulsion Event Sequence	II-4
II-2	Acceleration Environment	II-5
II-3	Propellant Physical Properties	II-6
II-4	Propulsion System Criteria	II-10
III-1	Dielectrophoretic System Mass for Mission A ₁	III-6
III-2	Representative Polymeric Bladder and Diaphragm Positive Expulsion Systems	III-10
III-3	Polymeric Bladder and Diaphragm Evaluation Summary	III-18
III-4	Device Weights for Polymeric Bladders and Diaphragms	III-26
III-5	Polymeric Bladder/Diaphragm Testing	III-28
III-6	Ring-Reinforced Diaphragm System Mass	III-44
III-7	Convolute Spherical Diaphragm Mass	III-44
III-8	Operating Pressure Differential for Various Bladders and Diaphragms	III-49
III-9	Summary of Metallic Ring-Reinforced Diaphragm Technology Programs	III-52
III-10	Metallic Bellows Evaluation Summary	III-54
III-11	Expulsion Bellows Programs	III-55
III-12	Metallic Bellows Configuration	III-57
III-13	Metal Bellows System Mass	III-62
III-14	Summary of Trap Designs	III-74
III-15	Surface Tension System Mass	III-74
III-16	Settling Rocket Requirements, Mission A ₁	III-80
III-17	Settling Rocket Requirements, Mission A ₂	III-81
III-18	Settling Rocket Requirements, Mission B	III-82
III-19	Settling Rocket System Mass	III-85
III-20	Capillary/Bellows System Mass	III-90
IV-1	Propellant Outflow Schedule, Missions A ₁ and A ₂	IV-3
IV-2	Mission A ₁ Thermal Criteria	IV-4

IV-3	Results of Thermodynamic Analysis for Mission A ₁ , OF ₂ Propellant Tank	IV-6
IV-4	Results of Thermodynamic Analysis for Mission A ₁ , B ₂ H ₆ Propellant Tank	IV-7
IV-5	Results of Pressurant Storage Analysis for Mission A ₁	IV-16
IV-6	Results of Thermodynamic Analysis for Mission A ₂	IV-19
IV-7	Results of Pressurant Storage Analysis for Mission A ₂	IV-21
IV-8	Propellant Outflow Schedule, Mission B	IV-23
IV-9	Results of Thermodynamic Analysis for Mission B	IV-26
IV-10	Pressurant External Leakage for Mariner '71 Propulsion System	IV-29
IV-11	Pressurant External Leakage for Mission A ₁ Propulsion System	IV-31
IV-12	Pressurant External Leakage for Mission A ₂ Propulsion System	IV-32
IV-13	Pressurant External Leakage for Mission B Propulsion System	IV-33
IV-14	Pressurant Amounts Contained in Saturated Propellants	IV-35
IV-15	Helium Gas Evaluation	IV-38
V-1	Baseline Tank Dimensions	V-1
V-2	Tank Packaging Considerations	V-9
V-3	Metal Property Summary	V-11
V-4	Metal and Composite Tank Material Parameters	V-13
V-5	Metal Propellant Tank Mass	V-17
V-6	Critical Buckling Pressure Differential for Baseline Spherical Tanks	V-19
V-7	Metal and Composite Tank Mass Comparison	V-21
VI-1	Two versus Four Propellant Tanks, Mission A ₂	VI-5

VI-2	Spherical versus Cylindrical Tankage	VI-6
VI-3	Composite Tank Evaluation	VI-10
VI-4	Propellant Acquisition Concept Comparison	VI-14
VI-5	Possible Failure Modes	VI-15
VI-6	Relative Comparison for Mission A ₁	VI-16
VI-7	Relative Comparison for Mission A ₂	VI-17
VI-8	Relative Comparison for Mission B	VI-18
VI-9	Propellant Acquisition Concept Rating	VI-26
VI-10	Ratings with Simplified Approach	VI-27
VI-11	Ratings with Bridgeman Method	VI-29
VI-12	Mass Summary for Selected Propulsion Subsystems	VI-36
VII-1	Effects of Changing Propellants on Baseline Propulsion System	VII-2
VII-2	Propellant System Changes Resulting from a Total Impulse Increase to 10 ⁶ lb _f -sec	VII-5

SUMMARY

The contractual program is being conducted in two separate phases. During Phase I, the utility of current propellant acquisition techniques was investigated and the best acquisition, pressurization, and tankage propulsion subsystems were selected for Mars and Grand Tour spacecraft. Detailed analyses and design of the selected acquisition systems will be performed in Phase II. The three baseline missions include two 1-yr Mars Orbiter missions and a 10-yr Grand Tour mission to the outer planets. The space storable propellants OF_2 and B_2H_6 are used for one Mars orbiter, while the second uses N_2O_4 and $\text{CH}_3\text{N}_2\text{H}_3$ (MMH) earth storables. A nitrated hydrazine monopropellant is employed for the Grand Tour spacecraft.

Results of the Phase I system evaluation and selection are presented in this volume. Detailed information on current propellant acquisition techniques is included. Evaluations of propellant acquisition techniques, propellant tank configurations, and helium versus nitrogen stored-gas pressurization are presented for each of the three reference missions. Surface tension devices are clearly shown to be the best propellant acquisition concept for all three missions. For both Mars orbiters, a two-spherical propellant tank configuration is preferred; for the Grand Tour, the single tank should be spherical. Helium pressurant provides advantages over nitrogen for both of the separately stored Mars orbiter systems and for the Grand Tour blowdown pressurization system. The results presented also show that the Mars orbiters should employ a single pressurant storage sphere with helium stored at the nominal propellant temperature and an initial pressure of 4000 psia.

SYMBOLS

a	acceleration, ft/sec ²
A _b	effective bellows area, ft ²
b	dome height, ft
b _i	inside height of liner dome, ft
Bo	Bond number, dimensionless
C	constant or correction factor, dimensionless
d	distance, ft
d _s	settling distance, ft
D	diameter, ft
E	voltage, volts
E _m	modulus of elasticity, psf
F	thrust, lb _f
F _b	bellows spring force, lb _f
F _p	polarization force, lb _f
g	Earth gravitational acceleration, 32.17 ft/sec ²
h	liquid height, ft
H	cone height, ft
I	field intensity, volts/ft
I _{sp}	specific impulse, lb _f -sec/lb _m
I _t	total impulse, lb _f -sec
K	dielectric constant, dimensionless
K _b	bellows spring rate, lb _f /ft

ℓ	length, ft
L	tank length or characteristic dimension, ft
m	mass of propellant, lb_m
M	spacecraft mass, lb_m
P	pressure, psfa
P_b	burst pressure, psfa
ΔP_c	capillary retention pressure differential, psf
ΔP_{cr}	critical buckling pressure differential, psf
ΔP_e	entrance pressure loss, psf
ΔP_f	flow pressure loss, psf
ΔP_h	hydrostatic pressure differential, psf
ΔP_v	static pressure reduction due to flow, psf
r	tank radius, ft
r_d	radius of spherical dome segment, ft
r_i	inside radius of liner, ft
r_m	maximum cone radius, ft
R	pore radius, ft
R_1, R_2	principal radii of curvature, ft
R_s	radius of curvature for spherical interface, ft
S	operating stress, psf
S_{cr}	critical buckling stress, psf
S_u	ultimate stress, psf
t	settling time, sec
t_t	total rocket operating time, sec

v	velocity, fps
V	tank volume, ft^3
V_c	volume of cylinder, ft^3
V_{cs}	volume of cylinder with hemispherical domes, ft^3
V_s	volume of sphere, ft^3
W_c	weight of cylindrical barrel section, lb_m
W_{cl}	cylinder liner weight, lb_m
W_{cs}	weight of cylinder with hemispherical domes, lb_m
W_{dl}	dome liner weight, lb_m
W_s	weight of sphere, lb_m
x	wall thickness, ft
x_c	wall thickness of cylinder, ft
x_s	wall thickness of sphere, ft
y	bellows displacement from null position, ft
β	kinematic surface tension (σ/ρ) , ft^3/sec^2
ϵ	permittivity, farads/ft
ϵ_o	permittivity of vacuum, farads/ft
$\nabla\epsilon$	permittivity gradient, farads/ft
θ	liquid-to-solid contact angle, deg
ν	Poisson's ratio, dimensionless
ρ	density, lb_m/ft^3
σ	liquid/gas surface tension, lb_f/ft
τ	settling factor, dimensionless

ϕ	cone angle, deg
ω	angle of divergence, radians

Subscripts

g	gas
l	liquid

I. INTRODUCTION

The problems associated with propellant orientation and control during zero g (near-weightlessness) are well publicized in the literature (Ref I-1 to I-4). During the coasting, unpowered phases of a space mission, drag forces acting on the spacecraft tend to position the heavier liquid propellant at the forward end of the tank, and the lighter ullage gas over the tank outlet. Therefore, a method for maintaining propellant at the tank outlet is required so that gas-free liquid is available to the rocket engine on demand. The propellant acquisition subsystem provides this method.

The investigation of space storable propellant acquisition devices is being conducted in two phases. During the first phase, current (developed or under development) propellant acquisition methods were evaluated and compared for possible application to spacecraft missions to Mars and the Grand Tour of outer planets. This study phase concluded with selection of the best propellant acquisition, pressurization, and tankage combination for each of the baseline missions. The propellant acquisition device was key in this selection. Results of the first phase are presented in this report. During the second phase of the contractual study, the propellant acquisition subsystem will be designed and analyzed. The results of the second phase will be summarized in the second volume of the final report to be published at a later date.

The study approach for Phase I which included five major tasks is presented in Figure I-1. The program objectives, mission criteria, and design guidelines, are discussed in Chapter II. During Task I, a preliminary rating system was formulated to compare the different propellant acquisition subsystems. An extensive survey was conducted early in the program to collect background information and data on propellant acquisition concepts. The survey included literature searches, personal contact with government agencies, aerospace companies and vendors. This survey effort did not uncover any new propellant acquisition methods except for the capillary/bellows device conceived under the recently completed NASA program, Contract NAS9-8939 (Ref I-5). The capillary/bellows device was evaluated further in this study under Task VIII.

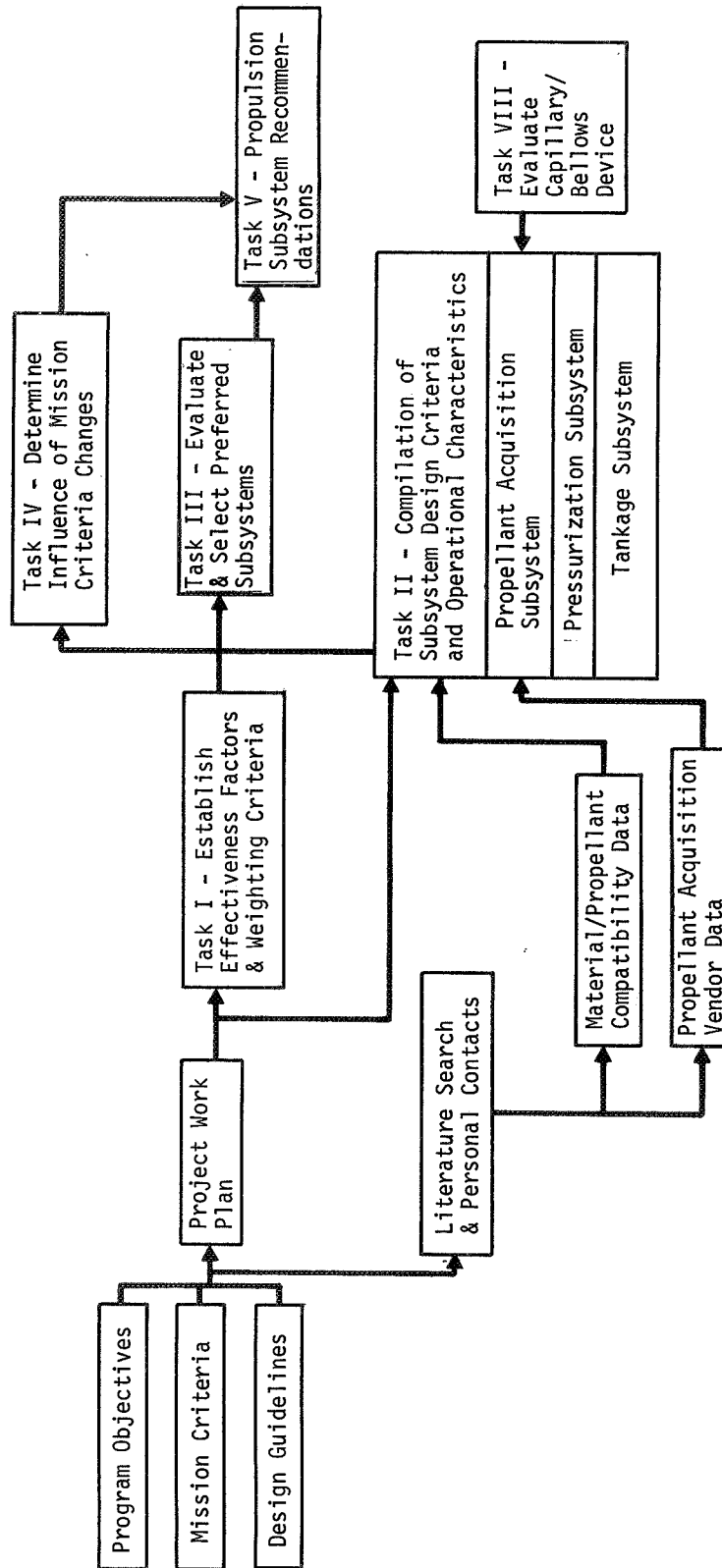


Figure I-1 Study Approach for the First Phase of the Program

As shown in Figure I-1, Task II was used to compile background information, design criteria and operational characteristics of the three propulsion subsystems. These data, along with the preliminary rating technique (Task I), were used in the comparative evaluation conducted during Task III. Based upon these comparisons, the best integrated propulsion subsystems were selected in Task III. The preferred systems were evaluated further in Task IV against possible changes to the baseline Mars and Grand Tour missions. The selected systems were recommended to JPL for approval (Task V).

As mentioned, program objectives, mission criteria and study guidelines are presented in Chapter II. The propellant acquisition devices evaluated during the study are discussed in Chapter III, and the pressurization system analysis is included in Chapter IV. Tank designs and packaging of the propulsion systems are presented in Chapter V, and the comparative evaluation of the propulsion subsystems and selection of the preferred systems are detailed in Chapter VI. A qualitative discussion of the influence of possible changes in the baseline mission requirements on the selected systems is presented in Chapter VII. Recommendations and conclusions for this first phase of the study are discussed in Chapter VIII.

II. PROGRAM OBJECTIVES, MISSION CRITERIA AND STUDY GUIDELINES

A. PROGRAM OBJECTIVES

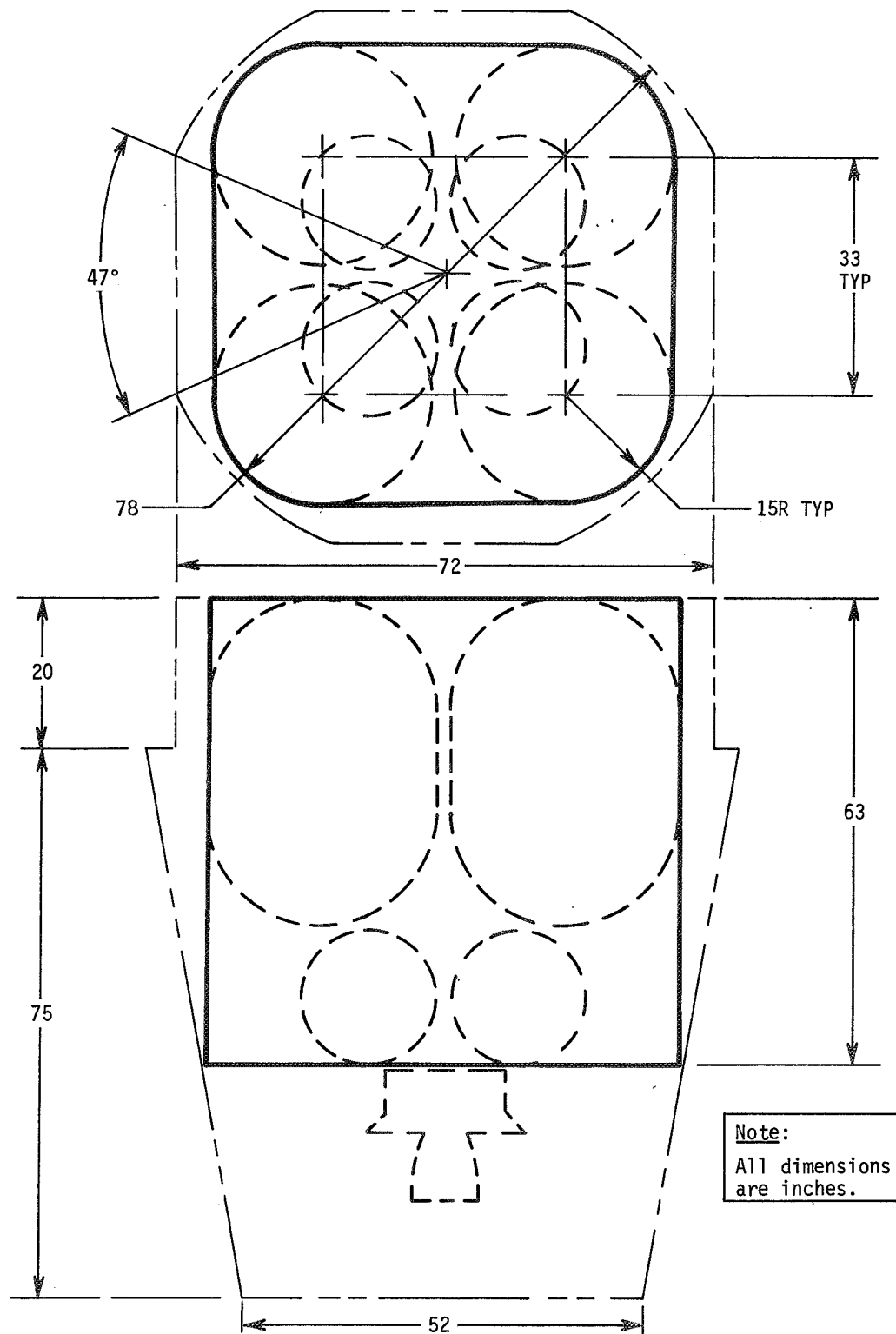
The program objectives were to investigate the utility of current (developed or under development) propellant acquisition methods and to select and recommend the best propellant acquisition, pressurization, and tankage subsystem combination to satisfy each of the baseline Mars and Grand Tour missions. The recommended propellant acquisition subsystem, with JPL approval, will be designed and analyzed during the second phase of the program.

B. MISSION CRITERIA

The baseline planetary missions are designated as Missions A₁, A₂ and B. The latter is the multiple planet mission, Grand Tour, while A₁ and A₂ are Mars missions. The Viking spacecraft propulsion system envelope shown in Figure II-1 was used for the Mars missions, and the propulsion system envelope shown in Figure II-2 was used for the Grand Tour mission. The corresponding envelope gross volumes are 198 and 22 cu ft, respectively. Additional baseline mission criteria are presented in this section.

1. Mission Description and Engine Duty Cycle

Mission A₁ and A₂ - The Mars Orbiter Mission includes a ground hold of 30 days (maximum) prior to launch aboard the Titan IIID/Centaur. Transit time to Mars is 180 days followed by insertion into a 24-hour elliptical Mars orbit. The maximum Mars orbiting requirement is 90 days. The propulsion events are presented in Table II-1. There are two midcourse corrections, the orbit insertion, and as many as three orbit trims. The percent of loaded propellant expended during each engine burn is presented in the table. Mission acceleration environments are shown in Table II-2.

Figure II-1 Propulsion System Envelope, Missions A₁ and A₂ (Viking Orbiter Four-Tank Configuration)

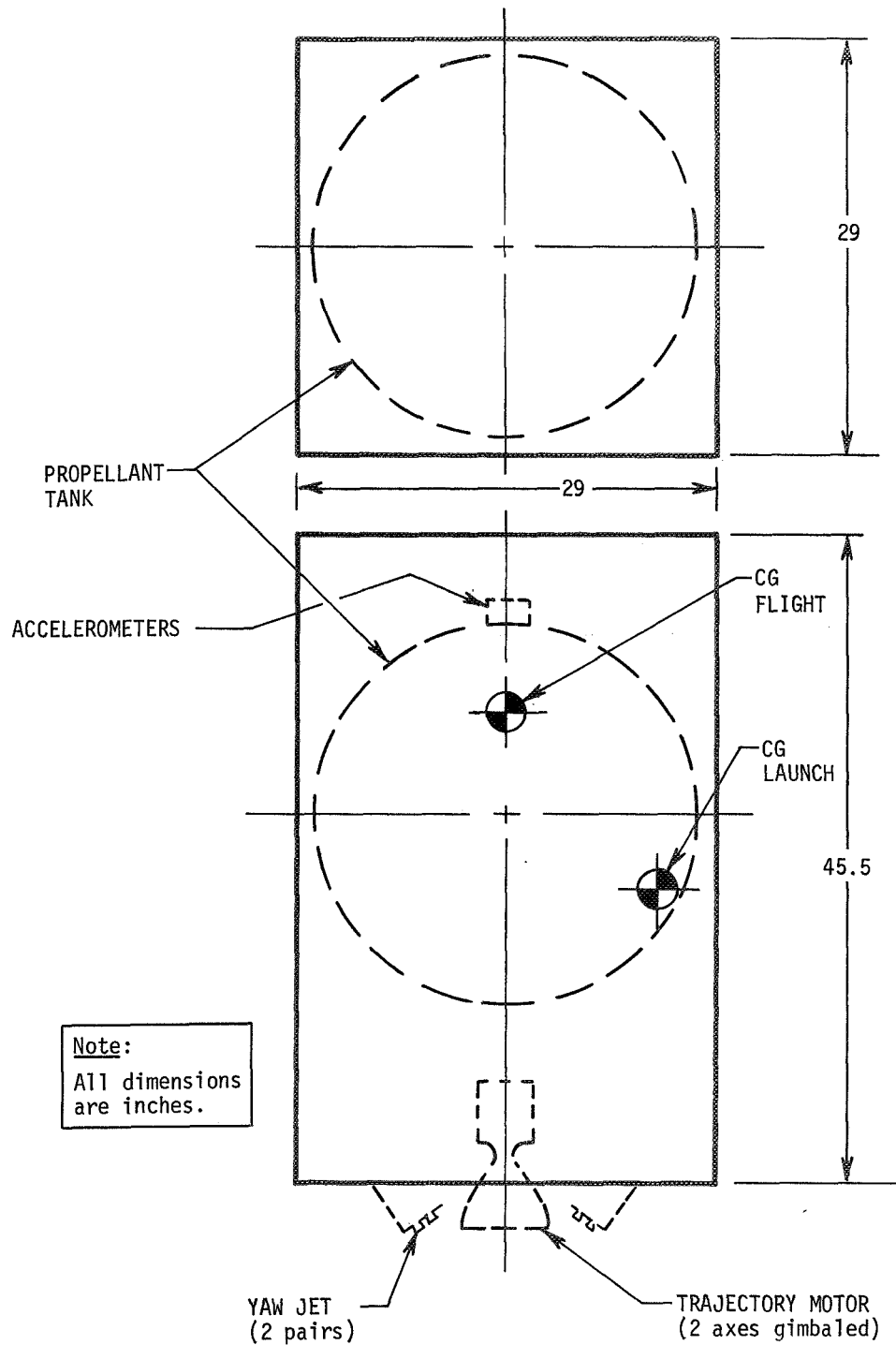


Figure II-2 Propulsion System Envelope, Mission B

Table II-1 Propulsion Event Sequence

Missions A₁ and A₂

EVENT	PROPELLANT LOAD EXPENDED (%)	EVENT TIME (DAYS)
First midcourse	0.6	Launch (L) + 5
Second midcourse	0.6	L + 160
Orbit insertion	95.0	L + 180
First orbit trim	1.3	L + 181
Second orbit trim	1.2	L + 225
Third orbit trim	1.3	L + 270

Mission B

EVENT	PROPELLANT LOAD EXPENDED (%)	EVENT TIME (DAYS)
Postlaunch	10.00	Launch (L) + 10
Pre-Jupiter	2.22	L + 493
Post-Jupiter	5.49	L + 531
Pre-Saturn	3.93	L + 1087
Post-Saturn	34.15	L + 1116
Pre-Uranus	10.89	L + 2310
Pre-Uranus	4.15	L + 2331
Post-Uranus	20.73	L + 2360
Pre-Neptune	8.44	L + 3272

Mission B - The Grand Tour Mission may include flybys of Jupiter, Saturn, Uranus and Neptune; the total mission time is approximately 3500 days. The nine propulsion events are presented in Table II-1. The first course correction maneuver occurs ten days after launch, while the last engine burn (pre-Neptune) takes place 3272 days after launch. The percent of loaded propellant expended during each engine burn is presented in the table; the total (nominal plus 3σ) velocity requirement is approximately 320 meters per second. Mission acceleration levels are shown in Table II-2. The launch vehicle for this mission is a Titan IIID/Centaur/Burner II (1440).

Table II-2 Acceleration Environment*

	Mission A ₁	Mission A ₂	Mission B
AXIAL - POSITIVE			
Boost Phase - Maximum	3.8	3.8	3.8
Spacecraft Engine			
Maximum	0.156	0.0495	0.0253
Minimum	0.133	0.0400	0.0202
AXIAL - NEGATIVE	10^{-7}	10^{-7}	10^{-7}
LATERAL	0.0002	0.0002	0.0002
*Accelerations are expressed in Earth g.			

2. Propellants

Mission A₁ and A₂ - Mission A₁ utilizes the space storable propellants oxygen difluoride (OF₂) and diborane (B₂H₆) while Mission A₂ employs the earth storables nitrogen tetroxide (N₂O₄) and monomethylhydrazine (CH₃N₂H₃) as the baseline propellant combinations. Physical property data for these propellants, as well as those for other propellants considered during the program are presented in Table II-3. The possibility of replacing the monomethylhydrazine with neat hydrazine (N₂H₄) for Mission A₂ was considered during the study.

Mission B - A monopropellant, 75/25 wt% hydrazine/hydrazine nitrate (75/25 - N₂H₄/N₂H₅NO₃), was the baseline propellant. A possible propellant change to hydrazine was also considered.

Table II-3 Propellant Physical Properties

PROPELLANT	FUELS			OXIDIZERS		
	DIBORANE (B ₂ H ₆)	MONOMETHYLHYDRAZINE [N ₂ H ₃ (CH ₃)]	NEAT HYDRAZINE (N ₂ H ₄)	NITRATED HYDRAZINE (75/25-N ₂ H ₄ /N ₂ H ₅ NO ₃)	OXYGEN DIFLUORIDE (OF ₂)	NITROGEN TETROXIDE (N ₂ O ₄)
Density lb _m /ft ³	30.3 (-210°F) *	55.6 (40°F) †	63.8 (40°F) §	69.8 (40°F) ¶	92.3 (-210°F) *	92.5 (40°F) §
Viscosity, lb _m /ft-sec	1.9 × 10 ⁻⁴ (-210°F) *	7.8 × 10 ⁻⁴ (40°F) †	8.9 × 10 ⁻⁴ (40°F) §	24 × 10 ⁻⁴ (40°F) ¶	1.54 × 10 ⁻⁴ (-210°F) *	3.4 × 10 ⁻⁴ (40°F) §
Surface Tension, lb _f /ft	1.43 × 10 ⁻³ (-210°F) *	2.46 × 10 ⁻³ (40°F) †	4.9 × 10 ⁻³ (40°F) §	3.84 × 10 ⁻³ (40°F) **	9.19 × 10 ⁻⁴ (-210°F) **	1.85 × 10 ⁻³ (68°F) §
Freezing Point, °F	-265 *	-63 §	35 §	3 ¶	-371 *	12 §
Boiling Point, °F	-135 *	193 †	235 §		-230 *	70 §

*J. S. Whittick, et al.: *Physical Properties of Liquid Oxygen Difluoride and Liquid Diborane: A Critical Review*. SRI Report No. 951581-4, Stanford Research Institute, Menlo Park, California, July 1, 1967.

†S. S. Miller: *Liquid Propellant Manual, Unit No. 11, Monomethylhydrazine*. Chemical Propulsion Information Agency, Silver Spring, Maryland, Dec. 1966 (Confidential).

§*Engineering Property Data on Rocket Propellants (U)*. AFRPL-TR-68-100, Rocketdyne Division, North American Rockwell Corporation, Canoga Park, California, May 1968 (Confidential).

¶Data supplied by Jet Propulsion Laboratory.

**Calculated by Sugden Parachor method described by P. I. Gold and G. J. Ogle: "Estimating Thermophysical Properties of Liquids, Part 8 - Surface Tension." *Chemical Engineering*, May 19, 1969.

3. Propulsion System

Missions A₁ and A₂ - The baseline system schematics for the two Mars missions are presented in Figures II-3 and II-4. The tank outlets are pointed toward Earth during launch. Total impulse is 400,000 lb_f-sec for both missions. Engine thrust levels are 1000 lb_f and 300 lb_f and propellant mixture ratios are 3.0 and 1.55 for Missions A₁ and A₂, respectively. Additional system criteria are presented in Table II-4.

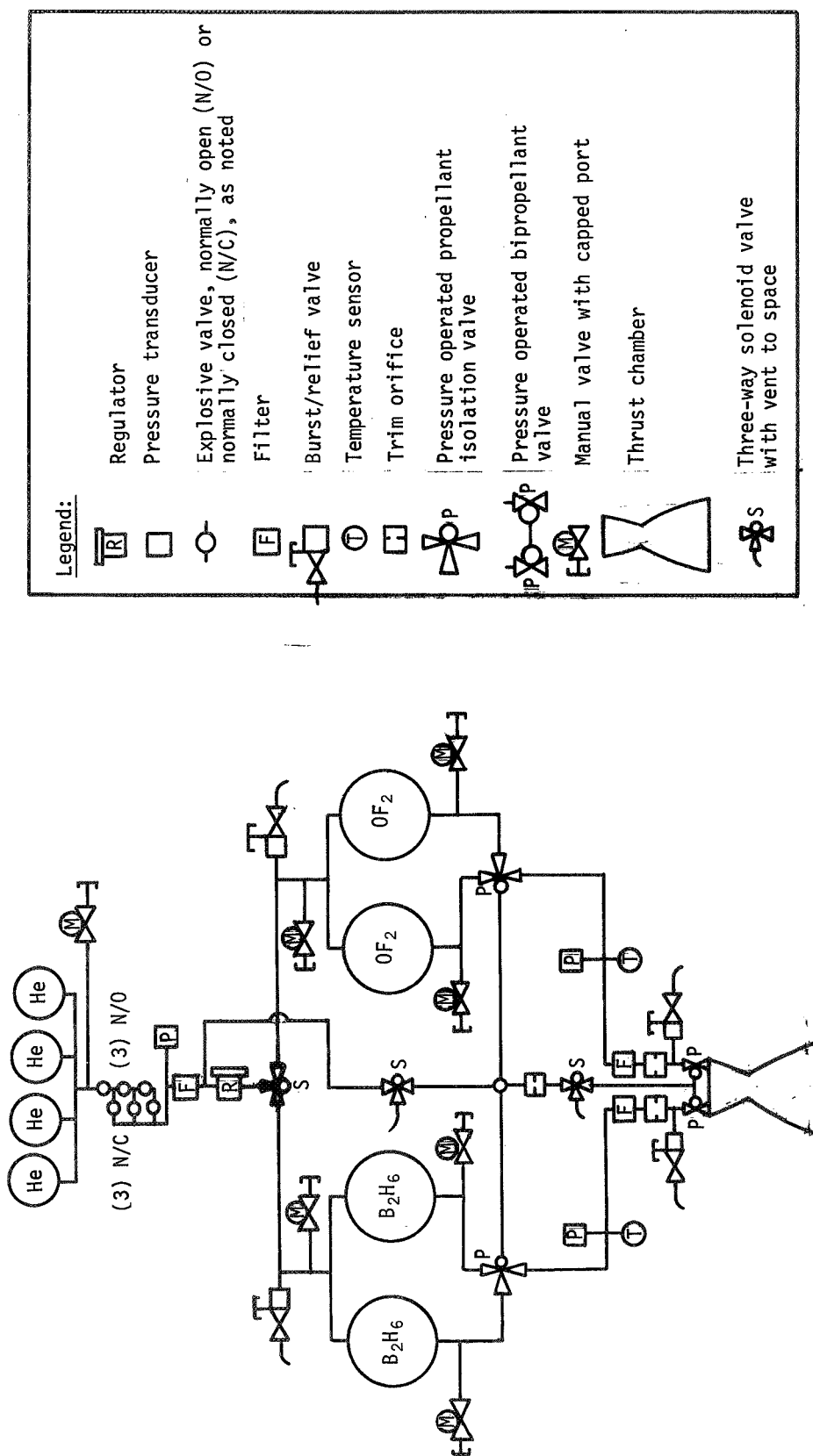
Mission B - The propulsion system schematic is presented in Figure II-5. As in the Mars missions, the tank outlet is oriented toward Earth during launch. The propulsion system criteria for this mission are also presented in Table II-4. Engine thrust level is 25 lb_f and the vacuum specific impulse is 255 lb_f-sec/lb_m.

4. Pressurization Subsystem

Stored-gas pressurization is employed for all missions. The pressurant may be nitrogen or helium for the Mars and Grand Tour missions. The latter uses a blowdown system as shown in Figure II-5.

5. Propellant Tankage

The baseline tanks are spheres or cylinders with hemispherical end domes. For Missions A₁ and A₂, either two or four propellant tanks may be employed. The baseline four-tank configuration uses a parallel tankage arrangement. For Mission B, only one tank is used.

Figure II-3 Baseline Propulsion System Schematic for Mission A₁

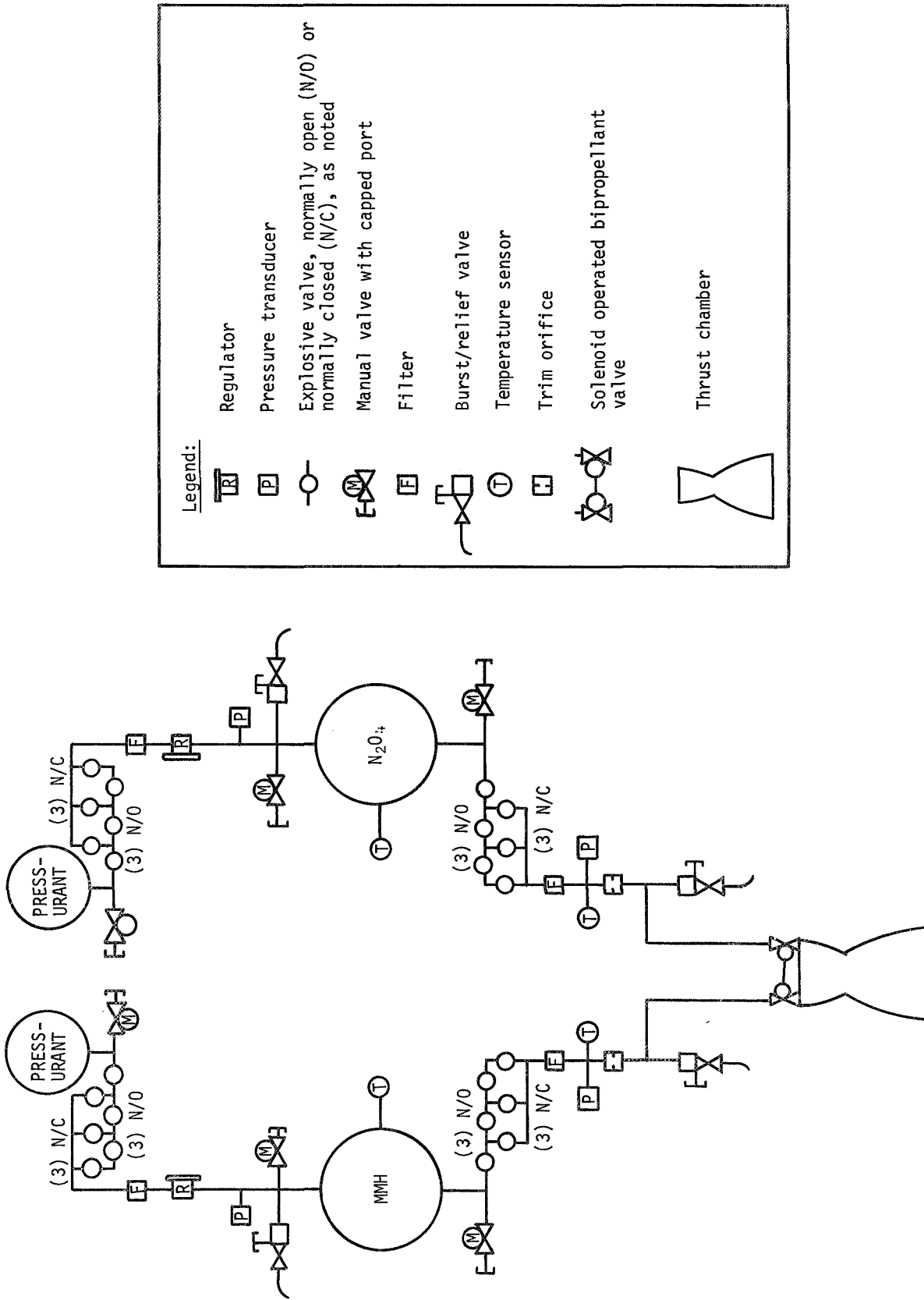


Figure II-4 Baseline Propulsion System Schematic for Mission A2

Table II-4 Propulsion System Criteria

	MISSION		
	A ₁	A ₂	B
Propellants	B ₂ H ₆ /OF ₂	MMH/N ₂ O ₄	75/25-N ₂ H ₄ /N ₂ H ₅ NO ₃
Propellant Temperature, °R			
Range	210-280	500-580	475-575
Nominal	250	500	500
Propellant Density, lb _m /ft ³	30.3/92.3	54.8/90.5	69.8
Propellant Mass, lb _m	270/810	562/872	135
Tank Volume, ft ³	9.92	11.25	3.86
Initial Ullage, %	~10	~10	~50
Propellant Margin, %	4	4	4
Number of Burns	6	6	9
Thrust, lb _f	1000	300	25
Mixture Ratio	3.0	1.55	--
I _{sp} (vac), lb _f -sec/lb _m	385	290	255
Total Impulse, lb _f -sec	400,000	400,000	33,000
Minimum Impulse Bit, lb _f -sec	400	400	1.00
Propellant Tank Pressure, psia	~350	~350	~350
Chamber Pressure, psia	100	100	100
Tank Geometry		Spherical or Cylindrical with Hemispherical Ends	
No. of Propellant Tanks	2 or 4	2 or 4	1
Tank Material		Metal or Composite	
Pressurant		Helium or Nitrogen	
Propulsion Envelope, ft ³	198	198	22
Spacecraft Mass, lb _m	7500	7500	1124

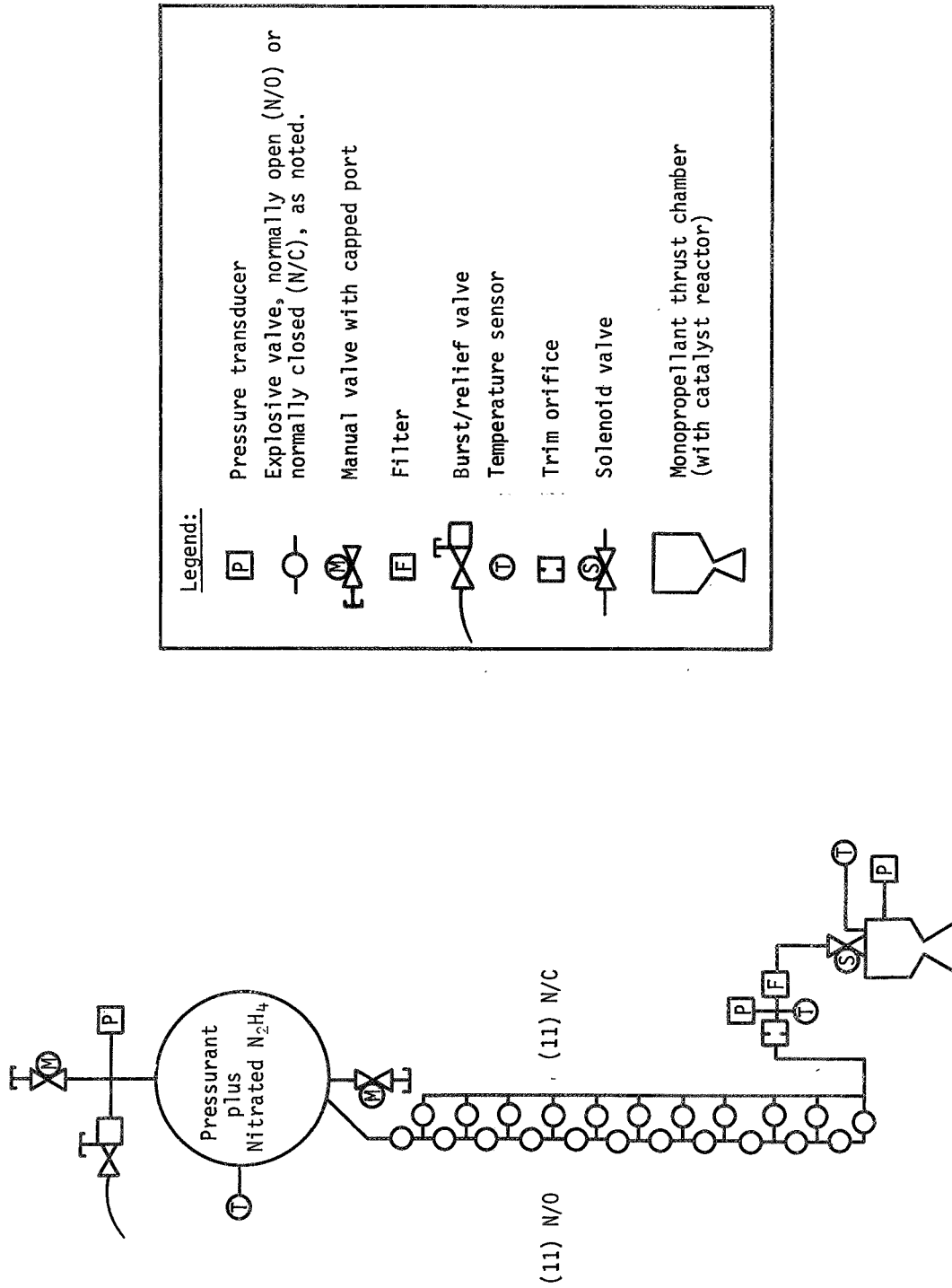


Figure II-5 Baseline Propulsion System Schematic for Mission B

C. STUDY GUIDELINES

The guidelines established for the study of the propellant acquisition, pressurization, and tankage subsystems are outlined in this section.

1. Propellant Acquisition Subsystem

The following classifications of acquisition methods were considered: surface tension devices, polymeric and metallic bladders, metallic diaphragms and bellows, dielectrophoresis, main engine start tanks, and auxiliary propellant settling rockets. Techniques already developed or under development were evaluated. A relatively small experimental task was conducted to evaluate the feasibility of the capillary/bellows device conceived under Contract NAS9-8939. These experimental results are presented separately in the Appendix. Background information, design criteria and operational characteristics were established for each method. Conceptual designs in the form of simplified schematics were to be made so that each method could be evaluated and compared for application to each of the baseline missions considering reliability, mass, performance repeatability, performance testability, state of development, and compatibility with adjacent components and propellants.

The mass attributed to each propellant acquisition device included the dry weight of the device plus any additional system mass resulting from the use of that device. One of the items included in the latter was residual propellant (outage) resulting from expulsion inefficiency which would have to be added to the baseline loaded propellant. However, the tanks were not resized for each acquisition device and the small increases in tank size and mass, which would have resulted from resizing, were neglected in the comparative evaluation of candidate concepts. As discussed in Chapter VI, no increase in tank size or loaded propellant quantity is required with the propellant acquisition system selected for each mission.

Interactions between the propellant acquisition subsystem and the pressurization and propellant tank subsystems were included. The intent for this first phase of the program was to select the best propellant acquisition concept for each mission -- not to provide an optimum design.

An evaluation of the influence of possible changes in certain mission constraints and propulsion system characteristics on the selection of propellant acquisition concepts was conducted. The following considerations and changes were included in the assessment:

- 1) Use of neat hydrazine in place of monomethylhydrazine for Mission A₂ and in place of 75/25 - N₂H₄/N₂H₅NO₃ for Mission B;
- 2) Increase in total impulse from 400,000 lb_f-sec to 1,000,000 lb_f-sec for Missions A₁ and A₂;
- 3) Decrease in minimum impulse bit from 400 lb_f-sec to 125 lb_f-sec for Mission A₁ and A₂;
- 4) Use of onboard accelerometers in place of preprogrammed time burns;
- 5) Series versus parallel arrangement of the propellant tanks;
- 6) Propellant tank loading constraints;
- 7) Impact of spacecraft sterilization.

2. Pressurization Subsystem

Based on the preliminary information available on the propulsion system, the preferred pressurant and storage and operating conditions were determined for the three reference missions in terms of subsystem mass, reliability, cost and schedule time. Interactions with the propellant acquisition and propellant tank subsystems were also evaluated.

Pressurization subsystem mass was defined as the sum of the pressurant mass (used and residual), pressurant storage vessel mass, and mass of propellant vaporized. Isothermal tank walls and environment were assumed for the coast periods on Missions A₂ and B. During engine burn periods, the pressurant storage and propellant tank boundaries were considered adiabatic. For Mission A₁, an environmental temperature varying linearly with time from 282°R in Earth orbit to 258°R in Mars orbit was employed. Other simplifying assumptions, presented in Chapter IV, were also employed.

A spherical pressurant storage vessel constructed of 6Al-4V titanium, with a safety factor of 2.2 based upon an ultimate strength of 165,000 lb_f/in.², was considered in the analyses for Missions A₁ and A₂. A factor of 1.1 on tank mass was to be used to account for attachments, penetrations, and welds. The propellant temperature range was 210 to 280°R for Mission A₁, 515 to 535°R for Mission A₂, and 475 to 575°R for Mission B. Other system conditions used for the analyses were:

- 1) An initial storage pressure range from 2,000 to 4,000 psia for Missions A₁ and A₂;
- 2) A gas storage temperature range of 210 to 530°R for Mission A₁, and 500 to 580°R for Mission A₂;
- 3) Propellant tank pressurant inlet temperatures from 210 to 530°R for Mission A₁, and 515 to 535°R for Mission A₂.

3. Propellant Tank Subsystem

The number of propellant tanks, tank size and geometry, and tank materials were determined considering mass, reliability, cost and schedule, and interactions with the propellant acquisition and pressurization subsystems. Two versus four tanks (Missions A₁ and A₂), spherical versus cylindrical geometry, and all-metal versus composite construction were evaluated. Propellant compatibility, tank mass, and fabrication were considered in selecting materials for both the propellant tanks and the acquisition devices.

III. CANDIDATE PROPELLANT ACQUISITION CONCEPTS

All the propellant acquisition concepts considered in this investigation are discussed in this chapter. The physical and operational characteristics of each device are discussed and an appraisal of reliability, mass, scalability and producibility, compatibility, and testability is presented for each concept.

A. DIELECTROPHORETIC SYSTEMS

1. System Description and Operation

Dielectrophoretic forces can be used to orient some propellants in a low-g environment. The electrical conductivity of the propellant must be low, however, to make this approach attractive. The polarization force may be used in the design of dielectrophoretic propellant acquisition devices (Ref. III-1):

$$F_p = \frac{1}{2}(I^2 \nabla \epsilon) \quad [\text{III-1}]$$

where F_p is the polarization force, I is the field intensity, and $\nabla \epsilon$ is the permittivity gradient. In a homogeneous fluid, the permittivity, ϵ , is constant and the gradient is zero, making the net polarization force zero as well. Fortunately, the permittivity gradient is large across the liquid-vapor interface of a dielectric liquid. This provides an electric force in a field of constant intensity that acts to orient the fluid. The permittivity gradient becomes a stepped function across the interface, $\nabla \epsilon = (\epsilon_\ell - \epsilon_g)$, where ϵ_ℓ and ϵ_g are the permittivities for liquid and gas, respectively. The force acting at the interface can be presented in terms of a pressure rise across the interface which, in turn, can be presented in terms of the liquid and vapor densities. The resulting basic equation for parallel plate electrodes is:

$$(\rho_\ell - \rho_g) a = -\frac{1}{2}(\epsilon_\ell - \epsilon_g) \nabla I^2 \quad [\text{III-2}]$$

where ρ_ℓ and ρ_g are liquid and gas densities, respectively, and a is the adverse acceleration.

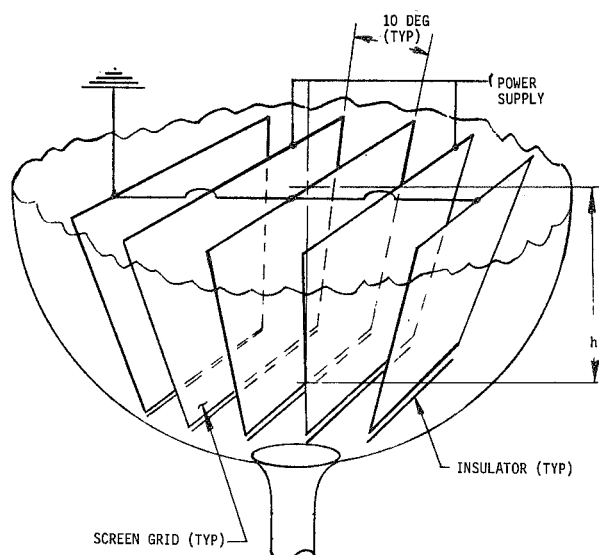


Figure III-1 Dielectrophoretic System

The use of parallel plate electrodes in a propellant tank under low adverse acceleration environments is unattractive as the liquid will tend to settle forward, away from the outlet, when all of the propellant is contained between the plates. A field intensity gradient tending to hold the propellant over the tank outlet is required under these conditions. This gradient can be achieved by decreasing the electrode gap in the direction of the tank outlet. A conceptual installation of the screen electrode grids in a fanned array with the apex at the tank outlet (Fig. III-1) is an example that achieves the desirable

field gradient. The field gradient within the diverging plates is:

$$I = E/\omega d \quad [\text{III-3}]$$

where E is the voltage across the plates and ωd is the grid spacing, ω being the angle of divergence and d the distance from the apex of the angle to the liquid-vapor interface.

Equation [III-2) can then be presented in terms of the impressed voltage and grid spacing:

$$E^2 = d^3 \omega^2 a \frac{(\rho_l - \rho_g)}{(\epsilon_l - \epsilon_g)} \quad [\text{III-4}]$$

The feasibility of using dielectrophoresis is dependent upon the electrical properties of the propellants. The propellants, monomethylhydrazine and nitrated hydrazine, are not good dielectrics because of their high electrical conductivities (on the order of 10^{-5} mho/cm). There would be too much electrical current flowing through the propellant, making the power requirements excessive.

The dielectric constant is another electrical property that must be considered. This is the ratio of the permittivity of the fluid to the permittivity of a vacuum:

$$K = \frac{\epsilon_l}{\epsilon_o} \quad \text{[III-5]}$$

The permittivity of the ullage gas should be very close to that of a vacuum, so Equation [III-4] can be written in terms of the dielectric constant:

$$E^2 = d^3 \omega^2 a \frac{(\rho_l - \rho_g)}{\epsilon_o (K - 1)} \quad \text{[III-6]}$$

The larger the dielectric constant for a propellant, the better electric it makes and, based on Equation [III-6], the smaller the required voltage.

From these considerations alone, both propellants for Mission have good dielectric properties. Dielectrophoresis is not attractive for either Missions A₂ or B. Based on information from Allied Chemical Company, OF₂ has an electrical conductivity of $< 10^{-10}$ mho/cm and a dielectric constant of 2.3. Diborane (B₂H₆) has a dielectric constant of 2.0, but its electrical conductivity is not available. Callery Chemical believes that the conductivity of B₂H₆ is less than that of OF₂, based on molecular structures.

The voltage that can be calculated from Equation [III-6] is the minimum voltage required to retain the propellant under the adverse acceleration. If this voltage is applied as a direct current, surface instabilities will occur; if it is applied at a high frequency, the power requirement becomes larger and another form of instability occurs. Therefore, the voltage must be applied in the form of a square wave with a frequency on the order of 0.1 cps. Because the voltage is squared as it appears in Equation [III-6], retention of the fluid is not affected if the waveform of the applied voltage is a square wave.

A typical dielectrophoretic propellant retention system consists of two major subsystems, the power supply and the screen grid assembly including the electrical feedthru assembly. The power supply converts 28 volts direct current from the spacecraft power system, into a high-voltage, low-frequency square wave. The size

and weight of the power supply depends upon the voltage required and the amount of power that will be consumed. A screen grid system positioned in the propellant tank in a fanned array, tapered toward the tank outlet, forms the desired capacitance plates required to orient the propellant (Figure III-1). The coarse-mesh, screen grid assembly uses insulator supports attached to brackets welded to the tank wall. Tubular rims supporting the screen grids are anchored to the insulator supports on the wall, and proper spacing between grids is provided by insulator rods.

The concept shown in Figure III-1 was evaluated for application to Mission A₁. In order to minimize the amount of power consumed, the dielectrophoretic system can be operated in two different modes. Prior to the first three burns, there is a large volume of propellant. If the grid height is approximately 16 inches, there will always be some liquid between the electrodes regardless of the location of the interface. Therefore, the sequence of operation would be:

- 1) Prior to the first midcourse correction, power is applied to the grids. The induced forces will act to settle the propellant into the grids. After allowing sufficient time to settle the propellant, the main engine is started and the dielectrophoretic system is turned off;
- 2) The second midcourse correction is accomplished in the same manner;
- 3) Prior to the insertion burn, the propellant is again settled with the dielectrophoretic system, but the power is left on after the burn is complete. From this point to the end of the mission, the amount of propellant remaining in the tank is too small to be reliably acquired and settled by any reasonable grid configuration. The fanned array will keep the propellant oriented if the power is left on;
- 4) The orbital trim burns are accomplished;
- 5) The system is turned off.

Using Equation [III-6], the voltage required for this system is 3000 volts. The amount of power required from the spacecraft power system depends upon a number of factors, such as the:

- 1) Total electrical resistance of the fluid;
- 2) Number of grids in the array;
- 3) Total capacitance of the system;
- 4) Frequency of the applied power;

- 5) Applied voltage;
- 6) Size of the charging resistor. (This resistor is added in series with the power supply output in order to limit the capacitor charging current);
- 7) Power supply efficiency.

The detailed design of this system would require a complex evaluation of the effects of all the above factors on the required power and the system performance. It is estimated that the power requirement for this system will be on the order of 4 watts, which is consistent with power requirements quoted for similar systems in Reference III-1.

The potential increase in propellant decomposition, caused by the imposed voltage, must be considered in designing a dielectrophoretic system. For Mission A₁, this effect is minor; the quantities of OF₂ and B₂H₆ decomposed were estimated to be about 3.5×10^{-6} lb_m and 1.8×10^{-6} lb_m, respectively. Materials in the screen grid assembly can be selected to be compatible with these propellants with the exception of materials for electrical insulators. More development is needed in this area, especially for OF₂. Nonmetallic insulators such as Teflon and Kel-F (and possibly ceramics) appear to be good candidates for B₂H₆, but they are questionable in OF₂.

2. System Evaluation

a. Reliability - The dielectrophoretic system is an active system consisting of many components. Major subassemblies are the screen grids and supporting electrical insulators, the electrical feedthrus and wiring, a power supply, and a dielectrophoretic sequencer. The probability of failure of the grids, insulators, feedthrus, or wiring is low and these failures were ruled out as unlikely.

Two catastrophic failure modes considered possible are

- 1) Failure of the portion of the spacecraft sequence system that operates the dielectrophoretic system;
- 2) Failure of the power supply.

Each of the catastrophic type failures could also occur to lesser degrees. Gas ingestion into the engine would occur and acquisition of the propellant would be accomplished in a degraded manner. Therefore, they are also considered to be anomalous failure modes.

b. Mass - The principal contributor to weight of the dielectrophoretic system is the power supply for units of the size under consideration. The screen grid system forms only a small fraction of the total system weight. Due to the manner in which this system is to be operated during the mission, the power consumption will be maximum during the Mars orbit because the power supply must be operated continuously. Power requirements become critical at this point because the solar panel efficiency is decreased. Therefore, some increase in the capacity of the spacecraft power system will be required by a dielectrophoretic system. The mass estimated for a 4-watt, 3000-volt system is presented in Table III-1.

Table III-1 Dielectrophoretic
System Mass for
Mission A₁

	TWO-TANK SYSTEM*	FOUR-TANK SYSTEM*
Power Supply	11 lb _m	12 lb _m
Electrodes, feedthrus	4	5
Vaporized Propellant	8	8
Additional batteries and solar panels	15	15
Total system mass	38 lb _m	40 lb _m
*Spherical or cylindrical geometry.		

c. Design Scalability and Producibility

1) Design Scalability - The system can be scaled over the range of interest, but redesign is required. As previously stated, the power supply is the heaviest subsystem in this type of retention device. Scaling will involve modification of the power package size in the interest of weight optimization.

2) Manufacturability - Much experimental work has been done with prototype systems but no flight systems have been built to date. Additional work on the power systems and electrical high tension feedthru techniques is required. Fabrication techniques are available.

3) Subscale Test Scalability - Complete geometric test scaling is possible through the use of nonmiscible fluids having attractive dielectric constants. For example, the performance of such a system was investigated by Dynatech using corn oil and silicone oil at 1 g (Ref III-1). Subscale drop tower and aircraft tests are also possible.

d. Compatibility with Adjacent Components and Propellants

1) Propellant/Material Compatibility - An aluminum screen grid assembly, compatible with the Mission A₁ propellants, can be used. As previously stated, the material selection for electrical insulation of the high tension feedthru and for the screen grid insulators could be a problem.

2) Pressurization System Compatibility - The propellant is in contact with the pressurant and is subject to gas dissolution and vaporization. Pressurant inlet temperature will not appreciably affect performance except for the secondary effects of propellant/pressurant contact.

3) Tankage Compatibility - This device can be used in any of the tanks considered in the evaluation without tank shape restriction.

4) Performance - The system is compatible with the Mission A₁ environment and engine duty cycle. If the number or duration of the orbital trim burns was changed, the same device would function properly and the power and voltage requirements would remain constant. This results from the continuous application of power after orbital insertion as mentioned previously. Variations in acceleration level in the negative direction affect the power supply requirement; increased voltage and power and a heavier power supply is required to retain propellant under higher negative accelerations.

e. Performance Testability

1) Verification of Operational Readiness - The operation of the power supply and its ability to apply the required potential to the grids can be verified. Settling and retention of the propellant, however, can only be demonstrated in a separate test program.

2) Development Status - Additional development is required on this type of device. Substantial work has been done in attempting to reduce power supply weight, but a flightweight power supply is still not available for systems of the size considered here.

B. POLYMERIC BLADDERS AND DIAPHRAGMS

1. System Description and Operation

Polymeric bladders and diaphragms are simple, effective, active devices that utilize an elastoplastic material to separate the liquid and gas volumes in the tank and provide positive expulsion of the liquid. Bladders are enclosed membranes or bags attached to the tank at the suction line. They function as a contact system where the driving mechanism is separated from the propellant. Diaphragms are morphologically similar to bladders, but the diaphragm is an open membrane that conforms with the tank wall and usually attaches near the tank equator. Bladders and diaphragms can be fabricated from metallic and/or nonmetallic materials and can be actuated mechanically, hydraulically, or pneumatically. The principal nonmetallic and combination constructions, polymeric and polymeric/metal materials, are the subject of this section. The discussion is oriented toward the gas pressurized systems (regulated and blowdown) in extensive use at this time. The information presented has been extracted from the program experience listed in Table III-2 and from References III-2 thru III-59.

a. Bladders - Polymeric bladder devices have been designed for liquid expulsion through collapsing, expanding, twisting, and squeezing actions. Bladder systems employing direct-acting mechanisms for twisting or squeezing are characterized by higher energy requirements, high weight, additional failure modes attributable to the actuation mechanism, and poor expulsion efficiency (Ref III-23). Generally, the volumetric efficiency of a bladder system that operates with a direct-acting mechanism is also severely degraded. Consequently, pneumatically actuated collapsing bladders and expanding bladders have received most attention.

Unbonded and independent multi-ply bladders have demonstrated increased expulsion cycle life at deep cryogenic temperatures (Ref III-2). However, inter-ply inflation, which results from pinholing in the polymeric film, can seriously limit the expulsion efficiency. An expanding bladder (expulsion produced by pressurizing the inside of the bag) controls the inter-ply inflation and circumvents the terminal collapsing problem. The cryogenic bladder materials, using about 10 plies of thin polymeric film, penalize the system weight and volumetric efficiency, but such bladder designs should produce expulsion efficiency greater than 98% for approximately 25 expulsion cycles (Ref III-3 and III-4). The cryogenic propellants for Mission A₁ would require this type of expanding bladder system (Fig. III-2).

Table III-2 Representative Polymeric Bladder and Diaphragm Positive Expulsion Systems

SYSTEM	VEHICLE	PROPELLANTS	PRESSURANT	MATERIAL	PROGRAM
Bladder	Transtage ACS	$N_2O_4/A-50$	N_2	TFE-FEP	PC211068
Bladder	Surveyor VPS	MON-10/MMH- H_2O	He	TFE-FEP	JPL950056
Bladder	Lunar Orbiter VCS	$N_2O_4/A-50$	N_2	TFE-FEP-A ₆ /TFE-FEP	
Bladder	Saturn S-IVB APS	N_2O_4/MMH	He	TFE-FEP	
Bladder	Apollo Service Propulsion System RCS	N_2O_4/MMH	He	TFE-FEP	NAS9-7182
Bladder	Apollo Command Module RCS	N_2O_4/MMH	He	TFE-FEP	NAS9-7182
Bladder	Apollo Lunar Module RCS	$N_2O_4/A-50$	He	TFE-FEP	NAS9-7182
Bladder	Mars Mariner '69	N_2H_4	N_2	Butyl FR6-60-26	JPL951939
Bladder	Mars Mariner '71	N_2O_4/MMH	N_2	TFE-FEP	JPL952460
Diaphragm	Transtage ACS	N_2H_4	N_2	EPR 132	AF04(695)-150
Diaphragm	Sterilizable Liquid Propulsion System	N_2O_4	N_2	TFE-FEP	JPL951709
Diaphragm	Viking Lander DPS	N_2H_4	N_2	EPT 10	NAS1-9000

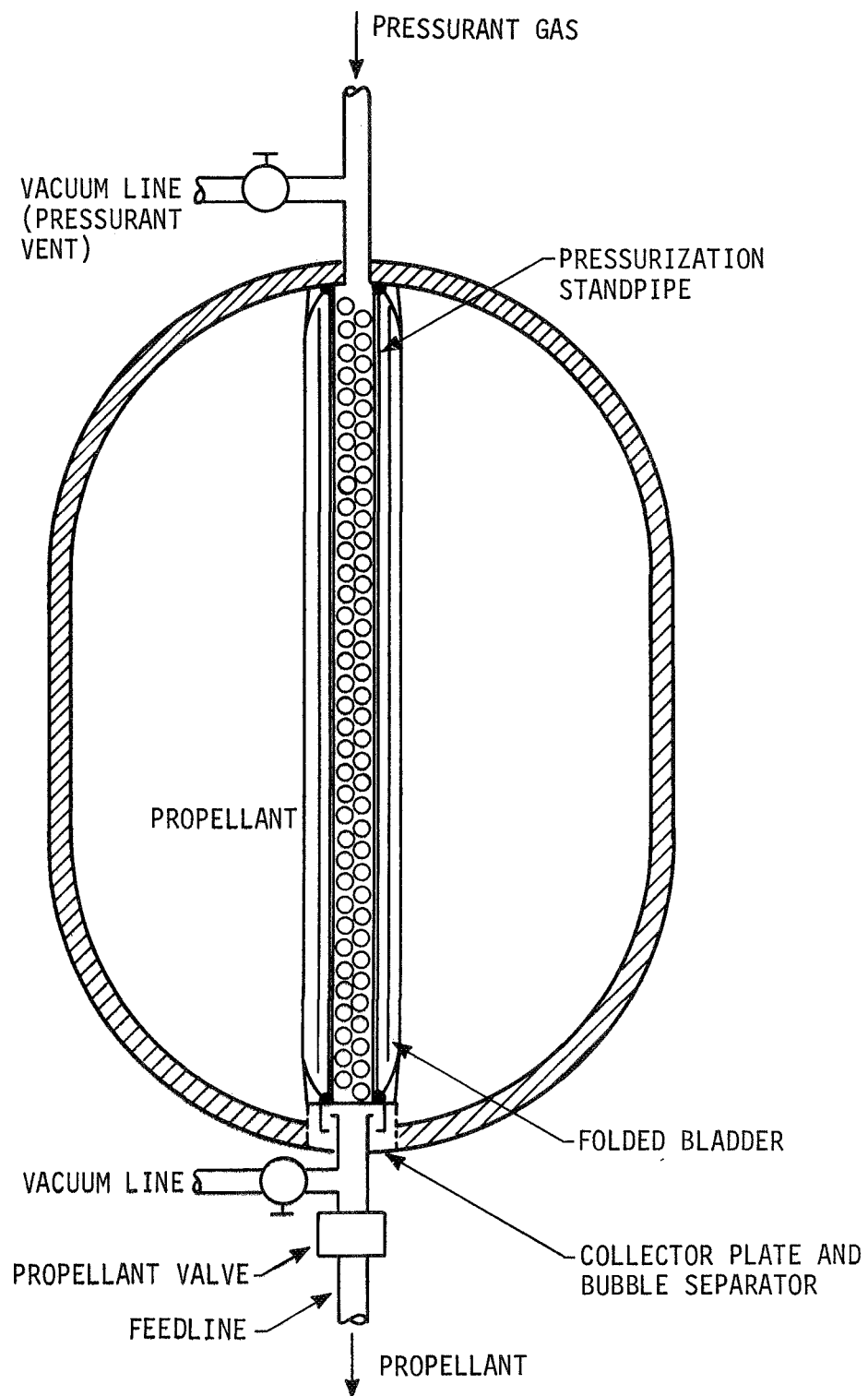


Figure III-2 Expanding Polymeric Bladder System for Mission A₁

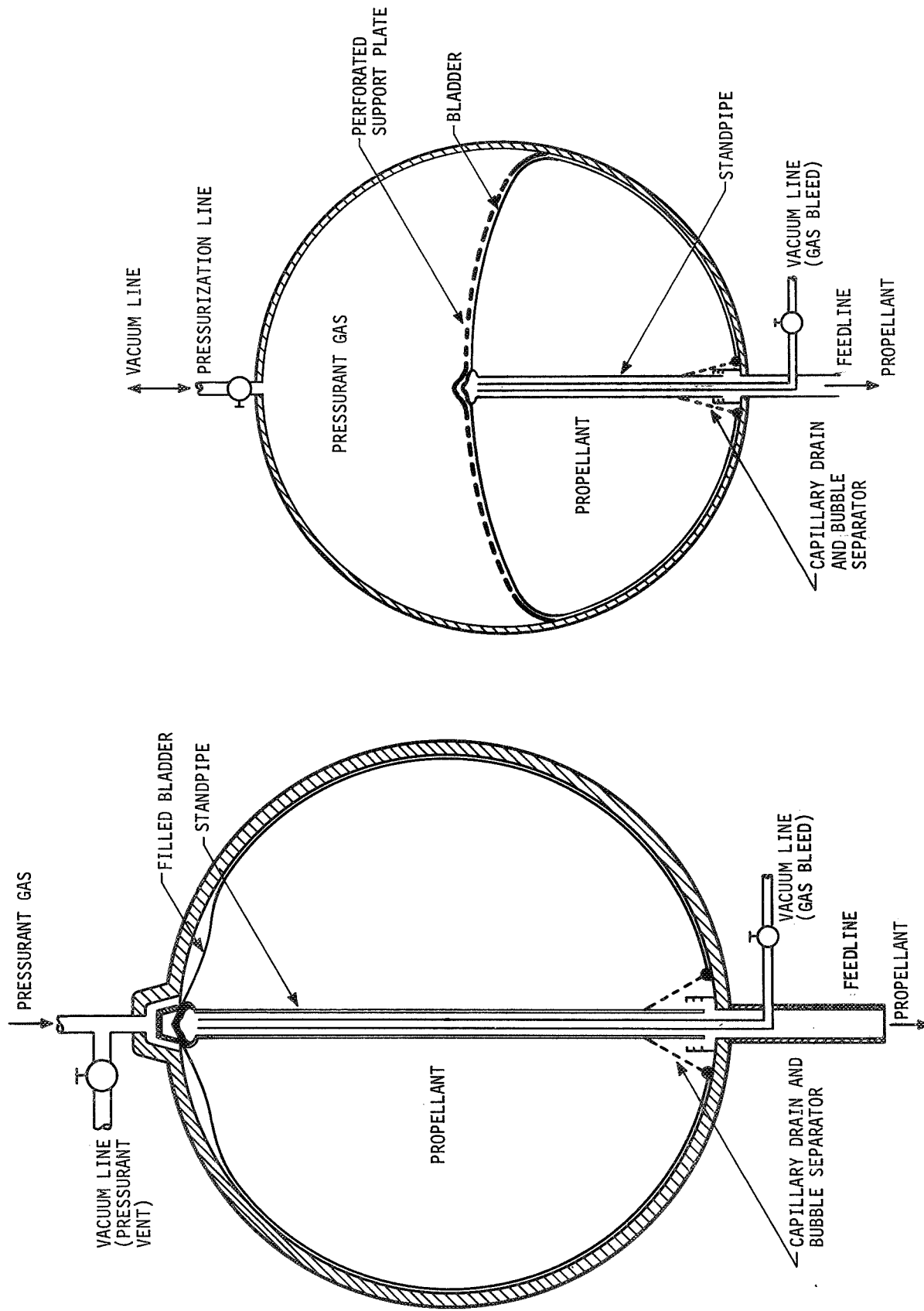
Filling an expanding bladder propellant tank can be most efficiently accomplished by vacuum loading. The pressurization standpipe and plumbing are evacuated to obtain maximum compactness for the folded bladder, followed by evacuation of the tank to enable propellant loading with negligible gas entrapment. If the tank will not support the compression stresses of a vacuum, a high-point overflow vent can be provided so that the tank can be fully loaded under internal pressure without trapping a gas bubble.

The standpipe supports the expanding bladder and acts as a distributing diffuser for the pressurization gas. The propellant drain is situated at the base of the standpipe and the overflow drain port (if necessary) is located at the top.

With a collapsing bladder, liquid expulsion is accomplished under the pressure of a gas introduced into the volume between the bladder and the tank wall. A collapsing bladder is currently preferred over an expanding bladder for the following reasons:

- 1) Internal pressurization (expanding bladder) tends to yield lower expulsion efficiency due to propellant that becomes trapped between the bladder and the tank wall;
- 2) At the fully loaded condition, the expanding bladder is tightly folded and creased while the collapsing bladder is filled with propellant. A flexural failure is more likely to occur with a folded bladder in the vibrational environment during booster operation, than with a loaded collapsing bladder;
- 3) More analytical knowledge and operational experience is available for externally pressurized bladders. As a result, the development costs for a collapsing polymeric bladder device should be lower.

For Missions A₂ and B, a pneumatically-actuated collapsing bladder system (Fig. III-3) was selected as the preferred design for the positive expulsion of earth storable propellants.

(a) Mission A₂ - Regulated Pressurant from External Storage

(b) Mission B - Blowdown Pressurization Integral with Propellant Tank

Figure III-3 Collapsing Polymeric Bladder System

Vacuum filling is the most desirable technique for loading propellant into collapsing polymeric bladders. The gas side of the bladder is evacuated to position the bladder smoothly against the tank wall. As the liquid side of the bladder is evacuated, there is no collapsing load to induce wrinkling and folding with the attendant high stresses that ultimately result in material failure. The propellant is "hard loaded" (tank completely filled) and then off-loaded to obtain the desired ullage volume and to expel any gas in the bubble trap. If the tank is incapable of sustaining the compressive loads under vacuum conditions, the bladder can be loaded against ullage pressure in the same way that most polymeric diaphragm systems are filled. In contrast to the diaphragm, which undergoes a minimum of contortion, the cycle life of a collapsing bladder will be compromised as it is squashed against the standpipe due to the vacuum on the liquid side prior to filling.

For the collapsing bladder, the standpipe provides a distributed drain and, when pressurant permeation is a problem, a gas phase separator. The standpipe can act as a support for the bladder, which helps to regulate the collapsing pattern during expulsion and prevents outlet blocking by the bladder.

The gas bleed line is used to evacuate the liquid side of the bladder so that the loading of single phase liquid propellant is possible. The liquid side of the bladder can be pressurized through the gas bleed line in the event of a ground abort so that the propellant can be drained without collapsing the bladder.

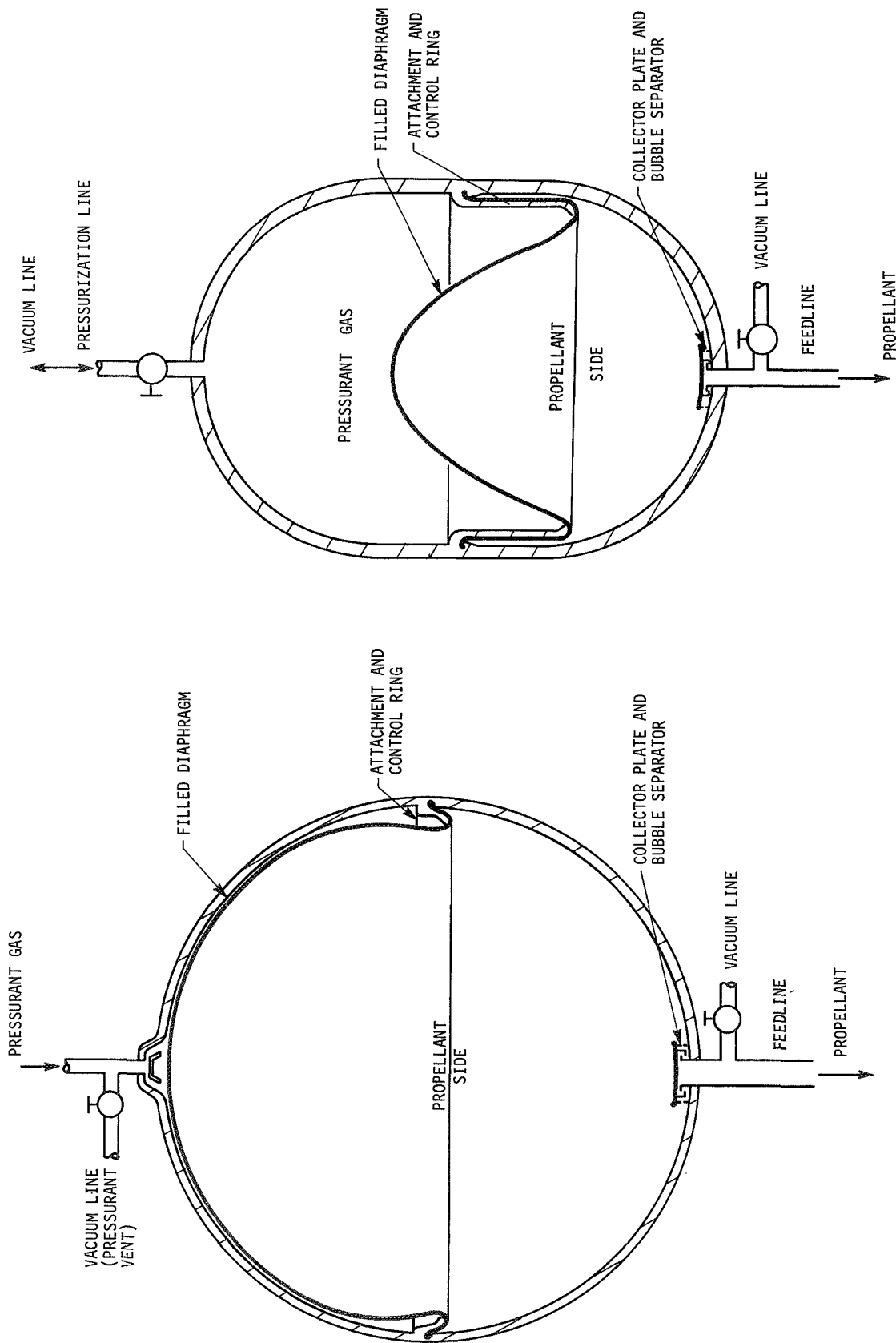
To prevent high pressure impingement on the bladder, the pressurant gas from external storage should enter the ullage volume through a throttling device.

b. Diaphragms - Polymeric diaphragms normally accomplish expulsion through a complete reversal of the barrier geometry, with translation produced by gas pressure in the ullage volume. A polymeric diaphragm undergoes less severe wrinkling and folding during expulsion with an attendant increase in cycle life of two to five times that of an equivalent bladder.

The diaphragm-to-tank attachment seal near the midplane of the tank complicates tank assembly and repair and may result in an excessively heavy design. Diaphragms for tanks with internal blowdown pressurization (e.g., Mission B) must withstand the most severe vibration and propellant slosh environments (occurring during launch) with relatively little support, as shown in Figure III-4(b). In this situation, the diaphragm can be easily contorted by motion of the bulk propellant. The excess material (diaphragm area to tank midplane area ratio) increases with tank length-to-diameter ratio. A diaphragm control ring is used for partial support in partly loaded tanks. Spherical tanks, which have small diaphragm area to midplane area ratios, may not need diaphragm support hardware if the polymeric material is sufficiently stiff. However, control rings become necessities as the L/D increases for cylindrical tanks.

Design alternatives have been proposed for controlling contortions in high L/D cylindrical tanks. Bathtub diaphragms and roll-and-peel diaphragms limit wrinkling and folding at partial propellant load conditions, and have the added advantage of being capable of undergoing a complete reversal. Bathtub (transverse) diaphragms are much heavier than conventional diaphragms, and only become attractive for an L/D where excessive control ring weights are incurred. Roll-and-peel diaphragms utilize an adhesive between the polymeric material and the tank wall to control diaphragm geometry at partial propellant load. Propellant compatibility with applicable adhesives is difficult to achieve, making roll-and-peel systems unattractive for long exposure applications.

Conventional polymeric diaphragm systems employing a diaphragm control ring to prevent excessive wrinkling in both cylindrical and spherical tanks, were selected as the preferred designs (Fig. III-4). The diaphragm control ring size and configuration depend upon the tank geometry and pressurization. Where external pressurant storage permits the use of a fully reversing diaphragm, as on Missions A₁ and A₂, the control ring is small. An integral blowdown pressurization system such as Mission B requires a larger control ring to stabilize the off-loaded diaphragm. The control ring size increases as the L/D of cylindrical tankage with blowdown pressurization is increased. However, the control ring on cylindrical tanks with external pressurant storage is constrained to small sizes to permit fully reversing diaphragm operation.



(a) Missions A_1 and A_2 - Regulated Pressurant from External Storage

(b) Mission B - Blowdown Pressurization Integral with Propellant Tank

Figure III-4 Polymeric Diaphragm System

Polymeric diaphragm systems for externally pressurized tanks can be vacuum-loaded like bladders without reversing the diaphragm. The ullage is evacuated to seat the diaphragm against the upper-half of the tank. Then the liquid side is evacuated and the propellant is loaded.

Loading against an ullage pressure is an alternative to vacuum loading reversing diaphragms and is the usual procedure for filling internal blowdown tankage. The ullage pressure holds the diaphragm in the expelled position, providing intimate contact between the tank wall and the polymeric material so that the potential bubble trapped on the liquid side is as small as possible. Normally, a vacuum is applied to the residual liquid side volume before the propellant is introduced. The filling of internal blowdown tanks must be carried out very carefully so that no significant pressure difference occurs across the restrained diaphragm which might strain or rupture the polymeric material.

c. Operational Characteristics - Polymeric bladders and diaphragms have the following advantages:

- 1) Recycle capability;
- 2) High expulsion efficiency;
- 3) Low actuation pressure differential;
- 4) Dynamical insensitivity to pressure level;
- 5) Adaptability to various tank shapes;
- 6) High volumetric efficiency;
- 7) Low system weight.

Disadvantages include:

- 1) Permeability to pressurant gas;
- 2) Permeability to propellant vapor;
- 3) Limited chemical and thermal compatibility.

A summary of polymeric bladder and diaphragm performance characteristics is given in Table III-3.

Table III-3 Polymeric Bladder and Diaphragm Evaluation Summary

DESIGN CHARACTERISTICS	BLADDER	DIAPHRAGM
Performance characteristics		
Expulsion efficiency, %	98	99.5
Scalability	Poor	Fair
Cycle life, cycles to failure*	5 to 35	10 to 500
Reliability	Fair	Good
Tank geometry	Volumes of revolution	Symmetrical volumes of revolution
Volumetric efficiency, % [†]	99.8	99.9
Maximum practical size, in.	60	60
Pressure drop, psi	~3	~10
Tank operating pressure range	Low → High	Low → High
Inherent cg control	No	No
Series tankage capability	No	No
Operational characteristics		
Simplicity	Good	Good
Series of partial expulsions	Yes	Yes
Off-load propellant limitations	Off-load not desirable	Off-load not desirable
Slosh control	Poor damping	Fair damping
Shelf life (verified propellant exposure)	30 days to 2 years	30 days to 1 year
Mission life, days verified	30 to 300	30 to 100
Environmental capabilities		
Permeable	Metal barrier needed	Metal barrier needed
Sealability	Good	Fair
Radiation sensitive	Yes	Yes
Deep cryogenic propellant	Limited	Limited
Mild cryogenic propellant	Limited	Limited
Earth storable propellant	Yes	Yes

*The lower values shown for both bladders and diaphragms are representative of Teflon; the larger values represent a good elastomeric film.

[†]Without devices to ensure good expulsion efficiency, phase separation, or dynamic control of the polymeric bladder or diaphragm.

The structural design of an expulsion device employing a bladder or diaphragm does not present an opportunity for a detailed stress analysis and associated material selection. There is little basis for the selection of a material thickness to satisfy structural requirements beyond sufficient elongation and ductility to withstand folding, buckling, and wrinkling without tearing or rupturing. The stiffness of thick bladders or diaphragms results in lowered expulsion efficiency while thin bladders or diaphragms sacrifice flex life and permeation resistance. Recommended thickness for polytetrafluoroethylene/polyfluorinated ethylene propylene (TFE/FEP) laminates is about 10 mils, whereas typical thickness for a comparable elastomer might be 40 mils. Bell Aerospace Company (Ref III-5) points out that "Material and functional life limitations are unique to a specific material, operating temperature, propellant, and L/D geometry. For any specific application, limitations are minimized by selection of the optimum combinations of these parameters within envelope and other system considerations."

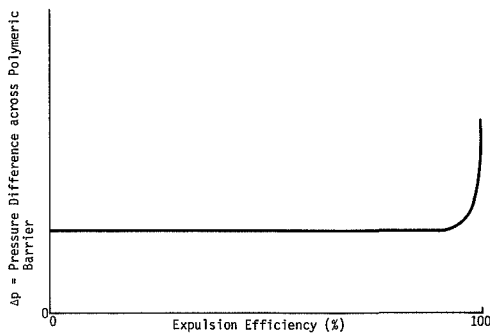


Figure III-5 Expulsion Characteristic of Polymeric Bladders and Diaphragms

Bell Aerospace Company, Dilectrix Corporation, and G. T. Schjeldahl Company (Ref III-5 thru III-7) claim expulsion efficiency of 99% for polymeric bladders. Both bladders and diaphragms exhibit the expulsion characteristic shown in Figure III-5.

The large increase in pressure difference required to force the last 2% of propellant out of the tank increases the risk of material failure. The expulsion geometry of diaphragms is more conducive to high expulsion efficiency than is the expulsion geometry of either expanding or collapsing

bladders. The expanding bladder has to empty about twice the terminal volume of a diaphragm. The collapsing bladder is contorted in folds and wrinkles that provide propellant pockets as contrasted with the smooth seating of the diaphragm against the tank wall. The gas phase separator may also trap additional propellant.

Polymeric bladders and diaphragms sustain very small pressure drops between the ullage side and the propellant side of the system during 95% of their operation. Consequently, the dynamics of expulsion are not significantly influenced by the tank pressure level.* The pressure difference between the ullage pressure and

*High ullage pressure does increase pressurant permeation by raising the gas concentration.

feedline pressure is the important propellant expulsion parameter. Tanks with polymeric bladders or diaphragms are capable of operation at low and high ullage pressures.

Oscillatory motion of the propellant, propellant pressure resulting from acceleration forces, and the process of liquid expulsion singly, or in combination, must not overstress or fatigue the bladder. The physical properties and fatigue resistance of bladders are heavily dependent upon the details of manufacturing techniques and material properties as well as the configuration and design. Bladders having negligible elasticity will not significantly influence the slosh mode. Bladders designed to act through membrane stresses (carry no bending moment), supplying negligible restraint in the dynamic system, have a relatively low weight compared with other positive expulsion systems. Bladders will generally exercise negligible elastic restraint on the liquid and will show little effect on the lower natural frequencies, although the flexing of severe bladder creases may contribute considerable damping. Concentric hoops on a diaphragm, similar to those of the Transtage monopropellant ACS, can prevent wrinkling that results in wear during sloshing (Ref III-8). Werkema (Ref III-3) contends that by proper design of a tank-bladder system, slosh can be minimized without seriously hampering bladder function or efficiency.

The polymeric materials of bladders and diaphragms should resist the corrosive action of the liquid propellant, and act as effective barriers against the loss of propellant and the permeation of pressurant. The materials from which bladders and diaphragms are made should be able to maintain their mechanical properties during the prolonged storage in contact with the propellant. There may be as much as a 30-day hold on the launch pad. The wind loads during the launch hold period can induce bladder or diaphragm fatigue and possible tear failure as a result of propellant slosh. This failure would be especially applicable to a bladder or diaphragm design with a free polymeric surface in the blowdown tankage for Mission B.* Both Missions A₁ and A₂ have a requirement for 270 days of operational status after launch; the estimated operational period for Mission B is 3272 days. During these long mission times, the polymeric materials must be able to withstand the force of pressurization (Missions A₁ and A₂) and must retain a high degree of flexibility and resistance to the creasing and folding that will occur during propellant sloshing at part load and during expulsion. For the cryogenics, OF₂ and B₂H₆, the bladder materials must retain these properties down to 210°R.

*No detrimental effect of liquid motion would be anticipated on a properly designed bladder or diaphragm that was supported by the tank wall when fully loaded with propellant.

A serious disadvantage of polymeric materials for long duration bladder and diaphragm applications is their permeability to pressurant gas and propellant vapors. The most severe problem of propellant vapor permeation has not been detrimental to small propulsion systems on short missions, but permeation may become a more serious problem for the longer missions and/or larger tanks. Propellant permeation to the ullage side of the bladder represents unusable propellant and exposes the pressurant system to the propellant vapor. Check valves are required in bipropellant systems to prevent intermixing of fuel and oxidizer vapors. Pressurant gas that permeates to the propellant side either dissolves in the liquid or exists as entrained free bubbles. These gas bubbles (free or from dissolved pressurant) can cause engine thrust perturbations or combustion instability.

Permeation is a rate process (Ref III-9), but the total quantity (equilibrium) of propellant that can be transported through the bladder or diaphragm is dependent on the ullage volume and not on the polymeric material. The expulsion device material only determines the permeation rate. Propellant vapor transport will continue until the partial pressure of the propellant vapor in the ullage is equal to the vapor pressure of the propellant. Similarly, the permeation of pressurant into the liquid side of the polymeric bladder or diaphragm will continue until the partial pressure of pressurant on the liquid side is the same as the partial pressure of that gas on the ullage side. Using conventional material to construct bladders or diaphragms for long duration missions will not prevent contamination of the propellant with pressurant because the permeability is great enough that an equilibrium pressurant bubble has sufficient time to form. An additional, redundant provision on the liquid side of the bladder or diaphragm, such as a capillary acquisition device acting as a vapor barrier over the outlet (Mariner '71 primary propulsion system design), would be required to ensure single-phase liquid expulsion.

The problem of permeation of the propellant and pressurant through a polymeric bladder was solved on the Lunar Orbiter velocity control system by the incorporation of a layer of aluminum foil to provide a bladder material of 2-mil TFE/1-mil FEP/ $\frac{1}{4}$ -mil Al foil/3-mil FEP (Ref III-10). Metal foils used in a thickness range of 0.0002 to 0.002 in. have a limited flex life with respect to pinholing due to cold working. The molding of metal foils into adherent conformance with spherical bladders or hemispherical diaphragms has been found difficult. Laminates of gold as well as aluminum and Teflon are troubled with nonuniformity of adherence

and formation of gas pockets (blisters). Chemical vapor deposited aluminum 0.0001- to 0.001-in. thick significantly reduced the N_2O_4 permeation of TFE Teflon while maintaining the basic structural properties of the Teflon (Ref III-11). A vapor deposited layer of aluminum 0.0003-in. thick reduced the permeation of N_2O_4 through a 10-mil sheet of TFE Teflon from 5 to 6 mg/in.²-hr to 0.1 mg/in.²-hr. Lead coatings of 0.0004 in. reduced N_2O_4 permeability to 0.2 to 0.02 mg/in.²-hr as compared with 13 to 20 mg/in.²-hr for the unclad Teflon film (Ref III-12). Gold foil (0.002-in. thick) lined carboxy-nitroso rubber (CNR) bladders suffered from delamination and fatigue cracking of the gold foil upon reexpansion after one expulsion cycle (Ref III-13 and III-14). The theoretically impermeable material had measured permeation rates of 0.16 to 4.6 mg N_2O_4 /in.²-hr and passed helium gas at 0.5 cc/15 min. The reduction in long term permeability accomplished to date has not been sufficient to justify the additional complexity and cost of metallized polymeric materials for application to the three reference missions.

The use of polymeric expulsion devices has been limited to small secondary propulsion systems with short storage requirements (<1 year). For applications involving longer storage periods and/or larger tanks, permeation may become a more serious problem. Particularly, the formation of larger gas bubbles (free or from dissolved pressurant) in the propellant, that can cause engine thrust perturbations or combustion instability as mentioned previously, must be prevented or controlled. Compatibility with propellant vapor and condensate and the propellant outage associated with the permeant must be considered in the ullage components and pressurant selection and the performance analysis. Nitrogen, helium, and solid propellant gas generators have been used successfully for expulsion pressurants.

2. System Evaluation

a. Reliability - The dynamics of vibration, wrinkling, and folding associated with ground and flight operations will induce stresses that can result in anomalous operation from pinhole leaks and possibly a catastrophic failure caused by tearing. Primary failure modes result from multiaxial tension forces. The rolling motion of buckled folds can precipitate mechanical fatigue and pinholing at the apex of double folds, and three-axis vibration has caused bladder tearing. If some degree of chemical incompatibility between propellant and bladder is present producing deterioration in the structural properties of the polymeric material or interlaminar blistering, aging can lead to a bladder failure under normally tolerable stresses.

Bladders have a higher element of risk than diaphragms in blowdown tankage. The unsupported surface area of a diaphragm will generally be smaller than that of a conventional bladder, even in the fully loaded condition. An alternative is to provide a perforated support cap for an asymmetrical bladder system. Diaphragms are more easily designed to cope with the free surface problem, but they still suffer from lack of local support by the tank wall. Nonsupport would also occur on Missions A₁ and A₂, since the tanks have an initial ullage of 10%.

Teflon FEP has experienced solvent stress cracking (analogous to stress corrosion in metals) under exposure to heptane, to alcohol to a lesser extent, or to freon only slightly. These cracks tend to propagate under operating stresses and eventually lead to premature failure of the polymeric material. The conditions of FEP stress, environmental pressure, and solvent exposure time required to produce stress cracking have not been established. However, the Mariner '71 Teflon bladder suffered solvent stress cracking as the result of vibration testing at operating tank pressure with isopropyl alcohol used as a referee propellant. The current opinion is that the critical conditions for cracking in the FEP are not met during normal cleaning operations. The greatest risk is encountered during system qualification and/or acceptance testing.

The only catastrophic failure of a bladder or diaphragm would be a tear that results in the major loss of propellant control and expulsion capability in a low-g environment. The single anomalous failure mode for bladders and diaphragms is from pin-hole leaks that permit excessive entry of ullage gas into the propellant volume and allow unplanned propellant loss to the ullage, reducing the total impulse available and increasing outage.

b. Mass - The bladder system mass estimates were based upon 10-mil thick Teflon bladders and standpipe designs similar to those employed on Mariner '71. Generally, a laminated construction of 5-mil polytetrafluoroethylene (TFE) next to the propellant for strength and chemical compatibility, and 5-mil polyfluorinated ethylene propylene (FEP) on the ullage side for permeation reduction and improved flexibility is employed. Dilectrix (Ref III-6) indicated that Teflon use on Mission A₁ is precluded because of the change in physical properties at cryogenic temperatures; in particular, the change in modulus that would render the Teflon inoperable in any type of folding and or creasing mode. Although

material compatibility problems exist for Mission A₁ propellants, Teflon density (0.08 lb_m/in.³) appears to be representative of the polymeric materials under development for fluorine oxidizers, and conservative for the polymeric materials under development for diborane. The structural properties of these developmental materials for use with OF₂ have not been characterized to the point where design criteria can be predicted. Multi-ply, thin-film bladder construction would probably be used with the cryogenic propellants of Mission A₁. Bell and Dilectrix (Ref III-5 and III-6) agree that Teflon would be satisfactory for Mission A₂, and probably for Mission B, because there do not appear to be detrimental aging effects on Teflon polymers in the earth storable propellants (N₂O₄, MMH, and hydrazine). However, Dilectrix recommends "a codispersion film comprising TFE and at least 20% FEP Product Code TE-9511 (high molecular weight) would be preferable for Mission A₂, and quite possibly for Mission B."

The diaphragm system mass estimates were based on 30-mil thick TFE/FEP Teflon for Missions A₁ and A₂, and 60-mil thick ethylene propylene terpolymer (EPT) or ethylene propylene rubber (EPR) for Mission B. The diaphragm system design for Missions A₁ and A₂ employed a completely reversing diaphragm. The Mission B system is similar to the N₂H₄ monopropellant ACS for Transtage.

The permeability of polymeric materials is so great that the ullage volume will be saturated with propellant vapor during the missions. Equilibrium concentrations of propellant vapor in the ullage will be reached within a few days. Metallized polymeric materials have been investigated for zero permeability systems, but the metal foils suffer from pinholing upon folding, and delamination from the polymeric material. Consequently, the permeation rate is still high enough to reach steady-state during these long-duration missions. Since the permeation transient is only slightly extended, metallized polymeric materials were not considered because of the additional weight and complexity.

Another problem associated with the polymeric film permeability is propellant saturation with pressurant gas and the formation of pressurant bubbles on the liquid side of the device. Helium permeation through polymeric films is so high that equilibrium is achieved in approximately one-half day. Nitrogen permeation is slower, on the order of the propellant vapor, with equilibrium occurring in a few days. Although the bladder or diaphragm provides efficient positive expulsion, a secondary and possibly

redundant system is required to separate the liquid and gas phases in the absence of a zero permeability polymeric material. A capillary screen device was employed for this function in the bladder standpipe and in the diaphragm collector plate shown in Figures III-2 thru III-4. The expulsion efficiency anticipated for the bladder system is 98% or more. The diaphragm for the spherical system should have an expulsion efficiency of 99.5%. The expulsion efficiency for the diaphragm in the cylindrical tanks may be degraded to about 99% by the less favorable geometry.

The mass estimates for both polymeric bladder and polymeric diaphragm expulsion systems considered for Missions A₁, A₂, and B are presented in Table III-4.

c. Design Scalability and Producibility

1) Design Scalability - The details of design, fabrication, attachment, and installation are primarily empirical and must rely on development testing. Consequently, a change in system size can require extensive redesign of the bladder or diaphragm expulsion system. New designs of comparable size can be developed from similar qualified systems, but design verification is needed.

2) Manufacturability - The ability to fabricate a bladder or diaphragm system is interdependent with the application. The character of the polymeric material is the principal consideration. Some materials can be molded (EPR); others are layed up on rotating mandrels by spraying (Teflon) or brushing (CNR); some materials require special or unique processes that must be developed to meet the particular needs of that design. In any event, manufacturing experience has been limited to maximum dimensions on the order of 60 in., which encompasses the technology requirements for Missions A₁, A₂, and B.

The leakage limits are critical to bladder or diaphragm system design and manufacture. Long duration missions should utilize all-welded tank construction to provide an absolute seal. Experience shows that an access port whose diameter is about one-fourth the tank diameter is required for installation of the bladder system into the tank. Such large ports are difficult to seal mechanically. The gas side of the propellant tank must be welded to the liquid side of the tank after the polymeric diaphragm has been installed. Welding of such systems has been accomplished with electron beam equipment.

Table III-4 Device Weights for Polymeric Bladders and Diaphragms*

Material Mission No. of Tanks	6Al ₄ -4V Titanium				2024 (T3) A ₂				304L Stainless Steel					
	A ₁		A ₂		B	A ₁		A ₂		B	A ₁		A ₂	
	2	4	2	4	1	2	4	2	4	1	2	4	2	4
Polymeric bladders														
Spherical expulsion hardware†	18.0	26.6	19.0	28.6	6.5	28.2	42.6	29.4	45.6	10.6	49.2	76.0	51.2	81.0
Trapped propellant	7.7	7.7	2.0	2.0	0	7.7	7.7	2.0	2.0	0	7.7	7.7	2.0	2.0
Outage	21.8	21.8	30.0	30.0	2.6	21.8	21.8	30.0	30.0	2.6	21.8	21.8	30.0	30.0
Spherical device mass	47.5	56.1	51.0	60.6	9.1	57.7	72.1	61.4	77.6	13.2	78.7	105.5	83.2	113.0
Cylindrical expulsion hardware†	18.4	27.8	19.4	29.6	6.5	29.0	44.6	30.0	47.0	10.7	50.2	79.2	52.2	83.0
Trapped propellant	7.7	7.7	2.0	2.0	0	7.7	7.7	2.0	2.0	0	7.7	7.7	2.0	2.0
Outage	21.8	21.8	30.0	30.0	2.6	21.8	21.8	30.0	30.0	2.6	21.8	21.8	30.0	30.0
Cylindrical device mass	47.9	57.3	51.4	61.6	9.1	58.5	74.1	62.0	79.0	13.3	79.7	108.7	84.2	115.0
Polymeric diaphragms														
Spherical expulsion hardware†	22.0	30.8	23.0	32.8	6.9	31.0	45.0	32.4	47.6	10.2	49.8	74.6	51.8	78.2
Trapped propellant	7.7	7.7	2.0	2.0	0	7.7	7.7	2.0	2.0	0	7.7	7.7	2.0	2.0
Outage	5.5	5.5	7.5	7.5	0.6	5.5	5.5	7.5	7.5	0.6	5.5	5.5	7.5	7.5
Spherical device mass	35.2	44.0	32.5	42.3	7.5	44.2	58.2	41.9	57.1	10.8	63.0	87.8	61.3	87.7
Cylindrical expulsion hardware†	21.2	29.4	22.6	30.6	6.6	30.2	42.2	31.6	43.4	9.5	49.0	68.6	50.4	69.8
Trapped propellant	7.7	7.7	2.0	2.0	0	7.7	7.7	2.0	2.0	0	7.7	7.7	2.0	2.0
Outage	10.9	10.9	15.0	15.0	1.3	10.9	10.9	15.0	15.0	1.3	10.9	10.9	15.0	15.0
Cylindrical device mass	39.8	48.0	39.6	47.6	7.9	48.8	60.8	48.6	60.4	10.8	67.6	87.2	67.4	86.8
*All figures presented are lb _m .														
†Includes mass of capillary screen device.														

Bladders should be fabricated smaller than the tank to avoid tears and pinholes due to wrinkling. However, shrinkage during curing must be controlled so that the bladder is large enough to seat against the tank wall without exceeding the elastic limit of the polymeric material. If yielding should occur, it is normally a local rather than uniform phenomenon which generates stresses that can lead to catastrophic failure.

A constantly recurring fabrication problem with multiple layer polymeric films is delamination. This is usually a local problem that results in blisters on the material. In general, these areas grow with continued loss of adhesion resulting in degraded mechanical properties of the polymeric laminate.

Teflon bladder fabrication for MMH and N_2O_4 bipropellant systems and EPR or EPT diaphragm molding for use with nitrated hydrazine are state-of-the-art processes. However, none of the materials for potential use with OF_2 has been formed or tested as a bladder or diaphragm. Many of these materials have not even been characterized. Those polymerics whose physical properties have been studied show characteristics that would make conventional manufacturing questionable, and it is problematical if satisfactory producibility could be achieved in the 1975 time period. Some polymeric hydrocarbons potentially useful with B_2H_6 , such as Mylar, polyethylene, and polycarbonate, show slight promise when multi-ply materials for diaphragm or expanding bladder designs are employed. Fabrication experience is available for the multi-ply construction with these polymeric hydrocarbons.

3) Subscale Test Scalability - Scalability for bladder or diaphragm testing is not required. Full scale system testing is possible and required for polymeric bladders and diaphragms. Structural testing, development testing, and qualification testing of polymeric bladders or diaphragms must be done full scale because of the expulsion action and inherent difficulty with scalability. Propellant compatibility and permeability tests can be performed on material samples. Table III-5 lists some tests required for polymeric bladder or diaphragm systems.

Table III-5 Polymeric Bladder/Diaphragm Testing

TEST ITEM	FULL SCALE	TEST DESCRIPTION
Material	No	Propellant decomposition Propellant permeability Pressurant permeability Polymeric material compatibility: Specific gravity Flexural modulus Ultimate tensile and elongation Compression set Hardness Tear strength Volume swell and linear shrinkage Blistering and delamination.
Functional evaluation	Yes	Leakage Cycle life Slosh Internal/external loads Temperature cycling Expulsion efficiency Expulsion kinematics: Polymeric material folding Liquid/gas phase separation

d. Compatibility with Adjacent Components and Propellants

1) Propellant/Material Compatibility - Material compatibility becomes a formidable problem for polymeric materials because of the known chemical activity between the propellants and the polymeric materials. However, the chemical kinetics are not known well enough so that rate processes can be predicted.

Chemical and thermal compatibility between the propellants and the polymeric materials are problems for Mission A₁. Chemically inert polymeric films having high flex life at cryogenic temperatures are not available for Mission A₁. Polymeric materials suitable for use in the presence of OF₂ (NBP 230°R) and B₂H₆ (NBP 325°R) are the subjects of current research (Ref III-15, III-16, III-12). Polymeric bladder and diaphragm designs for cryogenic applications employ the multi-ply material that retards pinholing by constraining the film to larger and smoother bends. The multiple layers of material (usually unbonded) function analogously to a labyrinth seal in controlling leakage between the gas side and the liquid side of the tank through the unavoidable pinholes. These leaks constitute an anomalous failure that might reach severe proportions during a long duration mission.

Only polyfluorocarbons can be considered for use with OF_2 because the hazards of fire and explosion exist with polymeric hydrocarbons in contact with OF_2 (Ref III-17). It is possible for OF_2 and fluorocarbons such as Teflon to react violently, although the initiation of these reactions is difficult (Ref III-12). HFB-2 (hexafluorobutylene-2) and perfluoro mono- and diisocyanates, in the synthesis stage, are materials with potential application (Ref III-15). Polyperfluorobutadiene is a chemically inert elastomeric polymer with predicted mechanical properties superior to Teflon (Ref III-16). However, bladder/diaphragm design data are not yet available for these new materials. Some polymeric hydrocarbons, such as polyesters (duPont Mylar), polyethylene (Union Carbide Zedel), and polycarbonate (GE 2346-63), are chemically compatible with B_2H_6 (Ref III-12). Teflon is another possible material.

It has been found that none of the polymeric materials selected for testing with either oxygen difluoride or diborane had a flex resistance of more than a few cycles at temperatures below 380°R in an inert Freon liquid. In tests with OF_2 , an FEP Teflon underwent about 8 cycles to failure. Mylar survived 5 to 7 cycles before failure in B_2H_6 (Ref III-12).

The best contemporary polymeric materials for bladders or diaphragms for use with oxygen difluoride and diborane are FEP Teflon and Mylar, respectively. However, the chemical and/or structural characteristics of both of these materials are considered unsatisfactory for the low temperature application of Mission A₁. There is no positive indication that adequate polymeric films will be found for OF_2 and B_2H_6 bladder or diaphragm expulsion systems.

There are several polymeric materials that are sufficiently inert for Mission A₂. Polyethylene and Teflon are candidates for MMH and Teflon is a good material for N_2O_4 . Poly (cyclized 1, 2-polybutadiene) tolyl urethane (CPBU) elastomeric composites may develop into superior bladder/diaphragm material for use with N_2O_4 within the development period 1975. CNR (carboxy-nitroso rubber) is an elastomeric material highly resistant to N_2O_4 , but it exhibits vapor permeability 80 times greater than Teflon. North American, Rocketdyne, has exposed Teflon bladders to N_2O_4 and MMH for one year and then expelled 99% of the propellants at 350 psig without incurring a bladder leak. There was no apparent degradation in the bladder seal and only 5 to 7% reduction in tensile strength. The selection of Teflon for Mission A₂ would provide valuable hardware interchangeability.

No experimental verification exists for polymeric material/propellant compatibility for Mission B application considering both the propellant and the 10-yr duration. Since nitrated hydrazine (75/25 $\text{N}_2\text{H}_4/\text{N}_2\text{H}_5\text{NO}_3$) is homologous with hydrazine (N_2H_4), an adequately stable polymeric material might be found for this application. Improvements in Teflon are being made, making it a leading prospect for Mission B. Ethylene propylene copolymers (EPR) and terpolymers (EPT) are chemically compatible elastomers in wide use with hydrazine. EPR and EPT suffer little structural degradation and produce only slight hydrazine dissociation when carbon black fillers are avoided. However, the rate of decomposition of nitrated hydrazine would probably be greater than that for hydrazine. Experimental assessment of the effects of long-term exposure of polymeric materials to nitrated hydrazine is a prerequisite for serious consideration of these materials for Mission B.

In summary, there are no polymeric materials suitable for use in bladders or diaphragms on either Missions A₁ or B at the present time. The best bladder and diaphragm materials for Mission A₂ are polyethylene or Teflon for MMH and Teflon for N_2O_4 .

2) Pressurization System Compatibility - All polymeric materials are permeable to helium or nitrogen pressurant gas. Attempts to provide zero-permeability bladders with metallic foil coatings show little promise of success for long duration missions. Consequently, there will be a problem of pressurant dissolution in the propellant. Gas saturation and subsequent formation of a pressurant bubble within the polymeric bladder can be expected. As a result, a liquid/gas phase separator is required in the outlet system.

3) Tankage Compatibility - Polymeric bladders and diaphragms can be successfully employed in almost any volume of revolution. Experience with spherical and cylindrical tankage is profuse. Spherical bladders may not perform as well as cylindrical bladders because of the larger girth dimension and continuous curvature that increase the wrinkling and folding during collapse.

The cross-sectional area to wall surface area ratio is the critical design parameter for diaphragm geometry. High values of this area ratio result in less diaphragm contortion during translation. Therefore, spherical tanks are a more desirable configuration for diaphragms than high L/D cylindrical tanks, that may require auxiliary tank and diaphragm structure or even novel designs such as roll-and-peel, or bathtub diaphragms. Tank size is presently a more significant limitation than tank shape on polymeric bladder or diaphragm applications. The maximum linear dimension to which polymeric bladders and diaphragms have been fabricated is on the order of five feet.

4) Performance - Bladders and diaphragms are not inherently limited by burn time variations, number of engine restarts, or acceleration variations. However, secondary effects of off-loading, which permits mechanical working of the polymeric material due to vibration, slosh, or off-axis acceleration, do contribute to deterioration of structural integrity.

e. Performance Testability

1) Verification of Operational Readiness - Acceptance testing of bladders and diaphragms can be performed by leak checking, vibration testing, and expulsion testing. Since bladders and diaphragms are not passive expulsion systems, the polymeric material is degraded with each exercise, increasing the potential of failure on the next expulsion in spite of acceptable performance during the test. Consequently, vibration and expulsion testing for bladder or diaphragm acceptance are not recommended.

Leak checking bladders and diaphragms can be difficult because of polymeric material permeability and trapping of gas pockets in folds or between the device and tank hardware. If the expulsion system is leak-tested with a gas pressurant, it is hard to distinguish the bubbles expelled due to general permeation (normal) from bubbles resulting from pinholes or tears (abnormal). The polymeric materials tend to squirm during collapse or seating against the tank wall. Periodically, trapped gas that may appear to be a leak is released. The Teflon bladders used on the bipropellant ACS and the EPR-132 diaphragms used on the monopropellant ACS for Transtage had significant leak checking problems attributable to these phenomena.* In contrast, the Teflon bladders for

*Transtage monopropellant ACS diaphragms were pressurized hydraulically (with liquid pressurant on the ullage side and gaseous nitrogen on the propellant side). Gas trapped in the wrinkles and folds of the diaphragm continued to discharge bubbles for several hours as the polymeric material continued to squirm after the diaphragm had been seated against the tank wall.

the primary propulsion system on Mariner '71 have not encountered the problem.* The polymeric material permeability and slow squirming action represent generic disadvantages to leak-checking bladders and diaphragms.

2) Development Status - Many bladder systems similar to a Mission A₂ system have been developed, qualification tested, and flown. The Apollo Lunar Module, Command Module and Service Module, the S-IVB Auxiliary Propulsion System, and Lunar Orbiter are prime examples. The Mariner '71 propulsion tankage is currently under development for a mission similar to Mission A₂. There has been no bladder or diaphragm development test experience with the nitrated hydrazine. The Mission B duration, which is an order of magnitude greater than any current experience, is the biggest risk factor and polymeric materials are not considered attractive at the present time. Full-scale geometry testing of any polymeric bladder or diaphragm designs for Mission A₂ can and should be performed if they are selected for use.

The test experience with polymeric materials for use with OF₂ or B₂H₆ cryogenic propellants has shown numerous compatibility and structural problem areas. At this time, the use of polymeric bladders or diaphragms cannot be recommended for Mission A₁. The product level development of polymeric films capable of chemical compatibility with the Mission A₁ propellants, while satisfying the structural integrity and performance requirements imposed by the cryogenic environment, are not envisioned within the 1975 time period (Ref III-5 and III-7).

Dilectrix (Ref III-6) indicated several state-of-the-art advances that may be anticipated for the 1975 time period. Increasing molecular weight of the raw polymer significantly increases flex fatigue life of the Teflon film structures. At least an order of magnitude increase in flex fatigue life in Teflon film composites fabricated from a high molecular weight FEP dispersion was measured in rolling fold crease tests at 12°F. Further improvements may be gained by optimizing the molecular weight of the TFE faction. Additional advances in the physical integrity of polymeric films may involve the incorporation of compatible fibrils within the film structure.

*The Transtage bipropellant ACS bladders were constructed of unbonded plies of Teflon, sealed at the neck only. Helium permeating the outer plies formed gas pockets trapped between the plies. The gas would then appear later on the propellant side after permeating the inner plies. Mariner '71 uses all-bonded bladders with no space between plies which appears to have aided leak checking.

C. METALLIC BLADDERS AND DIAPHRAGMS

The operational principle for these expulsion devices is similar to the polymeric bladders and diaphragms, as discussed in Section B. Liquid expulsion is achieved by collapsing or expanding a thin metal barrier located within the propellant tank. Metallic bladders developed to date, completely enclose the propellant and collapse under a positive differential pressure applied across the thin barrier during expulsion. Metallic diaphragm systems do not completely enclose the propellant and allow propellant contact with the tank. Diaphragms are available in at least two basic barrier designs: a preformed, metal sheet which unfolds into the propellant side; and a preformed, metal envelope which conforms to one-half of the storage tank and reverses itself during expulsion.

The metal barrier eliminates the permeation problems posed by the polymeric bladders and diaphragms and ensures more positive control (constrains movement) of the propellant. As with the polymeric devices, a physical barrier separates the ullage and propellant, which eliminates any intimate contact problems, e.g., pressurant solubility. On the other hand, the metallic diaphragms and bladders are much more sensitive to flexing, which work hardens the metal and tends to produce pinholes and cracks. As mentioned, the metal barrier affords a better constraint on liquid movement than does a polymeric device, but flexing will result under cyclic, unsymmetrical, and impulsive forces. Thermal cycling is also a critical consideration since it causes flexing of the metal due to expansion and contraction of the propellant.

The majority of the development work to date on these metallic barrier systems has not been aimed at planetary missions but, rather, at tactical weapons systems. The latter usually require a single, complete expulsion. The planetary missions considered in this program have a multiple partial-expulsion requirement with expulsions separated by days and even years. For Mission B, the diaphragm or bladder would be almost fully-expanded or collapsed for a low-g period of 912 days prior to the final engine burn (Table II-1). As a result, flexing of the metallic barrier is of much greater concern with the planetary missions.

Various techniques are used with tactical weapons systems to eliminate (or at least minimize) flexing prior to propellant expulsion. One method is to evacuate the pressurant side of the bladder or diaphragm. The resulting pressure differential (vapor

pressure on the propellant side and vacuum on the pressurant side) minimizes flexing by holding the metal membrane against the tank wall. The planetary missions, however, require that the propellant tanks be pressurized prior to launch, which precludes the use of such techniques. In fact, Mission B uses blowdown pressurization and the propellant occupies only half of the tank volume at launch.

1. System Description and Operation

Five different metallic bladder and diaphragm systems developed or under development are briefly described in the following paragraphs.

a. Ring-Reinforced Diaphragms - The ring-reinforced diaphragm (RRD) design, patented by Arde, Inc., consists of a thin, stain-

less steel shell stiffened by rings attached to the shell surface (usually by brazing) in planes parallel to the equatorial plane of the diaphragm (Fig. III-6). At completion of expulsion, the diaphragm is a mirror image of its initial shape. During expulsion, the rings roll with the shell to stabilize and control the rolling of the diaphragm and prevent collapsing (buckling) of the thin metal barrier. The controlled roll affords a recycling capability. The limiting factor on cycle life* is the amount of strain and work hardening imparted to the diaphragm shell. Arde is attempting to reduce this and improve cycle life performance (Ref III-60 and III-61). The initial approach used a hemispherical diaphragm shell with reinforcing rings (Fig. III-7, design a). Up to three reversals

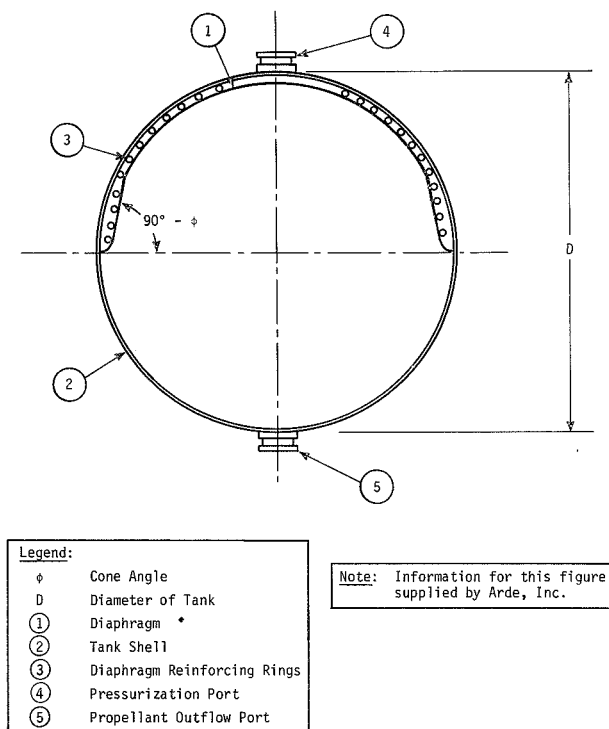


Figure III-6 Ring-Reinforced Diaphragm, Spherical Tank Assembly

*One cycle is two complete reversals.

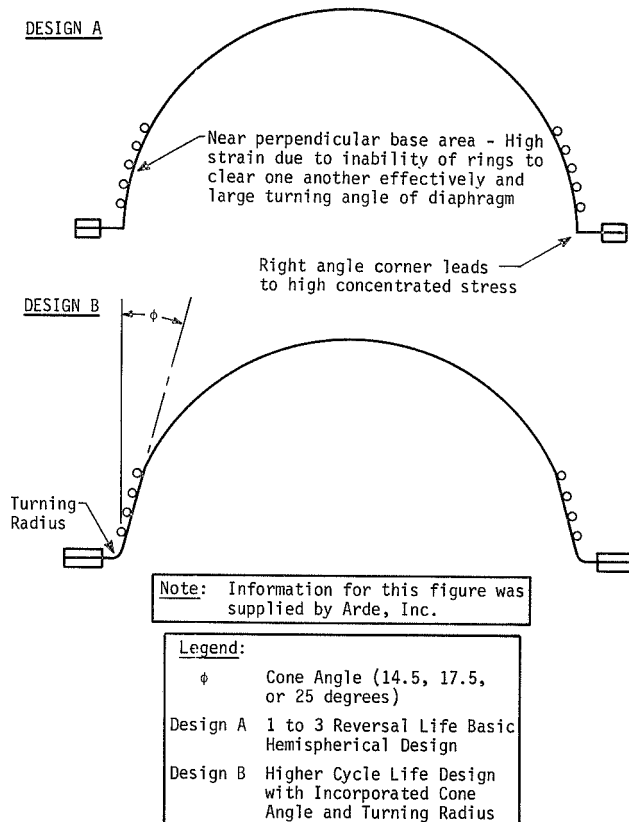


Figure III-7 Design Changes to Provide Higher Cycle Life

were achieved. The hemispherical diaphragm attachment to the tank was nearly perpendicular, as shown. The shell was modified in the next development step to incorporate a cone angle (ϕ) at its base and a turning radius at the attachment point (Fig. III-7, design b). Inclusion of the cone angle converts the hemisphere to a conospheroid which reduces strain hardening since ring clearance is increased and the turning angle at the base of the diaphragm is reduced. Arde presently supplies diaphragms (L/D of unity) with cone angles of 14.5 and 17.5 degrees (Ref III-61). Three to five reversals have been achieved with the 14.5-degree cone angle design, while five to seven reversals have been demonstrated with the 17.5-degree design using water, hydrazine, and liquid hydrogen as the test fluids. A 25-degree design is being developed to demonstrate 20 reversals (10 cycles), Ref III-60.

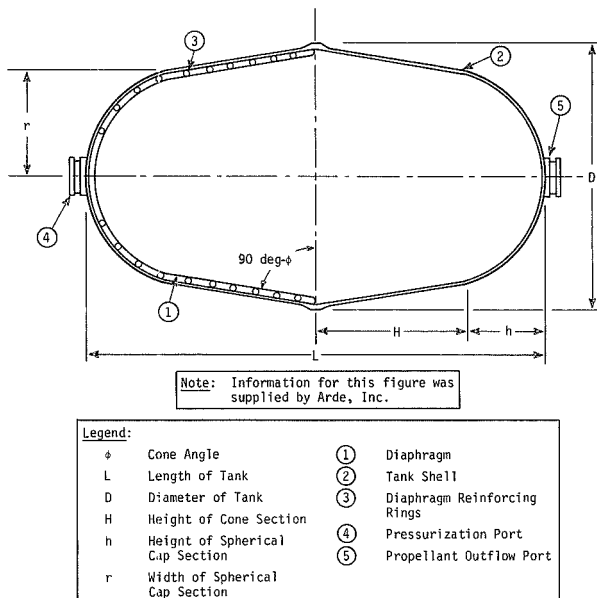


Figure III-8 Ring-Reinforced Diaphragm, Conospheroid Tank Assembly

Arde has developed diaphragms for application to conospheroid tanks* using a cone angle of 10 degrees (Fig. III-8). The 10-degree angle is the lowest practical size to obtain at least one reversal when $L/D > 1$ (Ref III-60). As with the $L/D = 1$ designs, an increase in cone angle increases cycle life but presents possible penalties in

*A conospheroid tank is used rather than a cylindrical tank to yield a greater volumetric efficiency.

volumetric efficiency and packaging geometry (the greater the cone angle, the more the conospheroid tank deviates from a cylinder).

For the 14.5- and 17.5-degree spherical and the 10-degree conospheroid designs, the maximum expulsion efficiency without plastically deforming the diaphragm is 95 to 96% (Ref III-60). It is possible to obtain a greater efficiency (to 99.5%) by plastically deforming the diaphragm. A pressure differential on the order of 200 psi is required (Ref III-62) for such deformation compared to an actuation pressure differential on the order of 10 psi without deformation.

The RRD system design can satisfactorily accommodate some flexing of the thin metal barrier. Since for this study the tanks are to be pressurized prior to launch (with no ullage on the liquid side), the diaphragm will be subjected to flexing corresponding to shifts in propellant volume for the entire mission, including prelaunch. Partial reversal test data show that for 1% volume change* the RRDs have undergone 5800 cycles before the appearance of pinholes (Ref III-61); however, for 30% volume changes, pinholes appeared after only 16 cycles (Ref III-60). The drastic change in cycle life is due to the fact that for a 1% volume change the reinforcing rings do not reverse upon themselves and the unsupported diaphragm area is only subjected to an 'oil canning' effect. Oil canning is independent of how far the expulsion process has proceeded, i.e., the number of rings reversed and the propellant remaining. For example, even if there were only 3% of the propellant left, the 1% volume cycling capability is still available. As evidenced by these data, the severity of thermal cycling with the ring-reinforced diaphragms is dependent upon both the magnitude and frequency of the temperature shifts during the missions. The temperature shifts corresponding to the 1% volume change are approximately 5°R for Mission A₁, 10°R for Mission A₂, and 23°R for Mission B. The slosh loads that may be encountered during the various missions appear to be a lesser problem than the thermal cycling. The elastic limit of the stainless steel diaphragm (Ref III-60) can support a relatively large strain. Test data for an 18-in. diaphragm that underwent sloshing in both the yaw and pitch axes (linear motion of ±1.5 in. at 3.75 cps) during outflow show no measurable degradation in the expulsion performance, i.e., the expulsion efficiency and number of reversals attained were identical to a diaphragm not subjected to slosh (Ref III-61).

*Based upon the total volume (capacity) of the diaphragm system.

b. Convolut Spherical Diaphragm - A convoluted spherical diaphragm (CSD) is composed of a series of circular convolutions formed from thin aluminum sheet. The diaphragm is positioned in the equatorial plane of a spherical tank and expands during expulsion to conform to one-half of the tank. Therefore, two diaphragms are needed per tank if the entire propellant tank volume is to be expelled (Missions A₁ and A₂); this requires two propellant outlets.

The CSD operates as a tensile strain-free membrane. Bell Aerosystems Company reports that by designing the convolution, as shown in Figure III-9, no membrane strain is introduced during expansion (Ref III-63). The node of each convolution tends to move in a straight line during expansion (Ref III-10) with the only strain resulting from bending. Diaphragm configurations that experience little (or no) stretching, such as these, require a relatively low differential pressure (on the order of 2 psi) for expansion (Ref III-63). For a 2-psi differential pressure, an expulsion efficiency of 98% can be obtained. For greater expulsion efficiencies (99.5%, or more) a ΔP of 14 psi is needed to plastically deform the diaphragm (Ref III-63).

Note: This figure was supplied by Bell Aerosystems Company (Ref III-63)

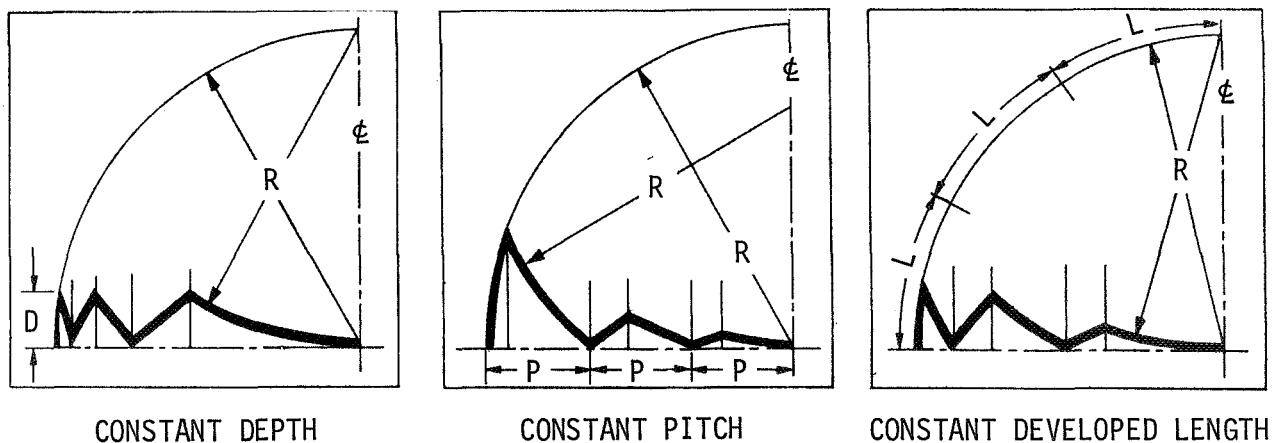


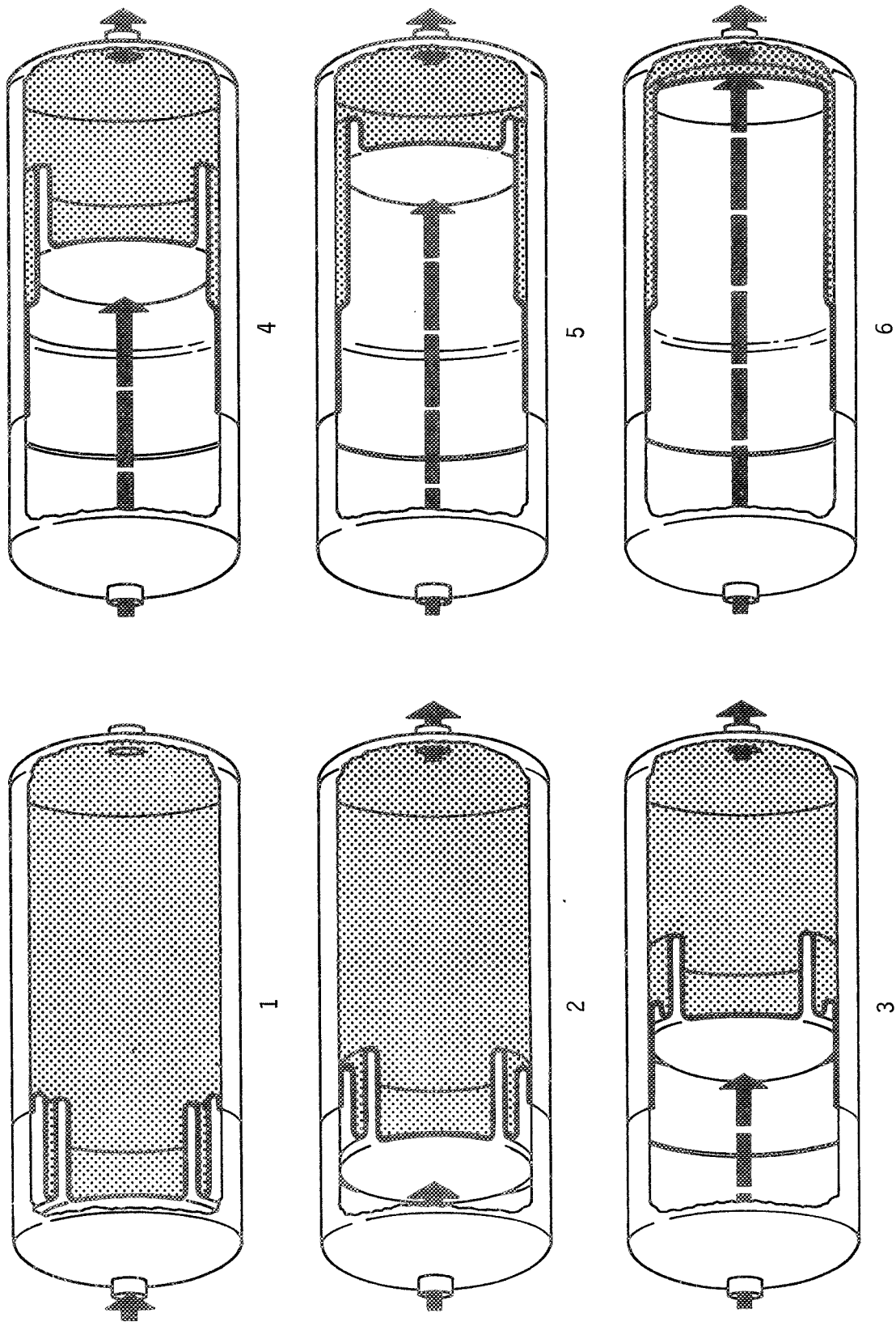
Figure III-9 Convoluted Diaphragm Design

The recommended operational procedure to reduce flexing prior to expulsion is to provide a vapor region on both liquid sides of the diaphragms with the pressurant side evacuated. This creates a pressure difference tending to hold the diaphragms against one another prohibiting diaphragm movement due to propellant thermal expansion, vibration, and slosh. However, this approach is not applicable to this study due to the pressurization and multiple burn requirements. A certain degree of thermal cycling can be satisfactorily tolerated with these devices (Ref III-63 and III-64). Also, the device is capable of partial expulsions encompassing volume shifts to as much as 20% of the maximum loadable propellant. As with the RRD designs, there is a tradeoff between the number of cycles and the magnitude of the volume shifts for these cycles. No data are available for the CSD under vibration and slosh under a pressurized condition.

c. Telephragm - The Bell Telephragm is a telescoping, rolling aluminum diaphragm limited to cylindrical tankage. During forming, the cylindrical barrier is telescoped into concentric cylinders, each with its predetermined roll radius. The Telephragm operates on the same principle as a rolling diaphragm -- the rolling of a thin-wall, ductile tube over a developed roll radius (Ref III-65). This will occur under a constant axial force (critical rolling load). The magnitude of the force is a function of tube diameter, wall thickness, rolling radius, and material properties.

Liquid expulsion, as provided by the Telephragm, is illustrated in Figure III-10. Expulsion begins with the rolling of the outer-convolution around its roll radius. A differential pressure on the order of 15 psi is required for operation; this ΔP will provide an expulsion efficiency of about 91% (Ref III-66). The remainder of the expulsion is performed by plastically expanding the unfolded Telephragm convolutes against the tank wall and aft bulkhead. Expulsion efficiencies to 98.5% can be obtained (Ref III-65) but only with differential pressures of 200 psi or more (Ref III-66). A reversing end-dome can be incorporated in the diaphragm to improve the volumetric efficiency. Volumetric efficiencies to 94% are attainable (Ref III-65).

As with the CSD design, the preferred operational procedure is to avoid diaphragm movement prior to expulsion by providing a vapor ullage on the liquid side of the diaphragm while evacuating the pressurant side (Ref III-65). The pressure difference will tend to hold the Telephragm firmly against the tank wall until the point of pressurization and expulsion. However, as discussed earlier, the propellant tanks for this study will be pressurized prior to launch. The Telephragm, as opposed to the RRD and CSD can tolerate little, or no, flexing of the diaphragm due to thermal expansion, slosh, and vibration or metal fatigue will result (Ref III-65). As a result, the Telephragm is not recommended for the planetary missions under consideration.



Note: This figure was supplied
by Bell Aerosystems Company.

Figure III-10 Telegraph Expulsion Action (Ref III-65)

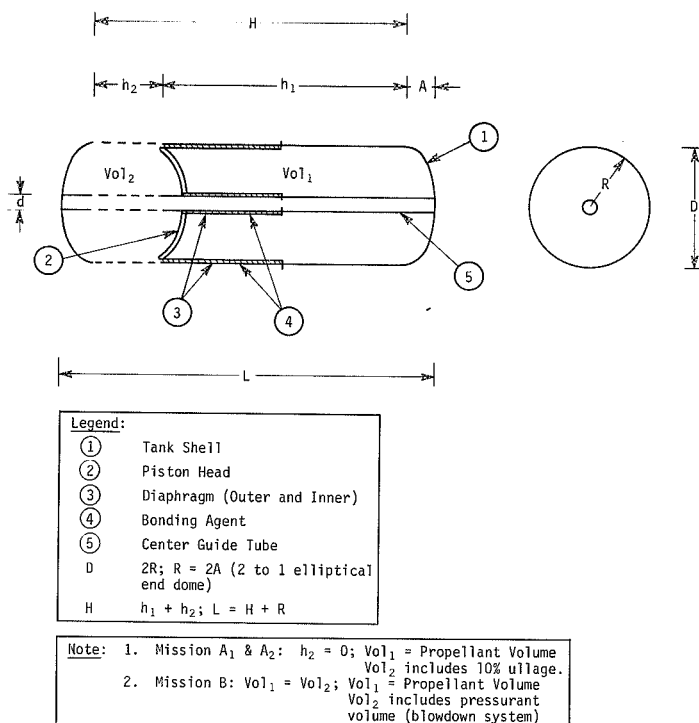


Figure III-11 Bonded Rolling Diaphragm System Geometry

d. Bonded Rolling Diaphragms - A bonded rolling diaphragm (BRD) consists of a thin, 1100 aluminum, cylindrical diaphragm approximately half the length of the cylindrical tank (Fig. III-11). The diaphragm attachment point is near the mid-plane of the cylindrical tank. When pressurized, the diaphragm rolls through the tank inverting itself and expelling propellant. The major problem with this kind of device is that it is subject to buckling if the pressure differential during expulsion exceeds the collapsing pressure of the diaphragm. One solution to this type of problem is to bond the diaphragm to the tank wall with an agent. This produces both a rolling and peeling process (Ref

III-67 and III-68). The bonding agent prevents the pressurant gas from acting on the sides of the diaphragm and collapsing the diaphragm. Teflon has been successfully used as a bonding agent (Ref III-68) and should be applicable for Mission A₂ and B. Silver has also been satisfactorily tested (Ref III-67) as a bonding agent and is proposed for Mission A₁, due to the low temperature requirement.

Rolling diaphragms, as shown in Figure III-11, are applicable only to cylindrical tanks. These designs usually include both a center-guide tube and 2-to-1 elliptical end domes. The guide tube stabilizes the piston-type head (prevents locking) during expulsion (Ref III-67 and III-69). The 2-to-1 elliptical end domes usually result from a compromise between volumetric efficiency, tank weight, and diaphragm operation. A flat piston head on the diaphragm is best considering only diaphragm operation (Ref III-68); however, if flat-end tanks were used to gain in volumetric efficiency, weights would be extreme. Hemispherical end-domes are advantageous from a mass standpoint but result in poor volumetric efficiency, if a flat piston head is used, or poor operating characteristics due to lateral loads acting on the piston head, if a hemispherical piston head is used (Ref III-68). A 2-to-1 elliptical piston head with a 2-to-1 elliptical dome tank is the best configuration for this program.

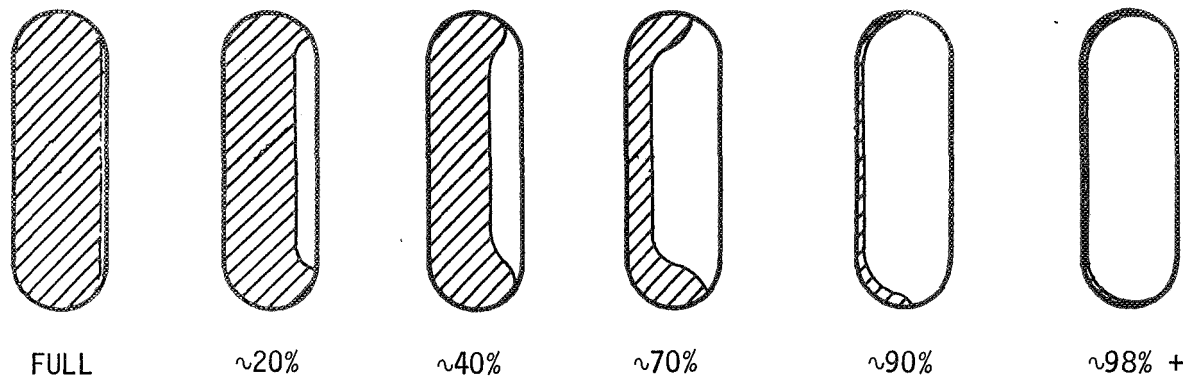
Based on a design similar to that shown in Figure III-11, an expulsion efficiency of 99.5% and a volumetric efficiency of about 82% are attainable for the baseline planetary missions. An expulsion efficiency to about 98% will require a ΔP of approximately 25 psi. For the 99.5% expulsion efficiency level, which results only with plastic deformation of the diaphragm, a ΔP of about 40 psi is needed.

As with the CSD and Telephragm devices, the preferred operational procedure to avoid flexing prior to expulsion, is to provide an ullage volume on the liquid side of the device. The device is held at the wall of the tank by the bonding agent and the pressure differential. The pressurization and multiple burn requirements for the baseline missions of this study preclude use of this technique, and flexing is a serious design consideration.

e. Transverse Collapsing Bladders - The transverse collapsing bladder (TCB) system, as described in Reference III-70, consists of a pressure shell and a deformable bladder. Support hardware includes pressure and discharge fittings, mounting provisions, indicators, and instrumentation ports. The pressure shell is the primary tank structure, and serves as a container for the bladder and base for mounting fittings, etc. The shell can be designed as either an all-welded, single-use structure or a flanged, refurbishable structure (Ref III-70). Shell construction materials include aluminum (conventional tankage), titanium (more sophisticated designs), and stainless or maraging steels (high temperature applications). The TCB system is limited to cylindrical tanks; an L/D as low as 1.1 can be used (Ref III-71 thru III-73).

The deformable bladder is comprised of thick- and thin-wall halves of 1100-0 aluminum joined by a longitudinal girth weld. An outlet fitting is located in the thicker half. The thin bladder half is the deforming section. During expulsion, reversal occurs on a transverse plane until the thin half nests within the nondeforming bladder half at propellant depletion (Ref III-70). A typical expulsion cycle is shown in Figure III-12.

The initial expulsion pressure differential across the bladder (10-in. diameter tank) is 2 to 3 psi and increases to 8 to 10 psi in accomplishing an expulsion efficiency to 98%. To achieve a greater expulsion performance, the differential pressure increases to about 16 psi, to plastically deform the bladder against the tank shell. With plastic deformation, an expulsion efficiency to 99.5% can be obtained.



Note: Information supplied by Aerojet Liquid Rocket Company.

Figure III-12 Typical Expulsion Cycle for a Transverse Collapsing Bladder (Ref III-74)

As with the BRD and Telephragm, the TCB has little, or no, flexing capability. (Aerojet has proposed the incorporation of a bellows attached to the tank (Ref III-74). The bellows would provide the additional volume when the propellant expands.)

2. System Evaluation

Based upon the discussion presented in Part 1, only the RRD and CSD are considered to be candidates for the planetary missions; these systems are evaluated further in the following paragraphs. The more limited flexing capability of the Telephragm, BRD, and TCB eliminated these systems from further consideration.

a. Reliability - Both the RRD and CSD are positive displacement devices ... they rely upon movement of the thin, metal barrier to expel liquid. Their catastrophic failure mode is a diaphragm rupture. The occurrence of pinholes in the diaphragm constitutes an anomalous failure for the RRD. These pinholes occur after several reversals from work hardening of the diaphragm material. The effect of system temperature level on pinholing and cycle life is negligible. Under an Air Force program, an RRD achieved seven complete reversals with LH_2 (-423°F), which compares identically to the number achieved at normal operating temperatures of 40 to 90°F (Ref III-61 and III-75).

Small cracks resulting either from diaphragm defects or off-nominal expansion (plastic deformation due to cocking, etc) of the diaphragm constitute an anomalous failure for the CSD. Detection of small cracks is difficult because there is no effective way of checking without an expulsion test; since the CSD cannot be cycled, an expulsion test cannot be performed. With proper quality control measures, small cracks due to material imperfections will not occur (Ref III-64); also, the diaphragm can be designed so its thickness can tolerate some small dents and scratches (during assembly and installation) as well as some limited asymmetric movement.

b. Mass - A summary of system mass for the RRD is presented in Table III-6. Diaphragm weights were obtained by scaling existing designs to the sizes considered in the study. For the spherical tanks, 17.5-degree cone angle diaphragms were used. No change in thickness was considered when a change in material was made. System mass consists of the diaphragm weight, weight of nonexpellable propellant (outage), weight of additional subsystems (such as screens over the tank outlet), and additional weight required due to changes in tank shape from the baseline. The outage penalty was based upon an expulsion efficiency of 95.5% due to the maximum allowable pressure differential (across the diaphragm) for the baseline missions being less than that needed to plastically deform the diaphragm. The need for a screen, or perforated plate, over the tank outlet to prevent gas ingestion during expulsion is discussed later in this section.

Table III-7 presents the CSD system mass for the different baseline missions. Diaphragm weights were based on 1100 aluminum having a thickness of 0.035 in. Two diaphragms per tank were used for Missions A₁ and A₂. Since Mission B uses a blow-down pressurization system with a 50 percent initial ullage, only one diaphragm is required. The system weight includes propellant outage based on an expulsion efficiency of 98%, weight for additional subsystems such as screens over the tank outlet, and weight required for mounting the diaphragms in the tanks.

c. Design Scalability and Producibility

1) Design Scalability - There have been no design problems associated with scaling of existing RRD tank assemblies. Arde has successfully scaled spherical assemblies ranging from 6- to 72-in. diameter.

Table III-6 Ring-Reinforced Diaphragm System Mass

Spherical Tanks					
Mission	A ₁		A ₂		B
Tank configuration	2 tanks	4 tanks	2 tanks	4 tanks	1 tank
Expulsion device	21.3	26.8	23.1	29.2	1.9
Tank loading and venting provisions	2.0	4.0	2.0	4.0	1.5
Trapped propellant	48.6	48.6	64.8	64.8	6.3
Total (lb _m)	71.9	79.4	89.9	98.0	9.7
Conospherical Tanks					
Mission	A ₁		A ₂		B
Tank configuration	2 tanks	4 tanks	2 tanks	4 tanks	1 tank
Expulsion device	45.8	61.4	50.6	69.9	4.1
Tank loading and venting provisions	2.0	4.0	2.0	4.0	1.5
Trapped propellant	48.6	48.6	64.8	64.8	6.3
Total (lb _m)	96.4	114.0	117.4	138.7	11.9
<u>Note:</u> Diaphragm material is 304L stainless steel and reinforcing rings are 308 stainless for missions A ₁ and A ₂ . For Mission B, 1100-0 aluminum was used.					

Table III-7 Convuluted Spherical Diaphragm Mass

MISSION	A ₁		A ₂		B
Tank configuration	2 tanks	4 tanks	2 tanks	4 tanks	1 tank
Expulsion Device	22.1	27.8	23.9	30.2	2.9
Tank loading & venting provisions	2.5	5.0	2.5	5.0	1.8
Trapped Propellant	21.6	21.6	28.8	28.8	2.8
Total (lb _m)	46.2	54.4	55.2	64.0	7.5

For the CSD design, scaling to sizes of interest for this program is possible without a major redesign and development effort since 26-in. and 54-in. diameter spheres have already been produced (Ref III-63). These sizes are well within the range of interest for this program.

2) Manufacturability - Arde has manufactured complete RRD tank-diaphragm assemblies using 304L stainless steel diaphragms with either 301 cryoformed or 304L stainless tanks. An 1100-0 aluminum diaphragm has been fabricated and the critical problem of joining the reinforcing rings to the diaphragm shell may be solved (Ref III-60).

For Mission B using nitrated hydrazine, an all-aluminum or a titanium tank/aluminum diaphragm system is required for propellant/material compatibility (Ref III-54). The all-aluminum system is the better choice since the titanium tank poses the additional problem of joining the aluminum diaphragm to the tank. Titanium cannot be used as a diaphragm material because of poor elongation properties.

Projections of the current technology to even larger sizes of RRDs indicate no manufacturing problems. There were problems such as metal thinning with the fabrication of large diaphragm sizes, i.e., larger than of interest in this program; however, with the 72-in. diameter conospheroid program (Ref III-60), such problems are apparently solved.

The CSD design presents no manufacturing problems. As mentioned, considerable experience already exists which is directly applicable to the missions considered here.

3) Subscale Test Scalability - For both the RRD and CSD, subscale testing is possible and, as mentioned, designs are scalable. Results, such as expulsion efficiency, can be easily scaled from volume and differential pressure considerations.

d. Compatibility with Adjacent Components and Propellants

1) Propellant/Material Compatibility - Considering the RRD, a 301 cryoformed stainless steel tank and 304L stainless steel diaphragm combination could satisfactorily be used for Missions A₁ and A₂. This is the only material combination presently developed. Aluminum and titanium are better materials for Mission A₂; however, titanium cannot be used as a diaphragm material (limited elongation) and the aluminum system needs further

development. The 301 cryoformed stainless steel is magnetic and, as a result, may not be desirable. Tests have shown that the permanent magnetic field is unaffected by outside induced fields (Ref III-76). For Mission B, any gain in compatibility easily offsets development/manufacturing considerations. The long duration mission, therefore, requires an all-aluminum or an aluminum diaphragm/titanium tank system.

The aluminum CSD should present no major problems from either propellant decomposition or material corrosion since aluminum is compatible with the propellants for all three missions (Ref III-54).

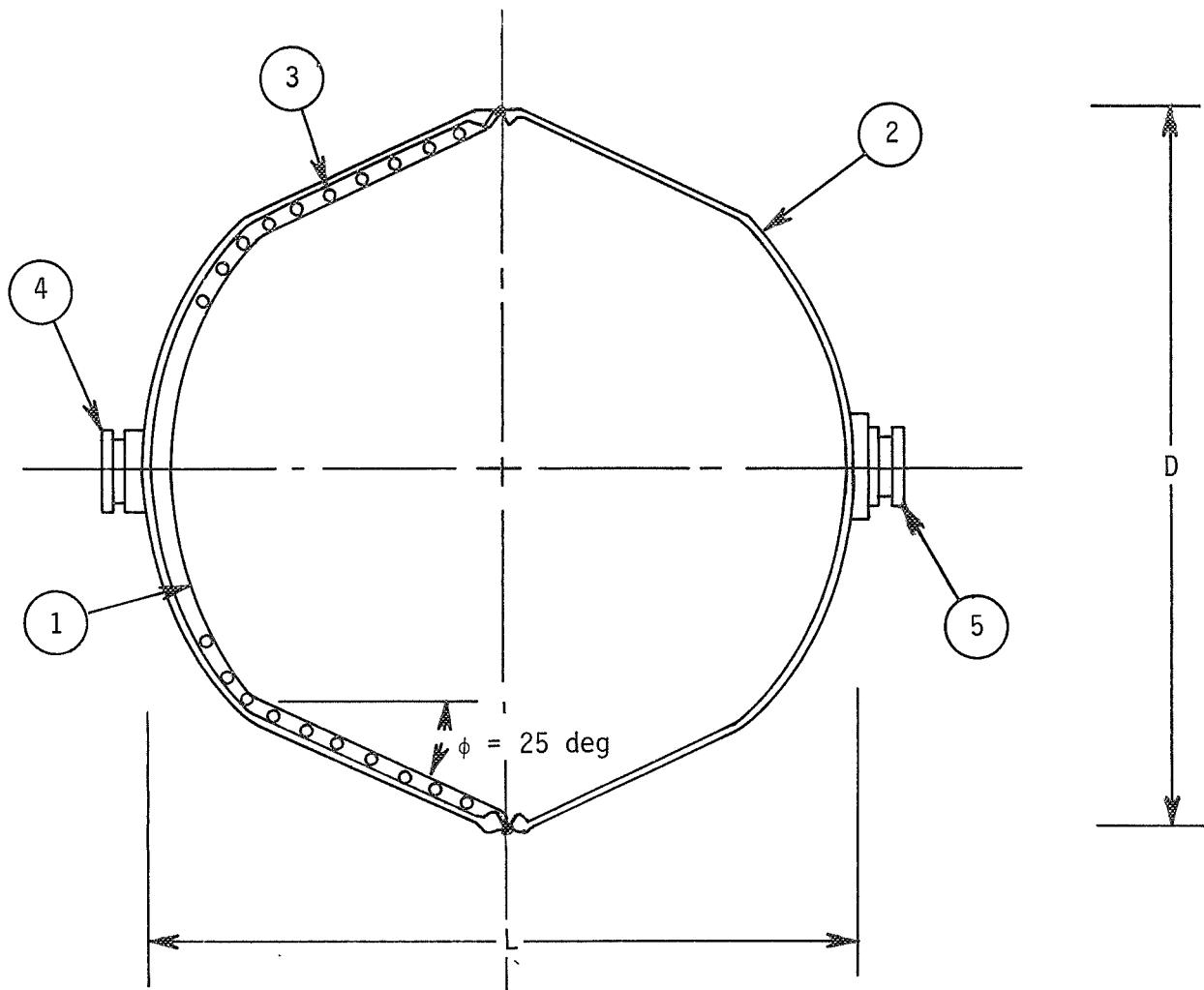
2) Pressurization System Compatibility - One of the more advantageous qualities of a metallic diaphragm device is that it provides a solid barrier between propellant and ullage. Problems associated with pressurant/propellant contact are eliminated.

3) Tankage Compatibility - The RRD is obtainable in either spherical, ellipsoidal, or conospheroid geometries, although it has been manufactured only in spherical and conospheroid shapes (Ref III-61). The basic diaphragm design is a conospheroid that can be fitted into a spherical or conospheroid tank.

For an improved cycle life to ten cycles, an RRD design ($\phi = 25$ degrees) is recommended (Ref III-60). This type of design is shown in Figure III-13. Use of a spherical tank with this diaphragm design will provide a relatively poor volumetric efficiency, and special tank tapers are recommended, as in Figure III-13, to improve volumetric efficiency. This shape will approximate a sphere with an L/D of unity, as shown. If a lower cycle life (5 to 7 reversals) is adequate, diaphragm designs with $\phi = 17.5$ degrees are available and are more easily adapted to spherical tankage (Ref III-60).

A conospheroid RRD ($L/D > 1$) can be used with a cylindrical tank, but only at a significant penalty in both volumetric and expulsion efficiencies. Only by use of special tapered tanks can an RRD be effectively employed for tankage with $L/D > 1$. There are L/D restrictions with a conospheroid tank based upon cone angle. For example, at a low cycle life (1 to 3 reversals), a cone angle of 10 degrees is adequate and the conospheroid tank is restricted to an $L/D \leq 5.67$; whereas, for high cycle life (20 reversals, $\phi = 25$ degrees), the conospheroid tank is limited to an $L/D \leq 2.14$.

The CSD is restricted to spherical tanks.



Legend:

- | | |
|--------|-----------------------------|
| ϕ | Cone Angle |
| L | Length of Tank |
| D | Diameter of Tank |
| ① | Diaphragm |
| ② | Tank Shell |
| ③ | Diaphragm Reinforcing Rings |
| ④ | Pressurization Port |
| ⑤ | Propellant Outflow Port |

Note: Information for this figure was supplied by Arde, Inc.

Figure III-13 Improved Cycle Life Diaphragm Tank Assembly

4) Performance

Duty Cycle and Mission Environment - There are no restrictions imposed on the mission duty cycle. RRDs have a demonstrated ability to be used either in a continuous, nonstop expulsion mode or in an intermittent, noncontinuous mode with the same performance (Ref III-61). No performance problems should be encountered because of the acceleration environment of the planetary missions. The acceleration load capability of the diaphragms is considerably above that expected for the three reference missions (Ref III-60) and accelerations twice nominal can be accommodated.

Convolutated spherical diaphragms also appear applicable to the multiple burn duty cycles of the three reference missions. Ability of the diaphragms to operate under both slosh and high lateral, or axial, accelerations also seems adequate for the missions under study. (No quantitative test data are available, however, for the maximum g levels.) Excellent center of gravity control during expulsion has also been demonstrated (Ref III-63).

As stated earlier, the ability of both RRDs and CSDs to tolerate diaphragm flexing, caused by propellant thermal cycling or vibration and slosh is somewhat limited and, as a result is a major design consideration. From the rather limited test data available, the RRD designs appear less sensitive to flexing of the diaphragm. If, for example, the propellant temperature excursions during the missions, result in only a 1% volume change, the RRD designs will satisfactorily withstand flexing to 5800 cycles (Ref III-61). However, more flexing data are needed at greater volume changes for the RRD design. Test data are needed for the CSD before an accurate assessment can be made with regard to its flexing capability.

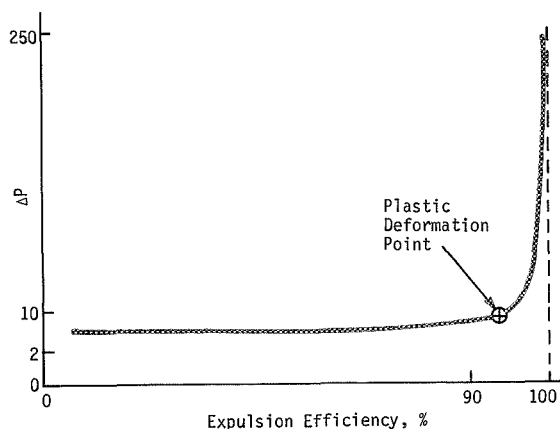


Figure III-14 Operating Pressure Differential for Bladders and Diaphragms as a Function of Expulsion Efficiency

The ΔP requirements for the CSD and RRD designs, to obtain expulsion efficiencies to 99.5%, cannot be satisfied by the baseline propulsion system pressure criteria if mission objectives are to be met. The differential operating pressure, typical for these metallic diaphragm devices, is shown in Figure III-14. The ΔP requirement is nearly constant to the point at which plastic deformation of the diaphragm begins. Beyond this point, the ΔP requirement increases sharply, as shown, since the metal diaphragm must

undergo plastic deformation. The plastic deformation pressure requirements are presented in Table III-8 for the CSD, RRD, and the other metallic diaphragm and bladder systems discussed earlier. The ΔP requirement for an expulsion efficiency of 99.5% is on the order of 200 psi for the RRD and 15 psi for the CSD. The operating ΔP , i.e., the pressure difference required to the point of plastic deformation, is about 10 psi for the RRD and 3 psi for the CSD.

Table III-8 Operating Pressure Differential for Various Bladders and Diaphragms

DEVICE	EXPULSION EFFICIENCY AT START OF PLASTIC DEFORMATION (%)	OPERATING ΔP UP TO DEFORMATION POINT (psi)	ΔP REQUIREMENT FOR STATED EXPULSION EFFICIENCY (psi)-(%)	REFERENCE
Spherical Ring-Reinforced Diaphragm (Stainless Steel)	95.5	10	200-99.5	III-62
Transverse Collapsing Bladder*	98	3	16-99.5	III-70
Convolutd Spherical Diaphragm	97	2	14-99.5	III-63
Telephragm*	90.6	15	>200-98.5	III-66
Bonded Rolling Diaphragm*	98	25	~40-99	III-69
*Presented for information only.				

The ΔP problem imposed by the metallic diaphragms is considered for Missions A₁ and A₂. The initial pressure of the pressurant gas (P_p) is 4000 psia. This pressure is reduced by the regulator to the tank pressure (P_T) which is 350 psia. The pressure of the propellant at the outflow port of the propellant tank (P_o) is P_T minus the ΔP required to operate the diaphragm. The flow orifice is sized to provide the desired flowrate to the engine at a constant upstream pressure (P_o) to produce the required chamber pressure (P_c). However, in providing an expulsion efficiency greater than approximately 95% for the RRD and 98% for the

CSD, the required diaphragm operating ΔP increases significantly causing a corresponding decrease in P_o . As P_o decreases, propellant flowrate and engine chamber pressure are reduced, as is the engine thrust level. The spherical RRD with a normal operating ΔP of about 10 psi is considered as a specific example. With a ΔP of 10 psi, P_o will be 340 psi and the orifice is sized to provide a flowrate giving the required chamber pressure of 100 psia. To obtain an expulsion efficiency of 99.5%, the diaphragm ΔP required is on the order of 200 psi and P_o will drop to 150 psia.

This decreases the flowrate to the engine by more than one-half. The severity of the degradation in engine performance will be different for the CSD and RRD; it is much worse for the RRD, due to its greater diaphragm plastic deformation ΔP requirement.

The difficulty in obtaining the higher and more desired expulsion efficiencies (to 99.5%) with the diaphragm devices is compounded for the Mission B propulsion system which uses blowdown pressurization. Near the end of the mission, tank pressure is only about 170 psia.

In comparing the CSD and RRD designs with the other candidate acquisition devices, the design point expulsion efficiencies of 98% for the CSD and 95.5% for the RRD were used because of the problems in providing higher operating ΔP to obtain higher expulsion efficiency. These design point expulsion efficiencies determined the amount of trapped propellant (outage) that was assigned as a mass penalty (Tables III-6 and III-7). However, the corresponding increases in tank size and mass were not considered.

Loading Considerations - Both the CSD and RRD designs employ vacuum loading techniques. The gas and liquid sides of the diaphragm are evacuated and then the propellant is loaded (Ref III-10 and III-60). A vapor bubble that can be collapsed once the system is pressurized is left on the liquid side. A capillary device is required over the outlet (or outlets in the CSD) to prevent any noncondensable gas formed within the tank by propellant decomposition and/or gas evolution from being ingested during liquid expulsion.

Passivation and Cleaning - For Missions A_1 and A_2 , the area between the two diaphragms of the CSD design would provide a contaminant trap which would be difficult to clean and passivate. The Mission B design presents less of a problem since only one CSD is used. Also, cleaning internal volumes having only one access port presents problems because adequate circulation of the cleaning fluid is difficult.

The RRD tank assemblies can be cleaned and passivated after final assembly. The cleaning or passivating fluid can be introduced on both sides of the diaphragm. However, with only one outflow port on each side of the diaphragm, as with the CSD, sufficient cleaning fluid circulation is difficult.

e. Performance Testability

1) Verification of Operational Readiness - The CSD cannot be tested prior to launch. Acceptance must be based on a statistical approach that decreases the confidence level for satisfactory performance. Only partial expulsion (15 to 20% of the total loadable propellant volume) can be demonstrated after assembly (Ref III-77). Unlike the CSD, the RRD can be acceptance-tested full-scale prior to launch because of its multi-cycle capability.

2) Development Status - RRDs have been commercially available since 1965. Flight-ready hardware, in both spherical and conospheroid shapes, has been manufactured and ground tested. A 72-in. diameter conospheroid tank with a high cycle life diaphragm design (Fig. III-13) and diaphragms able to operate satisfactorily under ± 20 -g lateral accelerations are presently being developed (Ref III-60). A 6-in. diameter RRD design for a hybrid engine was flown approximately two years ago by the Army, and launch of a N_2H_4 diaphragm tank assembly is planned for mid-1970 (Ref III-60). Table III-9 presents a summary of the RRD programs.

The development of the CSD is only in the preliminary stage. No flight-ready hardware has been made or flown. Only 20 diaphragms of this type have been made (Ref III-77).

Table III-9 Summary of Metallic Ring-Reinforced Diaphragm Technology Programs

CUSTOMER	TANK		DESCRIPTIVE COMMENTS	COMPLETED
	DIAMETER (in.)	SHAPE		
USAF Aero Propulsion Laboratory	6 23 72	Sphere Sphere Conospheroid	Concept demonstration 7 reversals at LH ₂ temperature (-423°F) Bulge formed shell demonstrated Complete diaphragm to be brazed and tested	1965 1966 Current
U.S. Army Missile Command	6	Sphere	Experimental liquid propellant engine - 40 diaphragms delivered for bench and missile flight tests (successfully flight tested)	1965
Jet Propulsion Laboratory	18	Sphere	Demonstration of multicycling flanged bladder tank assembly	1966
	18	Sphere	Welded tank bladder assembly Gold braze for demonstration of braze alloy compatibility with propellants	1969
	18	Sphere	Long term storability	Current
Aerojet Liquid Rocket Co. TVC Application	12	Sphere	Welded tank - diaphragm assembly <i>Qualified for Minuteman III</i>	1967
Aerojet Liquid Rocket Co.	12 33	Conospheroid Conospheroid	Subscale and full scale conospheroid for Advanced PBPS L/D = 1.6 Demonstrated hot gas expulsion of N ₂ O ₄	1967 1968
USAF Rocket Propulsion Laboratory	12	Sphere	5 to 10 yr propellant storage tests being conducted.	1969
NASA-Lewis Research Center (NAS3-12026)	13	Modified Sphere	Cryogenic propellants 20 reversal goal 11 reversals demonstrated to date	Current
Hamilton Standard	6	Sphere	Missile application ± 20 -g lateral ac- celerations 110-g axial accelerations	Current
Note: Information supplied by Arde, Incorporated.				

D. BELLOWS

1. System Description and Operation

Bellows are closed containers with convoluted side walls that allow an accordion action so that the internal volume can be varied through axial translation of the heads. The kinematics and structural requirements of bellows are particularly suited for cylindrical geometry. Other shapes are possible, but none are practical because of higher operating stresses and increased outage penalties produced by an inability to collapse completely. To obtain reasonable packaging efficiency, the system design must include both the tank and bellows in combination.

Metallic materials provide the advantages of a nonpermeable membrane between pressurant and propellant while preserving a multiple recycle capability of more than 500 cycles, good compatibility with the propellants so that long term storage and service life are possible, and operation over a temperature range from deep cryogenic to the boiling point for earth storable propellants. Control of propellant and structural dynamics are two major operational advantages characteristic of metallic bellows expulsion devices (Ref III-78). The movable action of the bellows under pressure, acceleration, or shock loads causes it to adjust to the fluid volume in the system. Consequently, there are no large voids* in which sloshing could take place. The encapsulated fluid and the actuation pressure on the bellows provide two forms of damping that nearly eliminate vibrational problems. Metal bellows can accommodate a broad range of tank pressures; operation is dependent upon the bellows pressure differential. Table III-10 summarizes some nominal characteristics of both welded leaf and hydroformed bellows for positive expulsion applications.

Metallic bellows have been widely used in the aerospace industry as dynamic seals, flexible line joints, and accumulators, as well as positive expulsion devices. Table III-11 lists some programs that have utilized metallic bellows for positive expulsion of liquid propellants. Consequently, a large body of design technology has been accumulated from which repeatable and predictable bellows systems can be produced.

*The metal bellows system is, however, subject to propellant decomposition, which may form some gas.

Table III-10 Metallic Bellows Evaluation Summary

DESIGN CHARACTERISTICS	WELDED LEAF	HYDROFORMED
Performance characteristics		
Expulsion efficiency, %	98	98
Scalability	good	good
Cycle life, cycles to failure	>500	>500
Reliability	good	good
Tank geometry	Cylindrical	Cylindrical
Volumetric efficiency, %	85	85
Maximum size fabricated		
Diameter, in.	23	14
Length, in.	60	35
Pressure drop, psi	5	5
Expulsion pressure	Low → High	Low → High
Inherent cg control	Yes	Yes
Series tankage capability	No	No
Operational characteristics		
Simplicity	good	good
Duty cycle limitations	none	none
Off-load propellant limitations	none	none
Slosh control	good	good
Shelf life	10 years	10 years
Mission life, days verified	30	--
Environmental capabilities		
Permeation	Negligible	Negligible
Radiation sensitive	No	No
Deep cryogenic propellant	Yes	Yes
Mild cryogenic propellant	Yes	Yes
Earth storable propellant	Yes	Yes
High temperature environment	Yes	Yes

Table III-11 Expulsion Bellows Programs

COMPANY	CONTRACT NUMBER	FLUIDS	PROGRAM	VOLUME (in. ³)	MATERIAL	REF
Metal Bellows Corporation	--	Hydrazine and N ₂	Astronaut maneuvering back pack	21.0	300 SS	III-79
Metal Bellows Corporation	NAS9-6909	Hydrazine and H ₂ O	R&D	60.0	300 SS	III-79
Metal Bellows Corporation	AF04(611)-11545	Hydrazine and H ₂ O	Storage evaluation at Edwards	192.0	300 SS	III-79
Metal Bellows Corporation	NAS7-101	N ₂ O ₄ and UDMH	Study for Saturn use	10,000	300 SS	III-79
Metal Bellows Corporation	NAS9-4550	N ₂ O ₄ , A-50 & MMH	NASA	2,800	300 SS	III-79
Solar	NAS3-11755	Liquid Hydrazine	NASA	700	321 SS	III-80
Solar	NAS7-100	Hydrazine	NASA	463	Tank 6A ₂ -4V Bellows 321 SS	III-80
Sealol	NAS7-101	N ₂ O ₄ and UDMH	S-IVB/NASA	775	300 SS	III-78
Sealol	AF04(611)-68 C-0072	N ₂ O ₄ , UDMH & A-50	GEMINI	--	300 SS	III-78
Gardner	AF04(611)-67 C-0072	Liquid Fluorine	Shutoff valve seal	--	Inconel	III-81
Gardner	287847-29	--	Minuteman	--	347 SS	III-81
Belfab	--	N ₂ O ₄ , UDMH & A-50	NASA Program cancelled in acceptance testing	11,000	AM 350	III-82
Martin Marietta Corporation	NAS3-12017	Liquid Hydrogen	R&D	700	300 SS	III-83
Martin Marietta Corporation	NAS3-12053	Liquid Fluorine	R&D	1,040	300 SS	Current Program

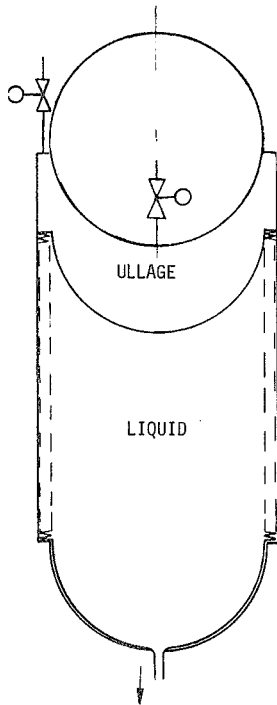


Figure III-15
Bellows in
Compression

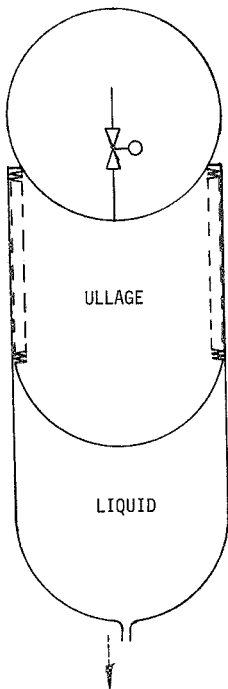


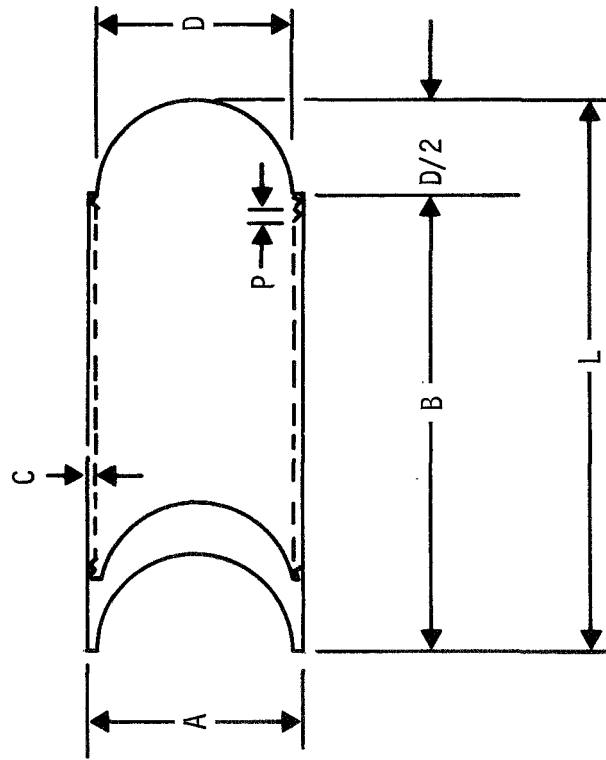
Figure III-16
Bellows in
Tension

Bellows can be designed to operate with the propellant on the inside and the pressurant on the outside, as shown in Figure III-15. Expulsion is achieved by collapsing the bellows with a higher pressure on the exterior. The alternative configuration (Fig. III-16) places the propellant outside the bellows so that expulsion is accomplished by expanding the bellows from an initial collapsed position with a higher interior pressure. The scheme with the propellant inside the bellows permits complete expulsion without the danger of convolution deformation which degrades the recycle capability and promotes premature failure. Applying the higher pressure to the outside of a bellows is preferable because it typically allows the bellows to operate in compression. Therefore, the externally pressurized system with the bellows in compression, shown in Figure III-15, was selected as the baseline configuration.

Design criteria for metallic bellows are intimately associated with the fabrication technique; a hydroformed side wall or a welded-leaf convolution construction must be selected. For low weight and high cycle life, a hydroformed bellows should use an L/D of two or greater while the welded-leaf bellows is better at an L/D nearer to one. Sealol contends that the L/D ratio is unimportant when the bellows is supported by the pressure tank (Ref III-78). Bellows with L/D up to 4 have been successfully built and used in a tank-supported configuration. The tank diameter criteria established for the baseline expulsion system designs, Table III-12, make the welded-leaf construction the best choice; however, cleaning and passivation are more difficult with this configuration.

Cycle life requirement can be designed into bellows by the proper selection of the pitch/span ratio which controls the plate stress level. In general, a weight reduction can be obtained by decreasing the metal thickness, decreasing the length/diameter ratio, and increasing the pitch/span ratio. Figure III-17 shows the influence of convolution and cylinder geometry on bellows weight. Higher cycle life is produced by decreasing material thickness and decreasing the pitch/span ratio, Figure III-18 (Ref III-78, III-84, and III-85). The obvious design decision is to select the thinnest gauge material consistent with dynamic stresses and corrosion rates. Corrosion rates on compatible metals as the result of propellant contact are on the order of one mil per year (Ref III-54).

Table III-12 Metallic Bellows Configuration



MISSION	NO. OF TANKS	VOL (in. ³)	DIAMETER A (in.)	LENGTH B (in.)	PITCH P (in.)	SPAN C (in.)	HEAD DIAMETER D (in.)	HEAD HEIGHT D/2 (in.)	TOTAL LENGTH L (in.)
A ₁	2	17,140	28.0	30.0	0.555	1.00	26.0	13.0	43.0
	4	8,570	20.0	29.5	0.447	0.75	18.5	9.25	38.75
A ₂	2	19,450	28.0	34.0	0.629	1.00	26.0	13.0	47.0
	4	9,725	20.0	33.5	0.508	0.75	18.5	9.25	42.75
B	1	6,670	18.0	29.6	0.448	0.75	16.5	8.25	37.85

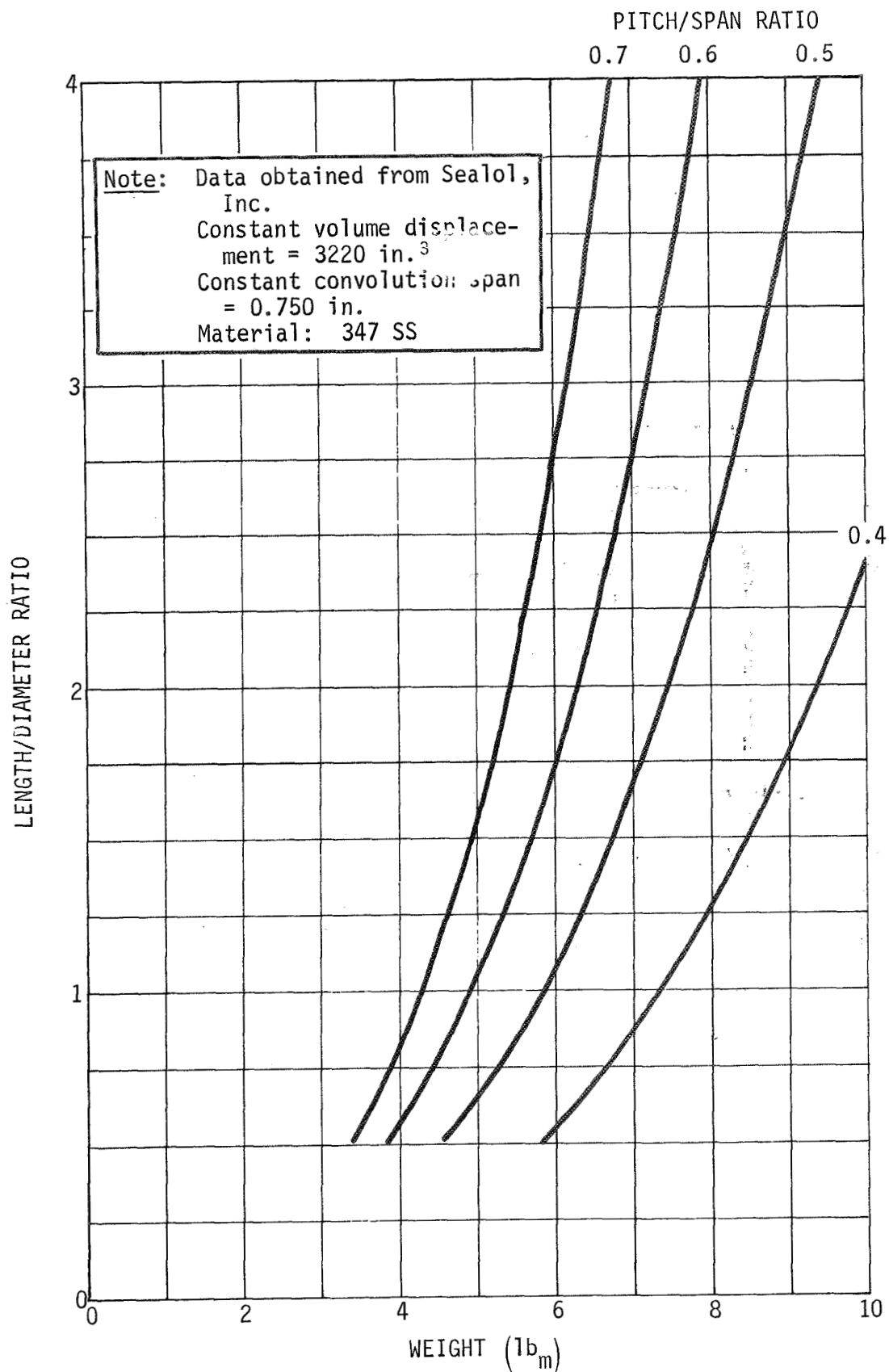


Figure III-17 Effect of L/D Ratio and Pitch/Span Ratio on Weight of Welded-Leaf Bellows

MCR-70-171

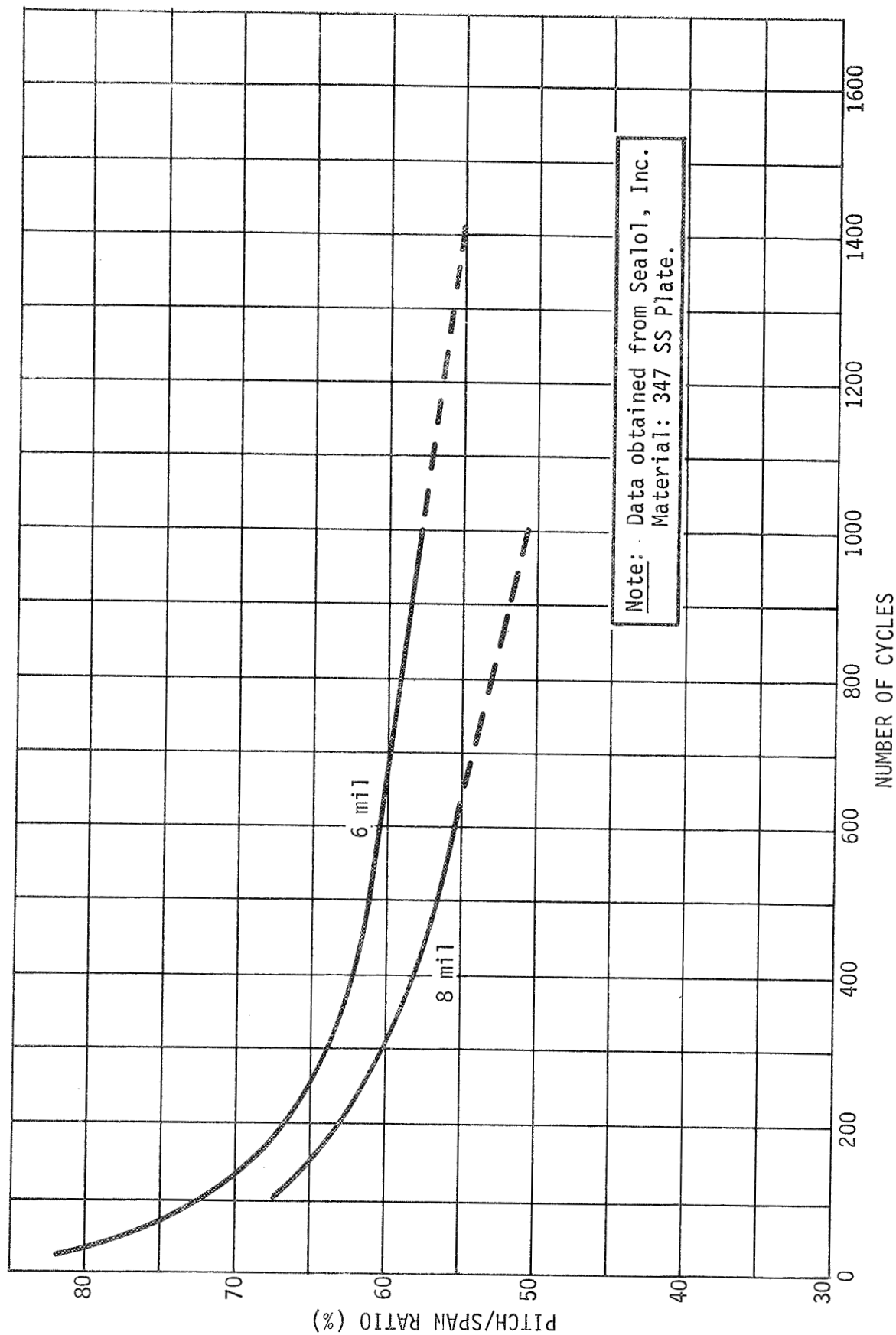


Figure III-18 Welded-Leaf Bellows Cycle Life as a Function of Pitch/Span Ratio

Since the fabrication of 20- to 30-in. diameter bellows will necessitate a minimum metal thickness of 8 mils to provide adequate stability during manufacture, no concession to wall thickness should be necessary for Missions A₁ or A₂ (Ref III-78 and III-86).

Reversing the upper dome of the tank or utilizing the pressurant gas storage bottle as the upper dome improves the volumetric efficiency at the expense of some additional tank weight (Ref III-78). With good head and convolution design, the bellows can achieve an expulsion efficiency of 98% with low pressure differences. However, the tank volumetric efficiency is limited to about 85% at the present.

2. System Evaluation

a. Reliability - Statistically, bellows are very reliable expulsion devices with no history of catastrophic failure in similar applications. Bellows have a single catastrophic failure mode -- when a material fracture provides sufficient separation to allow the propellant a preferential escape to the ullage volume rather than through the tank outlet (Ref III-87). A leaf-weld failure could cause this condition. Two modes of anomalous failure exist for bellows. Minor cracks and pinhole leaks, permitting pressurant gas to enter the liquid or the loss of propellant to the ullage volume, result in operational anomalies. Gas bubbles in the propellant ingested by the rocket engine can cause erratic and unstable combustion behavior. Propellant in the ullage volume contributes to outage and may cause corrosion damage to other system components. The second anomalous failure mode is nonsymmetrical leaf buckling, which results in unpredictable expulsion behavior and loss of expulsion efficiency.

The failure of a metal bellows device can be precipitated by excessive biaxial stresses* as a result of the dynamic mechanical environment from wind gusts during ground hold, launch vibration, or bellows system inertia forces due to vehicle perturbations in space. Fatigue fractures of any size can occur as the result of vibration or expulsion cycling. Corrosion from propellant contact can cause deterioration of the metal and bellows failure, particularly in porous areas of defective materials or welds and at interfaces between dissimilar metals where galvanic action can accelerate corrosion. The bellows wall convolutions and end dome welds form serious contamination trap areas that require stringent cleaning

*Combination of hoop compressive stress and longitudinal bending stress.

and passivation. Sealol states that methods have been developed to satisfactorily clean welded bellows (Ref III-78). Stress-corrosion cracking can produce more rapid failure rates than would be predicted from stress levels and corrosion rates individually. Weld areas are particularly susceptible to failure. Both hydroformed bellows and welded-leaf bellows have welds in the immobile support rings and head joints, but the welded-leaf construction can fail more easily at the hinge weld on each convolution. A higher total surface area for a bellows expulsion system may make it more susceptible to defective material failure from the probability standpoint.

b. Mass - Tank shapes are limited to cylindrical geometry with bellows. The system mass information presented in Table III-13 is based on a single material selection for both bellows and tank. However, there is no bellows fabrication experience using cryoformed 301 stainless steel, so the widely used 347 stainless steel was substituted for bellows material. The use of a cyroformed 301 stainless steel tank requires special manufacturing techniques employing compatible flanges for weld joints, because the cryogenic forming strength is lost in the heated area of a weld. The stainless steel expulsion bellows and tanks were designed with a safety factor of 1.5 on yield strength. A safety factor of 2.2 on ultimate strength was used for the aluminum and titanium materials. The bellows design parameters were:

Material thickness = 0.008 in.

Convolution geometry = 0.875 in./convolution.
(pitch)

The geometry selected for the bellows and tank results in a volumetric efficiency of nearly 88% and an expulsion efficiency of 98% for the bellows expulsion system.

c. Design Scalability and Producibility

1) Design Scalability - Some redesign will be required to optimize the system for a specific size and length/diameter ratio. The metal thickness required for forming bellows increases as the diameter increases. The bellows system is analytically predictable (based on empirical data) and scalable throughout the range of interest.

Table III-13 Metal Bellows System Mass

METAL	347 STAINLESS STEEL					2219 ALUMINUM					6AL-4V TITANIUM				
MISSION	A ₁		A ₂ [†]		B [†]	A ₁		A ₂	B	A ₁ [§]		A ₂	B		
NO. TANKS	2	4	2	4	1	2	4	2	4	1	2	4	1		
Cylindrical expulsion hardware	52.8	61.5	64.8	75.5	9.7	37.6	43.4	46.2	53.3	8.4	32.6	38.0	46.6		
Trapped propellant	0	0	0	0	0	0	0	0	0	0	0	0	0		
Outage	21.8	21.8	30.0	30.0	2.6	21.8	21.8	30.0	30.0	2.6	21.8	21.8	30.0		
Cylindrical device	74.6	83.3	94.8	105.5	12.3	59.4	65.2	76.2	83.3	11.0	54.4	59.8	76.6		
Special cylindrical tanks	174.0*	155.0*	186.0*	167.0*	27.6*	191.0	171.0	204.0	183.0	30.4	121.4	108.6	117.0		
Total mass, lb _m	248.6	238.3	280.8	272.5	39.9	250.4	236.2	280.2	266.3	41.4	175.8	168.4	193.6		
*Stainless steel for tank - 301 cryoformed.															
†Stainless steel is not the best material for use with N ₂ O ₄ due to possible adduct formation, or with MMH due to possible fuel decomposition. Stainless steel causes intolerable fuel decomposition with the nitrated hydrazine monopropellant.															
§Titanium is not recommended for use with OF ₂ because of shock sensitivity.															

*Stainless steel for tank - 301 cryoformed.

†Stainless steel is not the best material for use with N₂O₄ due to possible adduct formation, or with MMH due to possible fuel decomposition. Stainless steel causes intolerable fuel decomposition with the nitrated hydrazine monopropellant.§Titanium is not recommended for use with OF₂ because of shock sensitivity.

2) Manufacturability - Contemporary applications of bellows to propellant control have been limited to diameters of approximately 2 ft. However, designs as large as 30-in. diameter do not appear to present any major technical problems. Heavier presses and new dies would be needed, but the manufacturing techniques would remain the same.

In addition to the requirements for compatibility with the propellant, the metal must (1) remain ductile after welding; (2) possess good formability; and (3) provide a high allowable strain to density ratio. Stainless Steel Products expressed the opinion that titanium and aluminum do not have enough fatigue life for most bellows applications (Ref III-86). Titanium does not have the ductility required for bellows hydroforming. Sealol has fabricated pure titanium welded-leaf bellows and feels that the material is suitable for the proposed missions (Ref III-78). In any case, titanium would probably not be used with OF_2 because of the impact sensitivity of titanium with fluorine and OF_2 noted by various investigations (Ref III-88 thru III-90).

Hydroformed bellows may suffer some limitations on length and diameter which would preclude their consideration for 28-in. diameters. Stainless Steel Products states that the minimum diameter for hydroformed stainless steel expulsion bellows is presently about 7 in. (Ref III-86). In general, 0.006 in. is the minimum thickness for hydroformed stainless steel expulsion bellows up to 10-in. diameter. For larger diameters, thicker material is required. Welded-leaf bellows can be fabricated in any reasonable length or diameter. Welding technology presently limits the use of aluminum and titanium alloys in welded-leaf bellows (Ref III-87). Sealol is optimistic that new welding equipment will eliminate the weld burning and provide the manufacturing capability within the 1975 time period (Ref III-78).

Sealol has delivered units utilizing dissimilar metals. Metal bars which incorporated 304 stainless steel for joining to the bellows, a copper bond, and aluminum ends for joining to an aluminum housing were used for end fittings (Ref III-78). Transition pieces joining stainless steel to titanium are also available. The cost for these components are very high.

3) Subscale Test Scalability - No subscale testing is required on bellows systems. All important aspects of performance can be tested at full scale in a gravitational field. Since much of the bellows design technology is empirical, full scale testing is not only desirable, but necessary.

d. Compatibility with Adjacent Components and Propellants

1) Propellant/Material Compatibility - Metals with good compatibility characteristics and satisfactory structural properties are available for use with all of the cryogenic and earth storable propellants under consideration. The fabrication technology for stainless steel (OF_2 , B_2H_6) is more highly developed than that for titanium (MMH, nitrated hydrazine, N_2O_4).

2) Pressurization System Compatibility - Metals are essentially impermeable membranes to the propellant vapors, nitrogen, and helium in the wall thicknesses under consideration. The structural characteristics of bellows make them eminently suitable for both the regulated pressurization of Missions A₁ and A₂ and for the blowdown pressurization of Mission B.

3) Tankage Compatibility - Tankage is limited to cylindrical geometry by the bellows design for structural integrity and expulsion efficiency, and by the requirements for maximum volumetric efficiency. Spherical or ellipsoidal tank configurations would be impractical.

4) Performance (Duty Cycle and Mission Environment) - Bellows expulsion systems can be designed to meet all duty cycles and mission environments. Any combination of burn times, number of restarts, and acceleration variations (magnitude and direction) can be accommodated. Because some propellant decomposition and/or gas evolution occurs, a capillary bubble retention device is required over the tank outlet.

e. Performance Testability

1) Verification of Operational Readiness - The cycle life of well designed metallic bellows systems is so high that in-depth acceptance testing for leaks, vibration sensitivity, and expulsion efficiency can be conducted without performance degradation.

2) Development Status - Development and qualification tests have been performed on stainless steel bellows in smaller sizes than required for Missions A₁ and A₂. An 18-in. diameter welded-leaf bellows system similar to the design envisioned for Mission B was in qualification testing by Belfab when the program was cancelled. Sealol is fabricating a 27.5-in. O.D. welded bellows out of 8-mil stainless steel. Although no development test experience on 30-in. diameter bellows has been accrued, the structural, cycle life, vibration and performance test techniques employed to develop the smaller bellows systems should be applicable without modification. Solar has built 6-in. diameter hydroformed aluminum (1100) bellows (Ref III-80). Additional experience with titanium will be required to obtain the same level of confidence as that enjoyed with stainless steel.

E. SURFACE TENSION SYSTEMS

These systems differ from the other acquisition techniques presented in this chapter because they use the fluid intermolecular forces to provide the desired propellant orientation and control. These small capillary forces are dominant during the coasting, unpowered portions of the missions, and can be used to position and contain liquid over the tank outlet to provide gas-free liquid expulsion on demand.

Capillary phenomena have been studied both theoretically and experimentally since the eighteenth century when J. A. von Segner recognized that surface tension is dependent on temperature but not on pressure nor the form of the surface. Considerable work was done in the nineteenth century and early in the twentieth by many of the world's foremost physicists, notably Kelvin, Maxwell, Rayleigh, and Stokes (Ref III-91 thru III-94). A classical work with regard to interface shape and stability is the book by Bashforth and Adams (Ref III-95). During the late 1950s and early 1960s, there was a renewed interest in these earlier findings as aerospace companies, government agencies, and universities, explored the possibility of using surface tension forces to provide passive control of subcritically-stored fluids onboard spacecraft (Ref I-2 and III-96, for example). This more recent activity is summarized in two literature reviews (Ref III-97 and III-98).

A number of capillary systems have been developed and several have performed satisfactorily in flight. Included in the latter are systems used in the Agena, Transtage, and the Apollo Service Propulsion System (Ref III-99). Several current government programs are aimed at developing capillary systems to provide cryogenic propellant orientation and control (Refs III-100 and III-101).

1. System Description and Operation

Various capillary concepts typical of those developed, or under development, are presented in the following paragraphs. A discussion of their operational principles is also included.

Three system concepts are pictured in Figure III-19. Although the control device configuration is different in each propellant tank, as shown, the operational principle is based upon the relatively small pressure difference that exists across a liquid/gas interface due to intermolecular forces (Ref I-4). This capillary

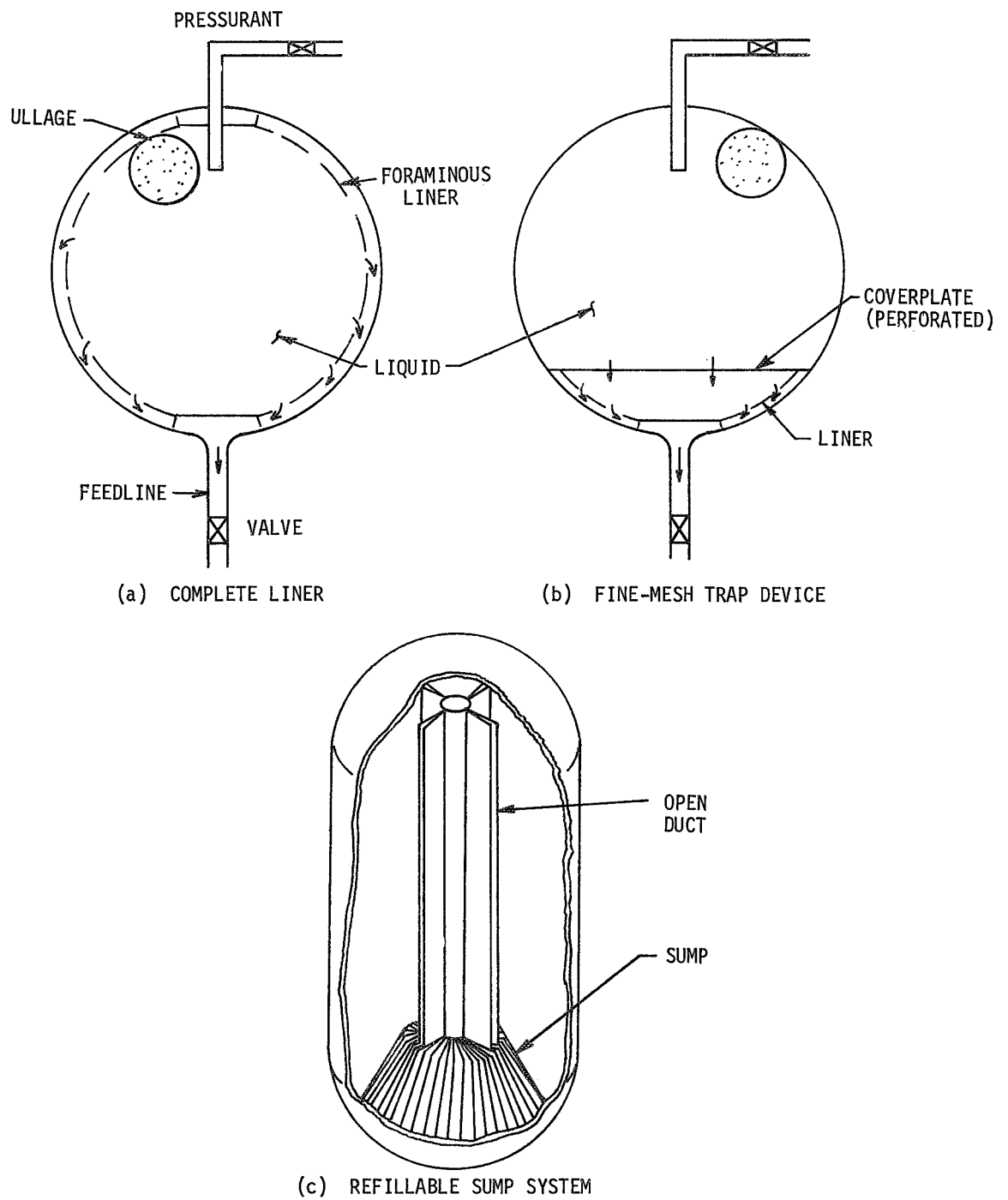


Figure III-19 Typical Capillary Concepts

pressure difference, ΔP_c , may be expressed at any point across the interface as

$$\Delta P_c = \left(\frac{1}{R_1} + \frac{1}{R_2} \right) \sigma \quad [\text{III-7}]$$

where σ is the liquid/gas surface tension and R_1 and R_2 are the principal radii of curvature at that point. For a spherical interface, the pressure difference is simply

$$\Delta P_c = \frac{2\sigma}{R_s} \quad [\text{III-8}]$$

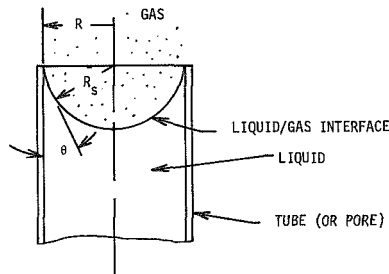


Figure III-20 Liquid/
Gas Interface Shape

where R_s is the radius of curvature. It is usually preferred for design practice to relate the capillary pressure difference to a more easily determined dimension, such as the tank or pore radius, R , rather than the radius of curvature. This can be done by introducing the relationship between the physical radius, R , and liquid-to-solid contact angle, θ , to the radius of curvature, as presented in Figure III-20. Then, rewriting Equation [III-8];

$$\Delta P_c = \frac{2\sigma}{R} \cos \theta \quad [\text{III-9}]$$

Capillary phenomena result from intermolecular forces; however, it is possible to represent these forces by the introduction of the two macroscopic parameters, contact angle and surface tension, and a measurable dimension, tank or pore radius. Surface tensions for the propellants of interest are presented in Table II-3. Contact angles have been measured for a number of liquid propellants in contact with aluminum (6061 T6), titanium alloy (ASTM B348-59T Grade 6), and 301 stainless steel (Ref III-102). The propellants include hydrogen peroxide (90%), nitrogen tetroxide, fuming nitric acid (Type III B), hydrazine, UDMH, and Aerozine 50 (50/50- N_2H_4 /UDMH). The measured contact angles varied from zero to two degrees. Based upon these results, the propellants considered in this study will exhibit near-zero contact angles when exposed to the aluminum and titanium tankage. As seen in Equation [III-9], the capillary pressure difference is a maximum when the contact angle is zero; however, whether the value is zero or two degrees, cosine θ is essentially unity. The maximum capillary pressure difference attainable for the propellants of interest is on the order of one psi, based upon a zero contact angle and use of the finest, practical screen available (325 x 2300 mesh).

The capillary concepts can be categorized as: gas-free liquid expulsion can be demonstrated under a minus 1-g test condition* (Fig. III-19a and III-19b); and system performance cannot be demonstrated under minus 1 g (Fig. III-19c). Systems that are testable in 1 g require the use of foraminous material, screen and/or perforated plate, with small (micronic) pore sizes to provide high capillary pressure differences. The latter are required to support the hydrostatic pressure differences that result under Earth's gravitational acceleration, g, expressed as;

$$\Delta P_h = \rho g h \quad [\text{III-10}]$$

where ρ is the liquid density and h is the liquid head. The capillary pressure difference must at least equal, or exceed, the hydrostatic pressure differences to stabilize the liquid/gas interface, i.e., prevent fluid transfer, at the surface of the foraminous material, and provide gas-free liquid expulsion. The pore size required can be expressed as follows:

$$R \leq \frac{2\sigma}{\rho g h} (\cos \theta) \quad [\text{III-11}]$$

or

$$R \leq \frac{2\beta}{h g} (\cos \theta) \quad [\text{III-12}]$$

where β is the kinematic surface tension, ft^3/sec^2 . The fuels possess a greater kinematic surface tension than do oxidizers; this is the case for any bipropellant combination of earth storables, space storables, or cryogenics. The fuels possess a slightly higher surface tension value and a correspondingly lower liquid density (Table II-3). As shown by Equation [III-12], a smaller pore size is required for the oxidizer because of its lower kinematic surface tension. The usual practice is to design the capillary device for oxidizer service and use the same design for the fuel.

The concept shown in Figure III-19a is a complete, foraminous liner positioned near (1/4 in., or less) the tank wall to provide: a passageway (annulus) between the liner and tank wall to the tank outlet; communication between the bulk propellant located anywhere in the tank and the annulus; and a porous surface at which surface tension forces will stabilize the liquid/ullage interface. The liquid outflow path during expulsion is shown in the figure. The bulk liquid is depleted by flowing into the annulus and out the

*The minus 1-g test condition is provided by inverting the propellant tank (liquid drain port pointed upwards, away from Earth) so the gravitational acceleration acts to position the heavier liquid away from the drain port.

tank. Since the annulus is an integral part of the outflow path, gas-free liquid can only be supplied provided that the annulus is full of liquid and the ullage is prevented from entering the annulus until the bulk propellant is depleted. The first requirement is satisfied by filling the annulus during loading; the second is met by selecting the mesh size (pore radius) to maintain this liquid condition. As discussed, the pore size must be small enough to at least balance hydrostatic pressure differences. For the minus 1-g tests, hydrostatic heads are the single, greatest design criterion in selecting pore size. However, the capillary pressure difference must be greater than the sum of all pressure differences tending to break down the liquid annulus by the ingestion of gas. During liquid outflow:

$$\Delta P_c \geq \Delta P_h + \Delta P_f + \Delta P_e + \Delta P_v \quad [\text{III-13}]$$

where ΔP_f is the pressure loss due to viscosity; ΔP_e is the pressure loss due to the bulk liquid entering the annulus; and ΔP_v is the static pressure reduction in the annulus due to flow. Selection of the proper pore size will stabilize the liquid/gas interface at the foraminous surface thereby maintaining the liquid prime in the annulus. Equation [III-13] is the fundamental relationship used to select the screen liner mesh size.

Gas-free liquid can be supplied continuously, or intermittently, until the bulk propellant is depleted. With further expulsion, ullage only is available to supply the annulus and will be ingested with outflow. The annulus, therefore, represents the residual propellant. It should be kept as small as practical so that expulsion efficiencies of 99%, or more, are achievable.

The second capillary concept, Figure III-19b, uses only a portion of the total liner concept as a start tank (trap) within the propellant tank. The foraminous liner is confined to the propellant acquisition device only, as shown, but provides the same function as in the complete liner. Communication between the bulk propellant (outside the trap) and the trap is achieved by propellant settling during engine burns. During the latter, provided that the magnitude of the vehicle acceleration and duration of the burn period are adequate (Ref III-103), the bulk propellant will be settled over the trap and will supply liquid to the device with continued outflow. The trap volume is sized to hold a sufficient propellant quantity so that gas-free liquid is supplied during the engine startup and during the propellant settling phase. With

each engine burn, some ullage will be ingested by the trap until the bulk propellant is settled. This amount must be considered in sizing the trap unless the coverplate on the trap (Figure III-19b) is designed to allow gas to be purged during burns as the trap is refilled with liquid. In this refillable case, the pores of the coverplate are selected large enough to be unstable under the vehicle acceleration during burn periods, and ullage may be completely, or at least partially, purged from the trap during each burn until the bulk propellant is depleted.

The trap volume is completely filled with liquid during tank loading and the initial ullage is positioned outside the trap. A vacuum fill is preferred, as with the full liner concept, to prevent wicking of the fine-mesh foraminous material and permit complete filling of the annuli and trap volumes with liquid (Ref III-104). Wicking will tend to trap gas in annuli and the acquisition device (trap). A vacuum fill technique will cause the liquid to vaporize rather than wick the foraminous material. If a vacuum fill is not practical, nonwicking material* may be used or techniques to vent the trapped gas either to the central ullage space or overboard may be employed (Ref III-104). Once the trap is full of liquid, it will remain so during the launch and boost phases if the tank outlet is pointed toward Earth. If the tank is launched with the outlet pointed away from Earth, the coverplate must provide stability and prevent liquid loss from the trap under the boost acceleration environment. The coverplate design must also assure that sufficient liquid is contained during low-g accelerations due to drag and attitude control maneuvers. Critical dimensionless design parameters for interface stability under static and dynamic conditions have been verified experimentally and are available in the literature (Ref III-105 and III-106).

The trap concept will provide expulsion efficiencies of 99.5%, or more, since propellant outage is the small annulus volume. The trap device is smaller and lower in weight than the total liner. Single-phase liquid expulsion of the trap volume can be demonstrated under minus 1 g.

The third concept, Figure III-19c, is designed to meet the low-g mission requirements only; fine-mesh material does not have to be used. The concept, as shown, relies upon capillary pressure differences to pump and contain liquid in the sump device over the

*As experimentally verified (Ref III-105), Dutch Twill cloth wicks even in 1 g due to its internal capillary network of warp and shute wires. On the other hand, perforated plate and square-weave screen do not wick.

tank outlet during the low-g periods of the mission (Ref III-107 and III-108). The vaned-sump is designed so that, when it is partially filled with liquid, a lower pressure will exist in the sump liquid than in any separated bulk liquid due to capillary forces. In practice this is achieved by use of tubes, plates, concentric cones, or other geometries, to provide closely-spaced surfaces. (This spacing, or gap size, becomes the R value in the capillary pressure difference equations.)

The cruciform-type duct connects the sump to regions where propellant may rest during low g. When the duct is only partially filled with liquid, a pressure deficiency exists in the liquid when compared to the bulk propellant. This condition results because the bulk propellant is less influenced by capillary forces since its characteristic dimension (R) approximates the tank radius, whereas the duct has a smaller dimension. The bulk liquid pressure will, therefore, be closer to that for the ullage. It will tend to flow into the duct because of this pressure difference. Since the liquid pressure in the sump is less than that in the duct due to the sump having smaller openings (smaller R values), the liquid will continue to flow from the duct into the sump. The basic design criterion is that the capillary pressure difference is greatest for the sump. If this is satisfied, the liquid pressure potential will pump liquid into the sump.

The interface stability provided by this simple capillary concept is much less than for the fine-mesh devices. Stability is, however, a lesser concern since the sump is refillable. The system can provide expulsion efficiencies of 99.5%, or more. Since fine mesh screen and perforated plate are not used, fabrication, assembly and cleaning are lesser considerations than with the fine-mesh screen devices.

2. System Evaluation

The screen/trap design, as shown in Fig III-19b, was selected for the comparative evaluation. This device can satisfy the system and mission requirements for the three planetary missions. Gas-free liquid expulsion performance can also be demonstrated for the full-scale trap using the baseline propellants under the minus one-g test condition.

The preliminary design is summarized in Table III-14. The designs are not refillable, i.e., ullage is not purged from the trap during engine burns. Materials of construction are aluminum for Mission A₁ and titanium for Missions A₂ and B. The screen materials were selected based upon compatibility and mesh size

requirements. Mesh sizes for the coverplate and liner are presented in the table. The lower minimum expulsion efficiency, 98.8%, for Mission B results because of the lower initial propellant loaded (50%) with the blowdown system.

a. Reliability - Surface tension devices are completely passive, i.e., they have no moving parts. Catastrophic failure of the device will occur when there is insufficient propellant in the trap to accomplish an engine start. An unexpected acceleration exceeding the trap stability design may cause loss of propellant from the trap; however, since the device is designed for minus 1-g testing, this would be unlikely during the actual mission. Propellant may also leave the trap device because of evaporation. The size of the reservoir may be increased to allow for evaporation. Designs could also incorporate capillary channels to pump liquid back to the trap.

An anomalous failure mode would be ullage penetration into the annulus. The anomalous failure may result from pore enlargement or an unexpected acceleration exceeding pore stability. As a result, some gas would be ingested during liquid outflow.

b. Mass - A compilation of device weight and weight penalties assessed for each mission is presented in Table III-15. Differences in the device weight between the spherical and cylindrical tanks are negligible.

The device itself is low in weight since it consists of foraminous material and thin plates. Because there is intimate contact between the ullage and the propellant, the device was penalized for dissolved pressurant and vaporized propellant (Chapter IV, Section B). Engine operation was assumed to end when the only propellant remaining was contained in the annulus. Gas-free propellant at the outlet can no longer be guaranteed beyond this point. The mass of the propellant remaining in the annulus (a measure of the expulsion efficiency) is the weight penalty due to outage.

c. Design Scalability and Producibility

1) Design Scalability - The design is scalable and can be applied to the tank sizes and shapes, propellants, and acceleration environments for this study (Ref III-99 and III-105).

2) Manufacturability - Similar systems have been fabricated, qualified, and flown successfully. Techniques for welding

Table III-14 Summary of Trap Designs (Prelim Analysis)

	Mission A ₁	Mission A ₂	Mission B
Refillable	No	No	No
Trap Volume, cu ft	0.34	0.38	0.11
Depth of Trap, ft	0.29	0.31	0.22
Screen:	Aluminum	Titanium	Titanium
Coverplate (Mesh)	200 x 1400	180 x 180	180 x 180
Liner (Mesh)	200 x 1400 Pleated	180 x 180 Pleated	100 x 100 Pleated
Expulsion Efficiency	≥99.6%	≥99.6%	≥98.8%

Table III-15 Surface Tension System Mass

	MISSION A ₁	
	2 Tanks (1b _m)	4 Tanks (1b _m)
Dry device weight (aluminum)	2.8	3.8
Propellant in annulus (outage)	4.7	5.9
Penalty for ullage-propellant contact	<u>7.7</u>	<u>7.7</u>
Total Mass	15.2	17.4
	MISSION A ₂	
	2 Tanks (1b _m)	4 Tanks (1b _m)
Dry device weight (titanium)	4.8	6.6
Propellant in annulus (outage)	5.8	7.3
Penalty for ullage-propellant contact	<u>2.0</u>	<u>2.0</u>
Total Mass	12.6	15.9
	MISSION B	
	1 Tank (1b _m)	
Dry device weight (titanium)	1.5	
Propellant in annulus (outage)	1.6	
Penalty for ullage-propellant contact	<u>0</u>	
Total Mass	3.1	

stainless steel and aluminum screen material are developed and have been in use for many years in the filter industry. More experience is required with the titanium; however, no major problems are foreseen.

A concentric liner made of flat screen material must be supported away from the tank wall to obtain the proper annulus gap width. A perforated plate may be used for support. By pleating the screen used for the liner, manufacturing problems are minimized. The pleated screen, because of its structural integrity, is self-supporting; the liner rests against the tank wall to form the annulus and no additional support is needed.

3) Subscale Test Scalability - Dimensionless numbers have been verified from previous tests with surface tension devices (Refs III-99 and III-105). Drop tower and bench tests have been used successfully.

d. Compatibility with Adjacent Components and Propellants

1) Propellant/Material Compatibility - The same material can be used to manufacture the surface tension device and the tanks. Aluminum screen material is available for Mission A₁, and titanium screen is available for Missions A₂ and B. Martin Marietta has demonstrated that devices fabricated with screen materials and representative metal joining techniques can be cleaned and passivated for the stringent requirements of fluorine service (Ref III-109).

2) Pressurization System Compatibility - Since there is intimate contact between pressurant and propellant, some pressurant will dissolve and some of the propellant will vaporize. This is discussed more fully in Chapter IV, Section B; however, it is not a serious problem.

Propellant may vaporize from the reservoir and condense elsewhere due to heat soak-back from the engine and external heating. The trap volume may be sized to allow for this or it may be desirable to provide channels from the trap coverplate to the opposite end of the tank. The channels will provide communication with the condensed propellant and trap.

3) Tankage Compatibility - The device is compatible with the tank sizes and shapes of interest.

4) Performance - Surface tension devices can satisfactorily meet the mission requirements. They can be designed to provide any number of short duration burns before and after the insertion burn. An expulsion efficiency of 99.6%, or more, can be provided for Missions A₁ and A₂ and 98.8%, or more, can be provided for Mission B.

e. Performance Testability

1) Verification of Operational Readiness - Surface tension devices can be designed and built to expel the actual propellants under the minus 1-g test condition. The full-scale device can be demonstrated. This test would be performed as an acceptance test of the actual flight article in order to demonstrate its compatibility, integrity, and performance. The capillary devices are not cycle limited.

2) Development - The Agena, Transtage, and Apollo SPS have successfully flown similar capillary systems. No additional development is required.

F. EXTERNAL SETTLING

In considering external settling systems for propellant acquisition, an analysis was conducted to define the system required for each of the baseline missions. An evaluation was then made on the use of these systems.

1. Analysis

To size a settling rocket system, the propellant settling rate must be established. If the rocket thrust is either too high or too low, optimum performance will not be obtained with respect to the amount of settling rocket propellant required. The drag of the spacecraft becomes significant if the thrust is small; this further complicates the analysis.

For a cylindrical tank, the optimum settling acceleration is obtained when the settling Bond number is 5.1 (Ref III-110). Therefore, a value of five for the settling Bond number was used for the analysis. This value should be adequate for a cylindrical tank and somewhat conservative for a spherical tank. From the Bond number equation,

$$Bo = \frac{\rho a r^2}{\sigma} \quad [III-14]$$

the optimum settling acceleration is determined as

$$a = \frac{5\sigma}{\rho r^2} \quad [III-15]$$

The settling time is the time between the firing of the settling rockets and the point at which the propellant is settled sufficiently to guarantee proper main engine start. Therefore, the time allowed for settling must take into account the worst possible initial orientation, sloshing and geysering at the inlet, and the rate at which bubbles leave the liquid. When there is a relatively motionless and gas-free volume of liquid located over the tank outlet, the main engine can be started. This liquid volume must be sufficient to fill the feedlines, start the engine and build the thrust to the point where the acceleration will continue the settling of propellant.

There are no relatively simple means of calculating the time required to settle propellants and accurately account for all the above factors for the wide range of propellant volume involved throughout the missions. However, free-fall equations can be used with a safety factor (τ) to estimate settling time (Ref III-111):

$$t = \tau \sqrt{\frac{2d_s}{a}} \quad [\text{III-16}]$$

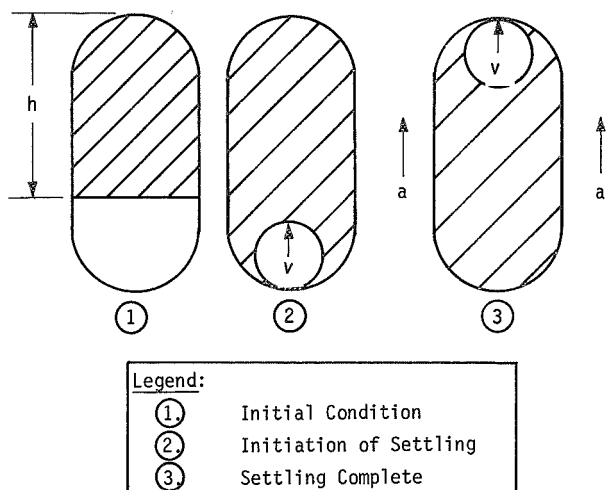
One free-fall time period is the time required for a particle of fluid to fall the desired distance (d_s). After five of these time units ($\tau = 5$), the fluid is sufficiently settled to permit engine start. The previously discussed optimum settling acceleration is employed in the calculation. The liquid is assumed to be oriented at the end of the tank opposite the outlet and the interface is assumed to be flat. Ultraconservative answers are usually obtained when this approach is applied to experimental data since geysering and sloshing due to settling are damped out, entrained gas bubbles are removed, and a relatively quiescent liquid is attained over the outlet within this time period.

Another method of determining the settling time in cylindrical tanks is to calculate the velocity of the interface (Ref III-111 and III-112):

$$\frac{v}{\sqrt{a}} = 0.48 \left[1 - \left(\frac{0.84}{Bo} \right)^{Bo/4.7} \right] \quad [\text{III-17}]$$

If the interface velocity is assumed constant, settling time is obtained as:

$$t = \frac{h}{v} \quad [\text{III-18}]$$



where h is the height of the liquid when the interface is flat as shown in Figure III-21. If the ullage volume is small, the settling time obtained is within 5% of that calculated using the free-fall equations. For large ullage volumes, this method is not applicable since v is not representative of the actual situation in the tank.

Figure III-21 Propellant Settling

The required settling rocket thrust is obtained from the initial mass of the spacecraft and the optimum settling acceleration:

$$F = Ma. \quad [\text{III-19}]$$

Since the spacecraft mass decreases throughout the mission as propellants are used, a corresponding increase in settling acceleration will occur. The total impulse and amount of propellant required for the external settling rocket system is obtained from the calculated settling rocket thrust, the total settling rocket operating time, and the propellant specific impulse:

$$I_t = Ft_t \quad [\text{III-20}]$$

$$m = \frac{I_t}{I_{sp}}. \quad [\text{III-21}]$$

The total settling rocket operating time is the sum of the individual settling times required to settle the main propellants for each main engine burn.

For Missions A₁, A₂, and B, the values calculated from the above analysis are presented in Tables III-16, III-17, and III-18, respectively. Both cylindrical and spherical main propellant tanks were considered for each mission; two- and four-main propellant tanks were considered for Missions A₁ and A₂. It was assumed that no venting of the main tanks was required and that propellant settling would be accomplished prior to each main engine burn.

2. System Evaluation

In order to facilitate the evaluation, a settling rocket system that appears to best match the mission requirements and provide the best overall performance was selected. This system, shown in Figure III-22, utilizes two cold gas jets (gaseous nitrogen) and includes its own independent supply tank, valves, and feedlines. The gaseous nitrogen is stored initially at 3000 psi and 500°R in a spherical 6Al-4V titanium tank. Explosively operated valves with redundant squibs are used to start and stop the rockets. The system illustrated has enough valves to accomplish the main burns required for Mission B. For Missions A₁ and A₂, the systems would not have the first three sets of squib valves because there are only six burns.

Table III-16 Settling Rocket Requirements, Mission A₁

	SPHERICAL		CYLINDRICAL	
	2 TANKS	4 TANKS	2 TANKS (L/D = 1.33)	4 TANKS (L/D = 1.7)
Optimum settling acceleration, ft/sec ²	0.0029	0.0046	0.0038	0.0074
Total rocket operating time, sec	897	635	843	574
Longest settle time, sec	207	146	196	135
Rocket thrust, lb _f	0.68	1.07	0.89	1.70
Total impulse, lb _f -sec	610	679	746	976
Settling rocket propellant mass, lb _m *				
Monopropellant N ₂ H ₄	3.1	3.4	3.7	4.9
Gaseous helium	4.5	5.0	5.5	7.2
Gaseous nitrogen	10.2	11.3	12.4	16.3
*N ₂ H ₄ I _{sp} = 200, He I _{sp} = 136; N ₂ I _{sp} = 60				
Spacecraft mass = 7500 lb _m				

Table III-17 Settling Rocket Requirements, Mission A₂

	SPHERICAL		CYLINDRICAL	
	2 TANKS	4 TANKS	2 TANKS (L/D = 1.46)	4 TANKS (L/D = 1.88)
Optimum settling acceleration, ft/sec ²	0.0035	0.0054	0.0050	0.0098
Total rocket operating time, sec	839	604	768	522
Longest settle time, sec	193	139	179	123
Rocket thrust, lb _f	0.82	1.26	1.16	2.28
Total impulse, lb _f -sec	685	761	891	1190
Settling rocket propellant Mass, lb _m *				
Monopropellant N ₂ H ₄	3.4	3.8	4.5	6.0
Gaseous helium	5.0	5.6	6.6	8.8
Gaseous nitrogen	11.4	12.7	14.8	19.8
*N ₂ H ₄ I _{sp} = 200, He I _{sp} = 136; N ₂ I _{sp} = 60				
Spacecraft mass = 7500 lb _m				

Table III-18 Settling Rocket Requirements, Mission B

	SPHERICAL TANK	CYLINDRICAL TANK (L/D = 1.79)
Optimum settling acceleration, ft/sec ²	0.011	0.0187
Total rocket operating time, sec	675	614
Longest settle time, sec	88	80
Rocket thrust, lb _f	0.38	0.65
Total impulse, lb _f -sec	259	401
Settling rocket propellant mass, lb _m *		
Monopropellant N ₂ H ₄	1.3	2.0
Gaseous helium	1.9	2.9
Gaseous nitrogen	4.3	6.7
*N ₂ H ₄ I _{sp} = 200, He I _{sp} = 136; N ₂ I _{sp} = 60		
Spacecraft mass = 1124 lb _m		

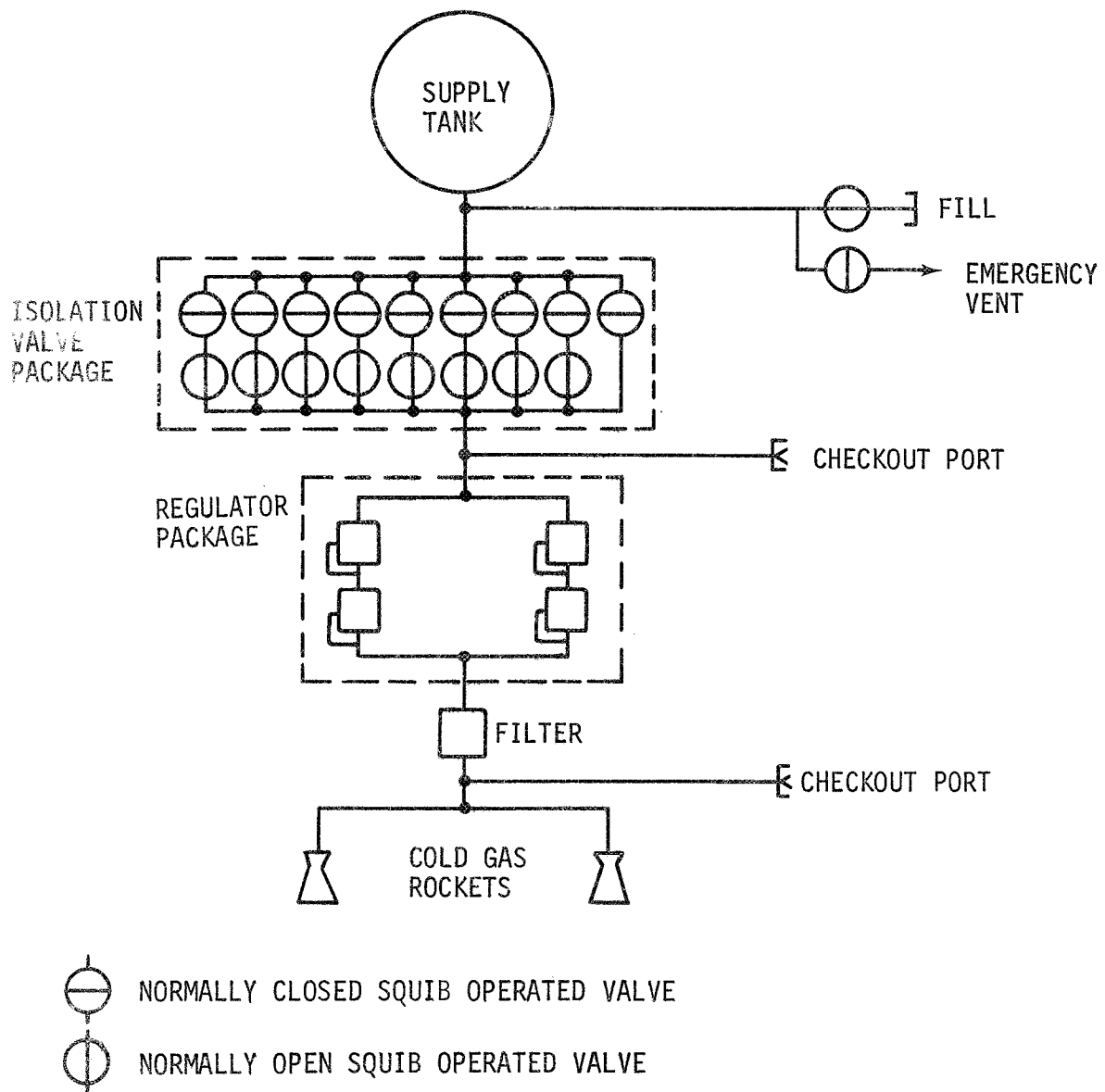


Figure III-22 Settling Rocket System Schematic

Prior to each main engine burn, a normally closed isolation valve is opened on command from the spacecraft sequence system. The quad-redundant regulator package reduces the supply pressure to the settling rocket operating pressure. After the settling system has operated for the necessary duration, the sequencer opens the main engine valves and closes the normally open settling rocket isolation valve.

From Tables III-16 thru III-18, it can be seen that the best settling rocket system performance is obtained with the two-spherical propellant tank configuration for Missions A₁ and A₂ and with the single spherical propellant tank for Mission B. These configurations were assumed for the evaluation.

a. Reliability - Determination of the possible failure modes is based on the components considered critical to the operation of the system. Those failure modes whose probability is extremely low in comparison to other possible modes were not considered. For example, the possibility of a catastrophic failure of the supply tank or lines was ruled out on this basis. There are three possible failure modes that would cause the system to become inoperative: (1) isolation valve fails to open; (2) isolation valve fails to close; and (3) the portion of the onboard computer and sequencer pertinent to the settling system fails to operate. In considering anomalous operation failure modes, there are two possible ways the system could fail that would not necessarily abort the mission: (1) failure of the regulator package to provide the proper outlet pressure; and (2) abnormal settling propellant gas leakage anywhere in the system.

b. Mass - Based on the calculated values and estimates, the mass of the settling rocket system is compiled in Table III-19. An increase in system mass would result from an increase in: (1) the required total impulse; (2) the required thrust; and (3) the settling propulsion system requirements to the point where mono-propellant rockets become desirable.

Table III-19 Settling Rocket System Mass

	MISSION A ₁ (lb _m)	MISSION A ₂ (lb _m)	MISSION B (lb _m)
Gaseous nitrogen	10	11	4
Supply tank	12	12	6
Valves, lines, regulator	17	17	20
Rockets	1	1	1
Vaporized propellant remaining in main tanks	8	2	0
Total system mass	48	43	31

c. Design Scalability and Producibility

1) Design Scalability - Any change in the quantity of propellant in the main propellant tanks prior to each burn, in the number of burns, or in the spacecraft dry weight, would cause a variation in the design. These changes are manifested in the settling rocket thrust and the amount of settling rocket propellant required. Within a certain range of variation, these changes would result in a resizing of the system in order to maintain optimum performance. As greater thrust and total impulse are required, a monopropellant rocket would become the more desirable system.

The redesign required for a monopropellant rocket would introduce many new problems. A catalyst would be required, a propellant acquisition device and pressurization system would be needed for the monopropellant, and consideration of propellant compatibility would be required. Because of these additional requirements, the monopropellant rocket system would be less reliable.

2) Manufacturability - All of the components required for the system have been manufactured for use in attitude control systems. The manufacture of this system should present no new problems.

3) Subscale Test Scalability - Full-scale tests of the cold gas rocket system, by itself, are feasible with parameters such as thrust, specific impulse, and settling rocket storability determined. The inherent problem with this system is that proper rocket operation does not necessarily mean that the propellants are settled. For systems such as bladders, orientation of the propellant is inherent in proper system operation.

Subscale tests to verify the propellant settling times may be desirable. The techniques for accomplishing these types of tests in a drop tower, or using aircraft, are well documented in the literature. Results can be scaled to the full-size system.

d. Compatibility with Adjacent Components and Propellants

1) Propellant/Material Compatibility - The compatibility between the propellant for the settling rocket system and the components of the system is the only area of concern since there is no contact with the main propellants. Use of gaseous nitrogen for the settling propellant presents no problem. The low boiling point of nitrogen makes it compatible with the spacecraft thermal environment.

2) Pressurization System Compatibility - The settling rocket system does not interface directly with the pressurization system; however, the propellant in the main tank is free to move about the tank when the settling system is not operating and there is contact between the pressurant and the propellant. This will affect the pressurant requirements, and pressurant gas solubility and propellant vaporization must be considered.

3) Tankage Compatibility - The shape of the main propellant tanks determines the magnitude of the capillary force which opposes the settling force. A spherical tank offers the least resistance to the settling force and therefore is the configuration requiring the smallest settling thrust and the least amount of settling rocket propellant.

The settling rocket thrust and propellant consumption increases as the L/D ratio for a cylindrical tank increases. Changing the configuration from two to four tanks increases the L/D ratio and causes a further increase in the settling rocket system's size and mass.

4) Performance - A settling rocket system should be capable of meeting the mission and duty cycle requirements. However, the impact on the guidance system must be considered in the application of external settling. The low acceleration levels of the settling rockets require highly-sensitive accelerometers to measure their contribution to the spacecraft velocity increment. The complexity and capacity of the sequencing system must be increased in order to accomplish the start up, shutdown, and timing of the burn duration. An acceptable way to integrate the settling propulsion system and the main propulsion system, so as to obtain the required small impulse bits, is essential.

e. Performance Testability

1) Verification of Operational Readiness - Other than the squib-operated valves, the entire settling rocket system could be functioned and acceptance-tested without any degradation of materials or performance. The squib valves present no new problem since they are qualified on a statistical basis.

2) Development Status - Similar systems have been developed, and used for attitude control and station keeping of satellites.

G. CAPILLARY/BELLOWS

1. System Description and Operation

The capillary/bellows system, a promising new concept devised under Contract NAS9-8939, *Advanced Propellant Management System for Spacecraft Propulsion Systems*, appears capable of satisfying the propellant orientation requirements of the reference missions. This concept, described in Martin Marietta New Technology Disclosure No. 46, employs a bellows accumulator to provide automatic refill of the bellows without the need for valving or other complicated apparatus.

The device consists of a metal bellows fitted with a fine mesh screen at its movable end (as opposed to a solid plate) and a cylindrical screen at its fixed end (Fig. III-23). The fixed end

is positioned over the tank outlet forming a propellant trap. Operation of the device is shown in Figure III-24. Following initial fill of the device and propellant tank, liquid is contained within the device by the capillary forces acting at the screen pores even though an appreciable negative acceleration is applied to the system (Fig. III-24a). The maximum capillary retention pressure across the screen is given by:

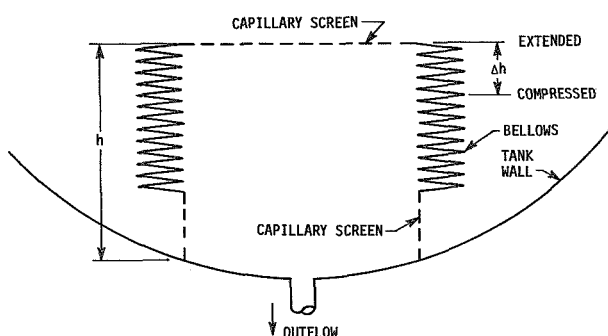


Figure III-23 Capillary/Bellows System

$$\Delta P_c = \frac{2\sigma}{R} \cos \theta \quad [\text{III-9}]$$

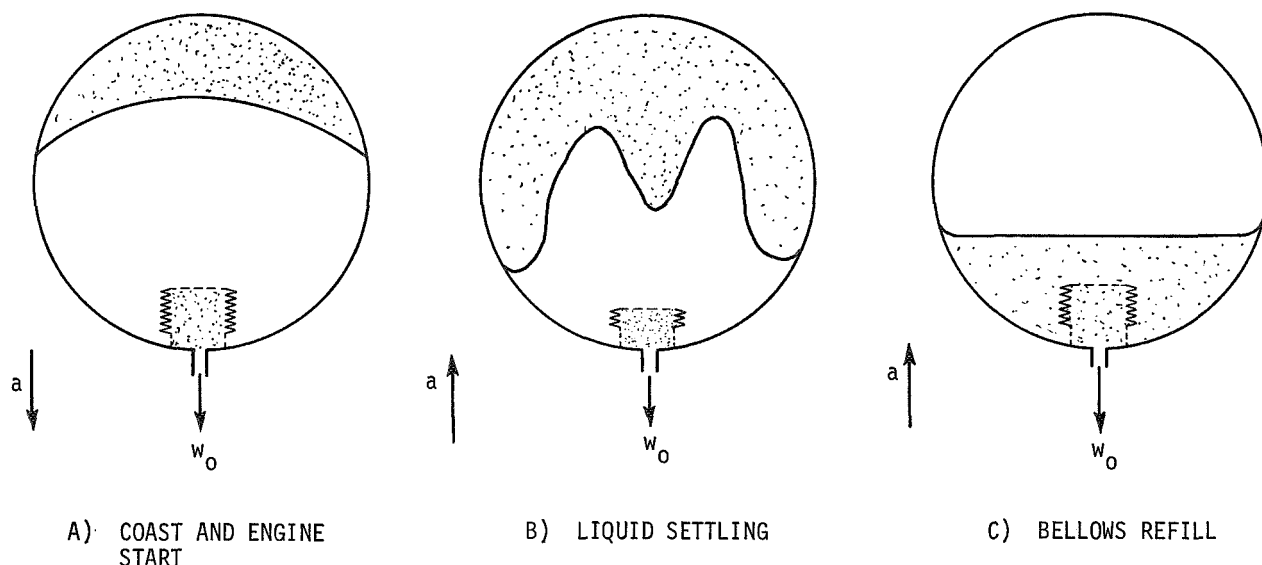


Figure III-24 Operation of the Capillary/Bellows Expulsion Device

The retention force provided by the screen material must be greater than the sum of perturbing forces including that resulting from the hydrostatic head within the device. The hydrostatic pressure acting on the screen is:

$$\Delta P_h = \rho a h \quad [\text{III-10}]$$

where h is the liquid head on the screen parallel to the acceleration vector. Equations [III-9] and [III-10] are used to determine the maximum acceleration the device can withstand without gas ingestion for a given pore size.

At engine start, propellant feed is supplied by the ullage pressure compressing the bellows. The surface tension force of the liquid at the capillary screen interface prevents gas penetration into the bellows reservoir during the compression cycle (Fig. III-24b).

In order for the bellows to be completely compressed (maximum expulsion from the trap), the product of the maximum pressure retention capability of the screen and the effective area of the bellows (A_b) must be greater than the force required to compress the bellows:

$$(\Delta P_c) A_b > F_b, \text{ or} \quad [\text{III-22}]$$

$$\left(\frac{2\sigma}{R}\right) A_b > K_b \cdot y \quad [\text{III-23}]$$

Where F_b is the bellows restoring force, K_b is the bellows spring rate, and y is the bellows travel from the null position. Finally, as liquid settles to the tank bottom as a result of engine thrust (Fig. III-24c), the device will automatically refill as liquid contacts the screen surfaces. The pressure difference across the device decreases to the pressure drop due to flow through the screens (ΔP_e) when liquid contacts the device surfaces. Under this condition, the spring force of the bellows is great enough to produce a reversal of the Equation [III-22] inequality, i.e.,

$$(\Delta P_e) A_b < F_b, \quad [\text{III-24}]$$

which causes the bellows to expand and the capillary/bellows trap refills with liquid.

The bellows restoring force is a product of its spring rate and the distance moved from its null position. As the bellows fills and moves toward its null position, the restoring force decreases. By proper choice of screen weave (which determines ΔP_c), effective area of the bellows, and bellows spring rate, the capillary bellows device can be designed so that its refill rate is greater than the outflow rate, and it will refill during an engine burn after propellant settling has occurred.

A test program to evaluate the feasibility of a capillary/bellows system was conducted as part of this program. The results confirmed that the device could be designed and fabricated. Feasibility of using the device for propellant acquisition was also established. The experimental evaluation is discussed in the Appendix.

2. System Evaluation

a. Reliability - Experience with capillary/bellows is limited to the experimental evaluation conducted during this program. However, metallic bellows have been widely used and are considered very reliable. The device is considered active in that the bellows does move; however, there are no other active components such as valves, linkages, or other mechanical devices. The screen involved is entirely passive.

Catastrophic failure of the device would allow the trapped propellant to escape. This type of failure could result from either a bellows leaf weld failure or a large opening in the screen material. An enlargement of a screen pore or a pinhole leak in a weld could cause an anomalous failure by allowing gas ingestion into the device.

b. Mass - The mass estimates were based on the devices tested, current state-of-the-art bellows manufacture, and fine mesh screen weights. Calculation of the mass of the device for Mission A₁ was based on 280 in.³ of trapped propellant for both fuel and oxidizer tanks. Both oxidizer and fuel devices for Mission A₂ were based on 226 in.³ of trapped fuel and 211 in.³ of trapped oxidizer using stainless steel material. For Mission B, the volume of propellant was 24 in.³ and a device constructed of titanium was assumed. Table III-20 presents the calculated system mass for each mission.

Table III-20 Capillary/Bellows System Mass

MISSION	A ₁ (2 TANKS) (lb _m)	A ₂ (2 TANKS) (lb _m)	B (1 TANK) (lb _m)
Mass of device	3.4	3.4	1.0
Vaporized propellant less He mass	7.7	2.0	0
Mass unexpelled propellants	7.1	8.6	0.4
Total mass	18.2	14.0	1.4

c. Design Scalability and Producibility - Scaling of capillary/bellows for other applications should be accomplished without major redesign. The only apparent limitation is the maximum diameter of metal bellows that can be fabricated. For a material thickness of 0.008 in., a diameter of 27 in. is the current state-of-the-art maximum for welded-leaf bellows. Capability of fabrication of hydroformed bellows is slightly less.

For capillary/bellows devices, the welded-leaf type metallic bellows is the better choice as the design length-to-diameter ratios are lower. An L/D of one is considered to be good design practice for welded-leaf bellows. Hydroformed bellows design favors an L/D greater than two, which results in a tall, slender device rather than the short, large diameter profile desired.

Welding currently limits the use of titanium and aluminum welded-leaf bellows, although they have been fabricated. Additional development is required with these materials. However, neither titanium nor aluminum bellows will have a fatigue life as high as stainless steel bellows because of the differences in mechanical properties. Also, titanium does not have the ductility required for fabrication of hydroformed bellows. Welded-leaf bellows have been made of stainless steel with aluminum ends for joining to aluminum tanks. The joining of titanium to stainless steel is also possible.

Fine mesh screen in stainless steel is commercially available up to 325x2300 mesh Dutch-twill weave, in aluminum to 200x1400 mesh Dutch-twill weave, and in titanium up to 180 mesh twilled weave.

d. Compatibility with Adjacent Components and Propellants - For all the missions, compatible materials are available from which to fabricate screens and bellows. Stainless steel would be used for Missions A₁ and A₂, and aluminum or titanium would be required for Mission B. However, use of an aluminum or titanium bellows for this application is considered questionable at this time.

With a capillary/bellows device, the pressurant contacts the propellant and gas solubility must be considered. The device can be employed with the tank geometries of interest and can be designed for most practical combinations of burn time and number of restarts.

e. Performance Testability - Capillary/bellows devices, like metallic bellows, are capable of numerous cycles when well designed. Development and qualification testing can be accomplished in depth without exceeding the cycle life. The actual devices chosen for a particular mission could be thoroughly tested prior to the mission without jeopardizing the inflight performance or operational life of the unit.

While development experience with capillary/bellows devices is limited, experience with its components, metallic bellows and screen, is considerable. Stainless steel bellows and fine mesh screen are both readily available and have undergone much development.

H. START TANKS

A start tank is a small tank or reservoir that may be located internal or external to the main propellant tank, and that provides sufficient propellant to start the main engine and settle the main tank propellants. After the propellants have been settled in the main tank, engine propellant requirements are supplied directly from the main tanks. The start tank concept is not a specific propellant acquisition device, but a method that may employ various acquisition techniques.

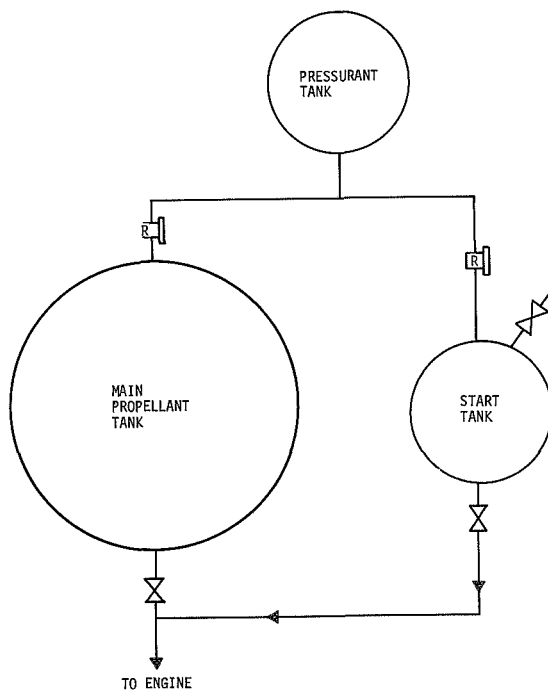


Figure III-25 Propellant Start Tank Schematic

Figure III-25 schematically illustrates how a start tank could be integrated into a main propulsion system. A propellant acquisition device is required within the start tank to maintain liquid at its outlet. In order to start the engine, the valve at the start tank outlet is opened allowing propellant to flow to the engine. After an engine burn time sufficient to ensure propellant settling in the main tank, the valve at the main tank outlet is opened, allowing the engine propellant requirements to be supplied from the main tank, and the start tank outlet valve is closed.

The volume of the propellant start tank for the operational cycle just described would have to be large enough to accommodate all the engine start requirements anticipated in the mission. However, if refilling of the start tank could be ensured during

thrust periods, the restart volume could be reduced. One possible method of refilling could be accomplished by venting the start tank ullage after the main tank propellants had been settled. The ullage venting allows the acquisition device to return to its original position and would allow propellant from the main tank to flow into the start tank. A disadvantage to this refilling process is added complexity to the design and operation of the pressurization system.

Various propellant acquisition devices could be used in the start tank system. Surface tension devices such as the propellant trap and the capillary/bellows are essentially internally mounted start tanks and have been discussed at some length in previous sections of this chapter. These devices could also be used in an external start tank; however, there would be no particular advantage to an external application since it would be more complicated to operate and would be a heavier installation.

Bladders, diaphragms, and bellows could also be used in external start tanks. Application of these devices in start tanks could provide flexibility and possibly weight reduction over use of these devices in the main propellant tank. In the start tank application, these devices would be required to orient only the start propellant and not the total propellant volume. However, valving and operational complexity, especially if recycling of the device is desired, would reduce reliability.

In a similar manner, dielectrophoresis could be applied to the start tank system. The grid size and voltage requirements would be reduced when compared to the requirements for a main tank system. However, the resulting weight savings would be nullified by the decreased reliability again developing from the valving and sequencing requirements.

Other start tank arrangements are possible. However, all the arrangements would employ a propellant acquisition system similar to the devices considered for the main propellant tank. Therefore, the evaluation applied to the acquisition concepts in the main propellant tank would equally apply to those devices used in the start tanks. For this reason and because of the reduced reliability, start tanks were not considered in evaluating propellant acquisition concepts.

IV. PRESSURIZATION SYSTEM

All of the baseline propulsion systems for the three missions considered in this program employ a stored-gas pressurization system. As shown in Figures II-3, II-4, and II-5, Mission A₁ and A₂ use a regulated pressurant supply from a separate storage container or containers, while Mission B utilizes a blowdown system with both pressurant and propellant contained in a single tank. The candidate pressurants for these systems were helium and nitrogen gas.

The primary objectives of the pressurization system analyses were: (1) to determine the effects of pressurant type (helium or nitrogen), propellant temperature, propellant tank pressurant inlet temperature, pressurant storage temperature and initial storage pressure, and pressurant leakage and solubility on pressurization system mass, and (2) to determine the effects of the same parameters on design and selection of the propellant acquisition system. An evaluation of the effect of number of propellant tanks on the pressurization system was also made. Results obtained from the analyses are presented in this chapter for each of the three reference missions.

The impact of the parameters of interest on the pressurization subsystem mass was established by conducting a propellant tank thermodynamic analysis and a pressurant storage analysis followed by evaluations of pressurant leakage and solubility. The tank thermodynamic analysis evaluated pressurant usage for each mission as a function of type of pressurant (helium or nitrogen), propellant temperature, and pressurant inlet temperature for cases with and without complete vapor barrier separation of propellant and pressurant. The quantity of propellants vaporized was also determined as a function of these parameters, and the resultant pressurant usage data were then used in conducting the pressurant storage analysis. This analysis evaluated the amount of pressurant stored and the mass of the pressurant storage tank as a function of type of pressurant, initial pressurant storage pressure, pressurant storage temperature, and pressurant usage. After completing the pressurant storage analysis, pressurant leakage and solubility were evaluated. The pressurization subsystem mass was determined as the sum of the pressurant mass stored (used and residual), the storage container mass, mass of vaporized propellants, pressurant leakage mass, and dissolved pressurant mass.

Undue emphasis should not be placed on the absolute values obtained for pressurization subsystem mass because the pressurization studies were primarily conducted for comparative purposes only. Many of the ground rules and assumptions employed are not necessarily conservative and contingency factors were not included. When the thermal environment has been established and a detailed system design is available, more realistic values for the actual flight pressurization subsystem mass can be obtained by more stringent analytical techniques. However, the results obtained from this investigation do serve the intended purpose of providing the preferred pressurant type and storage and operating conditions for the three missions under consideration.

The second objective of the pressurization studies was accomplished by determining the effects of pressurant type and pressurant inlet temperature on the candidate acquisition concepts. Also of primary importance, the amount of propellant vaporized was considered in the design and selection of the acquisition device. Other pressurization system considerations investigated were pressurant solubility, permeation of positive expulsion materials, and surface tension device temperature sensitivity.

A. PRESSURIZATION SUBSYSTEM MASS

The tank thermodynamic and pressurant storage analyses conducted for the three reference missions together with the basic assumptions and ground rules employed are discussed in this section. The results are presented for each mission.

1. Mission A₁

The thermodynamic analysis for this mission, characterized by the space storable propellant combination of OF_2 and B_2H_6 , was conducted using the Martin Marietta OD041 computer program, *Analysis of Propellant Tank Pressurization*. The ground rules for the analysis were: (1) propellant tank operating pressure was 350 psia; (2) initial ullage was 10 percent; (3) propellant temperature range was 210 to 280°R with a nominal value of 250°R; (4) temperature of the tank insulation outer surface was equal to the conditioned environmental temperature that varied linearly with time from 282°R in Earth orbit to 258°R in Mars orbit; and (5) pressurant inlet temperature range was 210 to 530°R. The two-tank, spherical configuration was employed using the Mission A₁ propellant load and outflow schedule presented in Table IV-1.

Table IV-1. Propellant Outflow Schedule, Missions A₁ and A₂

	MISSION A ₁			MISSION A ₂		
	Burn Time (sec)	B ₂ H ₆ (lb _m)	OF ₂ (lb _m)	Burn Time (sec)	MMH (lb _m)	N ₂ O ₄ (lb _m)
Total loaded		270.0	810.0		562.0	872.0
First midcourse	2.5	1.62	4.86	8.3	3.35	5.2
Second midcourse	2.5	1.62	4.86	8.3	3.35	5.2
Orbit insertion	395.0	256.5	769.5	1317.0	534.0	828.5
First orbit trim	5.4	3.51	10.53	18.0	7.3	11.3
Second orbit trim	5.0	3.24	9.72	16.6	6.7	10.5
Third orbit trim	5.4	3.51	10.53	18.0	7.3	11.3

Tank external heat flux was calculated from thermal data provided by JPL for use with this investigation. The thermal data, listed in Table IV-2, were not readily usable for this analysis because of the differences of initial conditions, pressurant type and pressurant inlet temperature. Therefore, effective conductances were calculated and are also shown in Table IV-2. The effective conductances were calculated for each tank and each orbit as

$$K_{\text{eff}} = \frac{q/a}{\Delta T} \quad [\text{IV-1}]$$

where

q/a = heat flux into the tank, Btu/hr-ft²

ΔT = temperature difference between liquid and insulation, °R

K_{eff} = effective conductance, Btu/hr-ft²-°R.

Since the effective thermal conductance was essentially the same for both tanks in either Earth or Mars orbit and was about 0.001 Btu/hr-ft²-°R, this value was used as K_{eff} in calculating tank heating rates for the entire mission including transfer between planets. Tank heating rates were obtained from:

$$q = K_{\text{eff}} A_{\text{wall}} (T_{\text{ins}} - T_{\text{liq}}) \quad [\text{IV-2}]$$

Table IV-2 Mission A₁ Thermal Criteria

	EARTH ORBIT		MARS ORBIT	
	OF ₂	B ₂ H ₆	OF ₂	B ₂ H ₆
Temperature, top of insulation (T_{ins}), °R	282	282	258	258
Temperature, liquid (T_{liq}), °R	237	325	247	298
Effective thermal conductivity (k), Btu/hr-ft-°R	0.39×10^{-4}	0.54×10^{-4}	0.38×10^{-4}	0.45×10^{-4}
Heat flux (q/A), Btu/hr-ft ²	0.047	-0.05	0.01	-0.04
Thermal conductance (K_{eff}), Btu/hr-ft ² -°R	0.001045	0.001045	0.00091	0.001

The thermodynamic analysis was characterized by the following assumptions and calculations:

- 1) Pressurant inlet temperature was constant;
- 2) During pressurization and propellant outflow, the ullage, liquid, and tank wall temperatures were calculated separately;
- 3) During coast, the ullage liquid, and tank wall reached an equilibrium temperature instantaneously;
- 4) Without a vapor barrier, both heat and mass transferred could occur at the gas/liquid interface;
- 5) With a vapor barrier, only heat transfer could occur at the interface;
- 6) Mass transfer at the interface considered only propellant vapors;
- 7) The ullage gas was considered to behave ideally.

Condensation of gaseous nitrogen within the propellant tank was not considered in this analysis since it would be slight and could only occur at the minimum propellant temperature of 210°R. The worst case for nitrogen condensation would occur in the diborane tank since the ullage vapors are almost entirely gaseous nitrogen. At the 350-psia operating pressure, the saturation temperature of nitrogen is approximately 215°R and some condensation would occur on the 210°R tank walls and at the 210°R liquid surface. Thus, the nitrogen usage values at the minimum propellant temperature would have been slightly higher if condensation had been considered.

Helium and nitrogen usage for both propellant tanks was calculated for three propellant temperatures and four pressurant inlet temperatures. Tank pressure and ullage and liquid temperature histories were also obtained, and the effect of a vapor barrier (no propellant vaporization allowed) on propellant usage was determined at the nominal propellant temperature. The results for Mission A₁ are presented in Tables IV-3, IV-4, and Figures IV-1 through IV-5. Tables IV-3 and IV-4 show the results of the parametric analysis for the OF₂ tank and the B₂H₆ tank. Total helium and nitrogen quantities required as a function of both pressurant inlet and propellant temperatures for cases with and without a vapor barrier are presented in Figures IV-1 and IV-2, respectively. Of the parameters studied, pressurant inlet temperature and type of pressurant produce the greatest effect on pressurant usage. The mass of nitrogen required for pressurization is about six to seven times greater than that required for helium. This is essentially the nitrogen-to-helium molecular weight ratio. Pressurant mass required at the higher inlet temperature ranges 20 to 25 percent lower than that at the lower inlet temperatures. The effects of initial liquid temperature and use of a vapor barrier are not as significant as the other two parameters.

The amount of OF₂ vaporized with no vapor barrier in the tank is shown in Figure IV-3 as a function of pressurant inlet temperature, type of pressurant, and initial liquid temperature. The amount of B₂H₆ vaporized, on the order of 0.1 lb_m, is not shown since it was considered to be insignificant. At the lower pressurant inlet temperatures, the amount of OF₂ vaporized is about the same for helium and nitrogen. As the pressurant inlet temperature increases, the amount of vaporized propellant increases and is higher for nitrogen than for helium. The quantity vaporized increases approximately 35 percent for nitrogen pressurant and about 25 percent for helium as the pressurant inlet temperature increases from 210 to 530°R.

Calculated tank pressure and liquid temperature histories for both propellant tanks are shown in Figures IV-4 and IV-5. The environmental temperature used to calculate tank heat flux is also presented. Helium pressurant at 250°R was used in these calculations. The pressure histories are similar for both tanks. Prior to the first propulsion event, the tanks were pressurized from 100 psia to the operating pressure of 350 psia. Following the first engine burn, the pressure dropped immediately in both tanks because of the assumption that equilibrium is reached instantaneously.

Table IV-3 Results of Thermodynamic Analysis for
Mission A₁, OF₂ Propellant Tank

LIQUID TEMPERATURE (°R)	PRESSURANT	PRESSURANT INLET TEMPERATURE (°R)	VAPOR BARRIER	PRESSURANT USAGE (lb _m)	VAPORIZED PROPELLANT MASS (lb _m)
210 ↓ 250 ↓ 280 ↓	Helium ↓	210 300 400 530 210 300 400 530 210 300 400 530	No ↓ ↓ ↓ Yes ↓ ↓ ↓ No ↓	5.54 4.81 4.36 4.15 5.10 4.38 4.11 3.89 5.38 4.77 4.53 4.20 4.78 4.18 3.98 3.73	6.97 7.49 8.09 8.87 7.82 8.38 9.11 10.16 0 ↓ 8.57 9.23 10.06 11.09
210 ↓ 250 ↓ 280 ↓	Nitrogen ↓	210 300 400 530 210 300 400 530 210 300 400 530	No ↓ ↓ ↓ Yes ↓ ↓ ↓ No ↓	38.95 33.43 30.03 27.95 35.97 30.40 28.51 26.44 37.94 53.42 31.86 29.67 33.79 29.02 27.37 25.16	6.71 7.56 8.47 9.71 7.63 8.49 9.59 10.90 0 ↓ 8.43 9.36 10.51 11.99

Table IV-4 Results of Thermodynamic Analysis for Mission A₁, B₂H₆ Propellant Tank

LIQUID TEMPERATURE (°R)	PRESSURANT	PRESSURANT INLET TEMPERATURE (°R)	VAPOR BARRIER	PRESSURANT USAGE (lb _m)	VAPORIZED PROPELLANT MASS (lb _m)
210	Helium	210	No	5.61	0.10
↓		300	↓	4.94	0.11
↓		400	↓	4.70	0.10
↓		530	↓	4.37	0.11
250		210	↓	5.31	0.10
↓		300	↓	4.88	0.10
↓		400	↓	4.61	0.10
↓		530	↓	4.25	0.11
↓		210	Yes	5.49	0
↓		300	↓	4.89	↓
↓		400	↓	4.64	↓
↓		530	↓	4.31	↓
280		210	No	5.10	0.10
↓		300	↓	4.83	0.10
↓		400	↓	4.57	0.11
↓		530	↓	4.23	0.12
<hr/>					
210	Nitrogen	210	No	39.61	0.10
↓		300	↓	34.53	0.10
↓		400	↓	32.97	0.12
↓		530	↓	30.68	0.13
250		210	↓	37.72	0.10
↓		300	↓	34.18	0.11
↓		400	↓	32.51	0.12
↓		530	↓	30.17	0.13
↓		210	Yes	38.77	0
↓		300	↓	34.29	↓
↓		400	↓	32.66	↓
↓		530	↓	30.40	↓
280		210	No	36.33	0.10
↓		300	↓	33.94	0.11
↓		400	↓	32.15	0.12
↓		500	↓	29.77	0.14

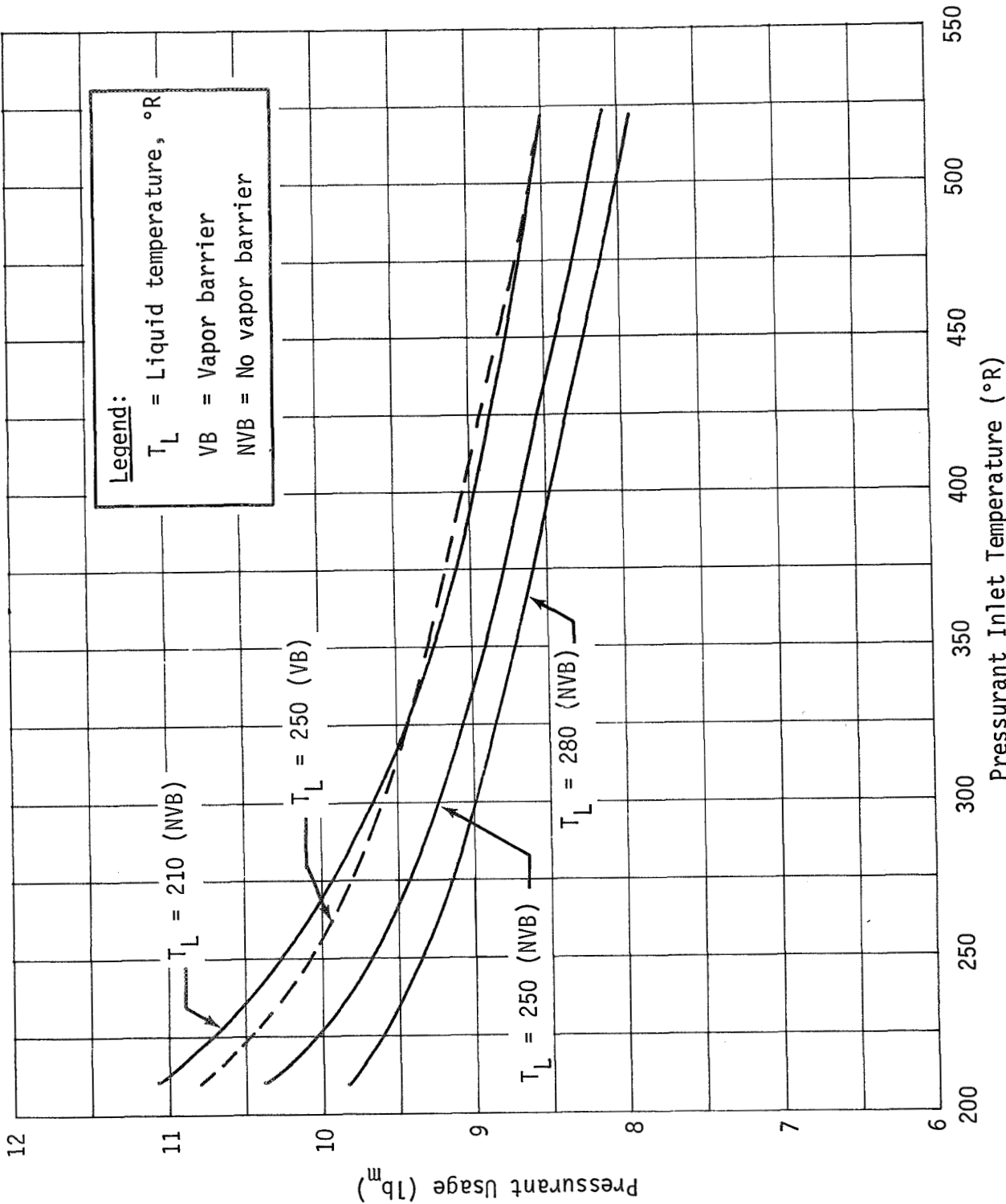


Figure IV-1 Total Helium Usage for Mission A1

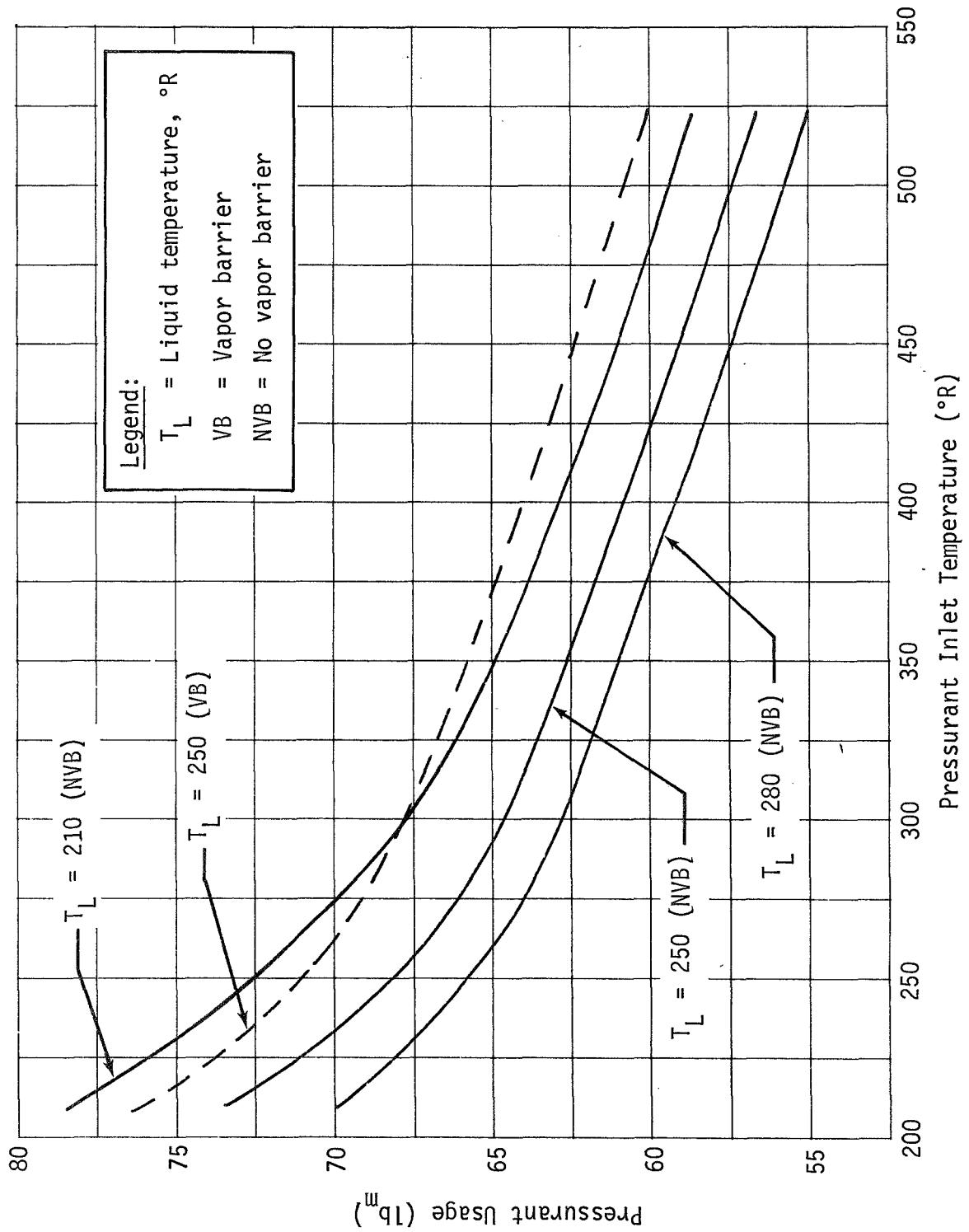
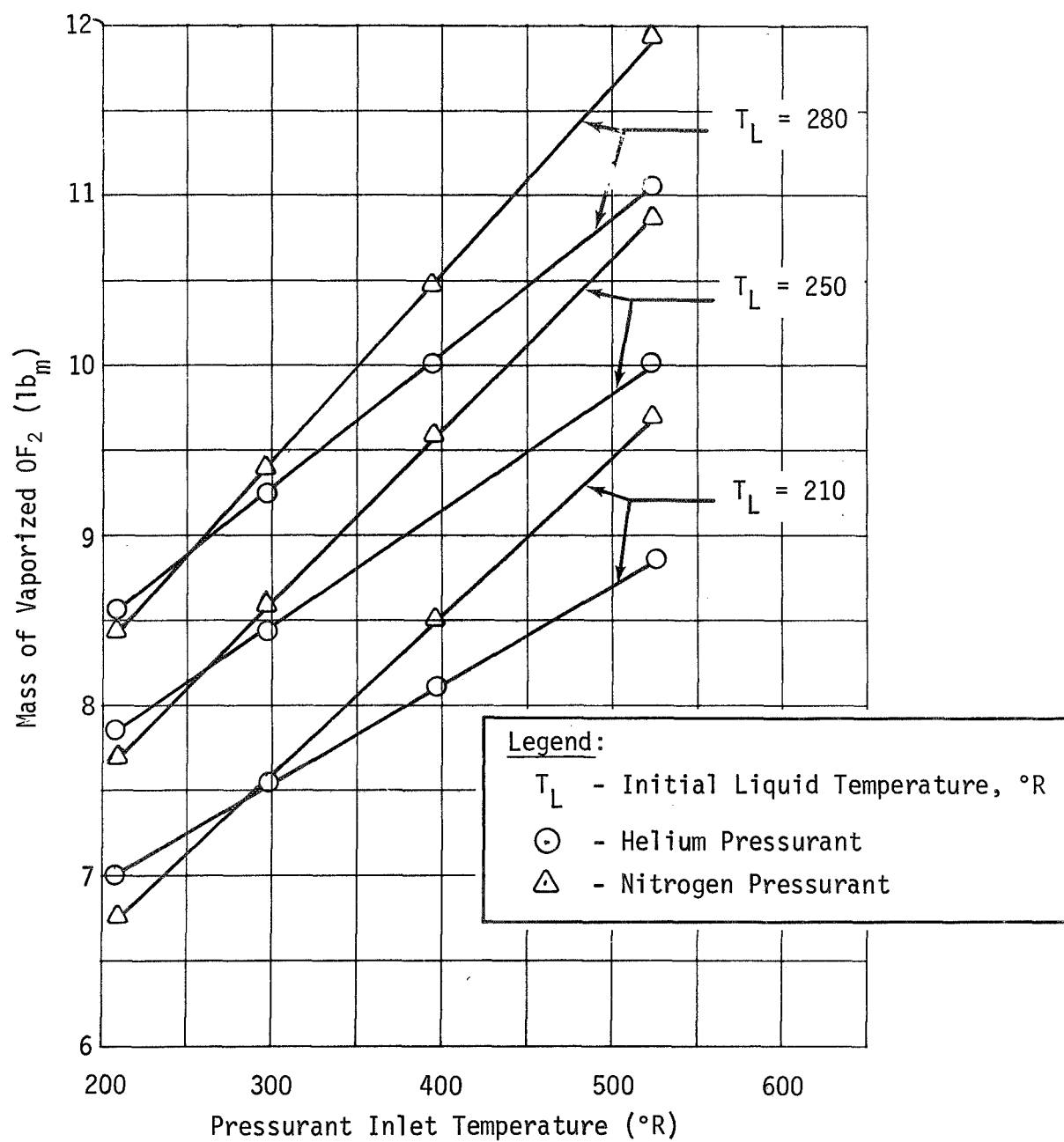


Figure IV-2 Total Nitrogen Usage for Mission A1

Figure IV-3 Mission A₁ Vaporized Oxygen Difluoride

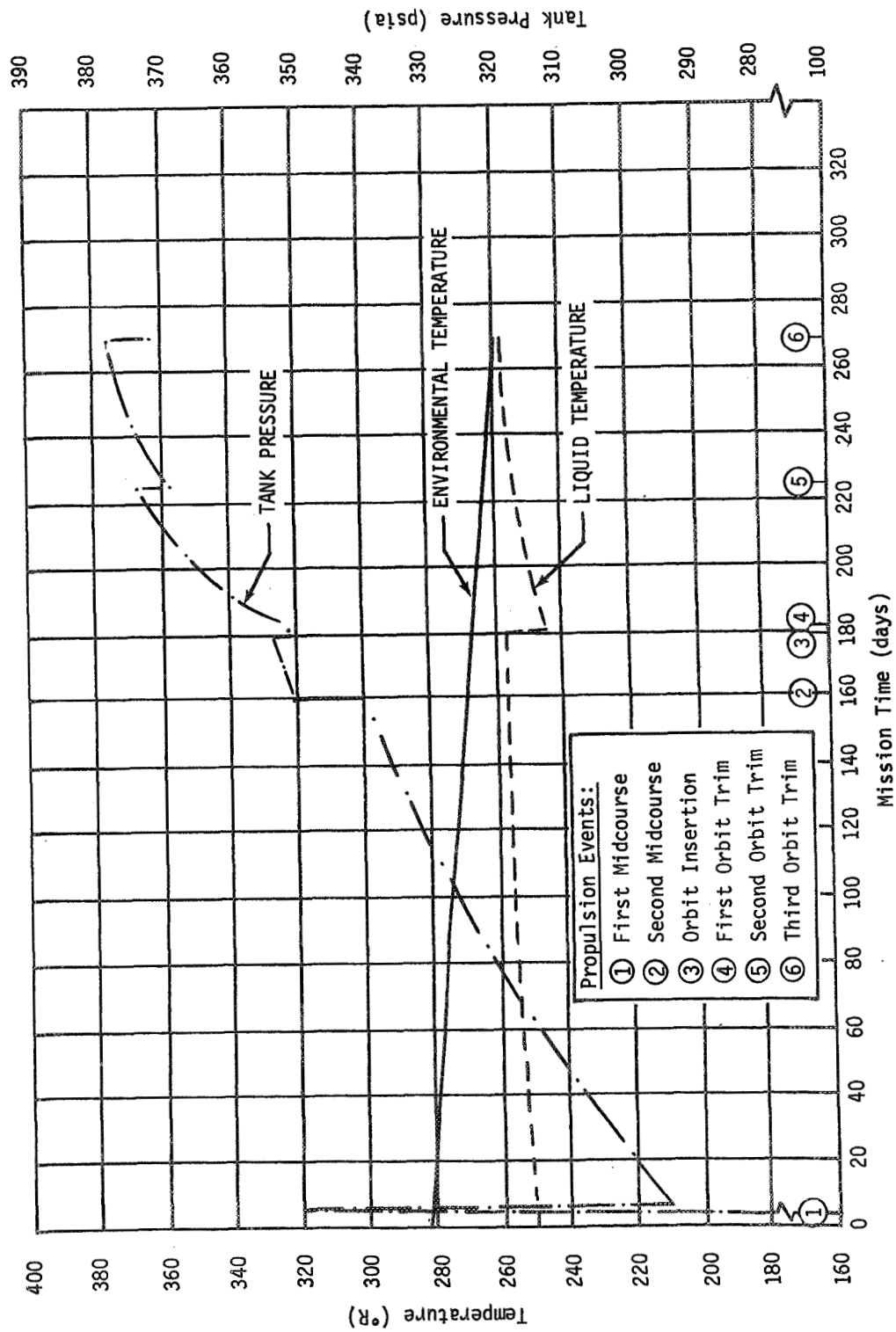


Figure IV-4 Pressure and Temperature Histories for Mission A₁ Oxygen Difluoride Tank (Helium Pressurant Entering at 250°R)

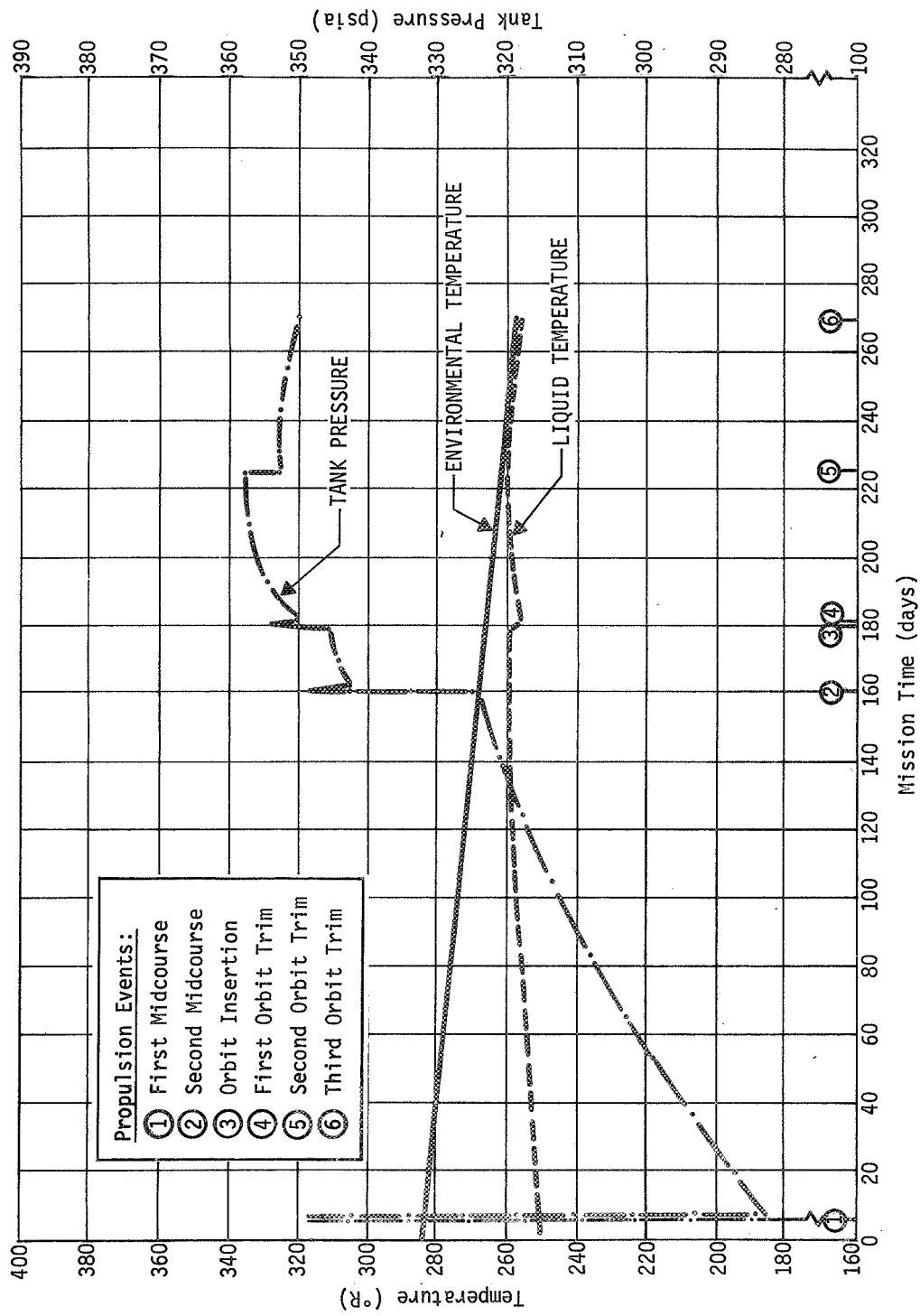


Figure IV-5 Pressure and Temperature Histories for Mission A₁ Diborane Tank (Helium Pressurant Entering at 250°R)

The pressure drop was 55 psi and 68 psi for the OF_2 and B_2H_6 tanks, respectively. After this drop, the tank pressures gradually rise due to environmental heating during the long coast period. Prior to the second propulsion event, the tanks were again pressurized to operating pressure. The third propulsion event (orbit insertion) used 95 percent of the loaded propellants. After this event, only 3.7 percent of the loaded propellants remained in the tanks. Prior to orbit insertion, both liquid temperatures showed a gradual increase from the initial value of 250°R . The OF_2 temperature increased 8 degrees while the B_2H_6 temperature increased 10 degrees during this time period.

Following the orbit insertion burn, the propellant temperatures decreased in both tanks due to the occurrence of vaporization which reestablished vapor/liquid equilibrium. During the burn period with pressurant inflow and propellant outflow, the ullage is enriched with pressurant and heat is transferred to the propellant. This produces a propellant vapor pressure greater than the partial pressure of propellant vapors in the ullage. Upon cessation of pressurization (end of the burn period), vaporization occurs until vapor pressure/partial pressure equality is attained. The B_2H_6 temperature decreased only 2 degrees while the OF_2 temperature decreased approximately 11 degrees because of the greater vaporization of OF_2 . Following these decreases, both liquid temperatures increased to and followed slightly below the environmental temperature. The tank pressures increased following both the third and fourth propulsion events. The OF_2 tank pressure increased 24 psi following the fourth event. This increase corresponds to the increase in the equilibrium (or liquid) temperature. The B_2H_6 tank pressure followed a similar profile, but the pressure rise was only 8 psi. Following the fourth propulsion event, tank pressures did not drop below the operating pressure and no pressurant was required for the remainder of the mission. These pressure and temperature profiles are representative of most of the other nominal propellant temperature cases analyzed.

Using information generated in the propellant tank thermodynamic analysis, the pressurant storage analysis for Mission A₁ was conducted. Two computer programs simulating the expansion of helium and nitrogen from a spherical container were employed. The helium gas expansion program is described in detail in Reference IV-1. The nitrogen program was developed by modifying the helium program; this involved changing the equation of state, enthalpy, and specific heat calculations from helium to nitrogen using data from Reference IV-2.

Criteria and ground rules employed for the pressurant storage analysis were: (1) Storage pressure range of 2000 to 4000 psia; (2) Minimum allowable storage pressure of 400 psia; (3) Storage temperature range of 210 to 530°R for helium and 400 to 530°R for nitrogen; (4) a 6Al-4V titanium pressurant storage tank with a safety factor of 2.2 based upon an ultimate strength of 165,000 psi; (5) A factor of 1.1 to account for bosses, welds, etc. in calculating tank mass.

The range of nitrogen storage temperatures considered was smaller than that for helium to circumvent nitrogen phase change during the expansion process. For example, if nitrogen gas were expanded through the pressure regulator from 3000 psia and 250°R to 350 psia by an isenthalpic process, the temperature would drop below the critical temperature (227°R) and two-phase fluid would result. The critical pressure for nitrogen is 493 psia. The temperature at which nitrogen can be stored to ensure that a phase change will not occur is dependent upon the storage pressure. At a storage pressure of 2000 psia, the nitrogen could be stored at approximately 310°R and, at 3000 psia, the storage temperature could be approximately 322°R without incurring a phase change during expansion to 350 psia. For this analysis, nitrogen storage temperatures of 400 and 530°R were selected since pressurant usage data were obtained in the thermodynamic analysis at corresponding values of pressurant inlet temperatures.

The primary objective of the pressurant storage analysis was to determine the storage tank size and amount of pressurant that must be stored in order to obtain a minimum pressure of 400 psia for the selected storage conditions and duty cycle. The point during the mission at which the minimum pressure occurred was a function of the pressurant outflow rates. The average pressurant outflow rate for each event was obtained by summing the pressurant usage data from both tanks and dividing by the duration time of each event. In all cases, the minimum pressure occurred at the end of either orbit insertion or the final propulsion event (third orbit trim). For the cooler pressurant inlet and storage temperatures, the minimum pressure occurred during orbit insertion; for the warm temperatures, the minimum pressure occurred during the final event.

An iterative procedure was used to calculate the tank size and amount of pressurant stored that would provide this minimum pressure during the expansion duty cycle. This iteration procedure is part of the computer program employed. An assumed mass of stored pressurant was input to the program along with the storage temperature, initial pressure and pressurant outflow rate. In the program, the gas was expanded according to the specified duty cycle and a minimum pressure was obtained. This minimum pressure

was then compared with the desired minimum pressure of 400 psia. If the difference was more than ± 1 psi, a new pressurant stored mass was calculated and the expansion process repeated for the same storage conditions and duty cycle until the minimum pressure calculated was 400 ± 1 psia.

The pressurant storage analysis was characterized by the following assumptions:

- 1) Tanks were isothermal;
- 2) Pressurant mass outflow rate was constant during each pressurization event;
- 3) Free convection heat transfer between the gas and isothermal walls was considered during each pressurization event;
- 4) During coast periods the gas reached an equilibrium condition with the wall.

Real gas thermodynamic and physical properties were used. The equations of state and enthalpy relationships for nitrogen and helium presented in References IV-2 and IV-3, respectively, were incorporated into the computer programs and used to calculate specific heats. The values calculated from these equations are in good agreement with actual data for the temperature and pressure ranges considered.

Results of the pressurant storage analysis are presented in Table IV-5 in terms of mass of pressurant stored and storage tank mass. For both pressurants, the mass of stored pressurant decreases as the storage temperature increases. However, at 530°R storage temperature, the mass of nitrogen stored is approximately seven times greater than that for helium. The initial storage pressure has the same effect upon storage mass as storage temperature except to a smaller degree. As the initial storage pressure increases from 2000 to 4000 psia, the mass of pressurant stored decreases approximately 1 to 2 pounds for helium and 7 to 8 pounds for nitrogen, depending upon the storage temperature. Changes in storage temperature have the opposite effect on storage tank mass. The mass of the storage tank increases as the storage temperature increases. This effect is directly attributed to the increase in storage volume which increases with temperature for both helium and nitrogen. This increase in tank mass is about 30 percent for both gases. It should be noted that the storage tank mass for the helium cases is slightly higher than that for nitrogen.

Table IV-5 Results of Pressurant Storage Analysis for Mission A₁

PRESSURANT	PRESSURANT STORAGE TEMPERATURE (°R)	INITIAL PRESSURANT STORAGE PRESSURE (psia)	MASS OF PROPELLANTS VAPORIZED (lb _m)	PRESSURANT USAGE (lb _m)	PRESSURANT STORED MASS (lb _m)	STORAGE TANK MASS (lb _m)	PRESSURIZATION SUBSYSTEM MASS (lb _m)
Helium	210	2000	7.92	10.42	16.09	65.09	89.10
	↓	2500	↓	↓	15.06	63.20	86.18
	↓	3000	↓	↓	14.43	62.76	85.11
	↓	3500	↓	↓	13.97	62.84	84.73
	210	4000	7.92	10.42	13.65	63.43	85.00
	300	2000	8.48	9.26	12.80	71.02	92.30
	↓	2500	↓	↓	11.98	68.40	88.86
	↓	3000	↓	↓	11.47	67.31	87.26
	↓	3500	↓	↓	11.12	66.97	86.57
	300	4000	8.48	9.26	10.86	67.13	86.47
Helium	530	2000	10.26	8.15	10.72	100.10	121.08
	↓	2500	↓	↓	10.20	96.93	117.39
	↓	3000	↓	↓	9.87	95.64	115.77
	↓	3500	↓	↓	9.65	95.11	115.02
	530	4000	10.26	8.15	9.49	95.10	114.85
	400	2000	8.59	61.02	76.74	65.18	150.51
	↓	2500	↓	↓	73.57	63.83	145.99
	↓	3000	↓	↓	71.74	64.45	144.78
	↓	3500	↓	↓	70.58	66.18	145.35
	400	4000	8.59	61.02	69.78	68.59	146.96
Nitrogen	530	2000	11.00	56.60	72.91	91.26	175.17
	↓	2500	↓	↓	69.53	88.65	169.18
	↓	3000	↓	↓	67.51	88.03	166.54
	↓	3500	↓	↓	66.71	88.66	166.37
	530	4000	11.00	56.60	65.21	89.93	166.14

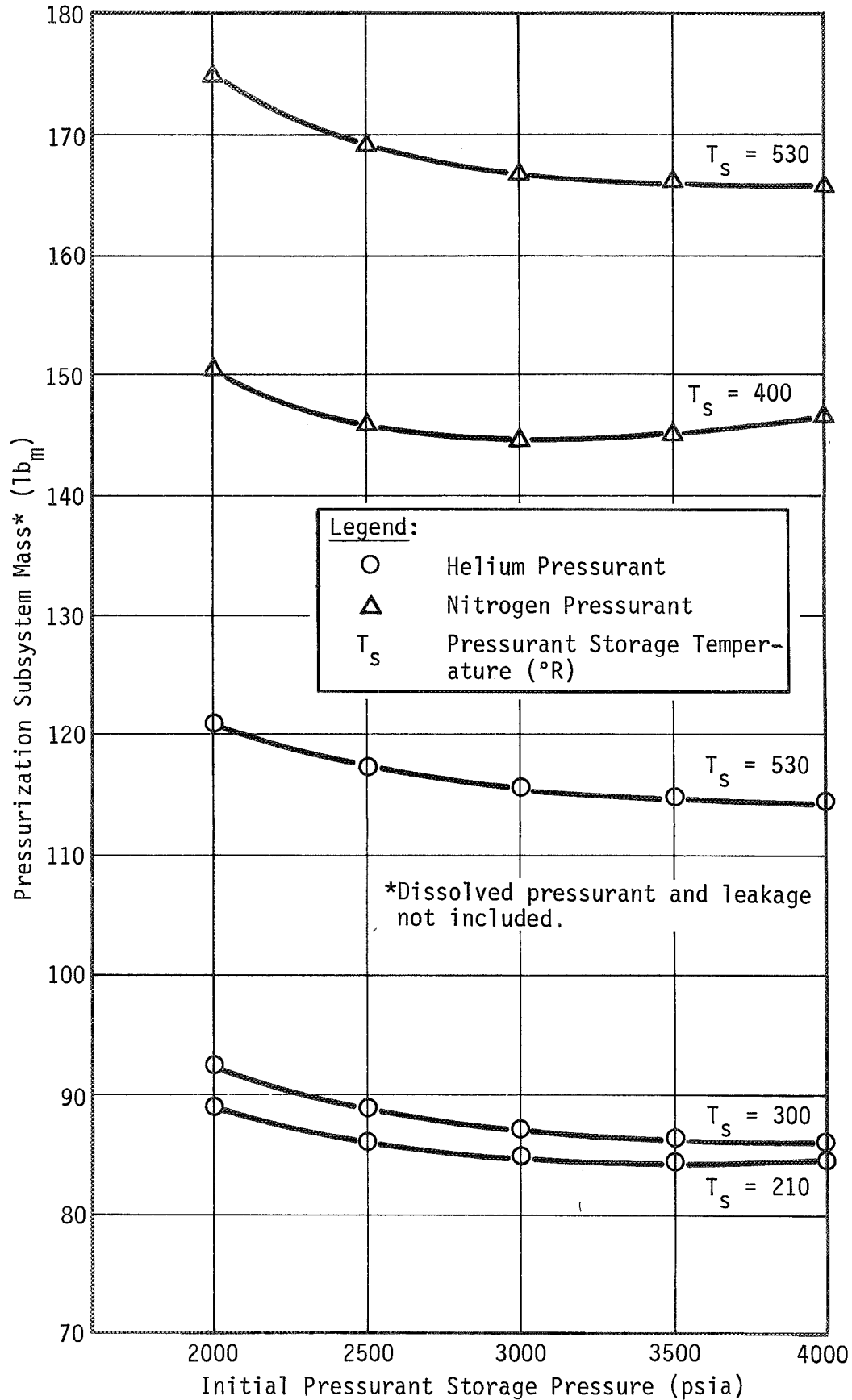
This again is attributed to the difference in volume. The changes in storage pressure produced an interesting effect on the storage tank mass. In four of the five cases studied, the tank mass decreased to a minimum and then increased again as the storage pressure increased from 2000 to 4000 psia. This minimum tank mass occurred at approximately 3500 psia for helium and at 2500 to 3000 psia for nitrogen, depending upon the storage temperature. For a storage temperature of 530°R, the minimum helium tank mass occurred at 4000 psia storage pressure which was the maximum pressure considered.

The results of the overall pressurization analysis are presented in Table IV-5 and Figure IV-6. Pressurization subsystem mass is shown as a function of type of pressurant, storage temperature, and initial storage pressure in Figure IV-6. The data presented are for the nominal propellant temperature only and for pressurant inlet temperatures that correspond to the storage temperatures. In this case, the pressurization subsystem mass is the sum of the mass of vaporized propellant, pressurant stored, and pressurant storage tank; dissolved pressurant and leakage are not included. Figure IV-6 clearly shows a significant reduction of about 30 to 40 percent in pressurization subsystem mass if helium is used as a pressurant instead of nitrogen. This figure also shows that there is approximately a 25% reduction in the subsystem mass when helium is stored at 300°R instead of 530°R. However, a further reduction in storage temperature to 210°R does not produce a significant reduction in subsystem mass. A definite minimum point for subsystem mass was obtained only at storage temperatures of 210°R for helium and 400°R for nitrogen. At the 300 and 530°R storage temperatures for helium and 530°R storage temperature for nitrogen, the pressurization subsystem mass only decreases slightly between 3000 and 4000 psia.

2. Mission A₂

The parametric analyses for this mission were conducted in conjunction with those for Mission A₁. Mission A₂ is characterized by the earth storable propellant combination of N₂O₄ and MMH. The thermodynamic analysis for Mission A₂ was also conducted using the OD041 computer program. The ground rules followed for this analysis were:

- 1) The tank wall was considered isothermal;
- 2) Propellant temperature range was 515 to 535°R with a nominal value of 525°R;
- 3) Pressurant inlet temperature was the same as liquid temperature;
- 4) Propellant tank operating pressure was 350 psia;
- 5) Initial ullage was 10 percent.

Figure IV-6 Mission A₁ Pressurization Subsystem Mass

The two-tank, spherical configuration was employed with the Mission A₂ propellant load and outflow schedule presented in Table IV-1. Helium and nitrogen usage for both propellant tanks was calculated at the nominal propellant temperature with and without a vapor barrier, for pressurant inlet temperatures equal to the propellant temperature. Pressurant usage values were also calculated for the case where the propellants, tank walls, and pressurant inlet temperatures decreased linearly from 535°R at the start to 515°R at the end of the mission. The parametric analysis also calculated the amount of propellant vaporized during the mission. Because of the low vapor pressure of MMH at the nominal propellant temperature, the analysis assumed this propellant to be nonvolatile and only the amount of N₂O₄ vaporized was calculated. This analysis also used the same assumptions that were used in the Mission A₁ analysis.

The results of thermodynamic analysis for Mission A₂ are presented in Table IV-6; they are consistent with the results obtained in the Mission A₁ analysis. Nitrogen usage for all cases investigated was again approximately seven times greater than the helium usage. These calculated usage values do not vary significantly for the small range of propellant and pressurant inlet temperatures investigated. Also, use of a vapor barrier has little effect on pressurant usage. Slightly more pressurant is required with a vapor barrier, since additional pressurant mass is required to compensate for the absence of propellant vapor in the ullage above the barrier. With no vapor barrier, the mass of vaporized N₂O₄ ranged from 1.5 to 2 pounds for all the cases considered.

Table IV-6 Results of Thermodynamic Analysis for Mission A₂

LIQUID TEMPERATURE (°R)	PRESSURANT	PRESSURANT INLET TEMPERATURE (°R)	VAPOR BARRIER	PRESSURANT USAGE (lb _m)	VAPORIZED N ₂ O ₄ (lb _m)
525	Helium	525	No	5.32	2.01
525	↓	525	Yes	5.38	--
535-515	↓	535-515	No	5.42	1.51
525	Nitrogen	525	No	37.30	1.79
525	↓	525	Yes	37.83	--
535-515	↓	535-515	No	39.44	1.51

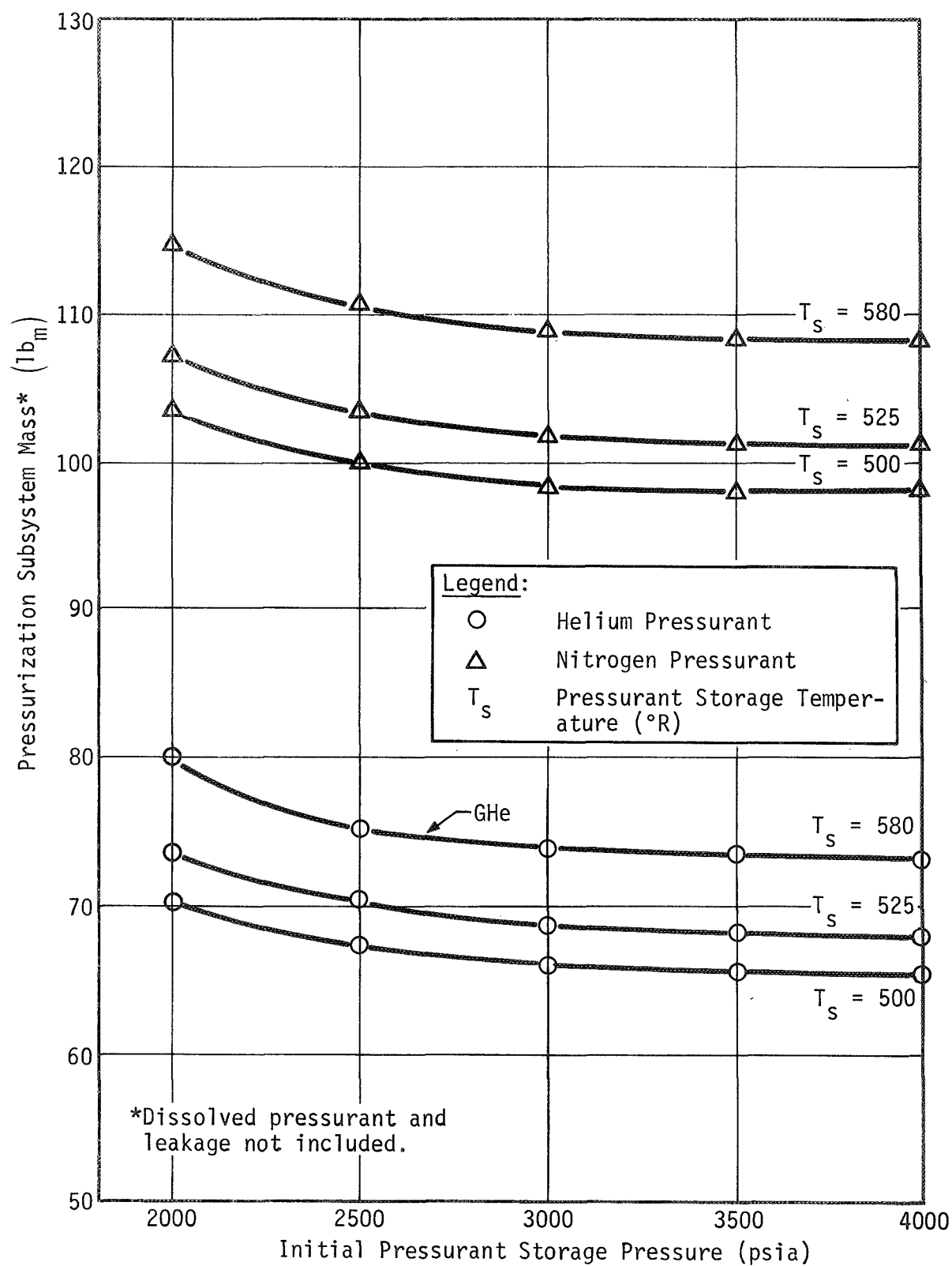
The pressurant storage analysis for Mission A₂ was conducted using the same method of analysis as was used on Mission A₁. This included using the same two gas expansion computer programs to evaluate pressurant stored mass and tank mass. The Mission A₁ analysis ground rules were used except that (1) pressurant storage temperature range was 500 to 580°R, and (2) pressurant usage for all cases corresponded to the nominal propellant liquid and nominal pressurant inlet temperature case. The average pressurant outflow rates were calculated in the same manner as in the previous analysis, i.e., the pressurant usage per event divided by event duration.

Results of the pressurant storage analysis are presented in Table IV-7. These results show that the pressurant stored mass is affected more by the type of pressurant than by any other parameter. The nitrogen mass stored is again seven times greater than the mass of helium stored, which is consistent with previous results and approximates the ratio of the molecular weights of the two pressurants. The change in pressurant stored mass is almost negligible with changes in storage temperature for either helium or nitrogen. The pressurant mass does decrease approximately 10 to 13 percent with an increase in storage pressure from 2000 to 4000 psia for both helium and nitrogen. The helium storage tank mass is slightly greater than the nitrogen tank mass due to the storage tank volumes. The results show that the tank mass is only slightly affected by changes in storage pressure for both helium and nitrogen. Changes in storage temperature from 500°R to 580°R increased the tank mass by about 15 and 20 percent for helium and nitrogen, respectively. The tank pressure and propellant temperature histories for this mission are not presented because they are essentially straight lines. These profiles result from the isothermal tank wall assumption and the fact that pressurant inlet temperature was equal to the propellant temperature.

The pressurization subsystem mass data for the Mission A₂ cases studied are presented in both Table IV-7 and Figure IV-7; again, dissolved pressurant and leakage are not included. As with Mission A₁, the helium system is much lighter than the nitrogen system. At the nominal propellant temperature, a 34 percent reduction in pressurization subsystem mass can be obtained by using helium instead of nitrogen. An optimum storage pressure was not obtained for the helium cases investigated. The data show that the pressurization subsystem mass approaches a constant value between 3500 and 4000 psia. The nitrogen cases did appear to establish an optimum storage pressure for subsystem mass at 3500 psia.

Table IV-7 Results of Pressurant Storage Analysis for Mission A₂

PRESSURANT	PRESSURANT STORAGE TEMPERATURE (°R)	INITIAL PRESSURANT STORAGE PRESSURE (psia)	MASS OF PROPELLANTS VAPORIZED (lb _m)	PRESSURANT USAGE (lb _m)	PRESSURANT STORED MASS (lb _m)	STORAGE TANK MASS (lb _m)	PRESSURIZATION SUBSYSTEM MASS (lb _m)
Helium	500	2000	2.01	5.32	6.98	61.70	70.69
	↓	2500	↓	↓	6.59	59.43	68.03
	↓	3000	↓	↓	6.35	58.37	66.73
	↓	3500	↓	↓	6.19	57.93	66.13
	↓	4000	↓	↓	6.07	57.83	65.91
	525	2000	↓	↓	6.96	64.46	73.43
	↓	2500	↓	↓	6.58	62.04	70.63
	↓	3000	↓	↓	6.34	60.90	69.25
	↓	3500	↓	↓	6.18	60.39	68.58
	↓	4000	↓	↓	6.06	60.26	68.33
Nitrogen	580	2000	2.01	5.32	6.94	70.50	79.45
	↓	2500	↓	↓	6.55	67.70	76.26
	↓	3000	↓	↓	6.32	66.44	74.77
	↓	3500	↓	↓	6.16	65.81	73.98
	↓	4000	↓	↓	6.04	65.59	73.64
	500	2000	1.79	37.30	46.95	54.65	103.39
	↓	2500	↓	↓	44.86	53.22	99.87
	↓	3000	↓	↓	43.60	52.97	98.36
	↓	3500	↓	↓	42.78	53.49	98.06
	↓	4000	↓	↓	42.20	54.42	98.41
Nitrogen	525	2000	↓	↓	47.05	58.23	107.07
	↓	2500	↓	↓	44.92	56.63	103.34
	↓	3000	↓	↓	43.65	56.28	101.72
	↓	3500	↓	↓	42.81	56.74	101.34
	↓	4000	↓	↓	42.22	57.60	101.61
	580	2000	1.79	37.30	47.20	65.70	114.69
	↓	2500	↓	↓	45.03	63.85	110.67
	↓	3000	↓	↓	43.73	63.40	108.92
	↓	3500	↓	↓	42.86	63.67	108.32
	↓	4000	↓	↓	42.24	64.41	108.44

Figure IV-7 Mission A₂ Pressurization Subsystem Mass

3. Mission B

The parametric analysis conducted for this mission was completely different from those for Missions A₁ and A₂. This difference is attributed to the Mission B characteristics, i.e., (1) single tank monopropellant system, (2) a blowdown mode for expelling propellant, and (3) duration time is 3272 days. The second characteristic eliminates the need for evaluating pressurant inlet temperature effects. The parametric analysis, instead, evaluated the effects of pressurant type and liquid temperature on pressurant mass and final tank pressure. Ground rules used for this analysis were:

- 1) Initial tank pressure was 350 psia;
- 2) Initial ullage was 50 percent;
- 3) Liquid temperature range was 475 to 575°R with a nominal value of 500°R;
- 4) The propellant load and outflow schedule, presented in Table IV-8, were derived from the contract statement of work data.

Table IV-8 Propellant Outflow Schedule, Mission B

	VELOCITY INCREMENT (mps*)	BURN TIME (sec)	PROPELLANT MASS (lb _m)
Total Load	320		135.0
Postlaunch	30.3	138.	13.5
Pre-Jupiter	6.7	31.	3.0
Post-Jupiter	16.8	75.	7.4
Pre-Saturn	11.8	54.	5.3
Post-Saturn	107.8	468.	46.1
Pre-Uranus	35.4	150	14.7
Pre-Uranus	13.5	57.	5.6
Post-Uranus	69.1	285.	28.0
Pre-Neptune	28.6	115.	11.4
* Meters per second.			

This analysis was also conducted using the ODO41 computer program. The assumptions used were the same as those for Mission A₂, i.e., isothermal tank walls, instantaneous equilibrium condition in coast, etc. The propellant was also assumed to be nonvolatile because of its low vapor pressure over the temperature range considered (at 575°R, vapor pressure = about 1 psia). The physical and thermodynamic properties of the 75/25 nitrated hydrazine used in this analysis were obtained from Reference IV-4.

Results of the thermodynamic analysis for Mission B are presented in Table IV-9. Pressurant mass values were calculated using the ideal gas law at the initial gas conditions. The initial pressure (350 psia) and volume (50% ullage) were fixed; the pressurant was either helium or nitrogen. The initial gas temperature, which was equal to the liquid temperature, was varied from 475 to 575°R. Because of the direct calculation of pressurant mass, the percentage change in this mass is directly proportional to the percentage change in both molecular weight of the pressurant and the initial temperature. As system temperature increased from 475 to 575°R, the required pressurant mass for this mission decreased from 0.53 to 0.43 pounds for helium and from 3.74 to 2.98 pounds for nitrogen. The difference in nitrogen and helium pressurant mass of approximately 3 pounds is relatively small in comparison to the difference for Missions A₁ and A₂. Therefore, the relative mass savings of a helium system for this mission is not as significant as for Missions A₁ and A₂. Final tank pressure at the end of the mission was not affected significantly by changes in either liquid temperature or type of pressurant. The small differences in final tank pressures between the helium and nitrogen cases are due to the differences in the properties of the pressurants such as thermal conductivities, densities, specific heats, etc. These properties affect the heat transfer calculations in the ullage.

The pressure history shown in Figure IV-8 was typical of the pressure histories obtained for Mission B. Liquid temperature history is not presented since temperature remained essentially constant with time because of the isothermal wall assumption.

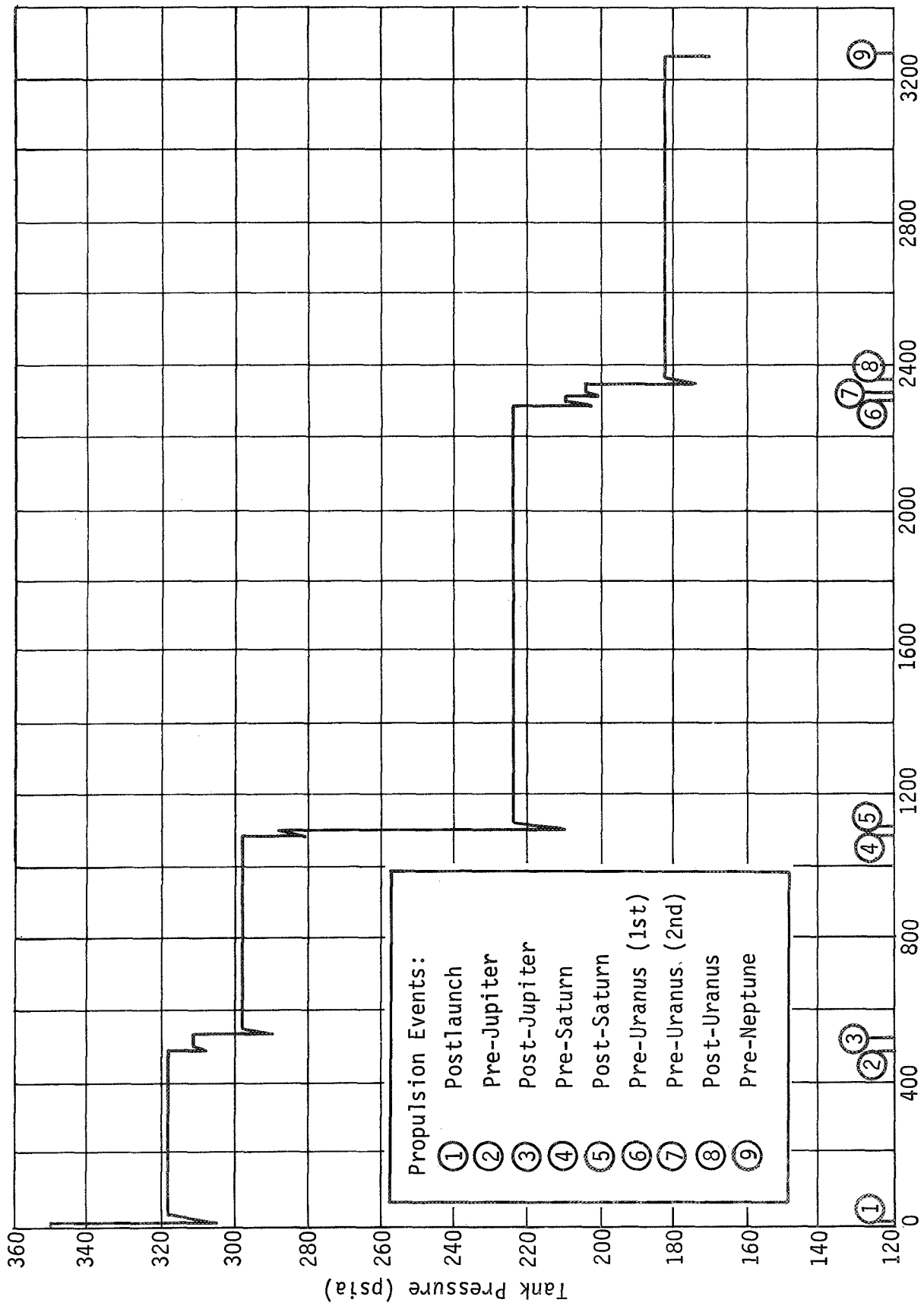


Figure IV-8 Mission B Tank Pressure History Using Helium Pressurant

Table IV-9 Results of Thermodynamic Analysis
for Mission B

TEMPERATURE (°R)	PRESSURANT	PRESSURANT MASS (lb _m)	FINAL TANK PRESSURE (psia)
475	Helium ↓	0.53	172.4
500		0.50	170.7
525		0.48	169.4
550		0.45	167.8
575		0.43	166.3
475	Nitrogen ↓	3.74	173.9
500		3.52	172.2
525		3.33	170.9
550		3.15	169.3
575		2.98	167.7

4. Pressurant Leakage and Solubility Considerations

All previous discussions concerning pressurization subsystem selection and mass calculations did not consider either pressurant leakage or solubility. Since all three missions under consideration are of long duration, both pressurant leakage and solubility of the pressurant in the propellants could have a significant impact on the selection of a pressurant. Pressurant solubility also has an impact on the selection of the propellant acquisition devices.

a. Pressurant Leakage Considerations - Pressurant leakage from the propulsion system increases pressurization subsystem mass and decreases propulsion system reliability. The impact of pressurant leakage on pressurization subsystem mass is considered here. Weight penalties due to pressurant leakage were evaluated using representative leakage rates for helium and nitrogen for Missions A₁, A₂, and B. For Missions A₁ and A₂, the approach for evaluating leakage was the same because mission duration and type of pressurization systems being considered are the same. With the A₁ and A₂ systems, pressurant leakage could occur from the pressurant storage tank, pressurization lines and control components, and propellant tanks. For Mission B, pressurant leakage could only occur from fill and vent components and lines and from the propellant tank since this is a blowdown system. Also, the duration of this mission is approximately an order of magnitude greater than that for Missions A₁ and A₂.

Realistic helium and nitrogen leakage values for the assembled propulsion systems of Missions A₁, A₂, and B were established using the baseline propulsion system schematics presented in Figures II-3, II-4, and II-5. Each propulsion system was divided into subassemblies. A representative leakage value for each subassembly was established from available leakage criteria and data for similar subassemblies from programs such as Mariner '71, Apollo Applications Program, and Titan III Transtage. The Mariner '71 Program was the primary source of data because of the similarity between its propulsion subassemblies and components and those for Missions A₁, A₂, and B. The Mariner '71 propulsion system schematic is shown in Figure IV-9 and the maximum external leakage specification values for each subassembly are presented as the asterisked numbers in Table IV-10.

After gathering the specification leakage values, a comparison between helium and nitrogen leakage was required in order to calculate the total leak rate of either helium or nitrogen. This comparison was made using the gas-to-gas leakage correlations presented in Reference IV-5. For Poiseuille (laminar) flow, which covers leakage rates between 10⁻¹ to 10⁻⁶ atm-cc/sec, the general expression for correlating volumetric flow for two different gases is given by:

$$\frac{Q_A}{Q_B} = \left(\frac{\mu_B}{\mu_A} \right) \left(\frac{P_1^2 - P_2^2}{P_3^2 - P_4^2} \right) \quad [IV-3]$$

where (P₁, P₂) and (P₃, P₄) are the pressure pairs for gases A and B, respectively, and μ_A and μ_B are the viscosities of the gases.

If the flow is molecular, the leakage path is long compared to the effective diameter of the hole. For this type of flow, the volumetric flow correlation is given by:

$$\frac{Q_A}{Q_B} = \sqrt{\frac{T_A}{T_B}} \times \sqrt{\frac{M_B}{M_A}} \times \left(\frac{P_1 - P_2}{P_3 - P_4} \right) \quad [IV-4]$$

where (P₁, P₂) and (P₃, P₄) are the pressure pairs, T_A and T_B are the temperatures and M_A and M_B are the molecular weights for gases A and B.

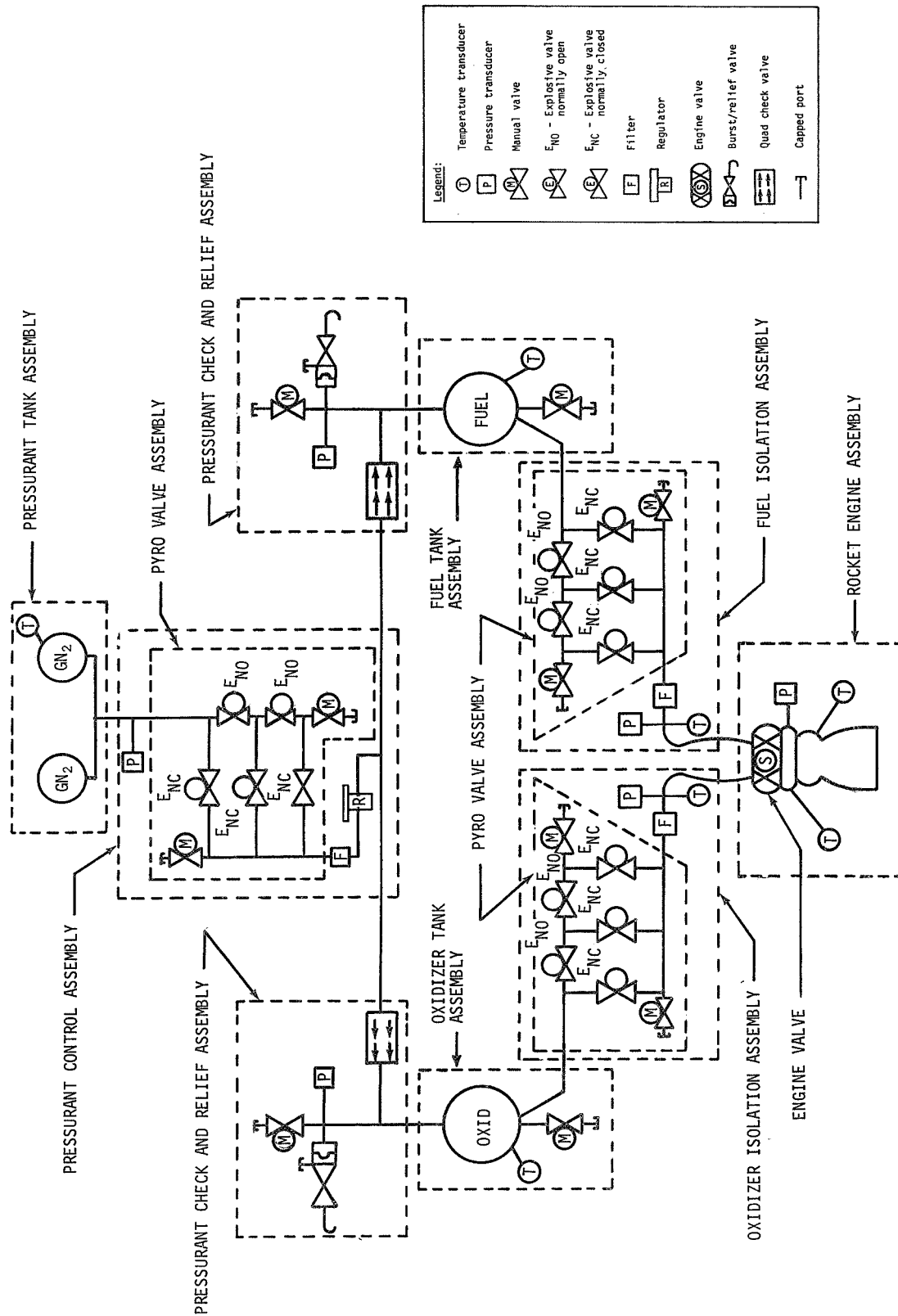


Figure IV-9 Propulsion System Schematic for Mariner '71

Table IV-10 Pressurant External Leakage for Mariner '71 Propulsion System

SUBASSEMBLIES AND COMPONENTS	LEAK CHECK CRITERIA	MAXIMUM HELIUM LEAKAGE RATE (scc/sec)	MAXIMUM NITROGEN LEAKAGE RATE (scc/sec)
Pressurant tank assembly (1) Pressurant tanks (2) Common manifold lines	GHe at 4000 psig & 70°R	$*2 \times 10^{-7}$	0.755×10^{-7}
Pressurant control assembly (1) Pressure transducer (1) Squib-operated valves, normally-closed (3) Squib-operated valves, normally-open (2) Manual service valves, (capped) (2) High capacity filter (1) Single stage regulator (1)	GN ₂ at 4000 psig	13.25×10^{-5}	$*5 \times 10^{-5}$
Pressurant check and relief assembly (2) Check valves (2) Pressure relief valves and burst disc (2) Manual service valves, (capped) (2) Pressure transducers (2)	GN ₂ at 380 psig & 70 ± 5°F	3.18×10^{-5}	$*1.2 \times 10^{-5}$
Propellant tank assembly (2) Oxidizer tank (1) Fuel tank (1) Manual service valve (capped) (2) Temperature transducer (2)	GHe at 300 psig	$*2 \times 10^{-5}$	0.755×10^{-5}
Total system leakage rate		18.45×10^{-5}	6.96×10^{-5}
*Specification values; all other values calculated from $Q_{He} = 2.65Q_{N_2}$.			

Both types of flow were considered for this evaluation. It was assumed that the gases were at the same temperature and had the same driving pressure differential. Under these conditions, the volumetric flow ratio of helium to nitrogen reduces to $Q_{\text{He}}/Q_{\text{N}_2} = \mu_{\text{N}_2}/\mu_{\text{He}}$ for Poiseuille flow and to $Q_{\text{He}}/Q_{\text{N}_2} = (M_{\text{N}_2}/M_{\text{He}})^{1/2}$ for molecular flow. Since gas viscosity is temperature dependent, Poiseuille flow varies with the temperature level; however, molecular flow is temperature independent. For Poiseuille flow at room temperature, $Q_{\text{He}} = 0.9 Q_{\text{N}_2}$, while for molecular flow, $Q_{\text{He}} = (28/4)^{1/2} = 2.65 Q_{\text{N}_2}$ at any temperature level. Since molecular flow results in a more conservative assessment producing a greater difference between helium and nitrogen leakage rates than does Poiseuille flow, the molecular flow mechanism was employed in comparing leak rates.

Using the molecular flow relationship, the volumetric leakage rate of helium or nitrogen was calculated for each Mariner '71 subassembly; these values are shown in Table IV-10 along with the total leakage rate calculated for the Mariner '71 propulsion system. It was assumed that the subassembly interface connections and all connections within each subassembly are completely welded. The leakage rate used on Mariner '71 for an interface weld is approximately 10^{-7} scc/sec of helium at operating pressure. Considering five subassembly interfaces, the total leakage rate for the welds (5×10^{-7} scc of GHe/sec) is negligible compared to the total leakage rate of all the subassemblies (6.96×10^{-5} scc of GHe/sec). The same approach was used in evaluating pressurant leakage for Missions A₁, A₂, and B, and the results are presented in Tables IV-11 thru IV-13. In terms of volume, helium leakage is approximately three times that of nitrogen; however, on a mass basis, helium leakage is about one-third that for nitrogen.

Since the total quantities of pressurant lost by external leakage are very small, the impact of pressurant leakage on pressurization subsystem mass is negligible. Even if the leakage evaluation were in error and the helium leakage was an order of magnitude greater, the mass of helium lost would still be negligible for Mission A₂ and would be from four to five percent of the helium loaded for Missions A₁ and B. These quantities still have no effect on the weight trade between helium and nitrogen pressurant. The only effect would be to slightly lower the final pressures in the pressurant and propellant tanks at the end of the mission.

Table IV-11 Pressurant External Leakage for Mission A₁ Propulsion System

SUBASSEMBLIES AND COMPONENTS	SOURCE	HELIUM LEAKAGE RATE (scc/sec)	NITROGEN LEAKAGE RATE (scc/sec)
Pressurant tank assembly (1) Pressurant tanks (4) Common manifold lines	Mariner '71 Program	4×10^{-7}	1.51×10^{-7}
Pressurant control assembly (1) Pressure transducer (1) Squib-operated valves, normally-closed (3) Squib-operated valves, normally-open (3) Manual service valve, (capped) (1) Pressure regulator (1)	Mariner '71 Program	13.25×10^{-5}	5×10^{-5}
Pressurant relief valve assembly (2) Relief valves and burst discs (2) Manual service valves (capped) (2) Check valves (2)	Mariner '71 Program	3.18×10^{-5}	1.2×10^{-5}
Propellant actuation assembly (1) Solenoid valves (2) Pneumatic isolation valves (2) Pneumatic bipropellant valves (2)	AAP Program	6×10^{-3}	2.26×10^{-3}
Propellant tank assembly (4) Oxidizer tanks (2) Fuel tanks (2) Manual service valves (capped) (2)	Mariner '71 Program	4×10^{-5}	1.51×10^{-5}
Total system leakage rate		6.20×10^{-3}	2.34×10^{-3}
<u>Pressurant Leakage Calculations:</u> Duration time = 2.335×10^7 sec GHe density = 3.66×10^{-7} lb _m /scc at 1 atm and 70°F GN ₂ density = 2.56×10^{-6} lb _m /scc at 1 atm and 70°F Total mass GHe leaked = $(2.335 \times 10^7)(3.66 \times 10^{-7})(6.20 \times 10^{-3}) = 0.053$ lb _m Total mass GH ₂ leaked = $(2.335 \times 10^7)(2.56 \times 10^{-6})(2.34 \times 10^{-3}) = 0.140$ lb _m			

Table IV-12 Pressurant External Leakage for Mission A₂ Propulsion System

SUBASSEMBLIES AND COMPONENTS	SOURCE	HELIUM LEAKAGE RATE (scc/sec)	NITROGEN LEAKAGE RATE (scc/sec)
Pressurant tank assembly (2) Pressurant tanks (2)	Mariner '71 Program	2×10^{-7}	0.755×10^{-7}
Pressurant control assembly (2) Pressure transducer (2) Squib-operated valves, normally-closed (6) Squib-operated valves, normally-open (6) Manual service valves (capped) (2) Filters (2) Pressure regulator (2)	Mariner '71 Program	2.65×10^{-4}	1×10^{-4}
Relief valve assembly (2) Burst and relief valve (2) Manual service valve (capped) (2)	Mariner '71 Program	3.18×10^{-5}	1.2×10^{-5}
Propellant Tank assembly (2) Oxidizer tank (1) Fuel tank (1) Temperature Transducers (2) Manual service valves (capped) (2)	Mariner '71 Program	2×10^{-5}	0.755×10^{-5}
Total system leakage rate		3.17×10^{-4}	1.20×10^{-4}
<u>Pressurant Leakage Calculations:</u> Duration time = 2.335×10^7 sec GHe density = 3.66×10^{-7} lb _m /scc at 1 atm and 70°F GN ₂ density = 2.56×10^{-6} lb _m /scc at 1 atm and 70°F Total mass GHe leaked = $(2.335 \times 10^7)(3.66 \times 10^{-7})(3.17 \times 10^{-4}) = 0.0027$ lb _m Total mass GN ₂ leaked = $(2.335 \times 10^7)(2.56 \times 10^{-6})(1.20 \times 10^{-4}) = 0.0072$ lb _m			

Table IV-13 Pressurant External Leakage for Mission B Propulsion System

SUBASSEMBLIES AND COMPONENTS	SOURCE	HELIUM LEAKAGE RATE (scc/sec)	NITROGEN LEAKAGE RATE (scc/sec)
Pressure relief valve assembly (1) Burst/relief valve (1) Manual valve (capped) (1) Pressure transducer (1)	Mariner '71 Program	1.59×10^{-5}	6×10^{-6}
Propellant tank assembly (1) Fuel tank (1) Manual service valve (capped) (1) Temperature transducer (1)	Mariner '71 Program	1×10^{-5}	3.77×10^{-6}
Total system leakage rate		2.59×10^{-5}	9.77×10^{-6}
<u>Pressurant Leakage Calculations:</u> Duration time = 2.83×10^8 sec GHe density = 3.66×10^{-7} lb _m /scc at 1 atm and 70°F GN ₂ density = 2.56×10^{-6} lb _m /scc at 1 atm and 70°F Total mass GHe leaked = $(2.83 \times 10^8)(3.66 \times 10^{-7})(2.59 \times 10^{-5}) = 0.0027$ lb _m Total mass GN ₂ leaked = $(2.83 \times 10^8)(2.56 \times 10^{-6})(9.77 \times 10^{-6}) = 0.0071$ lb _m			

For an order of magnitude higher helium leakage on Mission B, for instance, 0.027 lb_m would be lost and final tank pressure would be about 162 psia instead of the 171 psia calculated in the Mission B thermodynamic analysis. The calculated leakage of 0.0027 lb_m of helium would result in a decrease of only one psia to a final value of 170 psia. Even with an order of magnitude error in helium leakage, the system should be capable of satisfactory performance during the final Mission B pre-Neptune burn. Also, in any actual system, the total pressurant loaded always includes a leakage contingency that would offset some, if not all, of the slight effects resulting from even an order of magnitude error. Thus, leakage should not be a major consideration in selection of the pressurant.

b. Pressurant Solubility Considerations - When pressurant gas is allowed to contact a propellant, some of the gas dissolves in or is absorbed by the propellant. The equilibrium concentration of dissolved gas in the liquid is a function of the partial pressure of the pressurant gas in the vapor space (ullage) next to the bulk liquid and the temperature of the liquid. For propellants on which information is available, the equilibrium gas solubility has generally been found to follow Henry's Law for dilute solutions. This law states that the concentration of a gas in a liquid at equilibrium is directly proportional to the partial pressure of the gas in the vapor above the liquid. The constant of proportionality is called the Henry's Law constant which holds for a given system temperature; however, the value for this constant changes for a different system temperature. This has been demonstrated, in particular, for both nitrogen and helium in a variety of propellants (Ref IV-6 thru IV-15). In addition, the solubility of only slightly soluble inert gases generally increases with increasing temperature while the solubility of appreciable soluble inert gases may decrease with increasing temperature. As a general rule, the solubility of nitrogen is at least an order of magnitude greater than that of helium in most of the commonly used propellants. The solubility of both gases in oxidizers is almost an order of magnitude greater than their solubility in fuels.

In considering the different propellant acquisition techniques, it is seen that pressurant solubility is not a problem with impermeable barriers such as metallic diaphragms and bellows, as long as care is taken to minimize the dissolved gas content of loaded propellant. No additional gas can be added to the propellant across the impermeable metal barrier during system operation. The same is not true of surface tension, external settling, dielectrophoretic, or polymeric bladder acquisition systems. With sufficient exposure time, saturated propellants will result with all four of these systems since intimate contact exists between the pressurant and propellant in the first three systems, and polymeric bladders are semipermeable to gases and propellant vapors. On the Surveyor vernier propulsion system, for example, helium was found to permeate the Teflon bladder resulting in an equilibrium condition in the propellant (90-10 MON) after about 10 hours. At this point, as much helium was going from the propellant through the bladder as was entering the propellant through the bladder (Ref IV-16).

Data are available on the equilibrium solubility of both helium and nitrogen in the propellants of interest (Ref IV-6 thru IV-15). These data were used to calculate the equilibrium amount of pressurant dissolved in the propellants at the nominal system pressure and temperature, and the results are shown in Table IV-14. For Mission B, it was assumed that the dissolved solid, $\text{N}_2\text{H}_5\text{NO}_3$, did not affect the solubility of the gases in hydrazine. These results show that from the solubility standpoint, helium is a more desirable pressurant than nitrogen for all three missions. In addition, the very high solubility of nitrogen in both OF_2 and B_2H_6 in comparison to helium essentially rules out its consideration as a pressurant for Mission A_1 and any other long duration mission using these propellants, unless absolute separation of the propellant and pressurant is provided.

Table IV-14 Pressurant Amounts Contained in Saturated Propellants

MISSION	PROPELLANT	PROPELLANT QUANTITY (lb _m)	PROPELLANT TEMPERATURE (°R)	PROPELLANT TANK PRESSURE (psia)	PRESSURANT PARTIAL PRESSURE (psia)	DISSOLVED PRESSURANT (lb _m)	
						He	N ₂
A ₁	OF ₂	820	250	350	320	0.183	182.000
	B ₂ H ₆	270	250	350	349	0.027	45.200
A ₂	N ₂ O ₄	872	525	350	337	0.082	3.900
	MMH	562	525	350	349	0.012	0.428
B	75/25 ni- trated hydrazine	135 (101 lb N ₂ H ₄)	500	350	350	0.00038	0.0053

The dissolved pressurant quantities shown in Table IV-14 must be added to the pressurant quantities required to accomplish system pressurization only. From the quantities shown for all three missions, it is seen that the impact of gas solubility on the pressurant requirement is negligible for helium on all missions, and for nitrogen on Mission B. This is not the case with nitrogen pressurant for Missions A_1 and A_2 . An additional quantity of nitrogen, amounting to 227 lb_m for Mission A_1 and 4.3 lb_m for Mission A_2 , is required because of gas solubility if gas/liquid contact is not precluded.

B. EFFECTS OF PRESSURIZATION SUBSYSTEM ON ACQUISITION DEVICES

An analysis was conducted to evaluate the effects of pressurization related parameters on the selection of propellant acquisition devices. The pressurization variables that affect acquisition device performance are type of pressurant, propellant temperature, and propellant tank pressurant inlet temperature. These are manifested in the areas that were considered (1) temperature sensitivity of acquisition devices, (2) amount of propellant vaporized, and (3) solubility of pressurants in the propellants. The three areas impact the selection of both the acquisition device and the pressurization subsystem.

The temperature range over which the candidate acquisition devices can be employed has been discussed previously as each device was considered. For instance, materials for polymeric diaphragms that are suitable for use at the Mission A₁ temperatures are not available. In general, however, if an acquisition device concept is a serious contender for a mission, the temperature ranges investigated in the tank thermodynamic analyses do not present any significant design problems. Both propellant temperature and pressurant inlet temperature have negligible effects on acquisition devices over the ranges considered in this investigation.

Propellant vaporization does impact the selection of a propellant acquisition device. Devices that do not preclude vaporization of the propellant must receive a weight penalty equal to the mass of propellant vaporized in the tank at the end of the mission minus the mass of pressurant saved. This is the difference in gas residuals between devices allowing propellant vaporization and those precluding vaporization, and amounts to 7.7 pounds on Mission A₁ and 2.0 pounds on Mission A₂. For Mission B, the amount of vaporized propellant for devices not precluding vaporization was negligible. In assessing mass attributable to dielectrophoretic systems, settling rockets, surface tension devices, the capillary bellows device, and polymeric bladders and diaphragms, the above masses must be included in arriving at the total mass attributable to the acquisition device. The penalty does not apply to complete bellows systems or metallic bladders and diaphragms.

Of the three areas considered, solubility of pressurant in the propellants could have the greatest impact on the selection of both the propellant acquisition device and the pressurization subsystem. The quantity of pressurant that could be dissolved in the propellants was evaluated in the pressurant solubility analysis for the three reference missions. Both helium and nitrogen are soluble in the propellants, but the quantity of dissolved nitrogen would be much greater than that for helium. This is particularly true for Mission A₁. Dissolved pressurant would result with all acquisition devices that allow pressurant contact with the propellant. Little effect would probably result on the design of dielectrophoretic or external settling systems; however, pressurant solubility could have a considerable effect on the design of polymeric bladders and diaphragms and surface tension devices.

The amount of pressurant gas that will dissolve in the liquid propellant is dependent upon the partial pressure of the pressurant. Increasing the pressure will allow more pressurant to dissolve, while a pressure reduction will result in gas evolution. For each mission, changes in the partial pressure of the pressurant must be considered to determine the effects due to solubility.

The pressure profiles for the Mission A₁ fuel and oxidizer tanks are presented in Figures IV-4 and IV-5. Because the partial pressure of the propellant vapor is small, the tank pressure can be considered to be the partial pressure of the pressurant for the purposes of a conservative evaluation. The tanks are initially pressurized at 100 psia. If the transient periods of prepressurization and burn are neglected because of their short duration, it can be seen that there is a gradual increase in tank pressure throughout the mission. In general, the pressurant is being dissolved into the propellant throughout the mission as the pressure increases. There are some transient periods during which gas would be evolved; for instance, during the second orbital trim burn, the pressure drops about 6 psi. Within the next 20 days, the pressure then builds back up and finally exceeds the preburn level.

Missions A₂ and B had tank pressure histories completely different from those of Mission A₁. Tank pressure remained essentially constant at 350 psia for Mission A₂. For Mission B, there is a decrease in tank pressure throughout the mission. The tank is initially pressurized to 350 psia, so gas is always being evolved from the propellant as the pressure decreases. The tank pressure prior to the last burn is 185 psia as shown in Figure IV-8.

The maximum amount of evolved pressurant gas that could affect the operation of the propellant acquisition device can be determined based on the following assumptions:

- 1) Helium pressurant would be used;
- 2) The fraction of the gas evolved is proportional to the ratio of the pressure drop to the tank operating pressure (from Henry's Law considerations assuming propellant partial pressure is negligible);
- 3) The maximum pressure drop, ignoring short duration transients, is 6 psi for Mission A₁, zero for Mission A₂, and 165 psi for Mission B.

For polymeric bladders and diaphragms, any gas that is evolved on the liquid side of the barrier is a problem because it could be ingested by the engine. By considering the initial liquid volume and the above assumptions, a worst case estimate of the volume of evolved gas was made. The resulting quantities are shown in Table IV-15.

Table IV-15 Helium Gas Evolution

MISSION	TANK	AMOUNT OF He EVOLVED	
		BASED ON INITIAL LIQUID VOLUME (in. ³)	BASED ON PROPELLANT TRAP VOLUME (in. ³)
A ₁	OF ₂	18.1	0.7
	B ₂ H ₆	2.7	0.1
A ₂	N ₂ O ₄	0	0
	MMH	0	0
B	Nitrated		
	N ₂ H ₄	1.0	0.06

While the volumes are not excessive, no gas ingestion is desired. Thus, a screen device over the tank outlet is required with polymeric bladders and diaphragms to prohibit the evolved gas from entering the engine. This screen device would operate in the same manner as the coverplate of a propellant surface tension trap device by providing a gas barrier.

For a surface tension device, only the gas that is evolved within the device itself will have any effect. For devices that consist of liners, the liquid volume is small and the evolved gas could be purged. Of the many possible surface tension device configurations, a propellant trap would be most affected by gas evolution. For the conceptual surface tension device trap design, the amount of gas that could be evolved within the reservoir is also shown in Table IV-15.

If the trapped liquid is in contact with the coverplate, liquid will be forced out of the reservoir when gas is evolved since a lesser pressure difference is required to flow liquid through the coverplate than to flow gas because of the capillary retention capability. Based on the pressure histories presented in Figures IV-4, IV-5, and IV-8, a maximum of four drops in pressure could occur for Mission A₁ and there would be a single pressure drop for Mission B. Therefore, the maximum amount of propellant that could be lost from the trap is obtained by multiplying the amount of helium evolved within the trap (Table IV-15) by the expected number of pressure drops.

The amounts of propellant involved are small and can be easily accounted for in the design of the surface tension device. The maximum amount of propellant lost would be from the surface tension trap in the OF₂ tank. An amount of about 3 cu in., or about 0.16 lb_m, of propellant would be lost, and sufficient propellant would remain in the trap to resettle the lost 0.16 lb_m.

C. EFFECTS OF TWO VERSUS FOUR PROPELLANT TANKS ON PRESSURIZATION SUBSYSTEM

A qualitative evaluation was made to determine the impact on the pressurization system of four propellant tanks in place of the two-tank system employed in the previously discussed analysis. For spherical tanks, the net effect of changing to four tanks having the same total volume is to increase the total surface area which includes both the wall and gas/liquid interface areas. The increase in area produces an increase in the heat transfer rates that affects pressurant usage, propellant temperature, and gas residuals. In changing from two to four tanks, pressurant usage will increase because more energy will be transferred from the ullage to the tank walls and propellant. Propellant temperature

will tend to be higher because of the increased heat transfer across the gas/liquid interface. Increases in both pressurant usage and propellant temperature will produce higher gas residuals, i.e., pressurant gas plus propellant vapor.

The overall effect of increasing the number of propellant tanks from two to four will be an increase in pressurization subsystem mass; however, this increase should be small.

V. TANK DESIGN AND PACKAGING

A study of propellant tank design and packaging requirements was performed to supply pertinent tankage data to support the system evaluation phase of the program. Overall study guidelines for this phase of the program were discussed in Chapter II of this report. Briefly restated, the guidelines required an evaluation of two versus four tanks (Missions A₁ and A₂), spherical versus cylindrical geometry, and all-metal versus composite construction. The envelope constraints placed on the propellant tank study were also previously discussed in Chapter II. The Viking Orbiter propulsion envelope shown in Figure II-1 was used for Missions A₁ and A₂. The propulsion envelope shown in Figure II-2 was used for Mission B.

The baseline tank dimensions presented in Table V-1 were calculated from the propulsion system criteria given in Table II-4, Chapter II. For the cylindrical tanks, length-to-diameter ratios in the range of 1.3 to 2.0 were used. The helium pressurant storage tank dimensions, also given in Table V-1, were calculated from data obtained from the pressurization analysis discussed in Chapter IV.

Table V-1 Baseline Tank Dimensions

	MISSION		
	A ₁	A ₂	B
<u>Configuration</u>	<u>2 Tanks</u>	<u>2 Tanks</u>	<u>1 Tank</u>
Volume, ft ³	9.92	11.25	3.86
Spherical			
Diameter, in.	32.0	33.33	23.35
Cylindrical (hemispherical domes)			
Diameter, in.	28.0	28.0	18.0
Length, in.	37.18	40.89	32.20
<u>Configuration</u>	<u>4 Tanks</u>	<u>4 Tanks</u>	
Volume, ft ³	4.96	5.62	--
Spherical			
Diameter, in.	25.39	26.47	--
Cylindrical (hemispherical domes)			
Diameter, in.	20.0	20.0	--
Length, in.	33.98	37.58	--
Helium pressurant storage tank (spherical)			
Volume, ft ³	2.68	2.38	Integral
Diameter, in.	20.7	19.9	

A. PROPELLANT TANK PACKAGING CONSIDERATIONS

Various propellant tank configurations were evaluated for application in the specified propulsion system envelopes. Variations in number, size, and shape of the propellant tanks were considered in order to determine suitable tank packaging arrangements. A discussion of the packaging requirements for the reference missions is presented in this section.

1. Mission A_1 and A_2

A comparison of the baseline spherical and cylindrical tank requirements of Missions A_1 and A_2 presented in Table V-1 indicated that the Mission A_2 tanks are slightly larger than those required for Mission A_1 . However, since the difference was small, the Mission A_2 tanks were evaluated. The results are representative for both missions.

Two- and four-tank configurations of the baseline spherical and cylindrical tanks were evaluated. Figures V-1 and V-2 present possible packaging arrangements for two spherical- and two cylindrical-tank systems, respectively. Similar packaging arrangements for four spherical and four cylindrical tank systems are presented in Figures V-3 and V-4, respectively. All baseline tanks together with a pressurization storage sphere fit within the required envelope and present no packaging problems.

Certain propellant acquisition devices, the ring-reinforced diaphragm and the metal bellows, require tank shapes other than the baseline spheres or cylinders in order to improve volumetric and expulsion efficiencies. Figures V-5 and V-6 illustrate possible package arrangements for two- and four-conospheroid tanks, respectively. The 10-degree conospheroid tanks are applicable for ring-reinforced diaphragms. Metal bellows required a cylindrical tank with an inverted upper dome as discussed previously in Chapter III. Two- and four-tank arrangements of the special cylinders required by metal bellows are shown in Figures V-7 and V-8. Both the conospheroid and special cylindrical tanks fit the required envelope; no packaging problems are encountered with either two or four tanks.

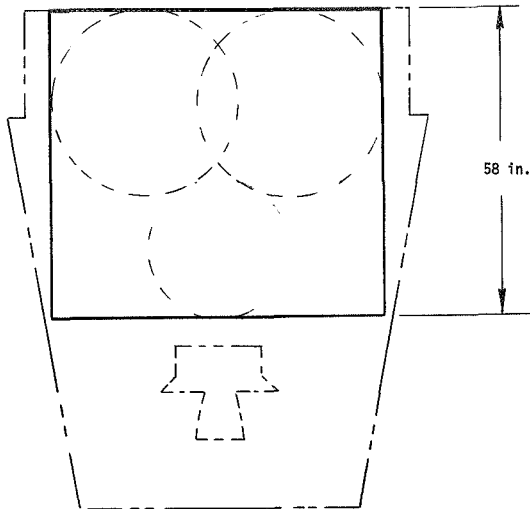
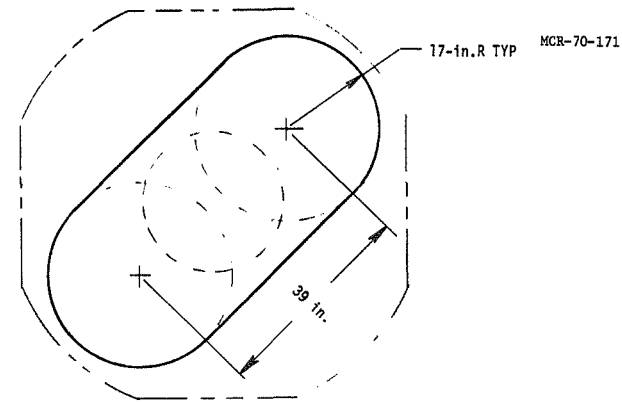


Figure V-1 Baseline, Two Spherical-Tank System

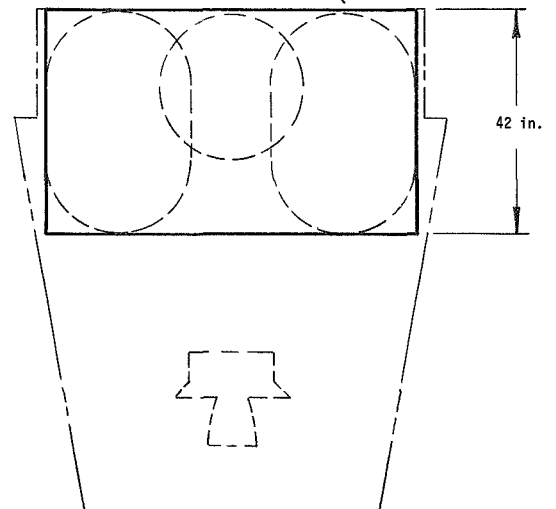
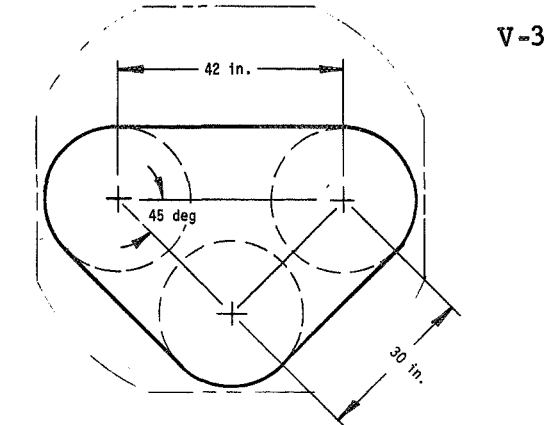


Figure V-2 Baseline, Two Cylindrical-Tank System

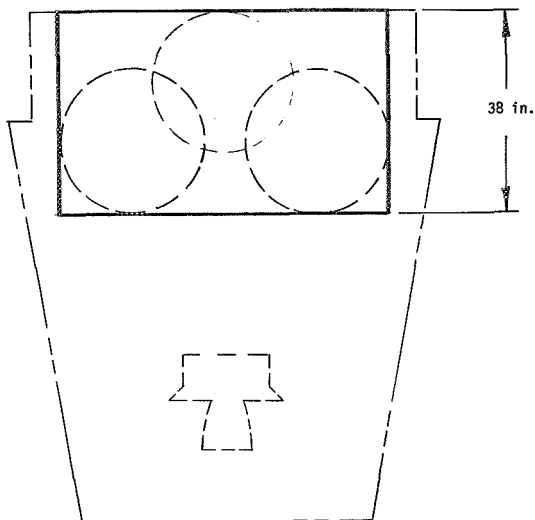
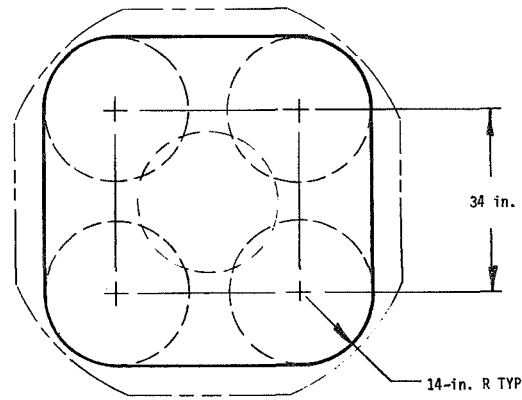


Figure V-3 Baseline, Four Spherical-Tank System

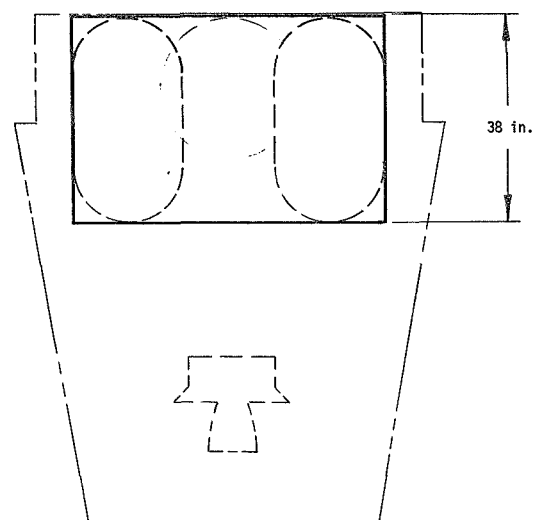
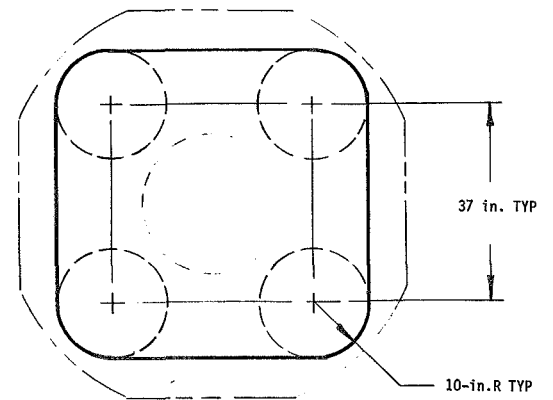


Figure V-4 Baseline, Four Cylindrical-Tank System

V-4

MCR-70-171

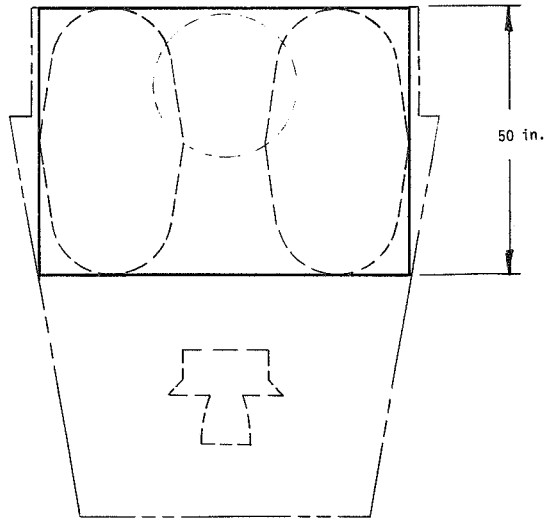
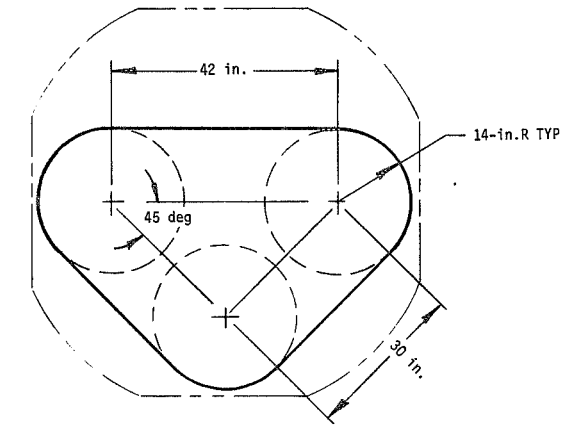


Figure V-5 Two Conospheroid-Tank System

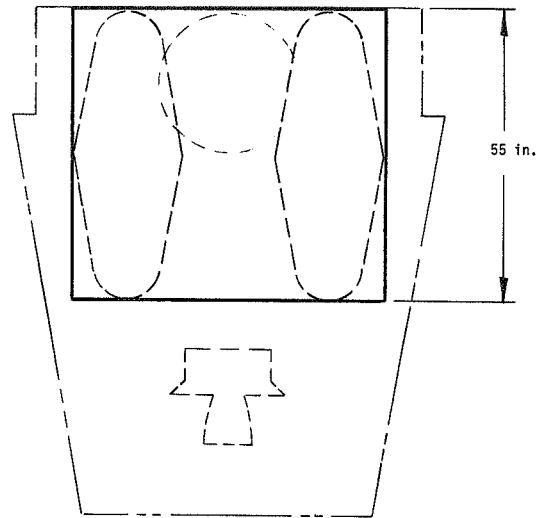
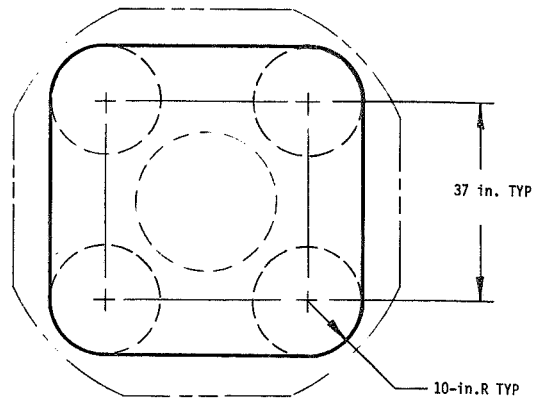


Figure V-6 Four Conospheroid-Tank System

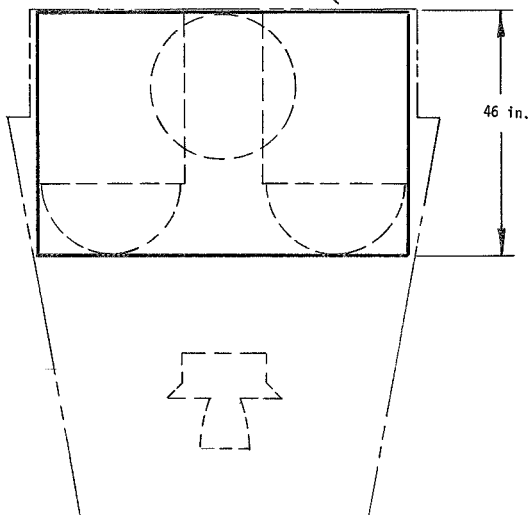
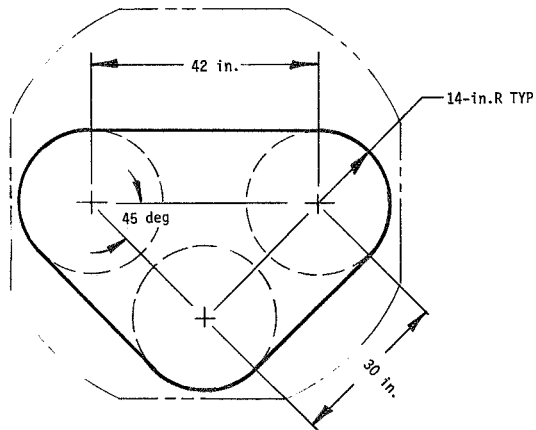


Figure V-7 Special Two-Cylinder Tank System

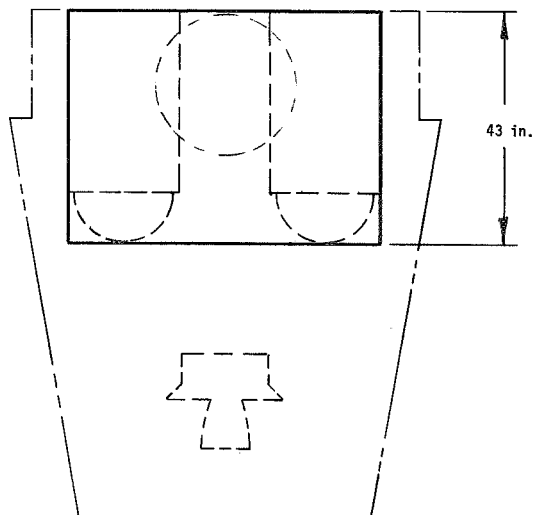
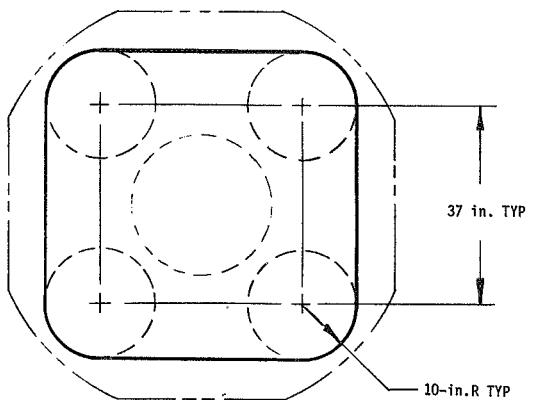


Figure V-8 Special Four-Cylinder Tank System

An evaluation of the practical growth limits for the spherical and cylindrical tankage arrangements over the baseline configuration was also made during the study. This evaluation indicated that the maximum diameter permitted by the propulsion envelope for two spherical tanks mounted side by side was approximately 37 inches. The tank volume corresponding to the maximum diameter is 36% greater than the baseline tank volume. For the four spherical-tank arrangement illustrated in Figure V-3, the evaluation indicated that an increase of 50% in propellant and pressurant volumes could reasonably be accommodated within the required envelope. The packaging arrangement for four spheres with a 50% increase in volume is shown in Figure V-9.

The envelope will easily accommodate the 50% growth tank systems in both the two and four cylindrical-tank configurations. This growth capability can be seen from Figure II-1 which describes the Viking Orbiter four-tank configuration. The Viking propellant tank volume is greater than the Mission A₂ baseline volumes by 126%.

2. Mission B

A study of propellant tank packaging was also performed for Mission B in a manner similar to that for the A₁ and A₂ missions. However, the packaging problem for Mission B is somewhat simplified because only one propellant tank is required for the mono-propellant system. The baseline spherical and cylindrical tanks for Mission B are shown in Figures V-10 and V-11, respectively. Neither of these configurations present any packaging problems.

When considering the growth potential of the propellant tank, it was found that the spherical tank volume could be increased by 50% and still remain within the limits of the envelope (Fig. V-12). However, when considering the growth potential of a cylindrical tank, a growth factor of 50% is too large if the baseline length-to-diameter ratio is maintained. Interference between the propellant tank and the engine system would occur, as shown in Figure V-13. If the length-to-diameter ratio of the propellant tank were reduced, the engine interference problem could probably be eliminated.

Packaging of 10-degree conospheroid tanks for use with the ring-reinforced diaphragm was also investigated. Figures V-14 and V-15 illustrate the arrangement for two tanks, each of baseline volume, but different length-to-diameter ratios. A tank with an L/D of 1.6 (Fig. V-14) can be acceptably packaged within the envelope while a tank with an L/D of 2.43 cannot (Fig. V-15). A special cylindrical tank for use with bellows results in crowding and possible interference with the engine as shown in Figure V-16.

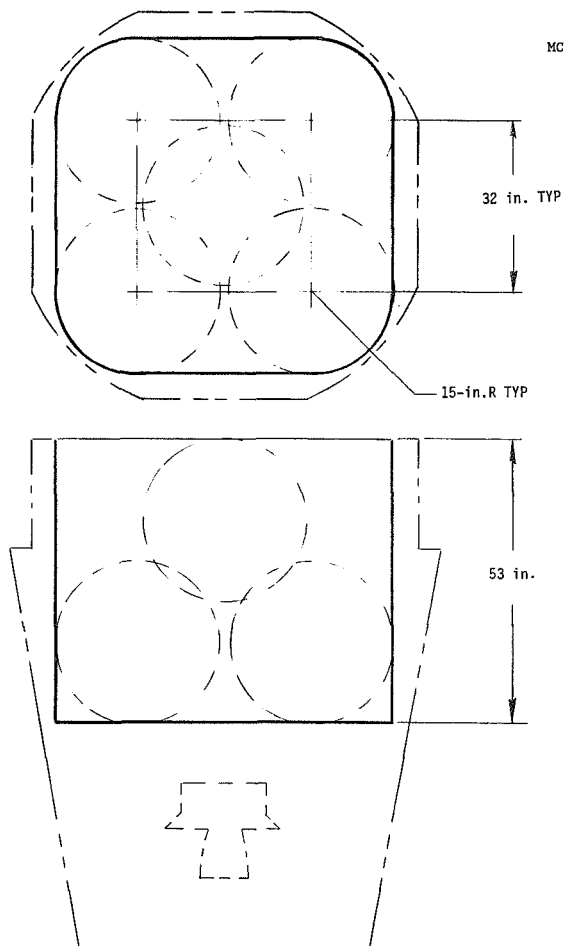


Figure V-9 Four Spherical-Tank Arrangement, 50% Volume Increase

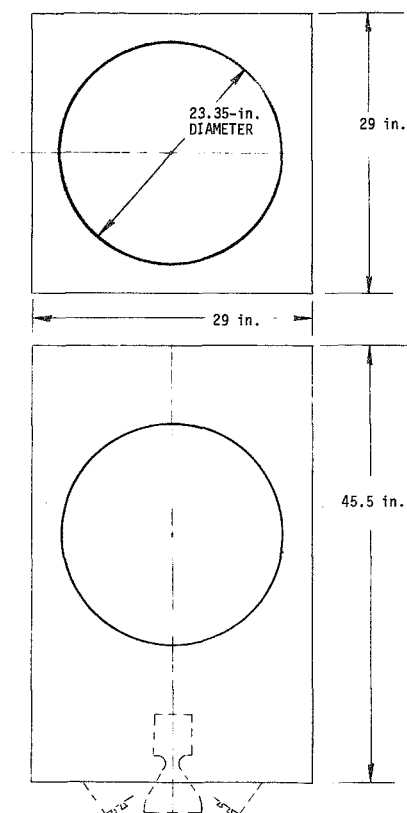


Figure V-10 Mission B Baseline Spherical-Tank System

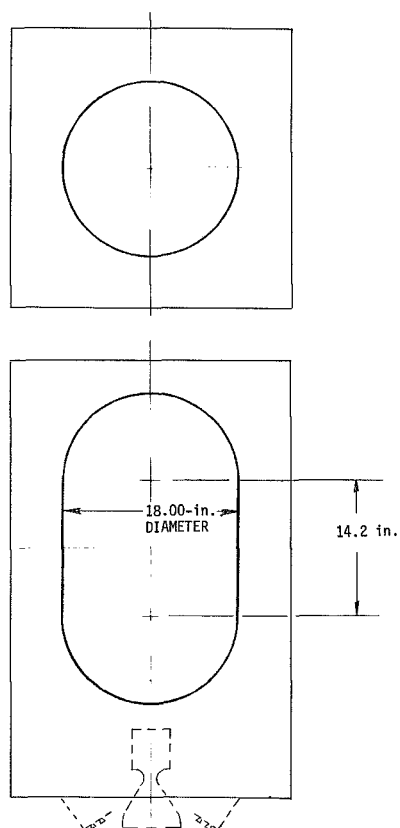


Figure V-11 Mission B Baseline Cylindrical-Tank System

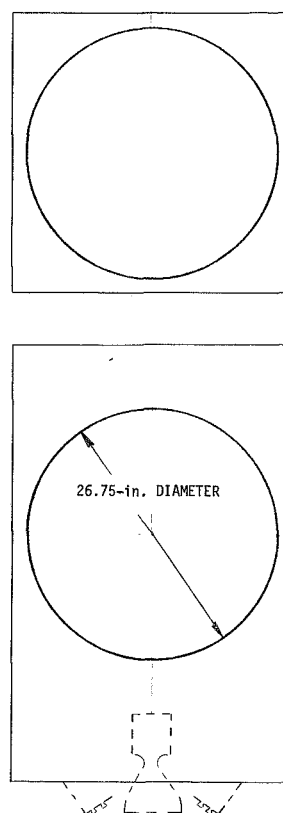


Figure V-12 Mission B Spherical Tank with 50% Volume Increase

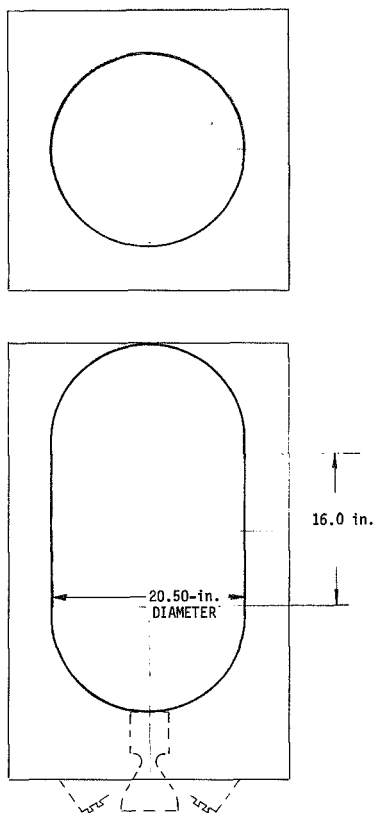


Figure V-13 Mission B Cylindrical Tank with 50% Volume Increase

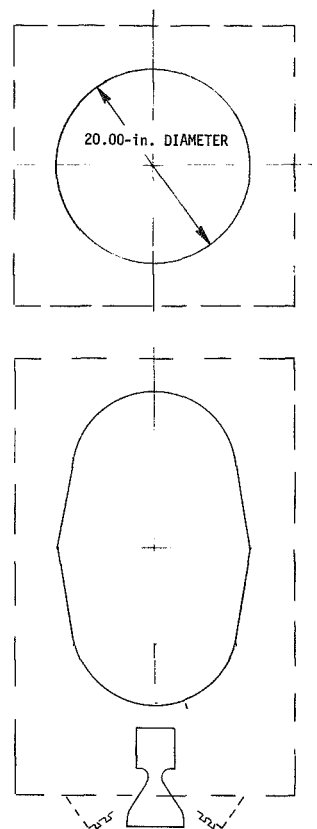


Figure V-14 Mission B Conospheroid Tank with L/D of 1.6

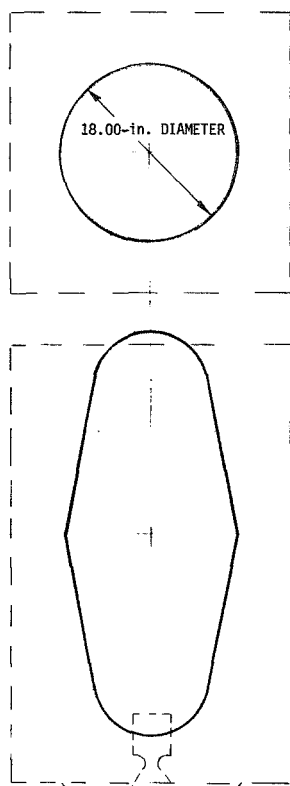


Figure V-15 Mission B Conospheroid Tank with L/D of 2.43

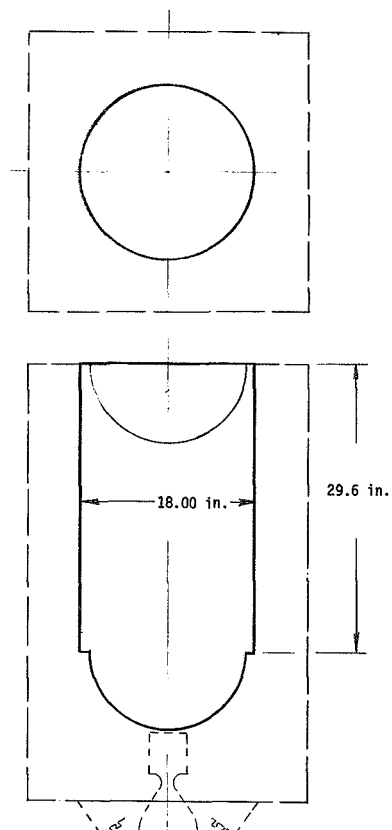


Figure V-16 Mission B Special Cylindrical Tank

3. Summary of Packaging Requirements

Tank package volume, total volume of tanks, tank package surface area, tank surface area, and meteoroid impact surface area were established for each packaging arrangement shown in Fig. V-1 through V-16. These data are summarized in Table V-2. Information on the Viking Orbiter system is included for comparison. The tank package volume is defined as the volume enclosing the propellant and pressurization storage tanks. The data presented for the A Missions are for Mission A₂ only; however, the relation between the tabulated parameters for each tank arrangement should be valid for Mission A₁ also. Because of the single tank system employed for Mission B, not all of the parameters shown for Mission A₂ are applicable. For Mission B, the tank package volume equals the propellant tank volume since it contains both propellant and pressurant.

B. TANK MATERIAL EVALUATION

Propellant tanks may be fabricated from all-metal material or may be composed of composite material. The evaluation of tank material in regard to strength, compatibility, and manufacturing considerations is discussed in this section.

1. Metal Tank Material

Information was compiled on the compatibility of various metals and nonmetals with the candidate propellants. This information is presented in Ref III-54 and III-55. Based on the compilation, eleven metal alloys were selected as candidate tank materials. Weldability, propellant compatibility, and strength-to-weight ratio for these materials are presented in Table V-3. From these considerations, it was concluded that acceptable materials for Mission A₁ are stainless steel or aluminum; titanium or aluminum are acceptable materials for Mission A₂ and B.

In choosing between stainless steel and aluminum for Mission A₁, it is noted that the 1100 and 6061 aluminum alloys and 304L, 321, 347 and 316 stainless steel alloys have low strength-to-weight ratios, and therefore offer an appreciable system weight penalty. Both the 301 cryoformed stainless steel and the three high-strength aluminum alloys (2024, 2014, and 2219) offer moderately high, and about equal, strength-to-weight ratios. It was concluded from weight considerations that the latter group of materials would be preferred.

Table V-2 Tank Packaging Considerations

	FIGURE NO.	ENVELOPE GROSS VOLUME (ft ³)	TANK PACKAGE VOLUME (ft ³)	VOLUME RATIO PACKAGE/ ENVELOPE	TOTAL VOLUME OF TANKS (ft ³)	VOLUME RATIO TANK/ PACKAGE	PACKAGE SURFACE AREA (ft ²)	TANK SURFACE AREA (ft ²)	AREA RATIO TANK/ PACKAGE	METEOROID IMPACT SURFACE AREA (ft ²)
Mission A ₂ (2-tank) Baseline Spherical Baseline Cylindrical Special Conosphere Special Cylindrical	V-1	198	60	0.30	28	0.47	87	63	0.72	20.3
	V-2	198	60	0.30	28	0.47	90	65	0.72	17.3
	V-5	198	72	0.36	28	0.39	100	67	0.67	17.3
	V-7	198	66	0.33	35	0.53	95	87	0.92	17.3
Mission A ₂ (4-tank) Baseline Spherical Baseline Cylindrical Special Conosphere Special Cylindrical	V-3	198	80	0.40	28	0.35	109	76	0.70	25.6
	V-4	198	69	0.35	28	0.41	100	81	0.81	22.0
	V-6	198	100	0.51	28	0.28	124	88	0.71	22.0
	V-8	198	78	0.39	36	0.46	107	89	0.83	22.0
Mission A ₂ + 50% Four Spherical	V-9	198	115	0.58	42	0.37	135	129	0.96	26.0
Viking Spacecraft Four Cylindrical	II-1	198	138	0.70	63	0.46	151	143	0.95	26.0
Mission B Baseline Spherical Baseline Cylindrical Special Conosphere (L/D = 1.6) Special Conosphere (L/D = 2.43) Special Cylindrical	V-10	22	3.9	0.18	3.9	--	--	11.9	--	2.1
	V-11	22	3.9	0.18	3.9	--	--	12.6	--	1.8
	V-14	22	3.9	0.18	3.9	--	--	12.9	--	3.1
	V-15	22	3.9	0.18	3.9	--	--	15.3	--	1.8
Mission B + 50% Spherical Cylindrical	V-16	22	5.7	0.26	5.7	--	--	21.5	--	1.8
	V-12	22	5.8	0.26	5.8	--	--	14.8	--	3.9
	V-13	22	5.8	0.26	5.8	--	--	16.8	--	2.2

When weldability is considered, problems are encountered with the 301 cryoformed stainless steel. Welding anneals the material in the heat affected zone causing a reduction in strength. This could present problems in attaching support brackets, flanges, and some of the propellant acquisition subsystem candidates. This reduced strength might be overcome, but both cost and time would be involved in arriving at the best solution. The cryoformed 301 has another disadvantage in that it exhibits the characteristics of a permanent magnet. This could result in spacecraft compatibility problems by affecting or limiting the selection of components for the guidance system and payload science. Therefore, the cryoformed material displays enough disadvantages to eliminate it from consideration. Of the high-strength aluminum alloys under consideration, only the 2219-T87 alloy exhibits good weldability. It is therefore the preferred material for the Mission A₁ propellant tanks.

Because aluminum and titanium are compatible materials for the Mission A₂ and B propellants and because both exhibit good weldability, it is necessary to base the choice on their strength-to-weight ratios. It will be noted from Table V-3 that the 6Al-4V titanium has a strength-to-weight ratio some 30% higher than that for 2219-T87 aluminum; therefore 6Al-4V titanium is the preferred material for the Mission A₂ and B tankage.

2. Composite Tank Material

Continuous fiber-reinforced composites fabricated by filament winding offer attractive features for pressure vessel application. The strength-to-density properties of typical fibers are high, and the filament winding technique permits orienting the fibers exactly as needed to resist imposed stress. Pressure vessels tend to experience a well-determined stress state because the normal operating loads are due primarily to internal pressure. Consequently, one set of fiber orientations could be chosen and need not be perturbed due to unexpected internal load changes.

However, there are times when propellant vessels, because of vacuum loading techniques or tank support requirements, have significant external loads applied. In the case of "vacuum loading", it would be necessary to insert lugs, bosses or pads to distribute these loads into the tank. When the support fittings cannot be located on the tank polar axis, the strength of the supports added to a composite tank is lower than the strength of similar supports added to an all-metal tank.

Table V-3 Metal Property Summary

METAL	WELDA-BILITY	PROPELLANT COMPATIBILITY					ULTIMATE STRENGTH/WT $\left(10^6 \frac{\text{lb}_f\text{-in.}}{\text{lb}_m}\right)$	DENSITY $\left(\text{lb}_m/\text{in.}^3\right)$	OPERATING STRESS (1) (psi)
		OF ₂	B ₂ H ₆	N ₂ O ₄	MMH	N ₂ H ₄ + N ₂ H ₅ NO ₃			
6Al-4V Ti	A	C ^(a)	A	A	A	A	1.03	0.16	75,000
2024-T3 Al	C	A	A	A	A	A	0.66	0.10	30,000
6061-T6 Al	A	A	A	A	A	A	0.45	0.10	20,000
2014-T6 Al	C	A	A	A	A	A	0.66	0.10	30,000
2219-T87 Al	A	A	A	A	A	A	0.66	0.10	30,000
1100-0 Al	A	A	A	A	A	A	0.13	0.10	6,000
301 Cryo SS	C	A	A	B ^(b)	B ^(c)	C ^(c)	0.73	0.29	95,000
304L SS	A	A	A	B ^(b)	B ^(c)	C ^(c)	0.27	0.29	35,000
321 SS	A	A	A	B ^(b)	B ^(c)	C ^(c)	0.31	0.29	41,000
347 SS	A	A	A	B ^(b)	B ^(c)	C ^(c)	0.31	0.29	41,000
316 SS	A	A	A	B ^(b)	C ^(c)	C ^(c)	0.27	0.29	35,000

A - Good (a) - Impact sensitivity
 B - Acceptable (b) - Adduct formation
 C - Undesirable (c) - Propellant decomposition

(1) Operating stress = Ultimate stress/safety factor (2.2)

The principal difficulty that has prevented success in the application of filament-wound composites to pressure vessels has been the lack of a reliable liner system for gas or liquid containment. A liner is required because of both the porosity of typical resin systems used as the matrix for holding the fibers in place and the possible chemical attack on the resin by the gas or liquid. In addition, the matrix may experience severe cracking at the strain levels necessary to develop the strength of the fibers.

Elastomeric liners (e.g., neoprene) can be used where transient pressurizations are required and where permeation is not a problem. Where long term pressurization and/or zero leakage are required, as in most aerospace applications that utilize corrosive or toxic liquids or gases, a metal liner must be used.

The principal problem with the metal liner is strain compatibility. To develop its full capability, it is necessary to strain the glass filament to approximately 2.5%. The operating strain is about 1.15% if a 2.2 safety factor is required. While this strain is met easily by elastomeric liners, there is no metallic material that can remain elastic under this deformation, a necessary requirement to prevent liner buckling or fatigue failure. When an overwrap is used with a metal liner, the operating strain should be within the elastic strain limit of the metal. As an example, for aluminum and stainless steel, safety factor of 2.2, the operating strain is about 0.3% (Table V-4). For a Fiberglas overwrap, this strain limitation allows only a small fraction of the glass capability to be used; however, with a carbon overwrap, a strain of 0.3% will allow most of the wrap capability to be used, because carbon has a modulus approximately three times that of glass and correspondingly about three times the stress of glass at equal strains. Boron, like carbon, also has a high modulus and shows an advantage over glass when wrapped over metal liners.

When titanium is considered for the liner material, the operating strain is actually higher than either the aluminum or stainless steel previously discussed (Table V-4). It also overcomes the permeation and compatibility problems associated with an elastomeric liner. However, a titanium alloy such as 6Al-4V has such a high strength-to-weight ratio (Table V-3) that an all-metal tank is very competitive with a composite tank of the same volume (and design pressure) from a weight standpoint alone.

Table V-4 Metal and Composite Tank Material Parameters^(1, 2)

MATERIAL	OPERATING STRESS (psi)	OPERATING STRAIN (%)	MODULUS (10 ⁶ psi)	DENSITY (lb/in. ³)
2219-T87 Aluminum	30,000	0.30	10	0.10
Titanium 6Al-4V	75,000	0.47	16	0.16
Stainless Steel (301 cryoformed)	95,000	0.32	30	0.29
Carbon/epoxy	60,000 ⁽³⁾	0.3	20	0.055
	40,000 ⁽⁴⁾	0.3	13.3	0.055
Boron/epoxy	90,000 ⁽³⁾	0.3	30	0.070
	60,000 ⁽⁴⁾	0.3	20	0.070
<p><u>Note:</u> Operating stress = ultimate stress/safety factor (2.2) Modulus = stress/strain</p> <p>(1) Assumed: 0.020 in. thick aluminum liner 0.010 in. thick titanium liner</p> <p>(2) Safety factor of 2.2</p> <p>(3) Unidirectional composite properties</p> <p>(4) Balanced bidirectional composite properties in hoop direction of cylinder</p>				

When considering metallic liner materials for an application such as presented by Mission A₁ with the mild cryogenic propellants, the relative differences in the coefficients of thermal expansion can become significant. In particular, when aluminum (or any material) with a high coefficient is overwrapped with carbon/epoxy with a low coefficient and the resulting composite must operate over a wide temperature range, the physical separation of the two can become unacceptable.

While the significance of cost may vary greatly depending on usage, it should be noted that the high-strength filaments under consideration are also high-cost materials. At the present time, both the carbon and boron filaments cost between 350 and 400 dollars per pound. Another factor to be considered in evaluating the relative merits of the composite versus an all-metal tank should be the comparison of the cost of the metal liner to that of a metal tank. Assuming that each is made of the same material, it is possible, in certain cases, that the cost of the additional mass of material in the metal tank would be more than offset by the more costly fabrication requirements on the thin liner shell due to its delicate nature.

C. PROPELLANT TANK DESIGN AND WEIGHT ANALYSIS

1. Metal Tanks

The following equations were used to calculate tank weights for the spherical and the cylindrical with hemispherical dome tanks. An additional 10% was added to the calculated weights to account for welds and attachments.

Tank Volumes

$$V_s = 4/3 \pi r^3 \quad [V-1]$$

$$V_c = \pi r^2 l \quad [V-2]$$

$$V_{cs} = 2/3 \pi r^3 (3 L/D - 1) \quad [V-3]$$

Wall Thickness

$$x_s = \frac{Pr}{2S} \quad [V-4]$$

$$x_c = \frac{Pr}{S} \quad [V-5]$$

Tank Weight (Thin Wall)

$$W_s = \frac{3PV_s \rho}{2S} \quad [V-6]$$

$$W_c = \frac{2PV_c \rho}{S} \quad [V-7]$$

$$W_{cs} = \left(\frac{2PV_{cs} \rho}{S} \right) \cdot \left[\frac{(L/D - 1/2)}{(L/D - 1/3)} \right] \quad [V-8]$$

For conospheroid tanks, the following equations were employed to calculate metal tank weights. Again, 10% was added to account for welds and attachments.

Tank Volume

$$V = 2 \left[\frac{\pi}{3} H \left(r_m^2 + r_d r_m + r_d^2 \right) + \frac{\pi}{6} b^2 \left(3r_d + b \right) \right] \quad [V-9]$$

For $\phi = 10$ deg:

$$V = 7.737021 r_m^2 \left(\frac{L}{2} \right) - 2.74828 r_m^3 - 1.364267 r_m \left(\frac{L}{2} \right)^2 + 0.080188 \left(\frac{L}{2} \right)^3$$

$$H = 1.17364 \left(\frac{L}{2} \right) - 0.984914 r_m$$

$$b = 0.984814 r_m - 0.173644 \left(\frac{L}{2} \right)$$

$$r_d = 1.17364 r_m - 0.20695 \left(\frac{L}{2} \right)$$

Wall Thickness (thin membrane)

$$x = \frac{Pr_c}{S \cos \phi} \quad (\text{conical section, } r_m \geq r_c \geq r_d) \quad [V-10]$$

$$x = \frac{Pr_d}{2S \cos \phi} \quad (\text{spherical end domes}) \quad [V-11]$$

Tank Weight

$$W = \rho \left\{ \frac{2\pi}{3} \left[\frac{P^2}{S^2 \cos 2\phi} + \frac{2P}{S \cos \phi} \right] \left[H \left(r_m^2 + r_d r_m + r_d^2 \right) \right] + \left[\frac{\pi P}{S \cos \phi} \right] \left[r_d^3 + r_d b^2 \right] \right\} \quad [V-12]$$

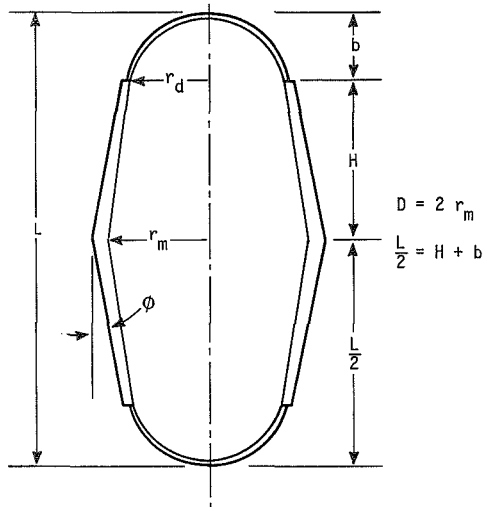


Figure V-17 Definition of Geometric Terms for Conospheroid

Geometric symbols used in these equations are defined in Figure V-17. All other symbols are defined in the list of symbols.

The baseline tank dimensions given in Table V-1 and the material properties presented in Table V-4 were employed in calculating mass of the metal propellant tanks. Mass of specially shaped tanks to accommodate specific propellant acquisition devices was also determined.

Volume of the special tanks was the same as the baseline tank volume with the exception of the

bonded rolling diaphragm tank as discussed in Chapter III, Section C. The design operating pressure for all tanks was 350 psia.

Results of the propellant tank mass calculations are presented in Table V-5. The baseline cylindrical tank hemispherical domes are half as thick as the barrel-section and are tapered to match the barrel. The conospherical tanks contain a varying thickness cone and domes half as thick as the minimum cone thickness. With one dome reversed, the bellows cylindrical tank employs end domes as thick as the barrel section. Two-to-one elliptical domes having the same thickness as the barrel section were used for the Telephragm and bonded rolling diaphragm cylindrical tanks. An additional propellant outlet port was added to the Mission A₁ and A₂ baseline spheres to accommodate the convoluted spherical diaphragm system (previously discussed in Chapter III, Section C). Figures presented for the special tanks also include acquisition device attachment mass. As noted in Table V-5, all of the other propellant acquisition concepts considered can be used with either the baseline spherical tanks or the baseline cylindrical tanks. Most of these can be used with both baseline geometries.

Table V-5 Metal Propellant Tank Mass* (lb_m)

MATERIAL MISSION NO. OF TANKS	6Al-4V TITANIUM (165 ksi UTS) [†]						2219 ALUMINUM (66 ksi UTS)						301 CRYOFORMED STAINLESS STEEL (210 ksi UTS) [‡]					
	A ₁		A ₂		B		A ₁		A ₂		B		A ₁		A ₂		B	
	2	4	2	4	1	4	2	4	2	4	1	4	2	4	2	4	1	4
Baseline tanks																		
Spherical	42.4	42.4	48.0	48.0	8.2	66.0	66.0	66.0	74.8	74.8	12.8	60.2	60.2	60.2	68.6	68.6	11.7	68.6
Cylindrical	46.9	49.5	54.4	56.9	9.7	73.3	73.3	77.4	85.0	88.9	15.2	66.8	66.8	70.5	77.5	81.0	13.8	81.0
Conospherical tanks for ring-reinforced diaphragms	Dissimilar metal with diaphragm					88.4	89.2	100.5	101.4	17.4	80.3	81.0	91.3	92.1				
Cylindrical tanks for Telephragms	Dissimilar metal with diaphragm					119.6	111.0	128.7	120.2	21.9	Dissimilar metal with diaphragm							
Cylindrical tanks for bonded rolling diaphragms	Dissimilar metal with diaphragm					147.7	130.7	159.0	142.0	22.8	Dissimilar metal with diaphragm							
Spherical tanks for con- volut spherical diaphragms	Dissimilar metal with diaphragm					68.0	70.0	76.6	78.8	12.8	Dissimilar metal with diaphragm							
Cylindrical tanks for metal bellows			130.0	117.0	19.4	191.0	171.0	204.0	183.0	30.4	174.0	155.0	186.0	167.0				

*Surface tension, polymeric bladder and diaphragm, external settling, dielectrophoretic, and capillary bellows propellant acquisition systems can be used with baseline tanks without weight addition. Tank mass for transverse collapsing bladders, same as baseline cylinders. Spherical tank mass for ring-reinforced diaphragms same as baseline spheres.

†Not recommended for Mission A₁ propellants.

‡Not recommended for Mission B propellants.

With some of the candidate propellant acquisition devices, it may be desirable to use vacuum loading techniques for filling the propellant tanks. The ability of the spherical baseline tanks to withstand vacuum loading without buckling was evaluated by means of theoretical equations taken from Ref V-1 and modified by an empirical correction factor. The correction factor was developed by Martin Marietta from industry-wide test results (Ref V-2) for different spherical pressure vessels of varying radius to wall thickness ratios, R/t . The correction factor is plotted in Figure V-18. The modified equation for the critical buckling stress in a spherical tank is given as

$$S_{cr} = \frac{C}{\sqrt{3(1 - \nu^2)}} \left(\frac{E_m x}{r} \right) \quad [V-13]$$

The critical buckling pressure differential is given as:

$$\Delta P_{cr} = \frac{2x S_{cr}}{r} \quad [V-14]$$

Combining Equations [V-13] and [V-14] and eliminating the wall thickness by means of the hoop stress formula for a sphere leads to the following equation for critical buckling pressure differential.

$$\Delta P_{cr} = C \frac{E_m P_b^2}{2S_u^2 \sqrt{3(1 - \nu^2)}} \quad [V-15]$$

Equation [V-15] indicates that the critical buckling pressure differential is dependent upon the material properties and independent of sphere size since the correction factor, C , is a function of r/x .

The results of applying Equation [V-15] to baseline tanks made of titanium, aluminum, and 301 cryoformed stainless steel are presented in Table V-6. The tanks were designed for a burst pressure of 770 psia (2.2 times the normal working pressure of 350 psia). To obtain the C -factor, the curve shown in Figure V-18 for a 99% probability of nonbuckling was used. The results of the calculations indicate that there is no buckling problem for the baseline spheres. The margin of safety for aluminum tanks is over an order of magnitude higher than that for the titanium or stainless steel tanks, however.

Table V-6 Critical Buckling Pressure Differential for Baseline Spherical Tanks

MATERIAL	POISSON'S RATIO	TANK RADIUS TO THICKNESS RATIO	CORRECTION FACTOR, C (99% PROBABILITY)	CRITICAL BUCKLING PRESSURE DIFFERENTIAL (psi)
6Al-4V Titanium	0.30	428.57	0.22	23.19
2219 Aluminum	0.33	171.43	0.47	209.43
301 Cryoformed Stainless Steel	0.3	545.45	0.168	20.5

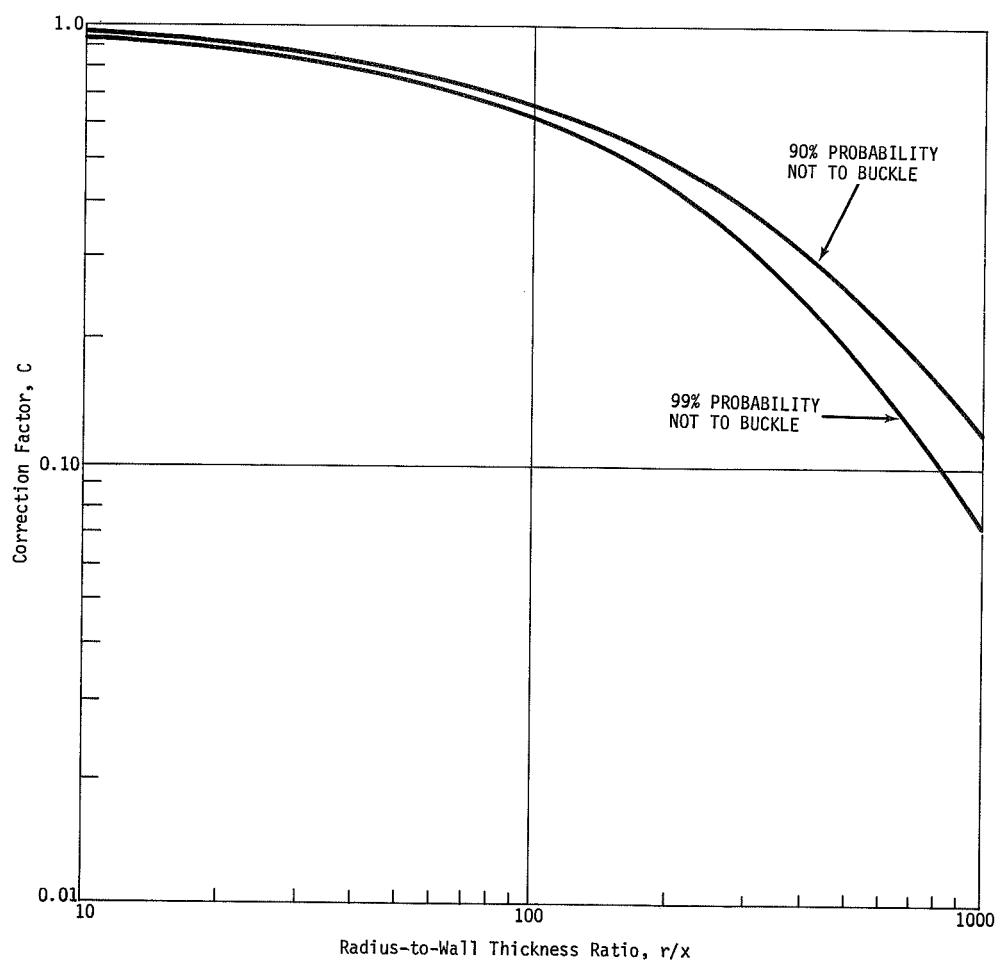


Figure V-18 Statistical Factor for the Design of Spherical Shells to Prevent Buckling in Compression

2. Composite Tanks

An evaluation was made on the use of composite tanks for the three reference missions. The primary objective was to determine if composite tankage offered a significant weight savings in comparison to an all-metal tank system. Use of the composite tanks was considered for both the 350-psia propellant tanks (all missions) and the 4000-psia pressurant storage container (Missions A₁ and A₂ only). This evaluation is discussed in the following paragraphs.

Providing tank attachments is more difficult for composite tanks than for metal tanks. Special attention is required in wrapping the composite structure at these points where additional wrapping thickness is required. The net result is a higher attachment weight for composite tanks than is required for all-metal tanks. This problem was not considered in detail. Instead, a comparison was made based on the tank shell only; the tank mass was determined by membrane strength requirements.

The following equations, together with Eq [V-6] and [V-7], were used to calculate composite tank weights:

$$W_{cl} = 2\pi r l x \rho \quad [V-16]$$

$$W_{dl} = 4/3\pi \left[r^2 b - r_i^2 b_i \right] \rho \quad [V-17]$$

Equation [V-17] describes the weight of an oblate spheroid shell.

The properties used for the determination of carbon/epoxy tank weights assume presently available material properties (Table V-4). It is expected that these properties will be improved significantly within the next five years. The weight of boron/epoxy tanks, though not calculated, would be comparable to those for the carbon epoxy. Boron/epoxy tanks are slightly stronger than carbon/epoxy tanks, but the higher density of boron/epoxy tends to offset this strength advantage. Carbon tends to be more attractive than boron since no significant increase in boron/epoxy properties is foreseen.

Calculated mass of the various composite tanks considered is presented in Table V-7. Masses are shown for Viking-sized tanks in addition to those for the mission propellant tanks and for the Mission A₂ pressurant storage tank. The metal tank weights listed do not include a 10% addition for welds and attachments.

Table V-7 Metal and Composite Tank Mass Comparison

	MISSION A ₁	MISSION A ₂	MISSION B	VIKING	MISSION A ₂ PRESSURANT STORAGE
Tank volume, ft ³ , in. ³	9.92 17142	11.25 19440	3.86 6670	25.46 44000	2.38 4113
Operating pressure (psia)	350	350	350	350	4000
Diameter (in.)					
Sphere	32.0	33.3	23.35	†	19.9
Oblate spheroid	37.6	39.0	27.3	†	23.2
Cylinder	28.0	28.0	18.0	36.0	--
Length (in.)					
Oblate spheroid	23.5	24.4	17.1	†	14.6
Cylinder with hemispherical domes	37.18	40.89	32.2	55.2	--
Cylinder with ellipsoidal domes	33.7	37.4	25.4	50.7	--
Mass, lb _m §					
Metal sphere					
Titanium	*	21.6	7.4	†	52.6
Aluminum	30.0	--	--	†	--
Metal cylinder with hemispherical domes					
Titanium	--	--	--	56.6	--
Composite oblate spheroid					
Titanium liner with complete carbon/ epoxy overwrap	*	24.4	6.3	†	47.0
Aluminum liner with complete carbon/ epoxy overwrap	23.2	25.8	6.9	†	--
Composite cylinder with hemispherical domes					
Titanium liner with carbon/epoxy overwrap on cylinder only	*	23.0	7.6	49.7	--
Aluminum liner with carbon/epoxy over- wrap on cylinder only	27.0	30.0	8.3	--	--
Composite cylinder with ellipsoidal domes					
Titanium liner with complete carbon/ epoxy overwrap	*	24.9	6.5	57.2	--
Aluminum liner with complete carbon/ epoxy overwrap	24.0	26.4	7.2	--	--

*Not considered due to propellant incompatibility

†Not considered because of packaging restrictions

§Shell only; attachments, penetrations, and welds not considered.

Comparison of these results indicates that there is very little weight advantage in using a composite tank when conditions dictate a metal liner be used for reasons of compatibility or permeability. In fact, it indicates that when a metal with a high strength-to-weight ratio is considered, an all-metal spherical tank can show a slight weight advantage over a composite (Mission A₂). This advantage shifts in favor of the composite only when (1) shapes of lower efficiency (cylinders or spheroids) are required due to packaging considerations, (2) metals with lower strength-to-weight ratios are required because of compatibility, or (3) when the pressure-volume factor becomes large enough to take advantage of the large quantity of low density composite material required. Therefore, it appears that no general statement can be made stating composite tanks are superior (or inferior) to metal tanks. Only when consideration is given to specific requirements (e.g., size, pressure, compatibility, and environment) and the emphasis to be placed on weight, cost and reliability is established, can a comparative evaluation be made.

VI. EVALUATION AND SYSTEM SELECTION

The information presented in Chapters III through V of this report was employed in evaluating the three propulsion subsystems considered in this investigation. These subsystems were the propellant tankage, propellant acquisition, and pressurization systems that comprise the propulsion system of interest. In evaluating the various options and possible approaches available for each subsystem, the primary goal was to select the specific propulsion system that offered the highest reliability and lowest mass for each of the reference missions. Minimum cost and schedule time were also considerations as were packaging and overall spacecraft compatibility.

In selecting the preferred propellant tank and pressurization subsystems, the effect of pertinent subsystem operating parameters, impact on the propulsion system envelope, and interaction with other subsystems were evaluated. The combination of hardware and operating conditions offering the most advantages in terms of mass, reliability, cost and schedule was then selected as the preferred system. This process was followed for each of the three reference missions.

Selection of a preferred propellant acquisition concept is not quite as straightforward a process. Each candidate concept possesses certain advantages and disadvantages. These vary from device to device and some are unique to one device only. In addition, some of the candidate concepts were developed for specific applications and are not as readily adapted to spacecraft as others. Metallic diaphragms are an example of this latter case. On the other hand, acquisition concepts such as settling rockets or surface tension systems can be adapted to a wide variety of applications. Thus, selection of acquisition devices is dependent more on mission and vehicle than are the other subsystems. Because of the above considerations, a rating system approach was employed to assess the relative merits of the different candidates and select the preferred concept for each reference mission.

The approach employed in evaluating each of the propulsion subsystems and the results obtained are presented in this chapter. The evaluation is discussed by subsystem, and the propulsion systems selected for each of the three missions under consideration are presented in the final section.

A. PROPELLANT TANK SUBSYSTEM

Number of tanks, size and geometry, and materials of construction were evaluated in the selection of the preferred propellant tank subsystem. The information presented in Chapter V was employed in this evaluation. The approach used in selecting the preferred system is presented in Figure VI-1.

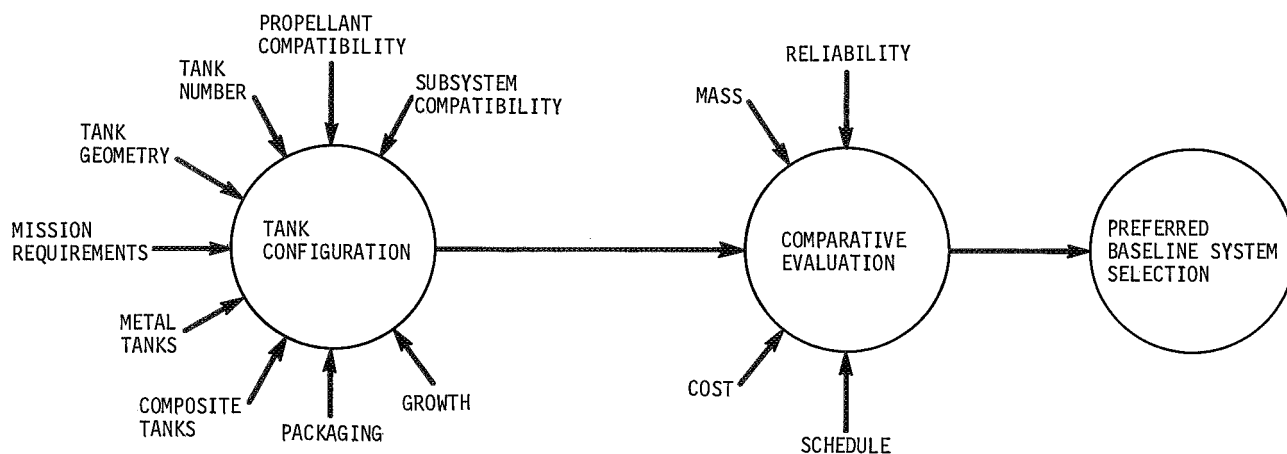


Figure VI-1 Propellant Tank Subsystem Evaluation

1. Number of Tanks

Two-tank and four-tank configurations were evaluated to determine which arrangement offered the most advantages for Missions A₁ and A₂. This was not a consideration for the Mission B single tank monopropellant system. An assessment was made of the impact that the number of tanks had on the propulsion system envelope and packaging, on other subsystems, and on spacecraft mass, reliability, cost and schedule.

a. Envelope - All baseline tanks fit within the reference envelope for all three missions. As shown in Table V-2, this is true for both the two-tank and four-tank configurations using either spheres or cylinders. In considering growth potential, two spherical tanks are limited to about a 36% increase in volume in a practical side-by-side packaging arrangement. Four spheres and either two or four cylinders can meet a 50% volume increase,

and two or four cylindrical tanks can meet a 126% growth requirement (equivalent to Viking Orbiter). A two- or four-tank design using baseline tanks in the Viking Orbiter reference envelope presents no spacecraft separation clearance problems. Adjustments can be made in the packaging arrangement to provide essentially the same clearance for either design. Thus, neither configuration affects the spacecraft to launch vehicle adapter ring or basic support structure.

Referring to Table V-2, it is seen that the propellant and pressurant tank package volume and package-to-envelope volume ratio are lower for the two-tank design. Between 10 and 20 ft³ of additional usable volume are available with the two-tank design. This space could be used for packaging additional electronics or other equipment inside the reference envelope. Thus, packaging advantages are provided by a two-tank design.

b. Impact on Other Subsystems - The tank package surface area is 13 to 16 ft² lower for a two-tank design than for a four-tank system, as shown in Table V-2. With a smaller package surface area, the insulation system for two tanks should be lighter and probably more reliable. Encapsulation, if required, should be lighter and easier to accomplish. If shadow shields are used, there should be less area and lower mass required with a two-tank design. Table V-2 also shows that the two-tank design offers meteoroid penetration advantages because of its smaller projected surface area. This area is the tank package area projected toward the aft end of the spacecraft.

Additional benefits are provided by a two-tank system in the areas of pressurant leakage, propellant usage, and lines and valves. In comparison to a four-tank system, two tanks have lower surface area, fewer weld joints, and fewer attachments and penetrations, all of which tend toward lower leakage. A potential propellant usage advantage is available with two tanks because a balanced outflow between two oxidizer tanks and between two fuel tanks, required in a four-tank, parallel-outflow design, is not necessary. Also, fewer lines and valves are needed for both pressurization and propellant outflow with a two-tank design.

From a guidance and attitude control system standpoint, little difference in slosh and dynamic loading should occur between a two- and a four-tank system. A slight, predictable center of gravity shift in the lateral direction will occur with a two-tank system during propellant outflow; an axial cg shift will occur with both designs.

The two-tank design should result in a slightly lower pressurization subsystem mass since pressurant usage, propellant temperature, and gas residuals should be lower because of the smaller propellant tank and gas/liquid interface area adjacent to the ullage. The four-tank system requires twice as many propellant acquisition devices as a two-tank design (with the exception of the settling rocket system), producing an increase in acquisition device mass and an attendant decrease in reliability.

From these considerations, it is seen that the two-tank design has less of an impact on other spacecraft subsystems than a four-tank system. With two tanks, advantages are gained in thermal control, meteoroid penetration, pressurant leakage, propellant usage, lines and valves, pressurization subsystem mass, and propellant acquisition.

c. Mass, Reliability, Cost and Schedule - As shown by the tank data in Table V-5 and by the acquisition subsystems mass data presented in Chapter III, the tank and expulsion device masses are lower for the two-tank design. The increased thermal control and meteoroid penetration mass implications, and the greater pressurization subsystem and line and valve mass for the four-tank design, result in an even greater difference in mass. Two tanks are also preferable in regard to reliability. The two-tank design has fewer tanks and welds to fail, lower leakage potential, less valving and line joints to fail, fewer acquisition devices to fail, a lower projected meteoroid impact area, and a potentially more reliable thermal control system. In considering schedule, the two-tank system has less welding and fewer attach points and penetrations to fabricate. Also, the inspection, cleaning, line attachment, and component test effort is less for two tanks. Therefore, fabrication and assembly time should be less for a two-tank design. The lower schedule time together with fewer components translates into lower tank, acquisition device, line and valve, and assembly and test costs for two propellant tanks in comparison to a four-tank design. This assessment shows that the two-tank configuration is lighter, more reliable, less costly, and can be fabricated and assembled in a shorter time than a four-tank system. A comparison of the pertinent items for Mission A₂ is presented in Table VI-1. Results of the evaluation also apply to Mission A₁.

Table VI-1 Two versus Four Propellant Tanks, Mission A₂

	SPHERES		CYLINDERS	
	2 TANKS	4 TANKS	2 TANKS	4 TANKS
Tank Mass, lb _m *	48.0	48.0	54.4	56.9
Package Volume, ft ³	60	80	60	69
Volume Ratio				
Package/Envelope	0.30	0.40	0.30	0.35
Tank/Package	0.47	0.35	0.47	0.41
Package Surface Area, ft ²	87	109	90	100
Tank Surface Area, ft ²	63	76	65	81
Meteoroid Impact Surface Area, ft ²	20.3	25.6	17.3	22.0
Leakage	Lowest	High	Low	Highest
System Hardware Requirements (propellant acquisition, lines, valves)	Lower	Higher	Lower	Higher
Propellant Acquisition Subsystem Mass	Lower	Higher	Lower	Higher
Pressurization Subsystem Mass	Lowest	High	Low	Highest
Reliability	Highest	Low	High	Lowest
Schedule Time & Costs	Lowest	High	Low	Highest
* 6Al-4V Titanium				

2. Size and Geometry

Baseline tanks for this investigation were spheres and cylinders with hemispherical domes. Special tanks required by some of the propellant acquisition concepts were also considered. These special shapes included conospheroids for one version of ring-reinforced metal diaphragms, cylinders with elliptical domes for bonded rolling metal diaphragms, and cylinders with one of the hemispherical domes inverted to provide the best volumetric efficiency arrangement for a metal bellows acquisition device. Selection of a specially shaped tank would have been given serious consideration only if mission or operational advantages could be provided. While the special tanks could be accommodated within the reference envelope, they presented a larger packaging requirement and mass than the baseline tanks, as shown in Tables V-2 and V-5. Also, as

Because spheres have a slightly smaller surface area and less weld joints, the pressurization subsystem mass and pressurant leakage should be potentially less with spheres than with cylinders. In considering propellant tank and acquisition device interaction, dielectrophoresis, settling rockets, polymeric bladders and diaphragms, capillary bellows, and surface tension systems can be employed in either baseline tank geometry. In fact, with the exception of the polymeric bladders and diaphragms, these acquisition concepts can be used in essentially any propellant tank. Metal bellows are limited to cylindrical tanks with reasonable L/D ratios; ring-reinforced metal diaphragms are adaptable to spheres or conospheroids. From a tankage standpoint, the best approach is to select an acquisition device compatible with the more advantageous tank configuration. A device that does not limit the choice of tank geometry while providing the desired operational characteristics offers obvious advantages.

Spherical tanks provide the lowest mass subsystem (Table VI-2); this is true for all three missions. They also have fewer welds to fail and a lower leakage potential, tending toward higher reliability. Spherical tanks have only one closure weld while cylinders have one closure weld plus a barrel section weld and a weld joint between the barrel and the other end dome. Because of less welding for spheres, the inspection and cleaning requirement should also be less. The result should be lower fabrication and assembly time for spheres. Spheres should also provide lower material, fabrication, assembly, and inspection costs.

Selection of spherical tanks for all three missions will provide a lighter, less costly, and more reliable propellant tank subsystem with schedule benefits over a system using cylindrical tanks. Advantages are gained in thermal control, pressurization, and fabrication by choosing spheres instead of cylinders.

3. Materials

In this investigation, three different metals were given primary consideration in selecting materials for construction of the propellant tanks. As discussed in Chapter V, these were 300-series stainless steel, aluminum, and titanium. Compatibility with the propellants was considered for each mission and the compatible materials were then compared to obtain the best propellant tank material. Pertinent metal properties are shown in Table V-3. All-metal tanks were also compared to a composite tank constructed of thin metal liners and carbon/epoxy overwrap.

a. Candidate Metals - The best materials for construction of the OF_2 and B_2H_6 propellant tanks for Mission A₁ are stainless steel and aluminum. Titanium is not a contender because of the possible shock sensitivity with OF_2 observed in some investigations (Ref III-54, and III-88 thru III-90).

Cryoformed 301 stainless steel, having greater ultimate tensile strength than other 300-series stainless steels, was considered along with 2014, 2219 and 6061 aluminum. These materials all exhibit excellent compatibility with the A₁ propellants. However, problems are encountered in welding cryoformed 301 stainless steel. The welding operation anneals the material in the vicinity of the weld causing a reduction in strength in this area with attendant loss of the cryoforming advantage. This would present problems in attachment of many of the propellant acquisition subsystem candidates. Methods of circumventing a reduction in strength can probably be found but each attachment requires separate consideration; both cost and time would be involved in arriving at the best solution. In addition, cryoforming presents another and perhaps more important disadvantage -- it exhibits the characteristics of a permanent magnet. This could result in spacecraft compatibility problems by affecting or limiting the use of various components in the guidance system such as magnetometers. Even if these factors could be circumvented or accounted for, additional cost and time would be involved. For these reasons, aluminum was selected as the preferred material.

Strength and weldability were the primary considerations in selecting an aluminum alloy. In regard to weldability, 2219 and 6061 aluminum possess comparable characteristics and both are superior to 2014. The ultimate strength of 2219 aluminum is about equal to that of 2014 and 30% greater than that of 6061. Therefore, since 2219 aluminum possesses the best combination of compatibility, strength and weldability, it was selected for the Mission A₁ propellant tanks.

Titanium and aluminum were the two prime materials considered for Mission A₂ since they exhibit the best compatibility characteristics with N_2O_4 and MMH. Stainless steel was eliminated for Mission B also, because it promotes excessive decomposition rates of hydrazine-hydrazine nitrate mixtures. Since titanium with its higher strength-to-weight ratio provides much lighter tanks, 6Al-4V titanium was selected for the propellant tanks for Mission A₂ and for the single tank for Mission B.

b. Metal Versus Composite Tanks - As discussed in Chapter V, three different composite structures were considered. These were (1) a wrapped cylinder with bare hemispherical domes, (2) a completely wrapped cylinder with elliptical domes, and (3) a completely wrapped oblate spheroid. The latter provided the lightest composite tank for all three missions. A weight comparison is shown in Table V-7 between an all-metal spherical tank and the various composite structures considered. The weights presented are for the tanks only without any consideration of attachments, penetrations, or welds. A safety factor of 2.2 on ultimate strength is reflected in all weights. With a 20-mil aluminum liner, the oblate spheroid is the lightest composite structure for all three missions, while a 10-mil titanium liner results in the wrapped cylinder with bare hemispherical domes lightest for Mission A₂, and an oblate spheroid again the lightest for Mission B.

A summary of the metal versus composite tank evaluation is presented in Table VI-3. A maximum weight savings of about 14 pounds for Mission A₁ and one pound for Mission B is potentially available with a composite tank structure. No savings are available for Mission A₂ as composites are from three to seven pounds heavier than the two titanium spheres. In actuality, composite tankage would probably provide no weight savings at all and could be heavier in all cases for this application for the following reasons:

- 1) Uncertainties exist in composite structure calculations. It is felt that the calculated weights more nearly indicate an equality between metal and composite tanks than the existence of an actual weight difference;
- 2) Composite tanks inherently result in heavier attachments and penetrations than metal tanks because the metal liner provides no attachment strength and this must be obtained with additional overwrap at the attachment points.

Table VI-3 Composite Tank Evaluation^{*†}

MISSION	OBLATE SPHEROID			CYLINDER COMPLETE OVERWRAP			CYLINDER BARREL OVERWRAP			METAL SPHERE		
	A ₁	A ₂	B	A ₁	A ₂	B	A ₁	A ₂	B	A ₁	A ₂	B
Metal [§]	1100 Al	Ti	Ti	1100 Al	Ti	Ti	2219 Al	Ti	Ti	2219 Al	Ti	Ti
Liner Thickness, mils	20	10	10	20	10	10	20	10	10			
Mass, lb _m [¶]	46.4**	48.8	6.3**	48.0	49.8	6.5	54.0	46.0**	7.6	60.0	43.2	7.4
Reliability	Unproven			Unproven			Fair			Good		
Leakage	Questionable			Questionable			Questionable			Good		
Thermal Compatibility	Bad	Good	Good	Bad	Good	Good	Bad	Good	Good	Good		
Vacuum Loading	No	No	No	No	No	No	No	No	No	Yes		
Fabrication Cost and Time	Higher			Higher			Moderate			Lower		

*Two tanks for Missions A₁ and A₂; one tank for Mission B.

†Carbon/epoxy overwrap.

§Ti was 6Al-4V Titanium.

¶The 10% weld and attachment weight allowance for metal tanks has been omitted for comparison; composite weights do not include attachment and penetration weights.

**Highest weight composite structure.

The use of composite tanks for cryogenic applications is questionable. The coefficient of thermal expansion of the overwrapped structure is near zero. This could result in serious problems with the liner buckling as it contracted away from the overwrapping in cooling from ambient to cryogenic temperatures. Composites could encounter problems whenever the operational temperature varies significantly from the fabrication temperature. For this reason, composite tanks should not be considered for the near-cryogen Mission A₁. Additionally, the cost and fabrication times for composite tanks are considerably greater than for metal tanks, the state-of-the-art position is not comparable, and reliability must be assessed as considerably lower than metal tanks, especially from a leakage standpoint.

In summary, all-metal baseline propellant tanks are probably equal in weight or even lighter than their composite counterparts. Also, metal tanks offer reliability, and cost and schedule advantages in comparison to composite tanks. This conclusion is

reinforced by the results obtained in comparing metal and composite tanks for the 126% larger two-tank Viking Orbiter configuration (Table V-7). For the bare tanks only, composite tanks constructed of a 10-mil titanium liner with carbon/epoxy overwrap are only 14 lb_m lighter than an all-titanium tank. This difference would disappear when considering welds, attachments and penetrations.

B. PROPELLANT ACQUISITION SUBSYSTEM

The propellant acquisition concepts considered in this evaluation were dielectrophoretic systems, polymeric bladders and diaphragms, metallic diaphragms, metal bellows, external settling rockets, surface tension devices, and the capillary/bellows concept. Metallic diaphragm devices considered were ring-reinforced diaphragms and the convoluted spherical diaphragm.

In evaluating the candidate propellant acquisition concepts, emphasis was placed on providing a thoroughly objective and impartial assessment in order to assure selection of the concept that is indeed best suited for use in the three specific missions of interest. As mentioned previously, a comparative evaluation of the many devices employing widely differing operational techniques was not as straightforward as, for instance, comparing two- and four-tank systems for containing propellants. As an example, the settling rocket system using separate gas storage, valving and cold gas rockets had to be compared to flexing metal diaphragms. To aid in the evaluation, a numerical rating system was developed and employed to establish a figure of merit for each concept. The concept receiving the highest figure of merit for each of the three missions was then selected as the preferred candidate for propellant acquisition. The detailed information compiled for each candidate concept, presented in Chapter III, was used in the evaluation. This overall approach for selection of the preferred concept is depicted in Figure VI-2. As shown, the evaluation also included consideration of the impact of the other two propulsion subsystems on propellant acquisition.

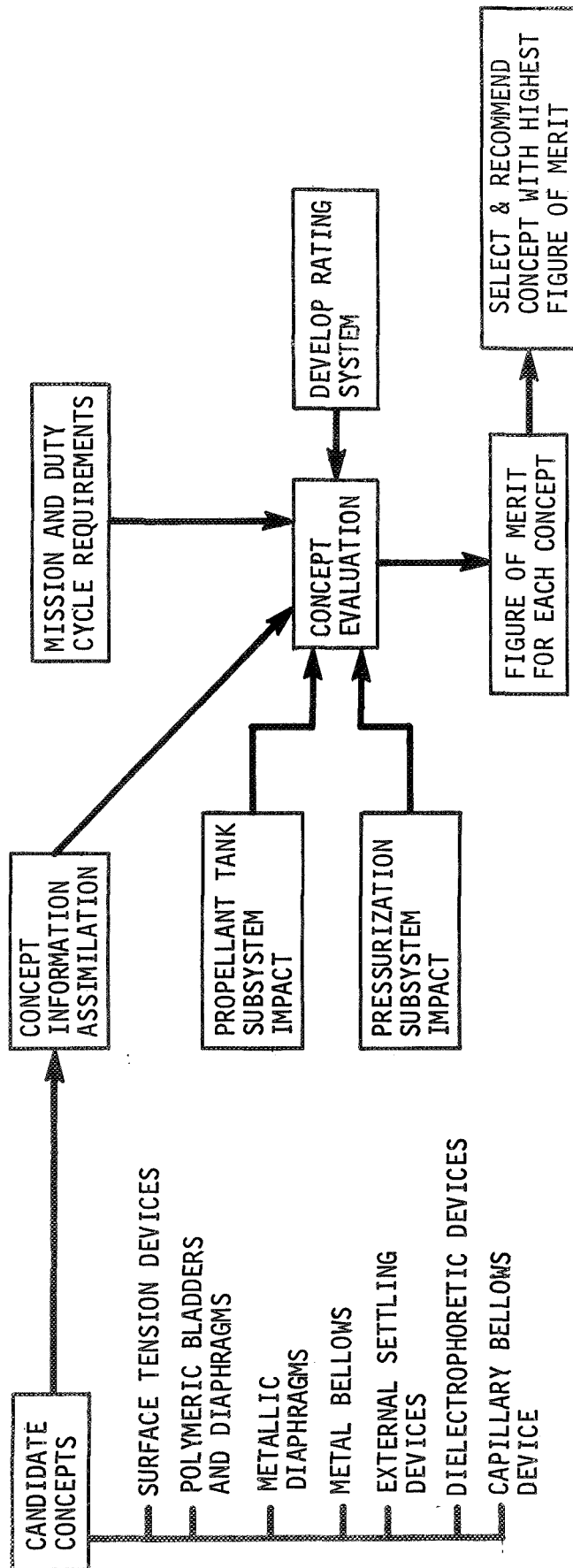


Figure VI-2 Evaluation of Propellant Acquisition Concepts

1. Rating System

The rating system employed in the evaluation was developed through an evolutionary process. Four separate evaluations using three different rating systems were conducted. Shortcomings or difficulties, encountered in various areas of the rating system, included the possibility that a system could be selected as best from a numerical rating standpoint, but not be able to meet the mission performance requirements and a mass evaluation that over-emphasized what in reality were small differences between candidate concepts. The problem areas were gradually eliminated as development of the final rating system progressed.

Prior to establishing a point rating system, a comparison of the candidate concepts was made. Presented in Table VI-4, the comparison shows surface tension devices possess more desirable propellant acquisition features than the other concepts, with dielectrophoresis, settling rockets and capillary bellows potentially second. Based on the information presented in Chapter III, possible failure modes for the various concepts were tabulated and used in the numerical rating. These modes together with an assessment of the probability of occurrence are shown in Table VI-5.

A relative comparison of the acquisition concepts was also made for each of the three missions using a point system from one to five where one was best and five was poorest. These relative comparisons are presented in Tables VI-6 thru VI-8 for Missions A₁, A₂, and B, respectively. Candidates considered not capable of meeting the mission requirements were not rated; this is discussed in more detail later in this section. The relative assessment shows surface tension first and settling rockets second for application on all three missions.

Two distinct areas are included in the system employed for the final evaluation. These are a performance assessment in terms of mission environment and duty cycle requirements and a rating schedule incorporating various rating categories. The performance capability of each candidate propellant acquisition concept for meeting mission requirements was assessed prior to rating the device. If the concept had serious limitations or would not perform adequately for the mission under consideration, it was not rated for that mission and was assigned a zero figure of merit. The reasons for assigning this rating were documented. Concepts considered capable of meeting performance requirements were then rated according to the rating schedule.

Table VI-4 Propellant Acquisition Concept Comparison

	DIELECTRO- PHORESIS	SETTLING ROCKETS	METAL BELLOWS	POLYMERIC BLADDERS	POLYMERIC DIAPHRAGMS	SURFACE TENSION	RING-REINFORCED DIAPHRAGM		CONVOLUTED SPHERICAL DIAPHRAGM	CAPILLARY/ BELLOWS
							SPHERE	CONOSPHERE		
Expulsion Efficiency, %	99.9	99.9	98.0	98.0	99.0-99.5	98.8-99.6	95.5	95.5	98.0	98.5
Volumetric Efficiency, %	99.9	99.9	88.0	98.5-99.6	96.4-98.9	99.9	98.0	98.0	98.0-99.9	99.5
Weight, lb										
Mission A ₁	38.0	48.0	182.6*	NA	NA	15.0	66.1	110.7	48.2	18.2
Mission A ₂	NA	43.0	232.8*	51.0	32.5	13.0	110.5	167.9	83.8	14.0
Mission B	NA	31.0*	NA	NA	NA	3.1	NA	NA	11.0	NA
Pressurant Solubility	Yes	Yes	No	Yes	Yes	Yes	No	No	No	Yes
Impact on Baseline Tanks	None	None	†	None	None	None	§	§§§	§	None
Duty Cycle Limitations	None	No. of Restarts	None	None	None	No. of Restarts	None	None	None	None
Off-Load Limitations	None	None	None	Yes	Yes	None	Yes	Yes	Yes	None
Cycle Life	>1000	Per Design	500 to 1000	<10 (Teflon)	~20 (Teflon) >50 (Rubber)	>1000	<10	<10	1 Reversal <1 Cycle	500 to 1000
Series Tankage Capa- bility	Yes	Yes	No	No	No	Yes	No	No	No	Yes
Fuel Decomposition Problems	No	No	Minor	Minor	Minor	Minor	Minor	Minor	Yes	Minor
Material Limitations	No	No	Yes	No**	No**	No	Yes	Yes	Yes	Yes
Additional Subsystems Required§§	Yes¶¶	Yes***	Yes†††	Yes†††	Yes†††	No	Yes†††	Yes†††	Yes†††	No

* Heaviest system.

§§ Additions to basic propulsion system.

† Major change (cylinder only).

¶¶ Power supply.

§ Minor (sphere only).

*** Concept is an additional subsystem.

¶¶ Series of partial expulsions not demonstrated.

††† Capillary bubble retention device required over outlet.

** No materials for cryogenics.

§§§ Major change (conosphere only)

†† 10-yr Life questionable.

Table VI-5 Possible Failure Modes*

CANDIDATE CONCEPT	CATASTROPHIC		ANOMALOUS	
	MODE	PROBA-BILITY	MODE	PROBA-BILITY
Polymeric Bladders and Diaphragms	Tear	4	Pinholing	1
Bellows	Leaf weld failure	5	Pinhole leak	4
			Snaking	5
Metallic Diaphragms	Tear	4	Pinholing	1
External Settling	Valve fails closed	5	Regulator shift	5
	Valve fails open	5	Gas leakage	4
	Computer/sequencer failure	5		
Capillary Bellows	Loss of trapped propellant	5	Gas ingestion w/outflow	3
	Leaf weld failure	5	Weld pinhole	4
Surface Tension	Loss of trapped propellant	5	Some gas penetration (flow annulus)	4
Dielectrophoresis	Power supply signal loss	5	Power supply degradation	5
	Power supply failure	5		
* Relative ratings - 1 through 5 where 1 represents high probability and 5 low probability.				

The rating categories considered in the rating schedule were (1) availability, (2) system compatibility, (3) reliability, (4) testability, (5) mass, and (6) design versatility. In the rating schedule, each of the six categories is allotted a maximum rating factor of one. Deficiencies in candidate concepts are penalized by subtracting fractions from the allotment according to the schedule. The magnitude of the penalties was determined by relative comparison. Intermediate weighting factors were determined by relative importance of the rating categories. The intermediate factors were then normalized so that the sum of the final weighting factors was 100%. This allowed the more important rating categories, such as reliability, to receive heavier weighting in the evaluation. A detailed discussion, including illustrations of this operations research approach for ranking or weighting various objectives, is presented in Ref VI-1. The weight factors employed were:

	<u>Percent</u>
Reliability	25
Mass	20
Testability	20
System Compatibility	20
Availability	10
Design Versatility	5

Depending upon the viewpoint of these rating categories, they can be considered either as stated or as an effective weighting of 20% for mass and 80% for reliability, since testability, system compatibility, availability, and design versatility may be looked upon as measures of or impacts on reliability.

* Finally, a figure of merit was established for each acquisition concept/mission combination being rated. This figure of merit was calculated as the summation of the rating factor - weighting factor products for all six rating categories. With this system, the maximum possible figure of merit was one.

The method used for establishing a figure of merit for each candidate propellant acquisition concept follows:

Performance Assessment

A. Candidate Concept Must Meet Mission Environment and Duty Cycle Requirements

- 1) Engine Duty Cycle (series of partial expulsions)
- 2) Vibration and Slosh
- 3) Acceleration
- 4) Thermal Environment

B. Candidate Concept Must Possess Certain Characteristics

- 1) No Major Compatibility Problems
- 2) Usable with Both the Fuel and the Oxidizer
- 3) Manufacturability Not Questionable
- 4) Repeatable Expulsion Performance

If the candidate concept cannot meet the mission performance requirements or is found deficient in the above areas, a zero figure of merit is assigned for the mission under consideration.

However, if the candidate is considered capable of meeting performance requirements, the candidate is rated for each mission according to the rating schedule.

Rating Schedule

A. Availability Maximum Rating Factor = 1.0

1) Development Status Maximum Allotment = 0.6

- a) Similar system developed and qualification tested - no penalty
- b) Only experimental development - subtract 0.2
- c) Only feasibility tests or less - subtract 0.6

2) Manufacturability Maximum Allotment = 0.4

- a) Similar system fabricated - no penalty
- b) New techniques required - subtract 0.2
- c) New technology required - subtract 0.4

B. System Compatibility Maximum Rating Factor = 1.0

1) Different design concept for fuel and oxidizer - subtract 0.2 Maximum Allotment = 0.2

- 2) Propellant/material compatibility Maximum Allotment = 0.2
 - a) Class 1* material only - no penalty
 - b) Class 2* material used - subtract 0.1
 - c) Compatibility problem (includes problem with fuel decomposition) - subtract 0.2
- 3) Tankage/Device Compatibility Maximum Allotment = 0.2
 - a) Cylindrical Tanks
 - 1) L/D restrictions out of study range - subtract 0.05
 - 2) Special tapers or domes required - subtract 0.05
 - 3) Not acceptable - subtract 0.1
 - b) Spherical tanks not acceptable - subtract 0.1
 - c) Two or four tanks not acceptable - subtract 0.1
- 4) Tankage/Device Cleaning Maximum Allotment = 0.15
 - a) Cleaning after assembly very difficult - subtract 0.1
 - b) Contaminant trap areas exist - subtract 0.1
- 5) Tankage/Device Passivation Maximum Allotment = 0.15
(applies to Mission A₁ with OF₂ only)
 - a) Contaminant trap areas exist - subtract 0.1
 - b) All areas inside tank cannot be passivated at operating pressure - subtract 0.1
 - c) Passivation cannot be conducted with complete tank/device assembly - subtract 0.15
- 6) Spacecraft Compatibility Problem Maximum Allotment = 1.0
- subtract 1.0
- C. Reliability Maximum Rating Factor = 1.0
 - 1) Device has moving parts - subtract 0.1 for
each moving part Maximum Allotment = 0.2
 - 2) Device requires additional subsystems beyond
the basic propulsion subsystem - subtract 0.1
for each additional subsystem Maximum Allotment = 0.2
 - 3) Catastrophic failure modes - subtract 0.1 for
each independent failure mode Maximum Allotment = 0.3
 - 4) Anomalous operation failure modes - subtract
0.05 for each independent failure mode Maximum Allotment = 0.3

*Class 1 materials are aluminum or stainless steel for Mission A₁ and aluminum or titanium for Missions A₂ and B; stainless steel is a Class 2 material for Mission A₂.

- D. Testability Maximum Rating Factor = 1.0
- 1) Device Has Cycle Limitations Maximum Allotment = 0.4
 - a) Greater than 50 cycles - no penalty
 - b) Less than 50 cycles - subtract 0.2
 - c) Less than 20 cycles - subtract 0.3
 - d) Less than one cycle - subtract 0.4
 - 2) Verification of Operational Readiness Maximum Allotment = 0.6
 - a) Acceptance test full-scale without performance degradation - no penalty
 - b) Acceptance test part of flight system and qualify remainder on statistical basis - subtract 0.3
 - c) Flight qualify on statistical basis only - subtract 0.6

- E. Mass Maximum Rating Factor = 1.0
- Comparison of total mass attributed to candidate device to the total mass attributed to the heaviest device under consideration.

Total mass attributed to a device is the summation of:

- 1) Dry weight of device only;
- 2) Residuals attributed to device that includes unexpellable, trapped propellant within the tank and any vaporized propellant in the ullage, minus savings in pressurant weight (based upon helium) resulting because of vaporized propellant;
- 3) Additional tank, line, or valve weight required by the device over weight of selected baseline tanks.

$$\text{Mass Rating} = \frac{\text{Wt Heaviest} - \text{Wt Candidate}}{\text{Wt Heaviest}}$$

- F. Design Versatility Maximum Rating Factor = 1.0
- 1) Design margin capability (consider $\pm 100\%$ of nominal values) Maximum Allotment = 0.2
 - a) Burn time limitation - subtract 0.1
 - b) Limitation on number of restarts - subtract 0.1
 - c) Acceleration limitation - subtract 0.1
 - 2) Design not calculable and performance predictable over size range from nominal to 1.5 times nominal - subtract 0.2 Maximum Allotment = 0.2
 - 3) New design required for each new size - subtract 0.3 Maximum Allotment = 0.3
 - 4) Testing required for each new size Maximum Allotment = 0.3
 - a) Verification only - subtract 0.1
 - b) Major evaluation - subtract 0.3

With this rating schedule, the penalty assessed against a candidate concept cannot exceed the assigned maximum allotment. For example, if a candidate concept had over three catastrophic failure modes, the penalty assessed could not exceed the maximum allotment of 0.3.

2. Performance Assessment

Each of the candidates was considered for application to the three reference missions. The approach used in evaluating the candidates for the one-year duration A_1 and A_2 missions was identical because these two Mars missions differed only in propellant combination, thrust level, and propellant outflow rates. A more stringent approach for assessing performance of the candidates was employed for the 10-year duration Mission B. Since minor or even negligible problem areas for a one-year mission can be magnified and compounded over a 10-year period to produce significant impacts, this close scrutiny was considered to be warranted. Compatibility, mission environmental sensitivity, response capability, and state-of-the-art considerations fall in this area. Candidate devices considered capable of meeting mission requirements are discussed in the following paragraphs by mission. The conclusions were reached after detailed consideration, from the standpoint of mission requirements, of the information presented in Chapter III.

a. Mission A_1 - All of the candidate propellant acquisition concepts, with the exception of polymeric bladders and diaphragms, were considered capable of meeting the performance requirements of Mission A_1 . Polymeric bladders and diaphragms were assigned a zero figure of merit for this mission because there are no developed polymeric materials that will perform satisfactorily at cryogenic temperatures either at this point in time or in the near future. In addition, no polymeric materials chemically compatible with OF_2 are sufficiently developed for use in this application.

The following concepts were contenders for Mission A_1 :

Dielectrophoretic Systems;	Bellows;
Surface Tension Devices;	External Settling System;
Ring-Reinforced Diaphragms;	Capillary/Bellows.
Convolute Spherical Diaphragms;	

b. Mission A₂ - Dielectrophoretic devices were eliminated from consideration for Mission A₂ since the high electrical conductivity of monomethylhydrazine precludes their use and a different acquisition concept would be required for the fuel. All other candidate systems were considered capable of providing satisfactory performance for the mission. Therefore, the contenders for Mission A₂ were:

Surface Tension Devices;	Convuluted Spherical Diaphragms;
Polymeric Bladders;	Bellows;
Polymeric Diaphragms;	External Settling System;
Ring-Reinforced Diaphragms;	Capillary/Bellows.

c. Mission B - Two-thirds of the candidate concepts were considered questionable in providing satisfactory performance for Mission B. The concepts eliminated were dielectrophoretic devices, polymeric bladders and diaphragms, ring-reinforced diaphragms, metal bellows, and the capillary/bellows. Dielectrophoretic devices were eliminated because of the high electrical conductivity of nitrated hydrazine, which makes the use of these systems impractical. The use of polymeric materials in bladders or diaphragms was considered questionable for a 10-year application. Unknowns involved with very long-term compatibility and the effect on requisite properties, including tensile strength and elasticity, indicate that these materials cannot be considered as serious contenders.

As discussed earlier in this chapter, aluminum and titanium are the metals considered for Mission B. Development, fabrication, and general state-of-the-art status of bellows using these materials are all inferior or unproven in comparison to stainless steel bellows. From a systems integration standpoint, use of bellows constructed of aluminum or titanium is considered questionable for the Mission B application. For these reasons, both metal bellows and the capillary/bellows device were assigned a zero figure of merit.

A similar assessment was made on ring-reinforced metal diaphragms for application to Mission B. Titanium cannot be used as a diaphragm material because of poor elongation properties; thus, an all aluminum or a titanium tank/aluminum diaphragm combination would be required. The latter presents a dissimilar metal joining problem. Feasibility tests have been performed with aluminum diaphragms, but it is felt that considerable development would

be required to perfect the manufacturing process and to obtain desired performance levels comparable to diaphragms using stainless steel. At this point in time, the system's capability to meet the mission performance requirements is considered questionable and a zero figure of merit was assigned. However, if an additional development time of about three years were available, this device might be a contender for Mission B.

The concepts considered capable of meeting the performance requirements of Mission B were:

Surface Tension Devices;
Convoluted Spherical Diaphragms;
External Settling System.

3. Concept Evaluation

a. Rating - All of the concepts considered capable of providing satisfactory performance for the three missions were rated by mission according to the schedule presented previously. Results of the evaluation are presented in Table VI-9 in terms of the numerical weighting factor - rating factor product, the figure of merit, and according to relative standing.

Comparing the figure of merit ratings, surface tension systems rate higher than any other system for all three missions. They rate higher than the second best external settling system by 28% for Mission A₁, 26% for Mission A₂, and 69% for Mission B.

b. Sensitivity Considerations - To ensure an impartial evaluation, the sensitivity of the rating results to the rating system employed was investigated. The first step was to compare the sum of the rating factors only, without considering weighting factors. Using this approach, no change in relative position occurred on either Mission A₂ or Mission B. The impact on Mission A₁ was minor, since changes occurred in the fourth and fifth positions only. Dielectrophoretic systems dropped from fourth to fifth while bellows went from fifth to fourth, and surface tension, external settling, and the capillary/bellows remained in the first, second, and third positions, respectively. This assessment tended to show that the ratings were relatively independent of the weighting fraction determined for each rating category. With this approach, surface tension systems rate higher than the next best system (external settling) by 19% for Mission A₁, 18% for Mission A₂, and 45% for Mission B.

The next step taken in evaluating sensitivity was to simplify the rating schedule and rerate the candidate system. In this case, reliability and mass were the only rating categories employed. The parameters and maximum allotments considered under reliability were: availability - 0.07; manufacturability - 0.06; testability - 0.07; moving parts and cycle limitations - 0.40; additional subsystems - 0.20; and catastrophic and anomalous operation failure modes - 0.20. The mass rating was determined in the same manner used in the more detailed primary rating method presented previously. The weighting factors used were reliability - 80% and mass - 20%. Results obtained are presented in Table VI-10. It is seen that little change occurred in relative positions of the candidate propellant acquisition systems. The important point is that surface tension systems again rate much higher than the second best system - 41% higher on Missions A₁ and A₂ and 105% higher on Mission B.

Table VI-10 Ratings with Simplified Approach

RATING	MISSION A ₁		MISSION A ₂		MISSION B	
	ACQUISITION METHOD	FIGURE OF MERIT	ACQUISITION METHOD	FIGURE OF MERIT	ACQUISITION METHOD	FIGURE OF MERIT
1	Surface Tension	0.82	Surface Tension	0.83	Surface Tension	0.90
2	External Settling	0.58	External Settling	0.59	CSD	0.44
3	Capillary/Bellows	0.53	Capillary/Bellows	0.54	External Settling	0.38
4	Dielectrophoresis	0.45	Polymeric Diaphragm	0.45		
5	Spherical RRD	0.37	Polymeric Bladder	0.40		
6	Metal Bellows	0.32	Spherical RRD	0.35		
7	CSD	0.23	Metal Bellows	0.30		
8			CSD	0.21		

The surface tension systems considered up to this point have been the type with designs testable in a 1-g environment. Since a low-g design surface tension system could also be employed for the three reference missions, the effect on rating with this type of system was determined. The resultant rating factor for testability changed from 1.0 to 0.7. Using the 20% testability weighting factor, the rating factor-weighting factor product dropped from 0.20 to 0.14, which produced a figure of merit for low-g design surface tension systems of 0.835 for Mission A₁, 0.840 for Mission A₂, and 0.870 for Mission B. These figures of merit are comparable directly with those shown in Table VI-9. This assessment shows that a low-g design surface tension system still rates first above all the other candidates on all three missions with a rating that is higher than the second best system by 20% on Mission A₁, 18% on Mission A₂, and 58% on Mission B.

A different operations research approach for evaluating multiple outcomes was also used to determine if any appreciable shift in ratings would occur. The Bridgeman method (Ref VI-2), as presented by Miller and Starr (Ref VI-3), which uses the product of the powers was employed. The figure of merit is obtained from:

$$\text{FOM} = (\text{RF}_1)^{\text{WF}_1} (\text{RF}_2)^{\text{WF}_2} (\text{RF}_3)^{\text{WF}_3} \dots$$

where FOM is the figure of merit, RF₁, RF₂, etc, are the rating factors for each category, and WF₁, WF₂, etc, are the corresponding weighting factors. With this method, any candidate system with a zero rating factor in any rating category automatically receives a zero figure of merit. This was the case for ring-reinforced diaphragms, convoluted spherical diaphragms, and bellows for both Missions A₁ and A₂, and for convoluted spherical diaphragms and external settling for Mission B. In fact, the only system that received a finite figure of merit for Mission B was surface tension. The rating factors and weighting factors obtained from the primary rating technique were employed; results obtained from the product of powers method are presented in Table VI-11. Again, changes in relative positions from those obtained by the primary rating technique are minor. Dielectrophoresis and capillary/bellows exchanged positions at the third and fourth level on Mission A₁, and polymeric diaphragms and external settling switched in the second and third positions on Mission A₂. The pertinent result, however, is that surface tension devices were again rated first by a large margin for all three missions. In comparison to the second best system, surface tension was higher by 39% on Mission A₁ and 31% on Mission A₂. With this method, surface tension was the only candidate for Mission B, as mentioned previously, and received a high figure of merit (0.935).

Table VI-11 Ratings with Bridgeman Method

RATING	MISSION A ₁		MISSION A ₂		MISSION B	
	ACQUISITION METHOD	FIGURE OF MERIT	ACQUISITION METHOD	FIGURE OF MERIT	ACQUISITION METHOD	FIGURE OF MERIT
1	Surface Tension	0.886	Surface Tension	0.892	Surface Tension	0.935
2	External Settling	0.639	Polymeric Diaphragm	0.682		
3	Dielectrophoresis	0.598	External Settling	0.655		
4	Capillary/Bellows	0.576	Polymeric Bladder	0.650		
5			Capillary/Bellows	0.581		

The results are not surprising when a comparison between the Bridgeman method and the primary rating technique using addition is made. Bridgeman's approach was developed primarily to allow comparison of numbers having mixed dimensions while maintaining dimensional integrity. However, the addition method is satisfactory when dimensions are the same or the factors are non-dimensionalized (Ref VI-3). The latter is the case in the primary rating technique.

These considerations show that the ratings of the various candidate propellant acquisition concepts are essentially insensitive to the rating technique employed. Even the straightforward comparison of features presented in Table VI-4 and the relative comparisons by mission made in Tables VI-6 thru VI-8 show surface tension systems to be preferred. The rating method, supported by the sensitivity considerations, merely quantizes the surface tension advantage.

c. Summary - Surface tension concepts are clearly shown by this evaluation to be the best system for all three missions. These devices are available and they exhibit good system compatibility. Using only the physical properties of the propellants and operating on established physical principles requiring no moving

parts, the surface tension systems possess the highest reliability of any of the candidate concepts. They also provide the least addition of mass to the complete propulsion system and possess highly versatile design characteristics. Since qualification testing can be conducted with the actual flight system and propellant to verify proper operation of a 1-g testable surface tension system, this design receives the maximum rating for testability. A surface tension system, designed for the operational low-g environment only (not testable full-scale in 1g), is penalized somewhat in testability but still maintains the overall preferential position by a considerable margin when compared to other acquisition concepts.

The cold gas, external settling system was the second-best system for all three missions even though it rated considerably lower than the surface tension systems, and was penalized in the areas of reliability, testability, and mass. The capillary/bellows device was third and fifth in the rating on Missions A₁ and A₂, respectively. It rated low in availability and was penalized in the areas of system compatibility and reliability. Approximately equivalent to surface tension systems in weight, they have a low impact on propulsion system mass. Dielectrophoretic systems were penalized somewhat in all categories and rate fairly low in availability, system compatibility and reliability. Reliability is down because of the requirement for a power supply and sequencer. Because of the previously discussed performance assessment, this system was considered for Mission A₁ only, and rated fourth.

Polymeric diaphragms and bladders, considered for Mission A₂ only, rated third and fourth, respectively. They received some penalty in all areas except availability. Limitations occurred primarily in reliability and design versatility. Bladders rate lower than diaphragms because of differences in testability and expulsion efficiency.

Ring-reinforced diaphragms rate lower with a conospherical tank than with a spherical tank because of the larger mass of the conospheroid. The candidate system considered included a cryo-formed 301 stainless steel tank. It was given a zero for system compatibility because of the permanent magnet properties discussed earlier. If a regular stainless steel tank had been considered, the device would have rated no higher than fourth or fifth on Mission A₁, and fifth or sixth on Mission A₂. The system compatibility rating would have increased but the mass rating would have decreased because of additional tank weight. Thus, this change would have no impact on selection of the preferred system.

Bellows received the maximum mass penalty on Missions A₁ and A₂ because they were the heaviest candidate considered for these missions. External settling received a zero mass rating on Mission B for the same reason.

Convoluted spherical diaphragms, having only a single reversal (one-half cycle) capability, rated low for all missions. They rate low in availability, system compatibility, and reliability, and were given a zero rating in testability because they must be qualified on a statistical basis only. Reliability is somewhat higher for Mission B because only one bladder or diaphragm is required for the one-tank system.

In summary, surface tension devices are the preferred propellant acquisition concept for all three missions, with an external settling system rated second for Missions A₁ and A₂. Because of the wide difference between ratings of the surface tension device and the second system (external settling) on Mission B, there is probably no real second, or backup, system presently available for this mission.

C. PRESSURIZATION SUBSYSTEM

The pressurization studies entailed making several comparisons and tradeoffs followed by the selection of a pressurization system for each of the three missions. This process is shown in Figure VI-3. Helium and nitrogen stored-gas systems were the candidates considered for Missions A₁ and A₂, and helium and nitrogen blowdown systems were the candidates for Mission B. For Missions A₁ and A₂, the pressurization system evaluation involved assessment of the effects of type of pressurant, initial pressurant storage conditions, pressurant inlet temperature, and pressurant storage tank construction. For the single-tank Mission B blowdown system, only evaluation of type of pressurant and system temperature impacts was required. The effects were noted in terms of the impact on subsystem mass, reliability, cost and schedule. The mass comparisons were based on the results presented in Chapter IV; the other comparisons are qualitative in nature.

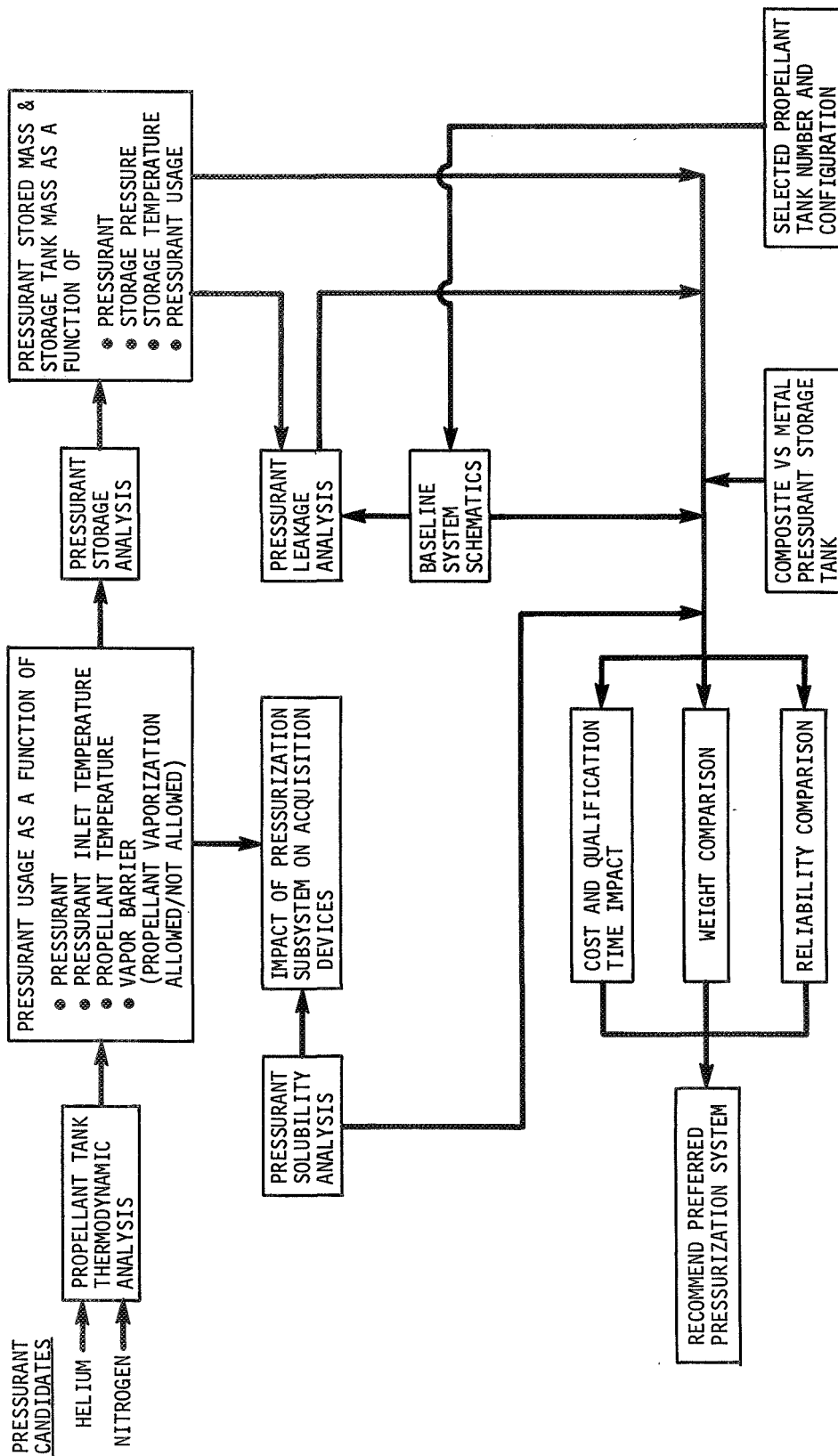


Figure VI-3 Pressurization System Evaluation

As discussed in Chapter IV, the calculated pressurization subsystem weights do not reflect either pressurant leakage or solubility in the propellants because, with the exception of nitrogen solubility in Mission A₁, neither make a significant impact on weight. For Mission A₁ and A₂, the mass comparisons considered the type of pressurant and pressurant storage conditions. The pressurization subsystem mass presented in Figures IV-6 and IV-7 and Tables IV-5 and IV-7 were employed. For Mission A₁, the lightest nitrogen pressurization subsystem was approximately 71% heavier than the lightest helium system of approximately 85 lb_m. For Mission A₂, the nitrogen pressurization system was approximately 50% heavier than the helium system at the nominal propellant storage temperature of 525°R. In Mission A₁ and A₂, the lightest system mass was obtained with pressurant stored at the lowest practical temperature and at the highest storage pressures. For Mission B, the mass comparison considered helium and nitrogen usages. As shown in Table IV-9, helium provides a 3-lb_m weight advantage over nitrogen; this small difference is not as significant as that for Missions A₁ and A₂. However, the mass comparisons for all three missions definitely favor helium over nitrogen with storage at the coldest practical temperature and high initial pressure.

The pressurization subsystem schematics employed in the evaluation were the same for both helium and nitrogen. Therefore, the impacts resulting from type of pressurant were the only considerations included in assessing system reliability effects. The results of the pressurant leakage analysis, presented in Tables IV-11 through IV-13, showed that helium leakage rate on a volumetric basis was almost three times greater than that of nitrogen. On a mass basis, this relationship is reversed; however, the total leakage quantities of either helium or nitrogen are not significant. Qualitatively, a pressurization system using helium would be less reliable than one using nitrogen because of the greater tendency for helium to leak. However, helium has been used extensively in both manned and unmanned propulsion systems with a high degree of success. The effects of pressurant solubility on system reliability might be more significant than that of pressurant leakage due to possible impacts on engine performance. The pressure drop through the propellant feed system can cause pressurant evolution that may change propellant flow rates and engine mixture ratio. Results of the pressurant solubility analysis, presented in Table IV-14, show that the difference between nitrogen and helium solubility ranged from one to three orders of magnitude, with nitrogen being the most soluble. Thus, unless the acquisition device precludes pressurant solubility, system reliability

will be degraded more with nitrogen than with helium. It appears that the reliability degradation of helium due to leakage is offset by that of nitrogen due to pressurant solubility.

Cost and schedule are related and are discussed together because any increase in schedule directly increases the cost. The important factors affecting cost and schedule are component development time, leak checking, and engine test and qualification time. Component development time is affected primarily by component leak check time. Equipment for direct measurement of nitrogen leakage is not available; helium leak checking equipment has been used extensively and requires minimum time for measuring leak rates. Nitrogen leak checks involve either bubble-type checks or leak checking with helium and converting to nitrogen. If nitrogen is used, the final assembled system leak check would have to be conducted using a tracer gas or other methods requiring additional time and cost. Any propulsion system using both nitrogen pressurization and acquisition devices that do not preclude pressurant solubility would require additional engine testing to determine the effect of nitrogen saturated propellants on engine performance. Additional engine cost and development time may be required to circumvent or eliminate problems due to nitrogen evolution. Therefore, it is concluded that using nitrogen pressurization would result in increased propulsion system cost and schedule over that for a helium pressurized system.

In considering number of tanks, geometry, and tank construction, the evaluation made for the propellant tanks also applies, in general, to the pressurant storage container for Missions A₁ and A₂. A single pressurant storage sphere provides a pressurization system that is lighter, less costly, more reliable, and available in a shorter time than a system using two or more tanks with either spherical or cylindrical geometry. The lower surface area and line and joint requirements result in a lower leakage potential. The preferred pressurant storage tank material is 6Al-4V titanium which provides a low tank weight.

Composite tanks were also considered for use as the 4000-psia pressurant storage container. An oblate spheroid fabricated with a 10-mil titanium liner and carbon/epoxy overwrap showed a 6-lb_m weight savings in comparison to the 53-lb_m, 6Al-4V titanium sphere for Mission A₂. Tank volume was 2.38 ft³. These weights are for the tank only; they do not include a weight assessment for welds, attachments, or penetrations. As with the propellant tanks when

attachments are considered, any weight savings would be small. In addition, metal tanks are preferable from reliability, schedule, cost and state-of-the-art considerations. Martin Marietta is presently investigating composite tanks for 2500-psia service under contract to NASA-LeRC, but to our knowledge, no composite tanks have been developed for use at 4000 psia. Also, composite tanks may be limited in operating temperature range by the large difference between coefficients of thermal expansion of the metal liner and the composite overwrap material. This limitation could eliminate the use of composite tanks at cryogenic temperatures and impair their use for high pressure storage at ambient temperature because temperature drops of 100°F could occur during expansion from high storage pressures. However, a titanium liner may present less of a problem in this regard than other liner metals.

Based upon the above evaluation, helium is the preferred pressurant for all three missions. For Missions A₁ and A₂, the helium should be stored at the nominal propellant temperature (250°R for A₁ and 500°R for A₂) with an initial pressure of 4000 psia. The resulting tank inlet temperatures are near the nominal propellant temperature. The pressurant storage tanks for Mission A₁ and A₂ should be a single sphere constructed of 6Al-4V titanium.

D. SELECTED PROPULSION SUBSYSTEMS

Based on the subsystem evaluations presented in the previous sections of this chapter, propulsion systems were selected for each of the three reference missions under consideration. For Mission A₁, the selected propulsion system includes helium pressurant stored at 250°R with an initial pressure of 4000 psia in a single metal sphere constructed of 6Al-4V titanium, two spherical propellant tanks constructed of 2219 aluminum (one for OF₂ oxidizer and one for B₂H₆ fuel), and an aluminum surface tension propellant acquisition system. A similar system was selected for Mission A₂ with the differences attributable to the propellant combination change. The selected Mission A₂ propulsion system employs helium pressurant stored at 500°R with an initial pressure of 4000 psia in a single metal sphere constructed of 6Al-4V titanium, two spherical propellant tanks constructed of 6Al-4V titanium (one for N₂O₄ oxidizer and one for CH₃N₂H₃ fuel), and a titanium surface tension propellant acquisition system. Helium pressurant was also selected for the single tank Mission B mono-propellant propulsion system. A titanium surface tension propellant acquisition system is contained in the spherical 6Al-4V

titanium tank. The pressurant and propellant temperature is 500°R and initial system pressure is 350 psia. The propellant is 75/25 wt percent $N_2H_4/N_2H_5NO_3$. Mass of the selected propulsion systems is itemized in Table VI-12.

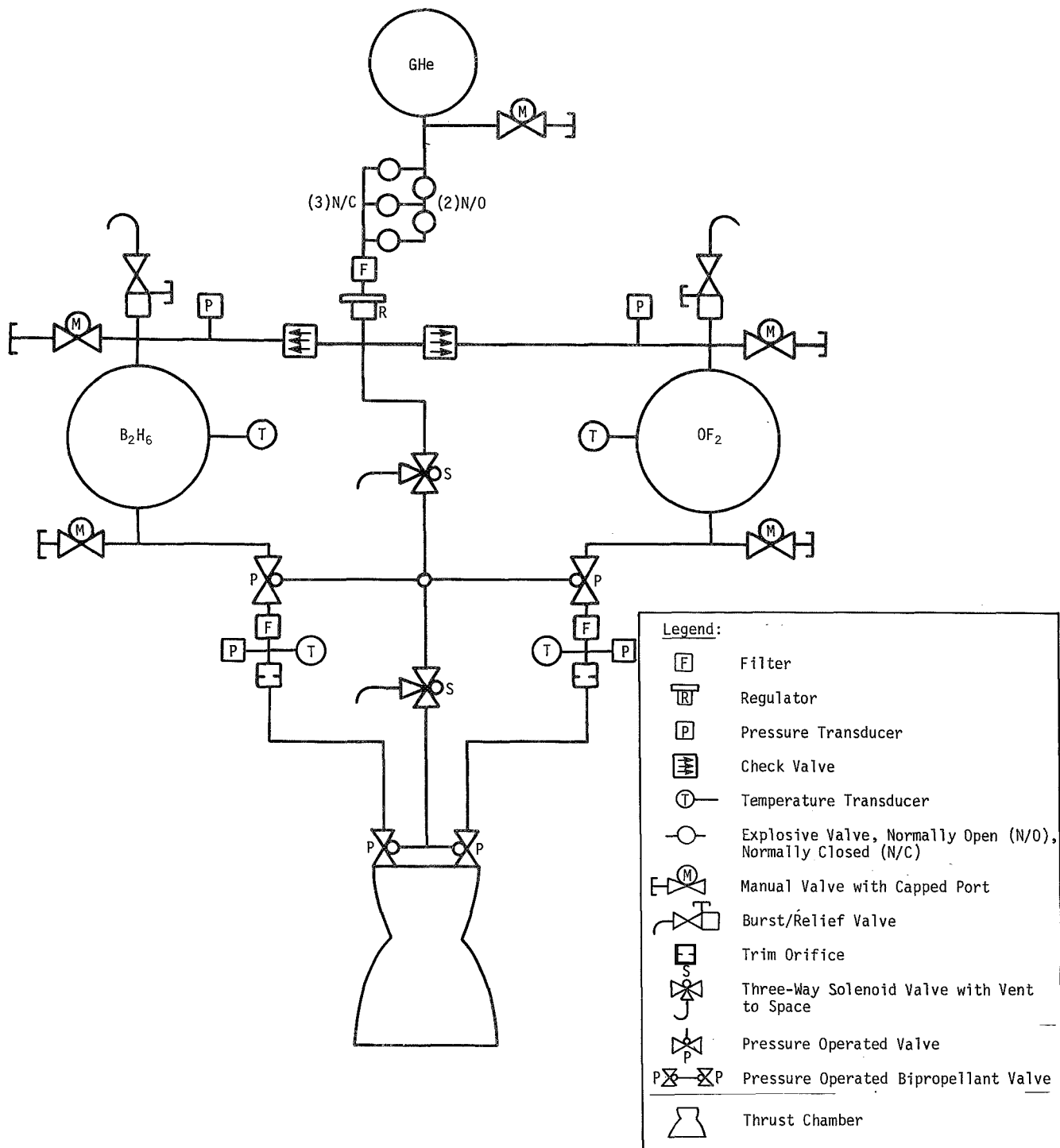
Table VI-12 Mass Summary for Selected Propulsion Systems

	MISSION		
	A ₁	A ₂	B
Pressurization Subsystem	86	66	0.5
Propellant Tank Subsystem	66	48	8.2
Propellant Acquisition Subsystem (Device Only)	3	5	1.5
Propellants	1080	1434	135
Total System	1235 lb _m	1553 lb _m	145.2 lb _m
<u>Note:</u> Line, valve, and engine weights are not included			

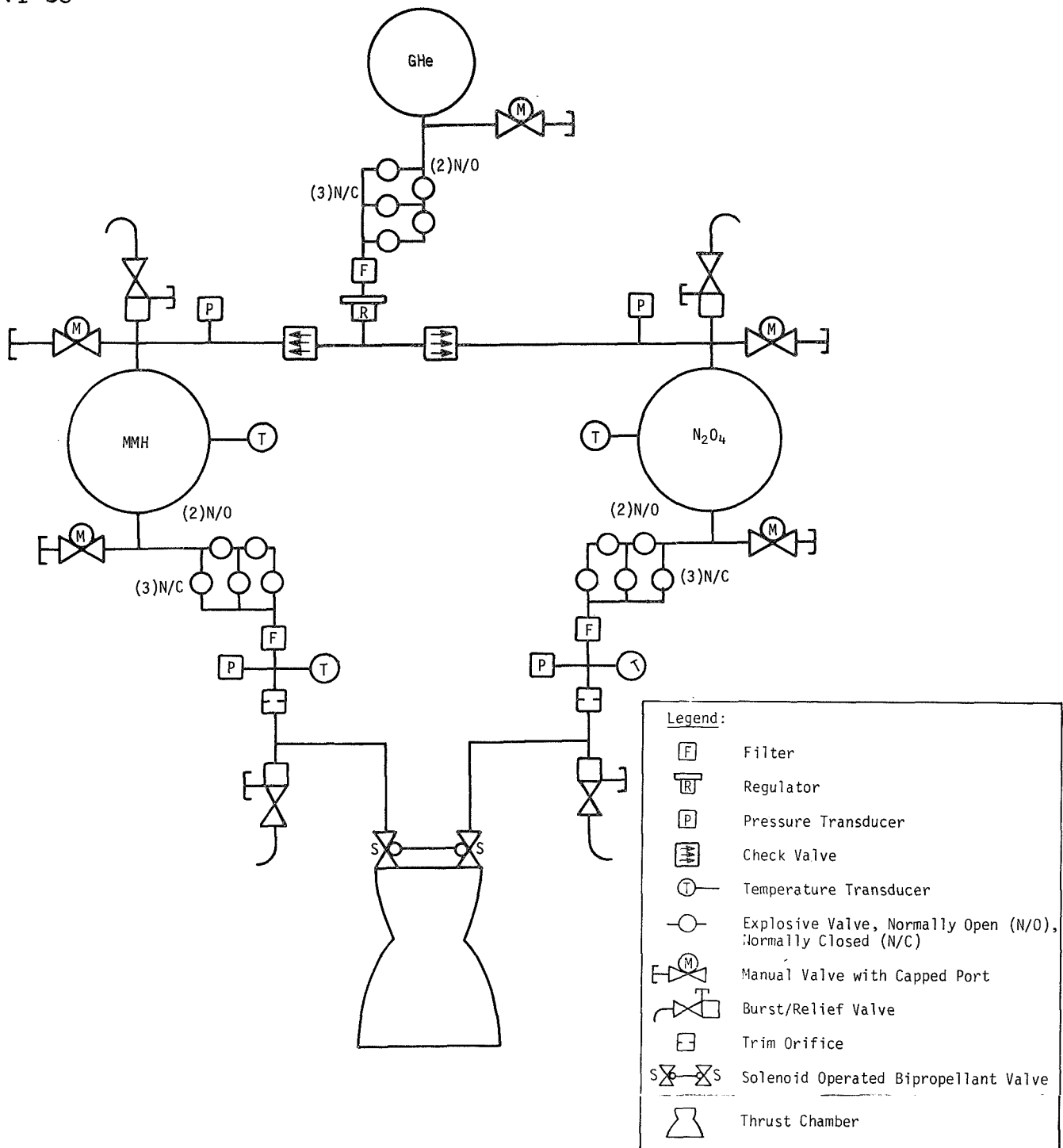
As discussed in the previous sections, the selected systems provide advantages in mass, reliability, cost and schedule over the other combinations considered. These benefits accrue from changes in the baseline propulsion system schematics for Missions A₁ and A₂ (Figures II-3 and II-4). The changes reflect the selection of a single pressurant tank and two propellant tanks for these missions. No change was required in the baseline propulsion system schematic for Mission B (Figure II-5).

The revised schematic for Mission A₁ is shown in Figure VI-4. Two check valves are included in the pressurization line to each propellant tank for propellant migration control. Considerable simplification was obtained in the propellant feedline system in comparison to the baseline schematics. In particular, the need for complicated three-way propellant isolation valves was eliminated in going to the two-tank configuration.

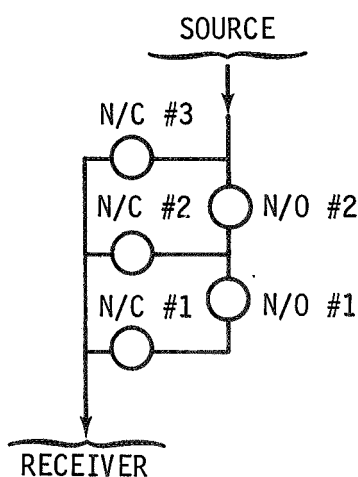
The revised propulsion system schematic for Mission A₂ is presented in Figure VI-5. It differs from the baseline schematic primarily in the pressurant storage and control assembly; with one pressurant storage tank, only one regulator and one set of pressurant isolation valves are required. Two check valves were included, as in the Mission A₁ system, for propellant migration control.

Figure VI-4 Revised Propulsion System Schematic for Mission A₁

VI-38

Figure VI-5 Revised Propulsion System Schematic for Mission A₂

The explosively-actuated isolation valve package used for both the Mission A₁ and A₂ systems includes two normally-open and three normally-closed valves. One of these packages is used for pressurant isolation on both Missions A₁ and A₂. In addition, the Mission A₂ system includes two of the valve packages for propellant isolation, as shown in Figure VI-5. The sequence of operation of these isolation valve packages is shown in Figure VI-6. Whenever the isolation valve package is left open between engine burns, the regulator maintains propellant tank pressure at 350 psia and propellant is isolated from the engine by the engine bi-propellant valve. For Mission A₁, after every burn the propellant is always isolated from the engine by the pressure-actuated feedline valves.



EVENT	EVENT TIME (DAYS)	EXPLOSIVE VALVE OPERATION
Start 1 st Midcourse	L + 5	Open N/C #1
End 1 st Midcourse		Close N/O #1
Start 2 nd Midcourse	L + 160	Open N/C #2
End 2 nd Midcourse		
Start Orbit Insertion	L + 180	
End Orbit Insertion		
Start 1 st Orbit Trim	L + 181	
End 1 st Orbit Trim		Close N/O #2
Start 2 nd Orbit Trim	L + 225	Open N/C #3
End 2 nd Orbit Trim		
Start 3 rd Orbit Trim	L + 270	

Figure VI-6 Operational Sequence for Explosively-Actuated Isolation Valve Packages, Missions A₁ and A₂

VII. INFLUENCES OF POSSIBLE CHANGES IN MISSION CRITERIA

Five areas were considered in qualitatively evaluating the impact of various changes in mission criteria and propulsion system requirements on the selection of propellant acquisition systems. These areas were: (1) Propellant Change Effects, (2) Propellant Tank Design Considerations, (3) Propulsion System Duty Cycle Effects, (4) Pressurization System Effects, and (5) Sterilization Effects.

A. PROPELLANT CHANGE EFFECTS

Two propellant changes were considered in the evaluation. These changes consisted of replacing the monomethylhydrazine in Mission A₂ with neat hydrazine and using neat hydrazine in Mission B in place of nitrated hydrazine. The effects of these changes are discussed in the following paragraphs.

1. Propulsion System Requirements

In order to evaluate the effect of the propellant changes on the propellant acquisition system selections, new propellant tank volumes and flow rates were calculated for each change. For Mission A₂, two different approaches were considered in calculating new volumes for the new propellant combination: (1) a mixture ratio was selected to provide equal volume tanks with a subsequent degradation in specific impulse; (2) a mixture ratio was selected for maximum specific impulse. It was found that use of the optimum mixture ratio resulted in the greater variation in tank volumes from the baseline mission requirements. Therefore, the optimum mixture ratio was used to evaluate the effect of the propellant change since this presented the worst-case situation.

For Mission B, the degraded specific impulse was obtained from Rocket Research Corporation (Ref VII-1). The other parameters used to size the propellant tanks (total impulse, ullage volumes, and propellant margins) in Mission A₂ and B were the same for both baseline and modified cases. Table VII-1 compares the new tank volumes with the baseline values for both Missions A₂ and B. New propellant flow rates were also computed for the propellant change, assuming the same thrust as the baseline values; these are also included in Table VII-1.

Table VII-1 Effects of Changing Propellants on Baseline Propulsion System

	MISSION A ₂		MISSION B	
	BASELINE	MODIFIED	BASELINE	MODIFIED
Propellant Combination	N ₂ O ₄ /MMH	N ₂ O ₄ /N ₂ H ₄	N ₂ H ₄ (nitrated)	N ₂ H ₄
I _{sp} (Vac), lb _f -sec/lb _m	290	296	255	230
Mixture Ratio	1.55	1.0	--	--
Total Propellant, lb _m	1434	1404	135	149
Fuel, lb _m	562	702	135	149
Oxidizer, lb _m	872	702	--	--
Volume Fuel Tank, ft ³	11.25	12.1	3.86	4.68
Volume Oxidizer Tank, ft ³	11.25	8.36	--	--
Propellant Flow Rate				
Fuel, lb _m /sec	0.405	0.507	0.098	0.108
Oxidizer, lb _m /sec	0.630	0.507	--	--

From the propellant tank volume data given in Table VII-1, it can be seen that the fuel tank volume increased 7.5% and the oxidizer tank volume decreased 25.7% for Mission A₂ by changing the propellant from monomethylhydrazine to neat hydrazine. For Mission B, the fuel tank volume increased 21%. However, if spherical tanks are used for each mission, the changes in tank radius from the baseline values are:

Mission A ₂	Fuel Tank	+0.3 in.
	Oxidizer Tank	-1.6 in.
Mission B	Fuel Tank	+0.7 in.

These radii changes are insignificant in regard to the geometric considerations in the selection of a propellant acquisition system.

2. Operational Effects on the Propellant Acquisition Device

An investigation of the effect of the proposed propellant changes upon the characteristics of the various acquisition devices was conducted to determine any possible operational limitations or constraints.

The representative surface tension system design used for comparative purposes for both Missions A₂ and B consists of a coverplate and annulus forming a propellant trap. The main function of the annulus is to provide gas-free propellant flow to the tank outlet port during engine operation. Therefore, the annulus design (annulus gap size and screen pore size) is a direct function of the propellant physical properties (surface tension, density, and viscosity), propellant outflow rate, and acceleration environment. The coverplate retains sufficient propellant at the tank outlet to feed the engine through the annulus during engine start periods. The retention capability of the coverplate depends upon the capillary pore size which is a function of the propellant properties. Therefore, for any propellant change in Missions A₂ and B, minor design changes could be incurred depending on the magnitude of the physical property and flow rate changes. Comparison of the physical properties affecting the surface tension system design indicates little change (Table II-3). The propellant flow rate variation, shown in Table VII-1, is also small. Finally, the total propellant mass change, indicated in Table VII-1, is negligible so that the vehicle acceleration level is essentially the same for baseline and modified cases. Considering all of these factors, no major redesign of the surface tension system hardware would be required.

Another operational factor influenced by the propellant change is the time required to settle the main propellants. The required settling time is defined by Equation [III-16]. Assuming constant thrust, no appreciable change in settling time would be required since both the propellant mass and tank dimensions do not change significantly for either Mission A₂ or B as a result of the propellant change.

For bladder or diaphragm operation, there would be no effect due to propellant physical property or flow rate change. Factors that affect these devices are mainly tank size and operating pressure; neither are significantly affected by the propellant change.

3. Storability and Compatibility

Presently, there are no long-term material compatibility data for times approaching the Mission B duration. Therefore, any consideration of compatibility for a 10-yr period will contain uncertainties since it must be based on available storability and compatibility data for much shorter time periods.

From data presented in References III-54 and III-55, the major storage problem associated with hydrazine fuels is one of accelerated fuel decomposition caused by catalytic action. For the three types of hydrazine fuels considered (monomethylhydrazine, nitrated hydrazine, and neat hydrazine), sensitivity to catalytic decomposition varies. The most stable of the three fuels is monomethylhydrazine; the least stable is nitrated hydrazine. The nitrated hydrazine rapidly decomposes when in contact with any catalytic material while neat hydrazine and monomethylhydrazine may be stored with milder catalysts, such as stainless steel, with only a slight increase in decomposition rates. Thus, replacement of the monomethylhydrazine in Mission A₂ by neat hydrazine leads to a more unstable storage condition, while replacing nitrated hydrazine with neat hydrazine on Mission B would create a more stable storage situation.

In order to evaluate the hydrazine fuel decomposition problem the propellant tank pressure rise resulting from decomposition of the nitrated hydrazine used in Mission B was estimated. The nitrated hydrazine blend was selected for analysis because it is the most unstable of the three hydrazine fuels and because the long duration of Mission B presents the worst case. A review of existing decomposition data indicated that no information was available for the Mission B fuel blend. However, Thiokol Chemical Corporation (Ref VII-2 and VII-3) investigated the decomposition of other nitrated hydrazine fuel blends with various materials. From these references, a method for estimating the propellant tank pressure rise due to fuel decomposition was obtained. This method was employed using the Mission B titanium tank and mission duration with a fuel blend of slightly lower hydrazine nitrate content than the baseline propellant. The analysis is not presented here because of the classified nature of the information. The reader is referred to the two Thiokol references if details are desired. The results of the estimate showed that the tank pressure rise due to propellant decomposition would be less than 10 psi over the 10-year mission. The Mission B fuel would probably produce a higher pressure rise; however, the increase would still be less than 10 psi. Therefore, it was concluded that long term propellant decomposition, and the resulting pressure rise, would not present a major problem in the design of a propellant system using titanium tanks.

B. PROPELLANT TANK DESIGN CONSIDERATIONS

The purpose of this study area was to determine if changes in propellant tank sizes or configurations could significantly influence the design or selection of propellant acquisition systems. Various aspects of propellant tank design are discussed in the following paragraphs.

1. Tank Volume Effect

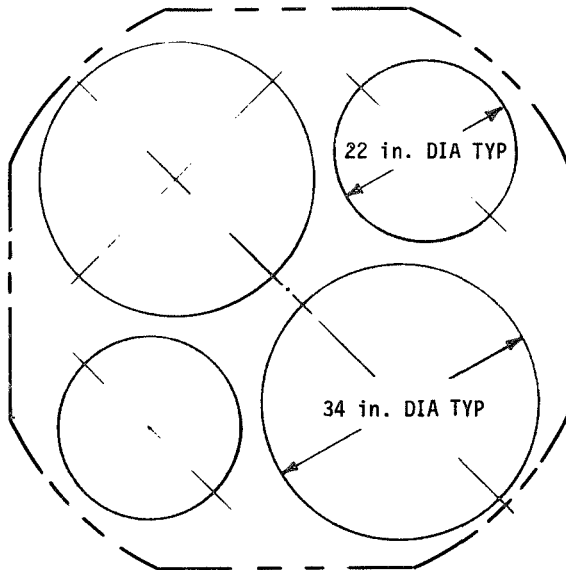
In order to determine volume limits, two ground rules were utilized in the investigation: (1) a total impulse of $10^6 \text{ lb}_f\text{-sec}$ was assumed for Mission A₁ and A₂; (2) the use of the Viking Orbiter propulsion envelope (Figure II-1) was required as a package limitation.

For the total impulse specified above, tank volumes using Mission A₁ and A₂ propellant combinations were computed. The specific impulse, mixture ratio, ullage, and propellant margins used in the calculation were the baseline values. The calculated propellant mass and volumes are presented in Table VII-2 for comparison with the baseline values shown. The difference in acceleration levels resulting from the additional propellant is also given. However, the acceleration change is due only to added propellant mass and does not include increased tankage weights due to the volume increase.

Table VII-2 Propellant System Changes Resulting from a Total Impulse Increase to $10^6 \text{ lb}_f\text{-sec}$

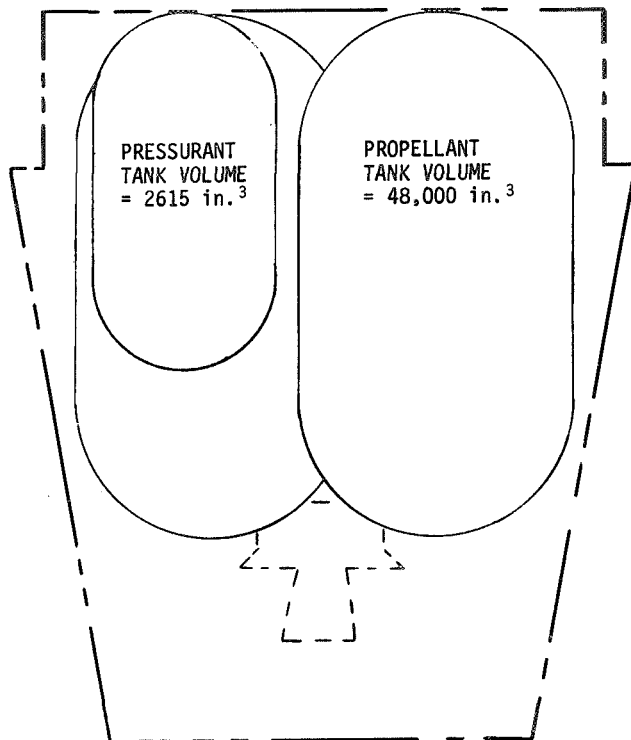
	MISSION A ₁		MISSION A ₂	
	BASELINE	MODIFIED	BASELINE	MODIFIED
Total Propellant, lb_m	1080	2860	1434	3795
Fuel, lb_m	270	715	562	1485
Oxidizer, lb_m	810	2145	872	2310
Volume Fuel Tank, ft^3	9.92	24.6	11.25	27.8
Volume Oxidizer Tank, ft^3	9.92	24.6	11.25	27.8
G-Level				
Full Propellant Tanks	0.133	0.108	0.04	0.031
Empty Propellant Tanks	0.156	0.15	0.05	0.047

In order to investigate packaging problems, Mission A₂ tank volumes for $10^6 \text{ lb}_f\text{-sec}$ were used because these volumes were larger than those required by Mission A₁. Two spherical tanks, 45 in. in diameter with a 27.8-ft^3 volume, could not be used since they will not fit within the envelope. Cylindrical tanks with hemispherical domes having a 27.8-ft^3 volume could be packaged into the envelope as illustrated in Figure VII-1. The enlarged conospheroid tanks for ring-reinforced diaphragms could not be used since engine interference occurred.



Since spherical or conospherical tanks create packaging difficulties, ring-reinforced diaphragms could not be used for the increased total impulse case. Polymeric bladders or diaphragms could be used; however, some redesign would be necessary to account for changes in length-to-diameter ratios. Use of surface tension systems are not affected by tank geometry changes and are, therefore, a desirable solution. Resizing of trap volumes might be required, but this is not a redesign of the basic system.

2. Series Versus Parallel Tankage



If multiple tanks are employed, two methods of manifolding or plumbing the tanks together are available. Series tankage is a feed system such as that used in the Apollo Service Module where one propellant tank expels into a second tank that, in turn, feeds the engine. Parallel tanks refer to a system with the tank outlets manifolded together in a common line that feeds the engine. Figure VII-2 schematically shows the differences between series and parallel arrangements. The series tankage arrangement is inherently simpler because pressurant gas need be added only to the first tank.

Figure VII-1 Cylindrical Tank Arrangement
for a Total Impulse of $10^6 \text{ lb}_f\text{-sec}$

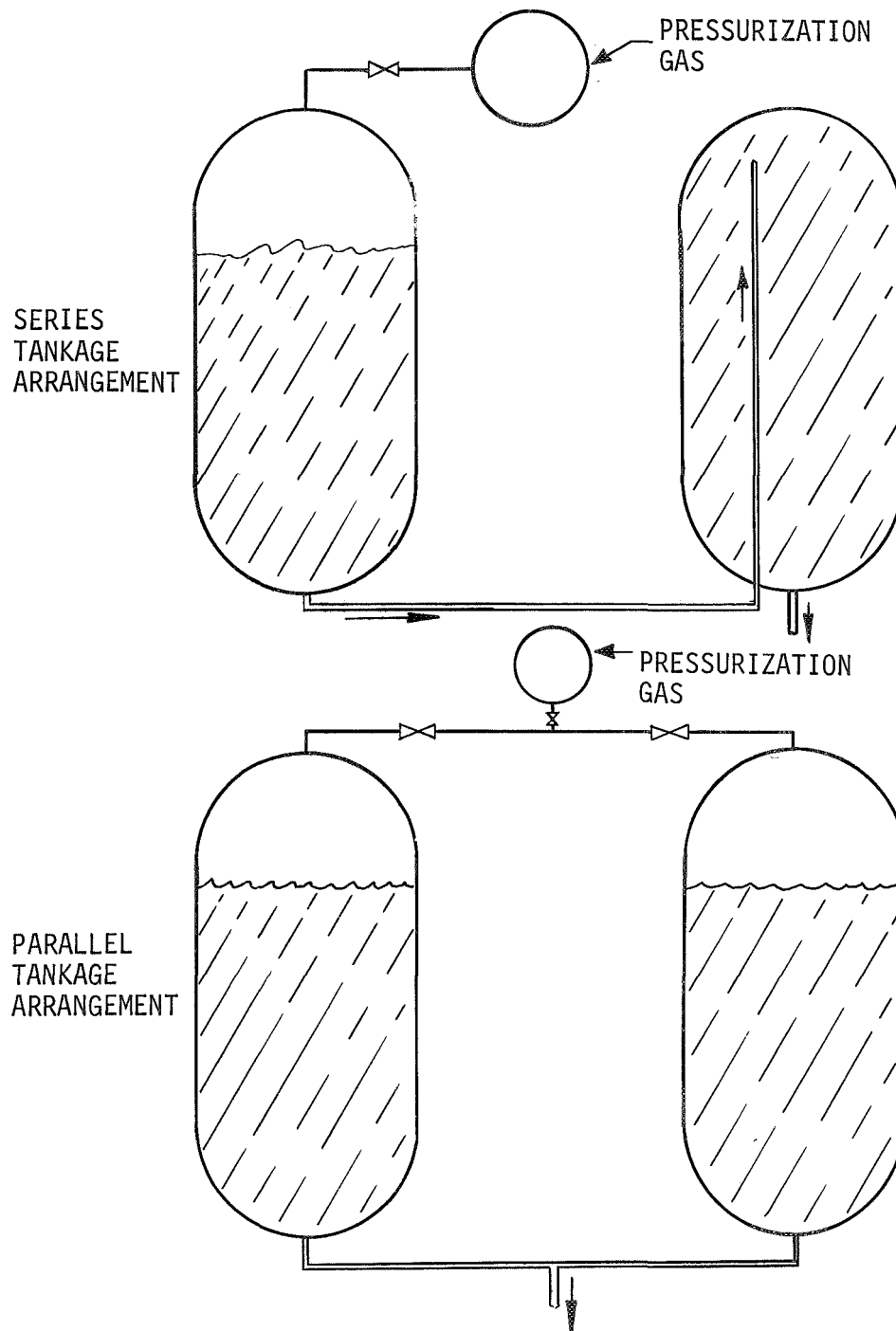


Figure VII-2 Comparison of Series and Parallel Tank Arrangements

When propellant is completely displaced from the first tank, the pressurant travels through the cross-over line to the second tank. In the parallel arrangement, both propellant tanks must be pressurized simultaneously. Furthermore, the parallel tanks require a balancing of both tank pressure and feedline pressure drop in order to assure equal propellant delivery from each tank. Therefore, its propellant feed system is more complex. However, parallel tanks do provide better control of center-of-gravity shifts during propellant expulsion.

With surface tension propellant acquisition systems, the series tankage arrangement would generally provide greater expulsion efficiency because only one propellant trap is required. The single trap requirement is a result of the complete emptying of the first propellant tank into the second. The parallel tanks require simultaneous emptying so that equal volumes of residual propellant remain in each tank. In general, positive barrier systems, such as diaphragms and bladders, cannot be used in series tankage systems.

3. Propellant Loading Considerations

The design or operational characteristics of the propellant acquisition system can impose limitations and constraints on the propellant loading process. Either vacuum or pressure loading may be employed. As previously discussed in Chapter III, the selection of technique to be employed depends upon the acquisition system being considered. Surface tension systems can generally employ either technique depending upon design details. No changes are required in the system schematics to accomplish loading by either technique.

The major consideration for the vacuum loading process is that the propellant tank be designed to withstand buckling loads. This is not a problem for baseline spheres as previously shown in Chapter V.

No restrictions on propellant off-loading are imposed by the use of surface tension systems or settling rockets. However, bladders and diaphragms would require complete filling followed by partial expulsion to achieve the desired off-load making it a much more involved process.

C. PROPULSION DUTY CYCLE EFFECTS

For Missions A₁ and A₂, consideration was also given to reducing the minimum impulse bit from the baseline value of 400 lb_f-sec to the Viking Orbiter requirement of 125 lb_f-sec (Ref VII-4).

Theoretically, there is no limiting minimum impulse bit below which the surface tension system cannot supply propellant. However, from a practical point of view, a large number of small magnitude impulse bits can lead to a depletion of propellant stored in the screen trap. This propellant depletion would result if the magnitude of the impulse bit was not sufficient to settle propellant so that the propellant supply was only from the trap. Therefore, if a large number of small pulses are required with a surface tension system, a constraint on the magnitude of the minimum impulse bit must be established, the propellant trap must be resized, or a surface tension system of different design must be employed.

Bladders, diaphragms, and bellows are not considered sensitive to pulse operation. However, uneven or varying propellant expulsion could occur due to stiffness of the material. Since the engine pulse operation is transient by nature, the uneven operation of the bladder or diaphragm will probably not affect the overall performance significantly. No test data is available to support this supposition, however.

Another possible propulsion system requirement considered was supplying the ACS system from the main propellant tank for Mission B. This would require additional propellant to supply the total impulse requirement of the ACS system and the ability to supply propellant at very low flow rates in a very small adverse acceleration environment. The only effect on the reference surface tension system would be the required increase in propellant trap volume. Outflow at very low flow rates in the adverse acceleration environment would not be a problem. The propellant trap will keep the propellant oriented over the outlet during the adverse accelerations, while preventing any gas contained in the trap from being ingested into the line.

The size of the bladders, diaphragms, and bellows used in the main tank would also have to be increased to accommodate the additional propellant. However, this is not considered a major problem. One operational problem that may be encountered with these acquisition devices is variations in flow rate to the ACS engine resulting from fluctuations in the pressure differential required to move the specific device. The ACS flow rates

are generally much smaller than those required for the main engine and, therefore, might be more susceptible to the pressure differential variations. The pressure differential variations might result, as previously discussed, from stiffness variations in the acquisition device material. The effect of the ACS flow rate variations may not significantly influence the system performance. However, it is a consideration that should be evaluated when ACS system requirements are known.

The effect of spacecraft onboard accelerometers on the operation of the propellant acquisition system was also considered. The use of an accelerometer, in general, eases the tolerances and repeatability required in the production of thrust. For example, the accelerometer, by monitoring velocity increment, can account for such things as thrust variations due to nozzle throat erosion or propellant flow rate variations, by allowing the propulsion system to operate for a longer period of time. This operation is extremely beneficial for long term missions such as the Grand Tour (Mission B) where communication time delays prevent real time control of the satellite from Earth-based tracking stations. However, it is the function of the propellant acquisition system to supply the proper amount of propellant to produce the required total impulse. Since total impulse actually determines the size of the propellant system, any probable degradation in thrust and specific impulse must be considered in the design of the system in order to assure that sufficient propellant is available. Therefore, the use of the accelerometer will assure more accurate utilization of propellant during the mission but will not reduce the uncertainties that must be considered in sizing the propellant system. The presence of an accelerometer would influence the magnitude and number of impulse bits required by the propulsion system; the impact of the impulse bit was discussed previously.

D. PRESSURIZATION SYSTEM EFFECTS

Replacing monomethylhydrazine in Mission A₂ and nitrated hydrazine in Mission B with neat hydrazine produces two effects on the pressurization system: (1) pressurization subsystem mass will vary; (2) the amount of dissolved pressurant will change. For Mission A₂, changing fuels decreased the total volume of the propellant tanks because of changes in fuel density and mixture ratio. This decrease in total volume will produce a proportional decrease in pressurization subsystem mass. For Mission B, changing fuels would increase helium usage because of the increase in tank volume.

Pressurant solubility in any of the propellants is not a significant problem if helium is the pressurant. However, for Mission A₂, changing fuels will reduce the solubility of helium by approximately an order of magnitude. For Mission B, the change in pressurant solubility is negligible due to changing fuels.

E. STERILIZATION EFFECTS

The recent program conducted by Martin Marietta for the Jet Propulsion Laboratory under Contract JPL 951709 (Ref VII-5 and VII-6) demonstrated the feasibility of loading, sealing, and heat sterilizing a liquid bipropellant (nitrogen tetroxide and monomethylhydrazine) propulsion system. After the sterilization process, the propulsion system was successfully fired. This type of sterilization process is not feasible for Mission A₁ since the sterilization temperature (275°F) is far above the critical temperature of the space storable propellants.

Sterilization of the Viking Lander will be accomplished before propellants are loaded. The propellants will be sterilized externally, if required, and loaded after the Lander has been sterilized. Thus, propellant compatibility with the system materials at the elevated sterilization temperatures will not be a major concern. Also, the ethylene oxide used in previous programs as a decontaminate will not be used in the Viking program. The Viking sterilization process consists of a series of dry heat cycles. Different requirements exist depending upon whether the sterilization is at a component or system level and whether flight acceptance, development, or qualification testing is concerned. The qualification sterilization cycle for components is the most severe, requiring a total time of 380 hours in a total of 8 cycles with the coldest contaminated point maintained at a minimum temperature of 275°F. The maximum surface temperature of the component may not exceed 282°F. If this Viking sterilization process were applied to the propellant acquisition systems considered in this study, the maximum temperatures would be below the threshold for any significant metallurgical effects in the metals considered. The only effect the elevated temperature would have on the metals would be the generation of stresses resulting from thermal expansion. Suitable design and mounting can minimize this problem.

For nonmetallic materials, such as polymeric products, the effect of heat sterilization can vary significantly ranging from insignificant changes in properties to changes sufficient to impair performance or destroy the usefulness entirely. A test program, concerned only with a dry-heat sterilization process, was conducted by Jet Propulsion Laboratory on polymeric materials used in the Ranger and Mariner spacecrafts (Ref VII-7). Additional test work has also been performed using ethylene oxide and dry heat in the sterilization process. References VII-8 and VII-9 present results from these test programs. A general conclusion to be reached from the results of all these programs is that special care must be exercised in the selection of polymeric materials for use in bladders, diaphragms, and seals when sterilization is a consideration.

The effect of sterilization on pyrotechnic devices used in squib valves was considered. A major consideration associated with these devices is that older conventional explosives cannot be used. However, new explosives that can withstand temperatures to 500°F are available. No development is needed. The most difficult design problem is associated with sealing materials such as epoxies that would outgas during sterilization. The outgassing products in some cases are noxious to the explosives.

VIII. CONCLUSIONS AND RECOMMENDATIONS

Only typical or representative missions were considered during Phase I of this investigation. The general mission and system criteria employed were sufficient for the comparative evaluations conducted, since the primary purpose of this phase of the effort was to define the preferred propulsion subsystem combination for each mission. Detailed designs were not required. The results clearly showed the preferred approach for the pressurization, propellant tank, and propellant acquisition subsystems. No attempt was made to optimize any of the propellant acquisition concepts against the mission criteria, since representative conceptual designs were adequate for comparison and selection.

A. CONCLUSIONS

1. Propellant Tank Subsystem

- 1) The two-tank configuration is preferable to the four-tank system for both Missions A₁ and A₂. The number of tanks was not a consideration for the single-tank Mission B monopropellant system;
- 2) Spherical tanks provide advantages over cylindrical tanks and specially-shaped tanks for all three reference missions;
- 3) Propellant tanks for Mission A₁, using OF₂ oxidizer and B₂H₆ fuel, should be constructed of 2219 aluminum. Tanks constructed of 6Al-4V titanium are preferred for both Mission A₂, using N₂O₄ oxidizer and CH₃N₂H₃ fuel, and Mission B, using 75/25 - N₂H₄/N₂H₅NO₃ monopropellant;
- 4) All-metal tanks should be employed since no significant advantages are provided by composite tanks.

2. Pressurization Subsystem

- 1) Advantages are gained by selecting helium pressurant for all three reference missions. Appreciable weight savings are provided using helium instead of nitrogen in both the Mission A₁ and A₂ separate stored gas systems; a lesser savings (lb_m) results for the lighter Mission B spacecraft which employs a blowdown pressurization system;
- 2) A single, spherical pressurant storage tank constructed of 6Al-4V titanium should be used for both Missions A₁ and A₂. Use of a composite tank for pressurant storage provides no advantage. A separate pressurant tank is not required for the Mission B system;
- 3) The pressurant storage spheres for Missions A₁ and A₂ should be initially loaded with helium to 4000 psia at the nominal propellant temperature (250°R for Mission A₁ and 500°R for Mission A₂). Thus, the pressurant and propellant tanks should probably be packaged together for optimum thermal control;
- 4) The Mission B propellant tank with 50% initial ullage should be pressurized to the 350 psia initial pressure with helium. Helium storage temperature is equal to the propellant temperature for this blowdown system; the nominal propellant temperature is 500°R.

3. Propellant Acquisition Subsystem

- 1) Surface tension devices are the preferred propellant Acquisition concept for all three missions;
- 2) These devices are lighter and more reliable than the other candidate acquisition systems and possess excellent availability, system compatibility, and design versatility characteristics;

- 3) On a relative basis, the figure of merit for surface tension devices is greater than that for the second best system by 28% for Mission A₁, 26% for Mission A₂, and 69% for Mission B;
- 4) The surface tension systems should be constructed of aluminum for Mission A₁, and titanium for Missions A₂ and B.

B. RECOMMENDATIONS

Based on the conclusions made from the evaluations, the preferred systems were recommended for approval at the Program Review held at JPL on 17 April 1970. After a thorough review of the program, the recommended systems were approved.

Phase II of the program will include the detailed design and analysis of surface tension propellant acquisition systems for Missions A₁, A₂, and B. The detailed prototype designs will be defined in terms of engineering drawings. The drawings will include overall dimensions, tolerances (where critical), materials of construction, and general fabrication requirements. The drawings will be to the level of detail required for engineering shop fabrication and assembly, but will not meet production drawing standards suitable for normal factory production line procedures.

The design will consider prelaunch, ground hold, launch, and postlaunch periods. The propulsion system schematics will be modified, as required, from the original JPL schematics to furnish a reliable and operational system. Any additional valving required for tank loading or draining will be shown. Handling, checkout and maintenance requirements will be defined for each system.

In conducting the detailed design effort, various surface tension concepts, in addition to a trap device, will be analyzed to achieve the best surface tension system for each of the three missions. As discussed and agreed to during the 17 April review, two basic surface tension concepts will be designed for each mission. The concepts will be different due to the two design approaches established at the meeting: (1) the surface tension device must be testable under the minus one-g condition; whereas (2) the other device will be designed to perform reliably under the operational environment only. During Phase II, JPL will furnish additional criteria so that the surface tension designs are further constrained to satisfy planned mission requirements.

IX. REFERENCES

- I-1. W. Unterberg and J. Congelliere: "Zero-Gravity Problems in Space Propellants." *ARS Journal*, Vol 32 (1962), p. 862.
- I-2. W. C. Reynolds: *Hydrodynamic Considerations for the Design of Systems for Very Low Gravity Environments*. Technical Report LG-1, Stanford University, Stanford, California, September 1961.
- I-3. E. Ring (Editor): "Special Zero Gravity Fluid Problems." *Rocket Propellant and Pressurization Systems*, Chapter 13. Prentice-Hall Book Company, Englewood Cliffs, New Jersey, 1964, pp. 116-152.
- I-4. T. E. Bowman and H. L. Paynter: "Weightless Liquids." *Science Journal*, Vol 2, No. 9, London, England, September 1966.
- I-5. D. L. Balzer, et al.: *Advanced Propellant Management System for Spacecraft Propulsion Systems, Phase I - Survey Study and Evaluation*. MCR-69-87, Contract NAS9-8939, Martin Marietta Corporation, Denver, Colorado, February 1969.
- III-1. E. J. Fahimian and M. Hurwitz: *Research and Design of a Practical and Economical Dielectrophoretic System for the Control of Liquid Fuels under Low Gravity Environmental Conditions*. Report No. 723, Contract NAS8-20553, Dynatech Corporation, Cambridge, Massachusetts, May 1967.
- III-2. F. Lark: *Cryogenic Positive Expulsion Bladders*. NASA TM X-1555, Lewis Research Center, Cleveland, Ohio, April 1968.
- III-3. M. J. Werkema: *Parametric Bladder Study, Phase I, (Orbital Refueling and Checkout Study, Lockheed Missiles and Space Company)*. G. T. Schjeldahl Company, Northfield, Minnesota, 23 June 1967.
- III-4. *Orbital Refueling and Checkout Study (Final Report), Volume III - Evaluation of Fluid Transfer Modes*. Part I, T1-51-67-21, pp (2-3) - (2-10). Contract NAS10-4606, Lockheed Missiles and Space Company, Sunnyvale, California, 12 February 1968.

- III-5. Letter from M. J. O'Connell, Bell Aerospace Company, Buffalo, New York, to Glenn F. Holle, Martin Marietta Corporation, Denver, Colorado, dated 5 March 1970.
- III-6. Letter from J. V. Petriello, Dilectrix Corporation, Farmingdale, Long Island, New York, to Glenn F. Holle and Howard L. Paynter, Martin Marietta Corporation, Denver, Colorado, dated 16 March 1970.
- III-7. Letter from M. J. Werkema, G. T. Schjeldahl Company, Northfield, Minnesota, to Glenn F. Holle, Martin Marietta Corporation, Denver, Colorado, dated 18 March 1970.
- III-8. R. G. Peterson and J. R. Taylor: "Positive Expulsion Tank for Titan III Transtage Hydrazine Attitude Control System," *Low Gravity Propellant Orientation and Expulsion*. Joint AIAA/Aerospace Corporation Symposium Proceedings, Los Angeles, California, 21-23 May 1968.
- III-9. J. C. Lee: "Counter-Permeation Phenomenon in Bladdered Expulsion Tank," *Low Gravity Propellant Orientation and Expulsion*. Joint AIAA/Aerospace Corporation Symposium Proceedings, Los Angeles, California, 21-23 May 1968.
- III-10. R. N. Porter and H. B. Stanford: *Propellant Expulsion in Unmanned Spacecraft*. Technical Report No. 32-899, Jet Propulsion Laboratory, Pasadena, California, 1 July 1966.
- III-11. D. F. Bazzare and J. V. Petriello: "Chemical Vapor Deposited Permeation Barriers in Teflon Expulsion Bladders," *Low Gravity Propellant Orientation and Expulsion*. Joint AIAA/Aerospace Corporation Symposium Proceedings, Los Angeles, California, 21-23 May 1968.
- III-12. R. F. Muraca, J. S. Whittick, and A. A. Koch: *Development of Techniques to Improve Bladder Materials and Test Methods*. Final Report JPL Contract 951484, Stanford Research Institute, Menlo Park, California, 17 June 1968.
- III-13. N. B. Levine: "CNR Expulsion Bladders," *Low Gravity Propellant Orientation and Expulsion*. Joint AIAA/Aerospace Corporation Symposium Proceedings, Los Angeles, California, 21-23 May 1968.

- III-14. R. L. Heilman: *Propellant Expulsion Bladder for the Saturn V/S-IVB*. RMD 5125-F1, Contract NAS8-21149, Thiokol Chemical Corporation, Denville, New Jersey, 1 July 1967 through 30 June 1969.
- III-15. H. C. Brown and A. R. Mukherjee: *Synthesis of Elastomers for Use with Liquid Fluorine*. Annual Interim Report, Contract NSR-10-005-047, Florida Engineering and Industrial Experiment Station, University of Florida, Gainesville, Florida, 15 September 1968.
- III-16. M. S. Toy: *New Fluorine-Containing Elastomers for Space-Propulsion Applications*. DAC-60520-F, Contract NAS7-603, McDonnell Douglas Corporation, Newport Beach, California, July 1968.
- III-17. L. M. Russell, H. W. Schmidt, and L. H. Gordon: *Compatibility of Polymeric Materials with Fluorine and Fluorine-Oxygen Mixtures*. NASA TN D-3392, Lewis Research Center, Cleveland, Ohio, June 1966.
- III-18. R. K. Anderson: "Apollo Teflon Bladder Design," *Low Gravity Propellant Orientation and Expulsion*. Joint AIAA/Aerospace Corporation Symposium Proceedings, Los Angeles, California, 21-23 May 1968.
- III-19. T. R. Barksdale, et al.: *Advanced Propellant Management System for Spacecraft Propulsion Systems, Phase I - Survey Study and Evaluation*. MCR-69-87, Contract NAS9-8939, Martin Marietta Corporation, Denver, Colorado, February 1969, pp 13-32.
- III-20. A. J. Bauman: *Some Design Characteristics, Large Expulsion Bladders for Nitrogen Tetroxide and Hydrazine*. Technical Report No. 32-862, Jet Propulsion Laboratory, Pasadena, California, 15 January 1966.
- III-21. J. Carhart, et al.: *The Evaluation of a Composite Teflon Aluminum Expulsion Bladder for Use in Nitrogen Tetroxide*. D2-100645-1, The Boeing Company, Seattle, Washington, May 1966.
- III-22. H. N. Chu, W. Unterberg, and J. C. Lee: *Final Report, Improvement of Efficiency and Life of Expulsion Bladders*. R-7391, Rocketdyne, Canoga Park, California, 29 February 1968.

- III-23. *Development of Expulsion and Orientation Systems for Advanced Liquid Rocket Propulsion Systems.* SSD-TDR-62-712, Bell Aerosystems Company, Buffalo, New York, December 1962.
- III-24. *Evaluation of New Raw Material in the Fabrication of Teflon Bladder Film Structures.* Dilectrix Corporation, Farmingdale, New York.
- III-25. W. P. Fitzgerald, Jr.: *Study of Highly Fluorinated Heterocyclic Polymers for Cryogenic Bladder Applications.* Quarterly Letter Report No. 4, Contract No. NASw-1822, Whittaker Corporation, San Diego, California, 31 October 1969.
- III-26. R. A. Gould and L. M. Stayton: *The Use of Chemical Vapor Deposited Aluminum for Propellant Tank Liners and Expulsion Bladders (U).* 10th Liquid Propulsion Symposium, Vol I, Chemical Propulsion Information Agency, Las Vegas, Nevada, November 1968. (Confidential)
- III-27. J. Green: *Review of Materials Research, Rocket Fuel and Oxidizer Application.* Thiokol Chemical Corporation, Denville, New Jersey, 23 May 1962.
- III-28. J. Green and N. B. Levine: *Elastomeric and Compliant Materials for Liquid Rocket Fuel and Oxidizer Application.* RMD 5029-Q2, Thiokol Chemical Corporation, Denville, New Jersey, 1 June 1963 to 31 August 1963.
- III-29. J. Green and N. B. Levine: *Elastomeric and Compliant Materials for Liquid Rocket Fuel and Oxidizer Application.* RMD 5029-Q3, Thiokol Chemical Corporation, Denville, New Jersey, 1 September 1963 to 30 December 1963.
- III-30. G. H. Hopmier, B. D. Richardson, and B. L. Crasswhite: *Application for Positive-Expulsion Bladder Concepts to the Lance Feed System (U).* 10th Liquid Propulsion Symposium, Vol I, Chemical Propulsion Information Agency, Las Vegas, Nevada, November 1968. (Confidential)
- III-31. A. Krivetsky: *Research on Zero-Gravity Expulsion Techniques.* 7129-933003, Bell Aerosystems Company, Buffalo, New York, March 1962.

- III-32. J. Krusos: *A Study of Teflon Bladder Design Criteria for Use in the Expulsion Propellant Tanks of the Apollo-Saturn and Lunar Orbiter Vehicles*. Monthly Progress Report No. 7, Bell Aerosystems Company, Buffalo, New York, May 1966.
- III-33. J. N. Krusos, R. C. Higgins, and W. H. Dukes: *Design Criteria and Quality Control Studies for Teflon Expulsion Bladders*. 8460-933012, Bell Aerosystems Company, Buffalo, New York, March 1967.
- III-34. S. Levat Lehman, L. Jablansky, and J. Canavan: *Progress in Techniques of Propellant Expulsion for Army Weapons (U)*. 10th Liquid Propulsion Symposium, Vol I, Chemical Propulsion Information Agency, Las Vegas, Nevada, November 1968. (Confidential)
- III-35. N. B. Levine and H. Krainman: *Nitroso Rubber Expulsion Bladders for Nitrogen Tetroxide Application*. RMD 5094-Q2, Thiokol Chemical Corporation, Denville, New Jersey, December 1966.
- III-36. N. B. Levine and H. Krainman: *Nitroso Rubber Expulsion Bladders for Nitrogen Tetroxide Application*. RMD 5094-Q3, Thiokol Chemical Corporation, Denville, New Jersey, April 1967.
- III-37. N. B. Levine, H. Krainman, and J. Green: *Positive Expulsion Bladders for Storable Propellants*. AFML-TR-65-379, Thiokol Chemical Corporation, Denville, New Jersey, January 1966.
- III-38. N. B. Levine, H. Krainman, and R. C. Keller: *Nitroso Rubber Expulsion Bladders for Nitrogen Tetroxide Application*. RMD 5094-Q1, Thiokol Chemical Corporation, Denville, New Jersey, October 1966.
- III-39. N. B. Levine, W. R. Sheehan, and J. Green: *Nitroso Rubber Expulsion Bladders for Nitrogen Tetroxide Application*. ML-TDE-64-107, Part III, Thiokol Chemical Corporation, Denville, New Jersey, December 1965.
- III-40. H. R. Lubowitz, J. F. Jones, R. A. Meyers, and E. A. Burns: *The Development and Characterization of New Storable Propellant Bladder Materials*. 6104-6013-R000, TRW Systems, Redondo Beach, California, 15 February 1968.

- III-41. J. H. McKenna: *Compatibility of Materials of Construction with Hydrazine, Unsymmetrical Dimethylhydrazine, and Nitrogen Tetroxide*. IDC, The Martin Company, Denver, Colorado, 1959.
- III-42. R. F. Muraca, et al.: *Development of Techniques to Improve Bladder Materials and Test Methods, Addendum 1*. Stanford Research Institute, Menlo Park, California, 30 March 1969.
- III-43. J. V. Petriello: "Modifications in Fluorocarbon Bladder Structures in Improving Flexibility and Impermeability," *Low Gravity Propellant Orientation and Expulsion*. Joint AIAA/Aerospace Corporation Symposium Proceedings, Los Angeles, California, 21-23 May 1968.
- III-44. D. H. Pope and W. R. Killiam: *Positive Expulsion of Cryogenic Liquids*. NASA CR-55898, Beech Aircraft Corporation, Boulder, Colorado, June 1963.
- III-45. R. N. Porter: *The Fabrication of Seamless Teflon Propellant Expulsion Bladders*. Technical Report No. 32-914, Jet Propulsion Laboratory, Pasadena, California, 15 June 1966.
- III-46. R. N. Porter and H. B. Stanford: *Propellant Expulsion in Unmanned Spacecraft*. SAE Air Transport and Space Meeting, April 1964.
- III-47. *Program 706 Task 4 MPU Bladder Development*. SSD-TDE-63-278, Radio Corporation of America, Burlington, Massachusetts, 4 November 1963.
- III-48. J. W. Putt: "Experience with Teflon Positive Expulsion Bladders for the Surveyor Vernier Propulsion System," *Low Gravity Propellant Orientation and Expulsion*. Joint AIAA/Aerospace Corporation Symposium Proceedings, Los Angeles, California, 21-23 May 1968.
- III-49. *Reaction Control System Design Data for Space Vehicle Applications*. 8500-950008, Bell Aerosystems Company, Buffalo, New York, October 1965.
- III-50. J. Repar: *Flight and Experimental Expulsion Bladders for Mariner '69*. APCO #6935-2010 (SE), JPL Contract No. 951939, Accessory Products Company, Whittier, California, 17 July 1969.

- III-51. H. B. Stanford: *The Measured Permeability to Nitrogen Tetroxide of Some Potential Bladder Materials*. Technical Memorandum No. 33-123, Jet Propulsion Laboratory, Pasadena, California, 24 March 1963.
- III-52. *Study of Zero-Gravity Positive Expulsion Technique*. 8230-933004, Bell Aerosystems Company, Buffalo, New York, June 1963.
- III-53. *Technical Discussion of Measurement of Fluid Mass under Zero Gravity Conditions*. 3554-66, Bendix Corporation, Davenport, Iowa, 18 May 1966.
- III-54. P. E. Uney: *Compatibility of Storage Materials with Various Rocket Propellants*. SR 1660-69-20, Martin Marietta Corporation, Denver, Colorado, November 1969.
- III-55. P. E. Uney: *Compatibility of Storage Materials with Various Rocket Propellants*. Addendum SR 1660-69-20A, Martin Marietta Corporation, Denver, Colorado, January 1970.
- III-56. S. P. Vango: *Compatibility and Permeability of Nitroso Rubber*. Space Programs Summary No. 37-34, Vol IV, pp 206-207, Jet Propulsion Laboratory, Pasadena, California, 31 August 1965.
- III-57. S. P. Vango: *Determination of Permeability of Cast Teflon Sheet to Nitrogen Tetroxide and Hydrazine*. Technical Memorandum No. 33-35, Jet Propulsion Laboratory, Pasadena, California, 15 June 1966.
- III-58. M. J. Werkema: *Parametric Bladder Study, Phase II, (Orbital Refueling and Checkout Study, Lockheed Missiles and Space Company)*. G. T. Schjeldahl Company, Northfield, Minnesota, 7 December 1967.
- III-59. K. Wiederkamp: *Liquid Hydrogen Positive Expulsion Bladders*. NASA CR-72432, Contract NAS3-11192, Boeing Company, Seattle, Washington, May 1968.
- III-60. Series of personal communications between A. Cozewith, Arde, Inc., Mahwah, New Jersey, and P. E. Uney, Martin Marietta Corporation, Denver, Colorado, December 1969 to February 1970.

- III-61. *All-Metallic Positive Expulsion Systems*. Arde, Inc., Mahwah, New Jersey, 23 May 1969.
- III-62. Letter from A. Cozewith, Arde, Inc., Mahwah, New Jersey, to P. E. Uney, Martin Marietta Corporation, Denver, Colorado, dated 5 March 1970.
- III-63. *Zero Gravity Positive Expulsion*. Bell Aerosystems Company, Buffalo, New York.
- III-64. Letter from J. J. O'Connell, Bell Aerosystems Company, Buffalo, New York, to P. E. Uney, Martin Marietta Corporation, Denver, Colorado, dated 5 March 1970.
- III-65. *Proposal for a Feasibility Demonstration Program of an Advanced Positive Expulsion Propellant Storage Assembly for a Growth PBPS Application*. D8590-953001, Bell Aerosystems Company, Buffalo, New York, March 1969.
- III-66. W. Sanscrainte: *Telephragm Positive Expulsion Development and Demonstration Program (U)*. 8561-933004, Bell Aerosystems Company, Buffalo, New York, January 1969. (Confidential)
- III-67. D. W. Oliver and D. Miller: *Design and Evaluation of a Bootstrap Demand Monopropellant Gas Generator System (U)*. NOTS 4159, U. S. Naval Ordnance Test Station, China Lake, California, June 1967. (Confidential)
- III-68. Series of personal communications between R. W. Schwantes, Aerojet-General Corporation, Sacramento, California, and P. E. Uney, Martin Marietta Corporation, Denver, Colorado, December 1969 to March 1970.
- III-69. *Positive Expulsion Experience*. AFCS-0100-52, Aerojet-General Corporation, Sacramento, California, June 1968.
- III-70. *Transverse Collapsing Metallic Bladder Positive Expulsion Tanks*. 6710-69(03) ER, Aerojet-General Corporation, Fullerton, California, October 1969.
- III-71. Series of personal communications between W. D. Peters, Aerojet-General Corporation, Fullerton, California, and P. E. Uney, Martin Marietta Corporation, Denver, Colorado, December 1969 to March 1970.

- III-72. Letter from W. D. Peters, Aerojet-General Corporation, Fullerton, California, to P. E. Uney, Martin Marietta Corporation, Denver, Colorado, dated 27 February 1970.
- III-73. *Positive Expulsion Experience Report*. AGCS-0100-52, Aerojet-General Corporation, Sacramento, California, June 1968.
- III-74. *Transverse Collapsing Metallic Bladder, Tank Packaging Concepts*. 6710-69(04) ER, Aerojet-General Corporation, Fullerton, California, October 1969.
- III-75. D. Gleich and F. L'Hommiedieu: "Recycling Metallic Bladders for Cryogenic Fluid Storage and Expulsion Systems." AIAA Paper No. 67-444 presented at the AIAA 3rd Propulsion Joint Specialist Conference, Washington, D. C., 17-21 July 1967.
- III-76. W. H. Wright: *Nitrogen Tank Magnetic Testing*. AMR 183, General Electric, Philadelphia, Pennsylvania, December 1965.
- III-77. Series of personal communications between M. J. O'Connell, Bell Aerosystems Company, Buffalo, New York, and P. E. Uney, Martin Marietta Corporation, Denver, Colorado, December 1969 to March 1970.
- III-78. *Preliminary Conceptual Design for Space Storable Propellant Acquisition Devices*. Sealol, Inc., Warwick, Rhode Island, (Reply to Martin Marietta Corporation Inquiry No. ORF 69-01), September 1969.
- III-79. H. W. Johnson: *Metal Bellows Positive Expulsion Propulsion Systems for Space Vehicles*. Metal Bellows Corporation, Chatsworth, California, (Aerospace Corporation Symposium), 26 March 1964.
- III-80. D. A. Wendt: "High Expansion Metal Bellows with Non-Welded Convolution Edges for Propellant Expulsion System," *Low Gravity Propellant Orientation and Expulsion*. Joint AIAA/Aerospace Corporation Symposium Proceedings, Los Angeles, California, 21-23 May 1968.
- III-81. Letter from Vern Orth, Gardner Bellows Corporation, Van Nuys, California to Dennis Gilmore, Martin Marietta Corporation, Denver, Colorado, 20 November 1969.

- III-82. Personal communication between Elliot Thompson, The Belfab Corporation, Daytona Beach, Florida, and Dennis Gilmore, Martin Marietta Corporation, Denver, Colorado, November 1969.
- III-83. D. T. Covington and R. F. Fearn: *Cryogenic Metallic Positive Expulsion Bellows Evaluation*. NASA CR-72513, Martin Marietta Corporation, Denver, Colorado, January 1969.
- III-84. *Bellows Design Manual*. Belfab, Bailey Meter Company, Daytona Beach, Florida.
- III-85. *Designers' Guide for Positive Expulsion Tank Bellows*. 8230-933010, Bell Aerosystems Company, Buffalo, New York, February 1967.
- III-86. Letter from D. E. Williams, Stainless Steel Products Company, Burbank, California to T. R. Barksdale, Martin Marietta Corporation, Denver, Colorado, dated 11 March 1970.
- III-87. T. M. Trainer, et al.: *Final Report on the Development of Analytical Techniques for Bellows and Diaphragm Design*. AFRPL-TR-68-22, Contract AFO4(611)-10532, Battelle Memorial Institute, Columbus, Ohio, March 1968.
- III-88. C. J. Sterner and A. H. Singleton: *The Compatibility of Various Metals in Carbon with Liquid Fluorine*. WADD TR 60-436, Air Products, Inc., Allentown, Pennsylvania, August 1960.
- III-89. B. E. Dawson, A. F. Lum, and R. R. Schreib: *Investigation of Advanced High Energy Space Storable Propellant System*. RMD 5507-F, Thiokol Chemical Corporation, Denville, New Jersey, June-November 1962.
- III-90. N. A. Tiner, W. D. English, and S. M. Toy: *Compatibility of Structural Materials with High Performance O-F Liquid Oxidizers*. AFML-TR-65-414, Douglas Aircraft Company, Inc., Newport Beach, California, November 1965.
- III-91. Sir W. Thomson(Lord Kelvin): "Hydrokinetic Solutions and Observations." *Phil. Mag.*, Series 4, Vol 42, 1871, p 374.

- III-92. J. C. Maxwell: "Capillary Action." *The Scientific Papers of James Clark Maxwell*. University Press, Cambridge, England, Vol 2, 1890, pp 541 thru 591.
- III-93. J. W. Strutt (Lord Rayleigh): "On Waves." *Phil. Mag.*, Series 5, Vol 1, 1876, pp 257 thru 279.
- III-94. Sir G. G. Stokes: "On the Theory of Oscillatory Waves." *Cambridge Trans.* Vol 8, 1847.
- III-95. F. Bashforth and J. Adams: *An Attempt to Test the Theories of Capillary Action*. University Press, Cambridge, England, 1883.
- III-96. R. G. Clodfelter and R. C. Lewis: *Fluid Studies in Zero Gravity Environment*. ASD TN 61-84, Wright-Patterson AFB, Dayton, Ohio, June 1962.
- III-97. G. A. Hastings and D. W. Hill: *The Literature of Low-g Propellant Behavior*. CR-92081, Contract NAS9-5174, Lockheed Missiles & Space Company, Sunnyvale, California, May 1967.
- III-98. T. E. Bowman: *The Literature of Low-G Propellant Behavior 1966-69*. MCR-69-438, Contract NAS9-8939, Martin Marietta Corporation, Denver, Colorado, September 1969.
- III-99. S. C. DeBrock, *et al.*: "A Survey of Current Developments in Surface Tension Devices for Propellant Acquisition." Paper No. 70-685, presented at the AIAA 6th Propulsion Joint Specialist Conference, San Diego, California, 15-19 June 1970.
- III-100. H. L. Paynter, *et al.*: *Passive Retention/Expulsion Methods for Subcritical Storage of Cryogenics*. MCR-70-85 (Issue 7), Contract NAS9-10480, Martin Marietta Corporation, Denver, Colorado, September 1970.
- III-101. M. H. Blatt: *Low Gravity Propellant Control Using Capillary Devices in Large Scale Cryogenic Vehicles*. 584-4-513, Monthly Progress Report, Contract NAS8-21465, Convair Division of General Dynamics, San Diego, California, July 1970.

- III-102. G. A. Lyerly and H. Peper: *Summary Report - Studies of Interfacial Surface Energies*. NASA CR-54175, Harris Research Laboratories, Inc., Washington, D.C., 31 December 1964.
- III-103. T. E. Bowman: *Cryogenic Liquid Experiments in Orbit. Vol I - Liquid Settling and Interface Dynamics*. NASA CR-651, Martin Marietta Corporation, Denver, Colorado, December 1966.
- III-104. H. L. Paynter, et al.: *Capillary Systems for Storable Propellants*. SR 1660-67-8, Martin Marietta Corporation, Denver, Colorado, June 1967.
- III-105. H. L. Paynter, et al.: *Experimental Investigation of Capillary Propellant Control Devices for Low-Gravity Environments. Vol I - Summary Report*. NASA CR-110754, Martin Marietta Corporation, Denver, Colorado, June 1970.
- III-106. H. L. Paynter, et al.: *Experimental Investigation of Capillary Propellant Control Devices for Low-Gravity Environments. Vol II - Final Report*. NASA CR-110755, Martin Marietta Corporation, Denver, Colorado, June 1970.
- III-107. *Advanced Propellant Management System for Spacecraft Propulsion Systems*. P-68-114 (Vol I), Martin Marietta Corporation, Denver, Colorado, June 1968, p IV-10.
- III-108. *Capillary Retention Device Study*. P-69-142 (Vol I), Martin Marietta Corporation, Denver, Colorado, November 1969, p II-10.
- III-109. D. A. Fester and P. E. Bingham: *Evaluation of Fine-Mesh Screen Devices in Liquid Fluorine*. R-70-48631-010, Martin Marietta Corporation, Denver, Colorado, June 1970.
- III-110. M. E. Meadows: "Propulsion Requirements for Low-Gravity Liquid Settling," Paper No. 90, Proceedings of the Southeastern Symposium on Missiles and Aerospace Vehicles Sciences, American Astronautical Society, Huntsville, Alabama, 5-7 December 1966.

- III-111. J. F. McCarthy: "Zero-g Propulsion Problems." *Jet, Rocket, Nuclear, Ion and Electric Propulsion - Theory and Design*, W. H. T. Loh, Ed., Springer-Verlag, New York, New York, pp 644-727.
- III-112. H. M. Satterlee and M. P. Hollister: *Engineers Handbook: Low-G Propellant Behavior*, NASA CR-92083, May 1967.
- IV-1. *Pressurization System for Use in the Apollo Service Propulsion System, Computer Program Utilization Manual*. MCR-CR-66-39, Contract NAS9-3521, Martin Marietta Corporation, Denver, Colorado, July 1966.
- IV-2. T. R. Strobridge: "The Thermodynamic Properties of Nitrogen from 114 to 540°R Between 1.0 and 3000 psia, Supplement A (British Units)." *National Bureau of Standards Technical Note 129A*, U. S. Government Printing Office, Washington, D. C., February 1963.
-
- IV-3. D. B. Mann: "The Thermodynamic Properties of Helium from 6 to 540°R between 10 and 1500 psia." *National Bureau of Standards Technical Note 154A*, U. S. Government Printing Office, Washington, D. C., January 1962.
- IV-4. Data supplied by Jet Propulsion Laboratory, Pasadena, California.
- IV-5. P. H. Peters, E. E. Stone, and A. J. Bialous: *Leakage Testing Handbook*. Revised Edition, JPL Contract NAS7-396, General Electric Research and Development Center, Schenectady, New York, July 1969.
- IV-6. J. H. Robson, W. A. Cannon, and W. D. English: *Pressurization Systems Design Guide, Volume III - Pressurant Gas Solubility in Liquid Propellants*. NASA CR-97094, McDonnell Douglas Corporation, Newport Beach, California, July 1968.
- IV-7. *Pressurization Systems Design Guide - Volume IIB*. NASA CR-80315, Aerojet-General Corporation, Sacramento, California, July 1966.
- IV-8. *Nitrogen Saturated Propellants, YLR91-AJ-5 Rocket Engine (U)*. Report LR01, Contract AF04(694)-512, Order No. BSD-64-3, Aerojet General Corporation, Sacramento, California, June 1964 (Confidential).

- IV-9. B. Foran and B. B. Williams: *Solubility of Helium in Nitrogen Tetroxide, Aerozine 50, and Methyl Hydrazine*. SID65-232, North American Aviation, Inc., Downey, California, March 1963.
- IV-10. E. T. Chang and N. A. Gokcen: *Solubilities of N_2 , He, and Ar in Liquid N_2O_4* . ATN-64(9228)-4, Aerospace Corporation, El Segundo, California, October 1964.
- IV-11. E. T. Chang and N. A. Gokcen: *Solubilities of O_2 , NO, and N_2O_3 in Liquid N_2O_4* . TDR-469(5210-10)-6, Aerospace Corporation, El Segundo, California, May 1965.
- IV-12. E. T. Chang and N. A. Gokcen: *Journal of Phys Chem*, 70:2394 (1966).
- IV-13. E. T. Chang, N. A. Gokcen, and T. M. Posten: *Journal of Phys Chem*, 72:638 (1968).
- IV-14. D. A. Fester: *Study of Nitrogen Saturation of Titan II Propellants - Sampling and Analysis for Nitrogen Content*. TM 0444-65-1, Martin Marietta Corporation, Denver, Colorado, January 1965.
- IV-15. R. L. Beegle, D. L. Quick, and W. J. Flaherty: *Measurement of Helium and Nitrogen Solubility in Nitrogen Tetroxide, Monomethylhydrazine and Aerozine-50*. LM 0696-03-7 and LM 0696-03-8, Aerojet-General Corporation, Sacramento, California, May-June 1966.
- IV-16. M. E. Ellion, et al.: *Development of the Surveyor Vernier Propulsion System (VPS)*. AIAA Paper No. 66-593, presented at the AIAA Second Propulsion Joint Specialist Conference, Colorado Springs, Colorado, 13-17 June 1966.
- V-1. S. P. Timoshenko and J. M. Gere: *Theory of Elastic Stability*, 2nd Edition, McGraw-Hill, New York, 1961.
- V-2. G. Gerard and H. Becker: *Handbook of Structural Stability, Part III Buckling of Curved Plates and Shells*. NACA TN 3783.
- VI-1. C. W. Churchman, R. L. Ackoff, and E. L. Arnoff: *Introduction to Operations Research*. John Wiley & Sons, Inc., New York, New York, 1957, pp 136-153.
- VI-2. P. W. Bridgeman: *Dimensional Analysis*. Yale University Press, New Haven, Connecticut, 1922, pp 21-22.

- VI-3. D. W. Miller and M. K. Starr: *Executive Decisions and Operations Research*. Prentice-Hall, Inc., Englewood Cliffs, New Jersey, 1960, pp 161-165.
- VII-1. Personal communications between B. Schmitz, Rocket Research Corporation, Seattle, Washington, and J. E. Anderson, Martin Marietta Corporation, Denver, Colorado, 25 February 1970.
- VII-2. S. Tannenbaum, et al.: *Advanced Propellants Investigation for Prepackaged Liquid Engines (U)*. RMD 5046-F, Thiokol Chemical Corporation, Denville, New Jersey, June 1965. (Confidential)
- VII-3. R. M. Platz, et al.: *Advanced Packaged Liquid Propellants Research and Tankage Material (U)*. RMD 5074-F, Thiokol Chemical Corporation, Denville, New Jersey, May 1967. (Confidential).
- VII-4. *Viking Baseline Orbiter Conceptual Design Description*. Project Document No. 611-2, Jet Propulsion Laboratory, 1 March 1969.
- VII-5. H. F. Brady and D. DiStefano: *Sterilizable Liquid Propulsion System (Part I)*. MCR-68-119, JPL Contract 951709, Martin Marietta Corporation, Denver, Colorado, August 1968.
- VII-6. S. C. Lukens: *Sterilizable Liquid Propulsion System (Part II)*. MCR-68-119, JPL Contract 951709, Martin Marietta Corporation, Denver, Colorado, September 1969.
- VII-7. S. H. Kalfayan and B. A. Campbell: *Effects of the Thermal Sterilization Procedure on Polymeric Products*. Technical Report No. 32-973, Jet Propulsion Laboratory, Pasadena, California, 15 November 1966.
- VII-8. S. H. Kalfayan, B. A. Campbell and R. H. Silver: *Effects of Ethylene Oxide - Freon 12 Decontamination and Dry Heat Sterilization Procedures on Polymeric Products*. Technical Report 32-1160, Jet Propulsion Laboratory, Pasadena, California, 15 September 1967.
- VII-9. S. M. Lee and J. J. Licari: *Effects of Decontamination and Sterilization on Spacecraft Polymeric Materials*. C8-58/501, JPL Contract 951566, North American Rockwell Corporation, 12 January 1968.

MCR-70-171

APPENDIX

CAPILLARY/BELLOWS FEASIBILITY TEST PROGRAM

Bench tests were conducted to evaluate the feasibility of the capillary/bellows propellant acquisition device described earlier in Chapter III (Section G). The tests were conducted under Task VIII (Fig. I-1).

The objectives of the capillary/bellows investigation were to demonstrate (1) capability to design and fabricate the device within the current state-of-the-art; and (2) feasibility to provide engine restart capability for the missions identified in this contract. If the device proved feasible, then a secondary objective was to determine design criteria that should be considered in matching a capillary/bellows to a specific mission.

Specific test objectives, therefore, were to demonstrate that (1) the system was capable of being filled with liquid completely (no gas); (2) it could outflow liquid when covered with liquid; (3) it could outflow liquid in an adverse acceleration environment, i.e., the acceleration vector tending to position liquid at the opposite end of the tank away from the outlet and device; and (4) it was capable of refilling automatically.

A. EXPERIMENTAL APPARATUS

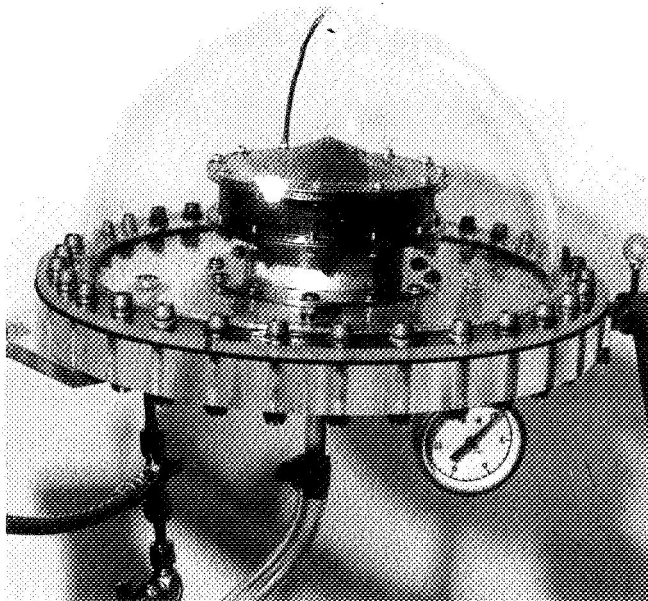


Figure A-1 Capillary/Bellows Test Setup

The test apparatus consisted of an 8-in. OD transparent tank and attachments for filling, pressurization, and outflow, as pictured in Figure A-1. The change in the direction of the gravity vector, from plus one-g to minus one-g, was achieved by rotating the tank through 180°. (The minus one-g condition has the liquid drain port at the top of the tank so that gravity tends to position liquid away from the outlet). Outflow was viewed through the clear, flexible Tygon tubing ($\frac{1}{2}$ -in. ID) connecting the outlet to a vented receiver tank. A Ramapo flowmeter (0 to 3 gpm) was installed in the outflow line.

The capillary/bellows device contained in the transparent tank was designed and fabricated full-scale to satisfy the monopropellant Mission B requirements* -- 25-lb_f thrust, total impulse of 33,000 lb_f-sec, and a specific impulse (vacuum) of 255 lb_f-sec/lb_m. The steady-state flowrate is readily determined to be 0.098 lb_m/sec. Methanol was selected as the test liquid because of handling considerations. Its physical properties, density, surface tension, and viscosity are less than those for N₂H₄ (nitrated), as shown in the tabulation.

	SURFACE TENSION [($\sigma \times 10^3$) lb _f /ft]	DENSITY (lb _m /ft ³)	KINEMATIC SURFACE TENSION [($\beta \times 10^4$) ft ³ /sec ²]	VISCOSITY [($\mu \times 10^3$) lb _m /ft-sec]
N ₂ H ₄ (Nitrated)	3.84	69.8	17.1	2.40
Methanol	1.55	49.4	10.1	0.402

The nitrated data are those presented in Table II-3 of the report. The methanol properties (at 20°C) were obtained from Ref A-1. Since capillary differential pressure, as explained earlier in Chapter III, is a critical design criterion, the liquid-to-solid contact angle (θ) is another pertinent property for similitude. Methanol is totally-wetting ($\theta = 0^\circ$), Ref A-1, which agrees well with the nitrated hydrazine, assumed to possess a contact angle in the range of 1 to 2 deg, as measured for neat hydrazine (Ref A-2).

*Although the capillary/bellows device is applicable to any of the three baseline missions, it appears to be most attractive for Mission B. Its attractive feature is the ability to refill. Mission B has a minimum impulse bit of 1.0 lb_f-sec whereas the value for the A₁ and A₂ missions is 400 lb_f-sec. The minimum impulse requirement is critical to propellant settling.

There are three predominant forces to be considered in designing the acquisition device (ignoring the inertial force of the bellows itself which is negligible): (1) the screen capillary force, (2) the liquid hydrostatic force, and (3) the bellows spring force. Referring to Figure III-23 of the report, the differential pressure corresponding to each force may be described as shown in Equations [III-9], [III-10] and [III-22], respectively.

The bellows were procured from Sealol, Inc.; they gave the following dimensions and operating characteristics for the bellows:

Material = 0.0025-in. thick, 347 SS

Diameter = 4.92-in. OD, 3.55-in. ID (effective area = 14.1 in.²)

Convolutions = 17 welded convolutions

Length (free length) = 1.19 in., stroke = 1.07 in.

Spring rate (K_b) = 3.33 lb_f/in.

Displacement = 15 in.³

The displacement volume corresponds to 0.429 lb_m of methanol. It was more than adequate since it provided liquid outflow durations from 2.3 to 10.7 sec (with no refill) for the range of steady flow rates, 0.04 to 0.19 lb_m/sec, during test. (The volume would provide 6.19 sec at the steady-state flow rate of 0.098 lb_m/sec for the nitrated hydrazine.)

Three acquisition devices were fabricated for test. The three basic components common to all three devices were (1) a top cone assembly, (2) a bellows assembly, and (3) the cylindrical screen assembly. An assembled device (No. 3) is pictured in Figure A-2. The cone assembly consisted of a mounting flange, 10-deg backup cone, and a screen cone. The screen was 304 stainless steel in each test article. The backup cone configuration is pictured in Figure A-3. It was formed from 0.024-in. thick stainless perforated plate with 0.026-in. diameter holes in a 60 deg array, providing an open area of 39.2%.

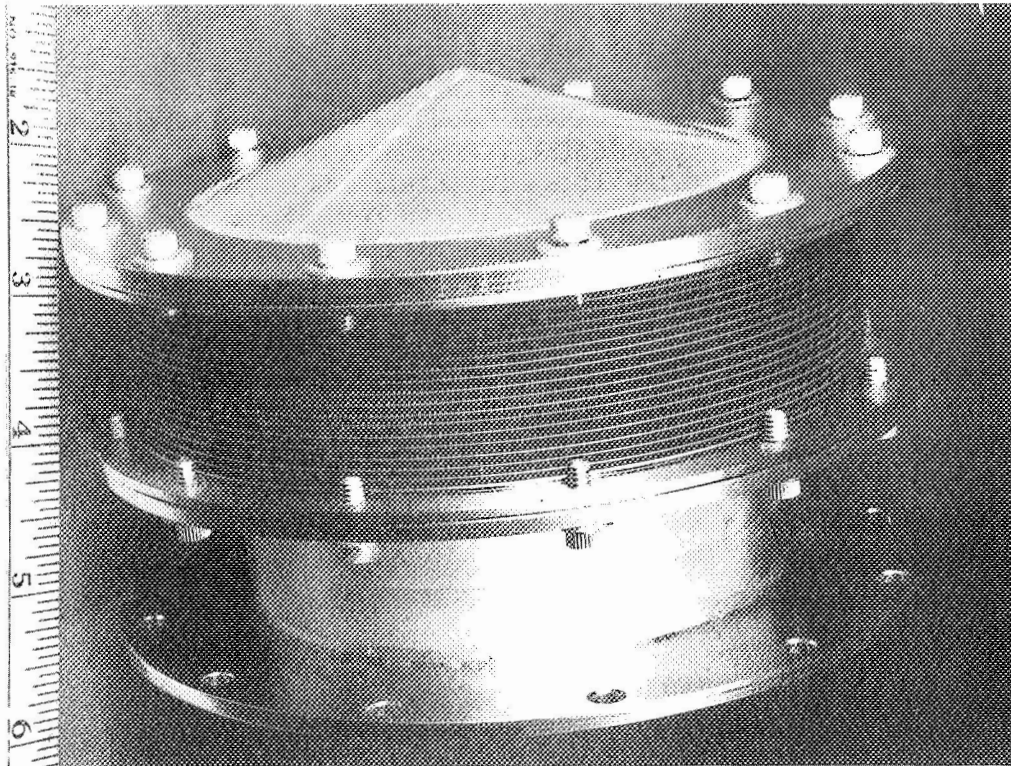


Figure A-2 Capillary/Bellows Device No. 3

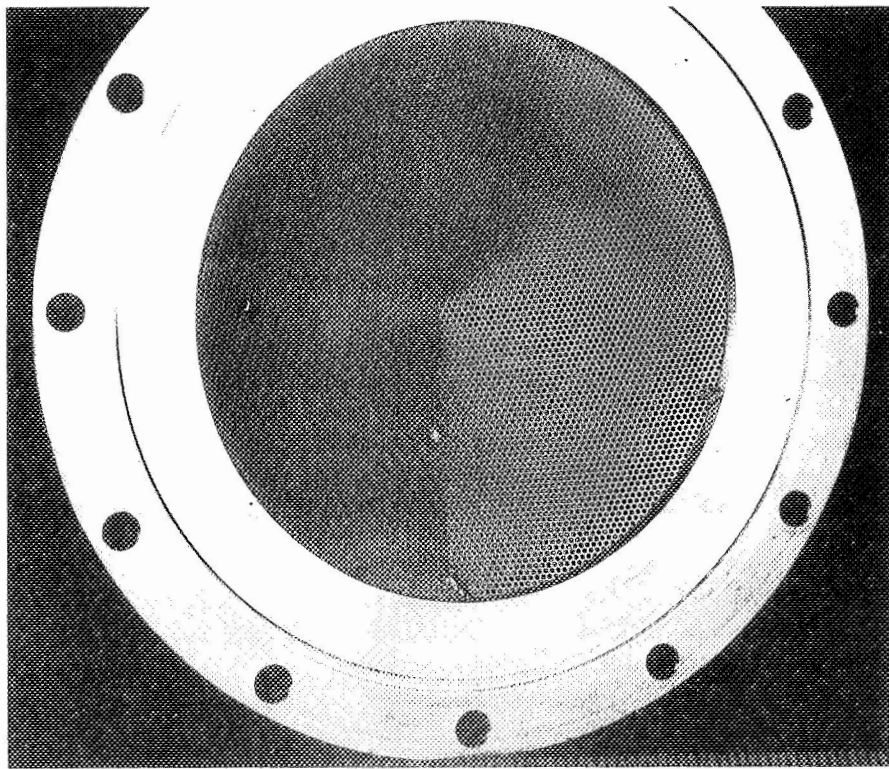


Figure A-3 Screen Backup Cone

The bellows assembly was described earlier. It was the welded-metal type with a nesting, ripple diaphragm, as shown. It had 347 stainless flanges 0.62-in. thick for attachments. The compression force-to-deflection relationship was checked and found to be nearly-linear (about $3.4 \text{ lb}_f/\text{in.}$) over 90% of its deflection.

The cylindrical screen section, Figure A-4, was 3.55-in. ID and 1.0-in. high. The Dutch-twill screen was supported by 0.020-in. thick plate with 0.125-in. holes to provide an open area of 36.2%.

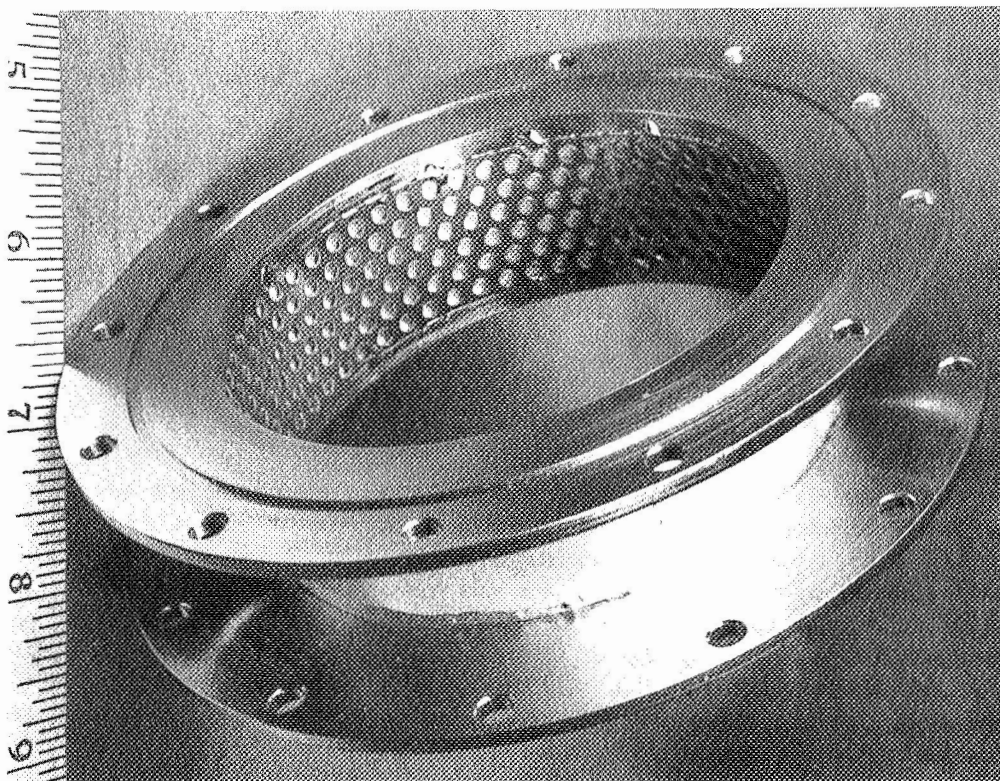


Figure A-4 Cylindrical Screen Assembly

Device No. 1 used 250x1370 mesh Dutch-twill weave screen on the cone and cylindrical assemblies with two bellows mounted in series instead of the one bellows shown in Figure A-2. Device No. 2 was identical to Device No. 1 except a compressive spring was mounted within the assembly, between the base plate and screen backup cone, to increase the effective bellows spring rate from 2.4 to $4.45 \text{ lb}_f/\text{in.}$ For device No. 3, the screen on the cone and cylindrical components was 80x700 mesh Dutch-twill weave. A single

bellows was used in this assembly, as shown in Figure A-2. The bubble point of each capillary component was checked prior to assembly. The 250x1370 mesh screen assemblies had a bubble point of 19.5 in. of H₂O (0.7 psi) in methanol, while the 80x700 mesh screen assemblies had a bubble point of 6.3 in. of H₂O (0.23 psi) in methanol. The actual bubble points of the assemblies were used in this effort rather than the more conservative micron rating data generally used in design.

In order for the capillary retention to be achieved during operation of the bellows, the gas/liquid interface at the screen surface must be stable. The Bo and ϕ number stability criteria for the acceleration vector acting normal and parallel to the screen surface, respectively, are discussed in detail in Ref A-3. For the 1-g bench tests, the Bo and ϕ numbers for the 80x700 screen, calculated to be 2.6×10^{-4} and 0.24, were below the critical stability values ($Bo \leq 0.84$ and $\phi \leq 1.00$).

B. TEST DESCRIPTION AND DISCUSSION OF RESULTS

Each of the four categories of 1-g tests performed is discussed separately.

1. Fill Tests

Fill tests were conducted with the outlet oriented both downward and upward. The tank was loaded through the outlet in each case. With the outlet oriented upward (away from Earth), the tank was completely filled, i.e., no gas remaining in the device. Fill tests with the outlet oriented toward Earth resulted in some gas trapped in the device below the conical-shaped top screen. This gas entrapment was due to wicking of the screen preceding the liquid fill level, thus sealing the screen pores and preventing gas escape. To alleviate this situation, a piece of 3/8-in. OD stainless steel tubing, 3/8-in. long, was fastened above the peak of the cone after providing a hole in the peak. A Dutch-twill disc (same mesh as the top screen) was then fastened in the open end of the tube. The addition of this small vent tube allowed all the gas to escape from the device so complete filling could be achieved.

All loading tests were made with the transparent tank vented.

2. Deflection Tests

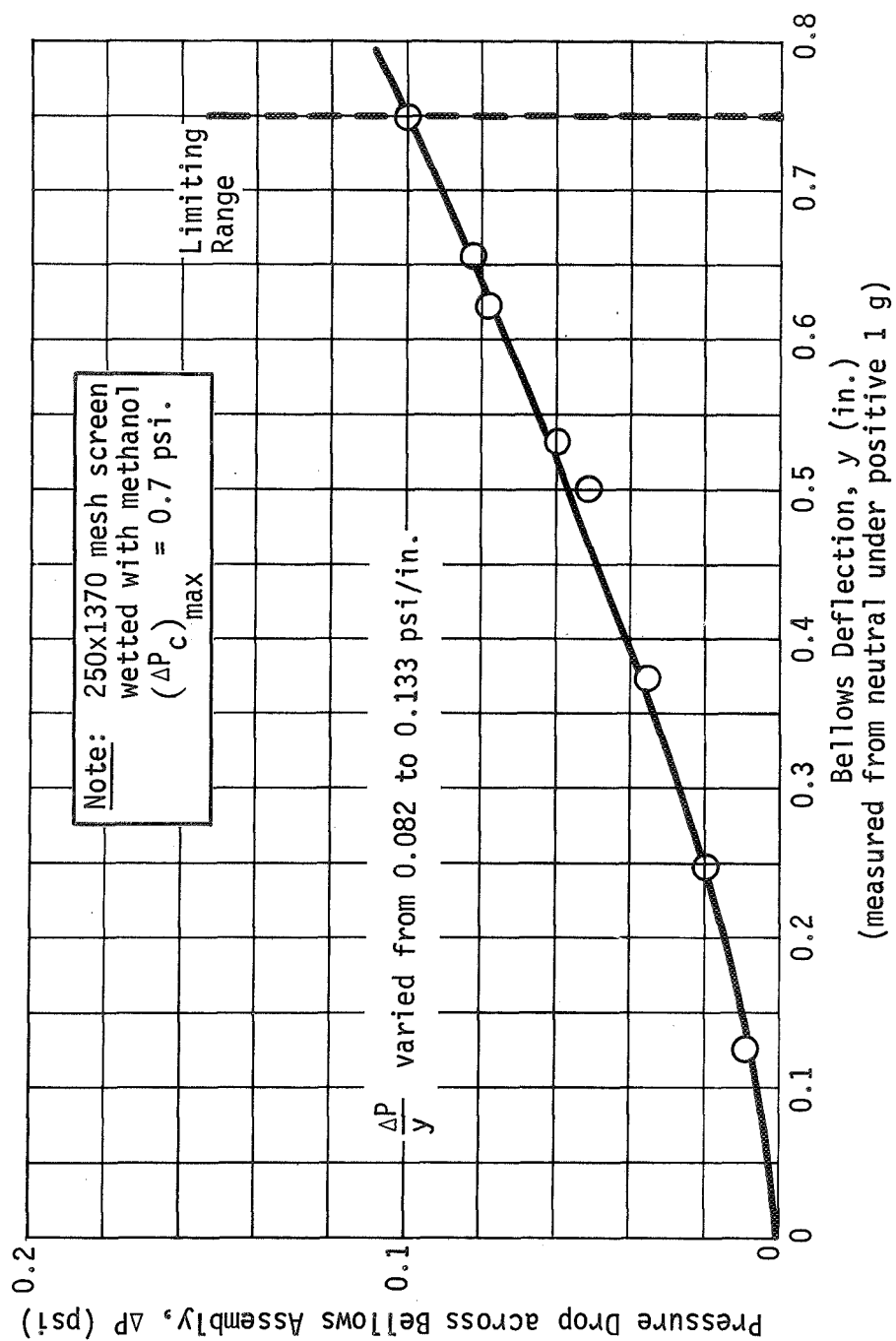
Tests for deflection of the bellows as a function of pressure drop across the capillary/bellows assembly were conducted with the test article mounted in the test fixture in a positive one-g position, i.e., with the outlet pointed toward Earth. The screens were wetted with methanol to establish a capillary pressure retention capability across the screen. Nitrogen gas was then used to pressurize the outside of the capillary/bellows device.

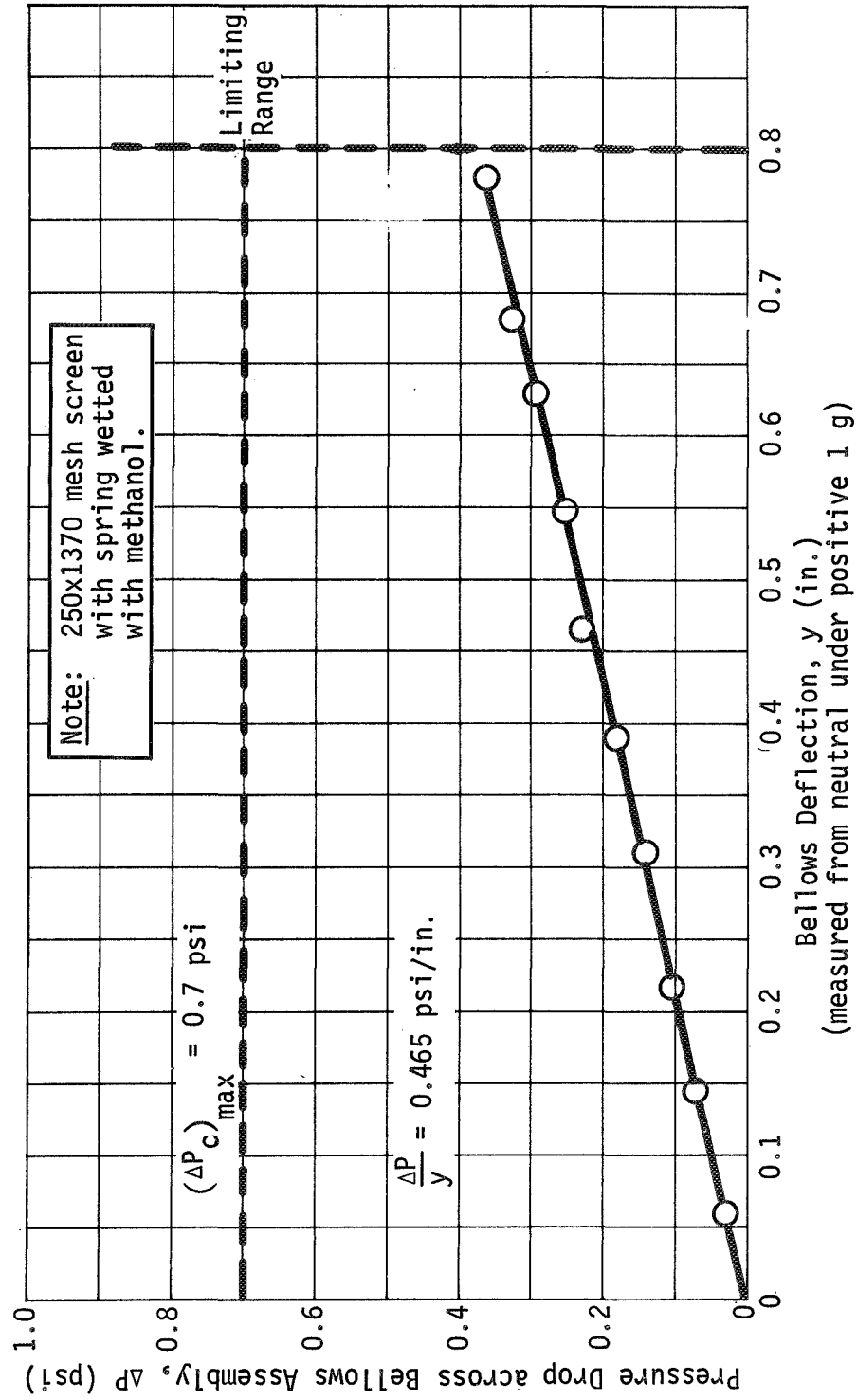
The pressure differential across the device was determined as a function of bellows deflection to provide a measure of pressure loss during outflow. The resulting pressure-deflection curves are presented in Figures A-5, A-6 and A-7 for the three devices tested. The data were plotted directly on each of the curves. The data shown in Figure A-5 indicate that Device No. 1 was slightly nonlinear. The maximum capillary pressure retention capability $(\Delta P_c)_{\max}$ of the 250x1370 mesh screen was 0.7 psi and for the 80x700, 0.23 psi. The data in Figure A-5 indicate a wide margin between the ΔP required to fully compress the bellows and the $(\Delta P_c)_{\max}$ of the screen. The margin is less for the other two test articles, although adequate.

3. Outflow under Adverse Acceleration

The adverse acceleration environment (minus one-g) was provided by rotating the test article so its outlet was at the top of the tank. Outflow from the device was in a direction opposite to the gravity vector. Pressure for outflow was provided by nitrogen gas entering through the pressurization/vent line. Outflow tests were conducted at flow rates of 0.04, 0.115, and 0.19 lb_m/sec . During these outflow tests, no liquid was in contact with the outside of the capillary/bellows device.

Four tests were conducted. In all tests, the bellows device was completely compressed before the screen capillary retention force was overcome, allowing gas to enter the device. Flow rate transients at initiation of flow were as great as 29.3 lb_m/sec with no gas ingestion.

Figure A-5 Calibration Curve, ΔP vs Bellows Deflection for Device No. 1

Figure A-6 Calibration Curve, ΔP vs Bellows Deflection for Device No. 2

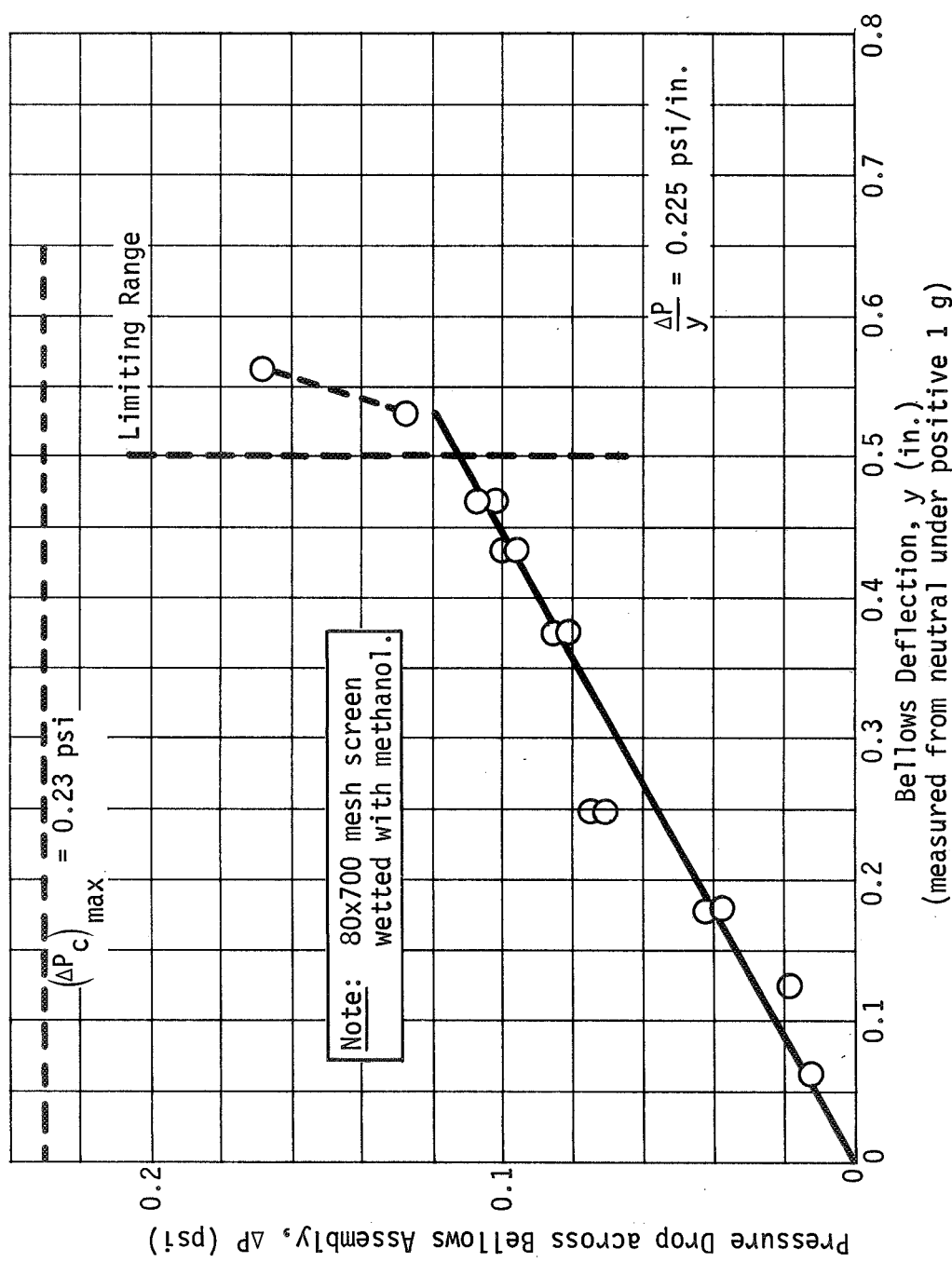


Figure A-7 Calibration Curve, ΔP vs Bellows Deflection for Device No. 3

4. Positive Acceleration Outflow Tests

Outflow tests under positive 1-g environment were made to investigate the refill characteristics of the capillary/bellows and the relationship between the bellows restoring force and the compressive force caused by flow losses through the screens. These tests were conducted with the tank outlet oriented downward. Pressurization for outflow was provided by nitrogen gas. Outflow tests were conducted on the entire devices, i.e., outflow through both the side and top screens, and outflow through the side screen alone.

Outflow tests on both screens were conducted with the tank liquid level so that the device was both full of, and covered by, liquid. During outflow, the bellows assumed a deflection consistent with the ΔP across it making it necessary to obtain steady-state conditions (constant deflection and flowrate) before taking data. Otherwise, the flow data would be in error due to the hysteresis of the bellows. During the test, the deflection of the bellows assembly was used to determine the ΔP across both screens using the data presented in Figures A-5 through A-7.

A second series was run to obtain pressure drop data on the side screen only. The tests were conducted in the same manner except that the liquid level in the tank was just below the top screen of the device at flow initiation. The device itself was full. Again, data were taken only after the bellows had reached a steady-state deflection. Due to the difficulty in accurately measuring the liquid level at flow termination, the flow loss was calculated from the measured bellows deflections, as shown in Figure A-8.

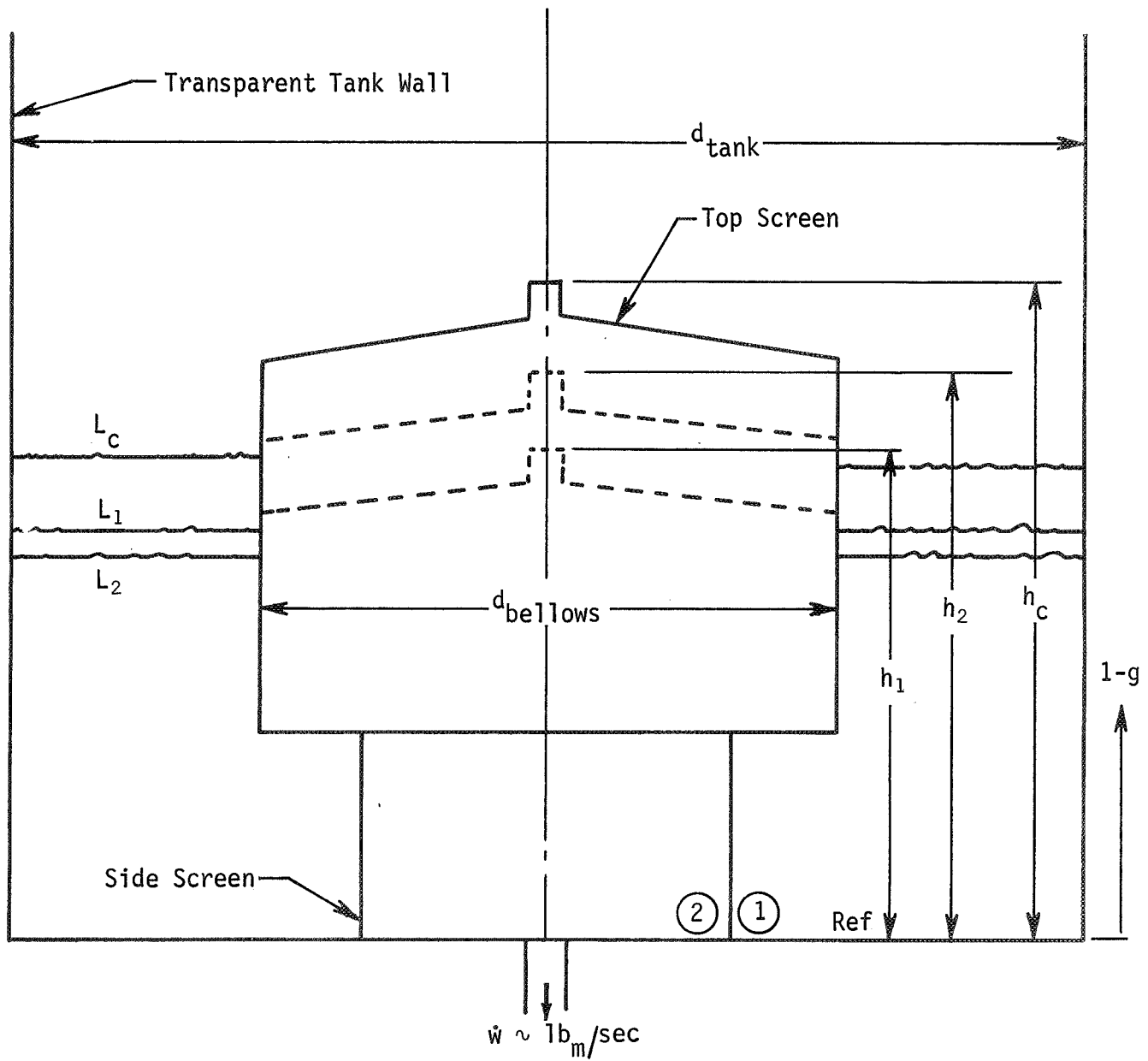


Figure A-8 Nomenclature Used in Determining Side Screen Pressure Drop

At flow initiation, the liquid level was L_c . At flow termination, the liquid level was L_1 . Due to the spring restoring force of the bellows, the device expanded after flow termination producing a further drop in liquid level to L_2 . The bellows deflections, measured from a common reference and corresponding to the three different liquid levels, are designated as h_c , h_1 , and h_2 . The measured deflections were used to calculate the flow loss by use of the following equation:

$$\Delta P_f = \left(\frac{\rho_l A_t}{A_t - A_b} + \frac{\Delta P}{y} \right) \Delta h \quad [A-1]$$

where

ΔP_f = pressure loss due to flow through the side screen only, psi;

ρ_l = liquid density, $\text{lb}_m/\text{in.}^3$;

A_t = cross-sectional area of tank, in.^2 ;

A_b = effective area of bellows, in.^2 ;

$\frac{\Delta P}{y}$ = bellows pressure rate, psi/in. ;

$\Delta h = h_2 - h_1$, in.

The measured Δh values and calculated ΔP_f values are presented in Table A-1 for each test run. Measured outflow rates are also given.

Table A-1 Test Data for Side Screen Flow Tests
(Methanol Was Fluid for All Tests)

Device No. 1
250x1370 Mesh Screen

RUN NO.	Δh (in.)	\dot{w} (lb _m /sec)	ΔP_f (psi)
11a	0.281	0.043	0.049
12	0.406	0.120	0.071
13	0.375	0.125	0.066
14	0.155	0.012	0.027
15	0.062	0.003	0.011
16	0.187	0.025	0.033
17	0.250	0.045	0.044
18	0.258	0.057	0.045
19	0.315	0.068	0.055
20	0.343	0.089	0.060

Device No. 2
250x1370 Mesh Screen

RUN NO.	Δh (in.)	\dot{w} (lb _m /sec)	ΔP_f (psi)
1	0.187	0.117	0.095
2	0.203	0.149	0.103
3	--	0.160	--
4	0.250	0.169	0.127
5	0.266	0.176	0.135
6	0.157	0.184	0.080
7	0.297	0.187	0.151
8	0.297	0.191	0.151
9	0.312	0.199	0.158
10	0.343	0.232	0.174

Device No. 3
80x700 Mesh Screen

RUN NO.	Δh (in.)	\dot{w} (lb _m /sec)	ΔP_f (psi)
21	0	0.020	0
22	0.047	0.058	0.013
23	0.031	0.080	0.008
24	0.015	0.119	0.004
25	0.047	0.130	0.013
26	0.031	0.138	0.008
27	0.031	0.144	0.008
28	0.031	0.150	0.008
29	0.047	0.157	0.013
30	0.047	0.164	0.013
31	0.047	0.175	0.013

Data from the tests are presented in Figures A-9, A-10, and A-11. Flow versus ΔP data are plotted for the cylindrical side screen alone and for both the side and top screens. Theoretical curves, based on the flow loss calculation method outlined in Ref A-4, are also presented in the illustrations. Relatively good agreement between the experimental and theoretical results was obtained for Devices No. 1 and 2, Figures A-9 and A-10, respectively. The experimental results for the third specimen show considerable scatter and deviation from the predicted results. The poor results in this case can be attributed to experimental error. Only small bellows deflections were produced with Device No. 3 resulting in the uncertainty in measurement having a greater impact on the calculated pressure drop. For example, an error of 0.030-in. in the measurement of h_1 will yield a 30% difference in the ΔP_f calculation.

C. CONCLUSIONS

A critical design consideration, as yet not discussed, is refill of the capillary/bellows device. Data presented in Figures A-5 and A-9 can be used to predict this capability for Device No. 1. Flow loss, ΔP_f , through the cylindrical screen only is nearly 0.1 psi at a flow rate of $0.12 \text{ lb}_m/\text{sec}$. At this condition, virtually no refill will take place during outflow since the pressure drop is nearly sufficient to collapse the bellows. If the device were completely covered with settled propellant, refill during outflow at this rate ($0.12 \text{ lb}_m/\text{sec}$) is achievable since the pressure drop is only 0.038 psi through both screens. The bellows restoring force is greater than the compressive force resulting from this ΔP_f of 0.038 psi. The device will not completely refill, but will fill to within 0.4-in. of the bellows neutral position, as shown in Figure A-5. Values for the refill rates are also available from these curves. For example, assume an engine restart at an outflow rate of $0.05 \text{ lb}_m/\text{sec}$. Also assume the burn has commenced to the point of compressing the bellows 0.75-in. before the side screen of the device is wetted with settled propellant. The flow loss, Figure A-9, of about 0.04 psi corresponds to a bellows compression of 0.4-in. The ΔP available for total flow through the side, cylindrical screen at a bellows deflection of 0.75-in.

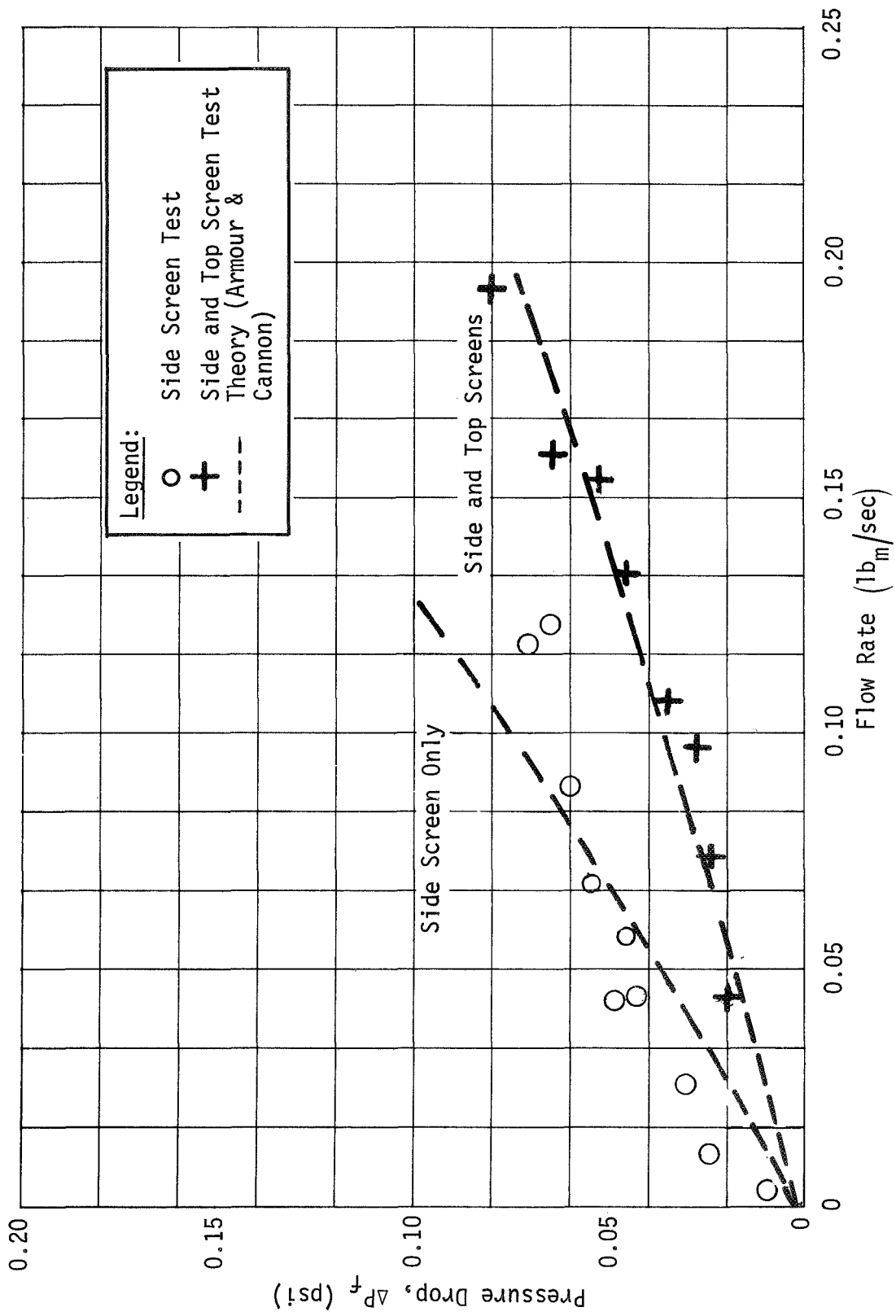


Figure A-9 Pressure Drop as a Function of Flow Rate for Device No. 1
(250x1370 Screen without Spring)

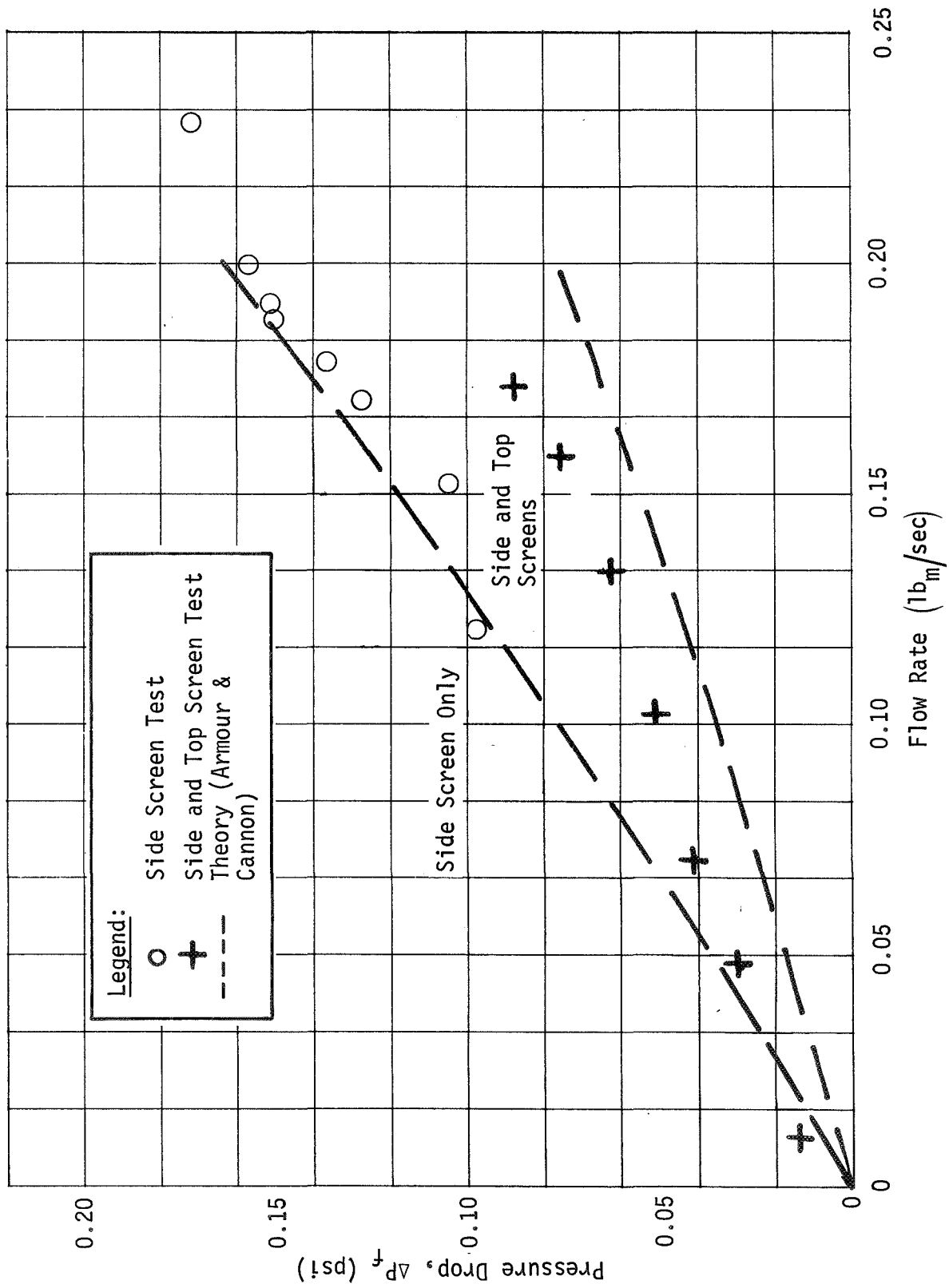


Figure A-10 Pressure Drop as a Function of Flow Rate for Device No. 2
(250x1370 Screen with Spring)

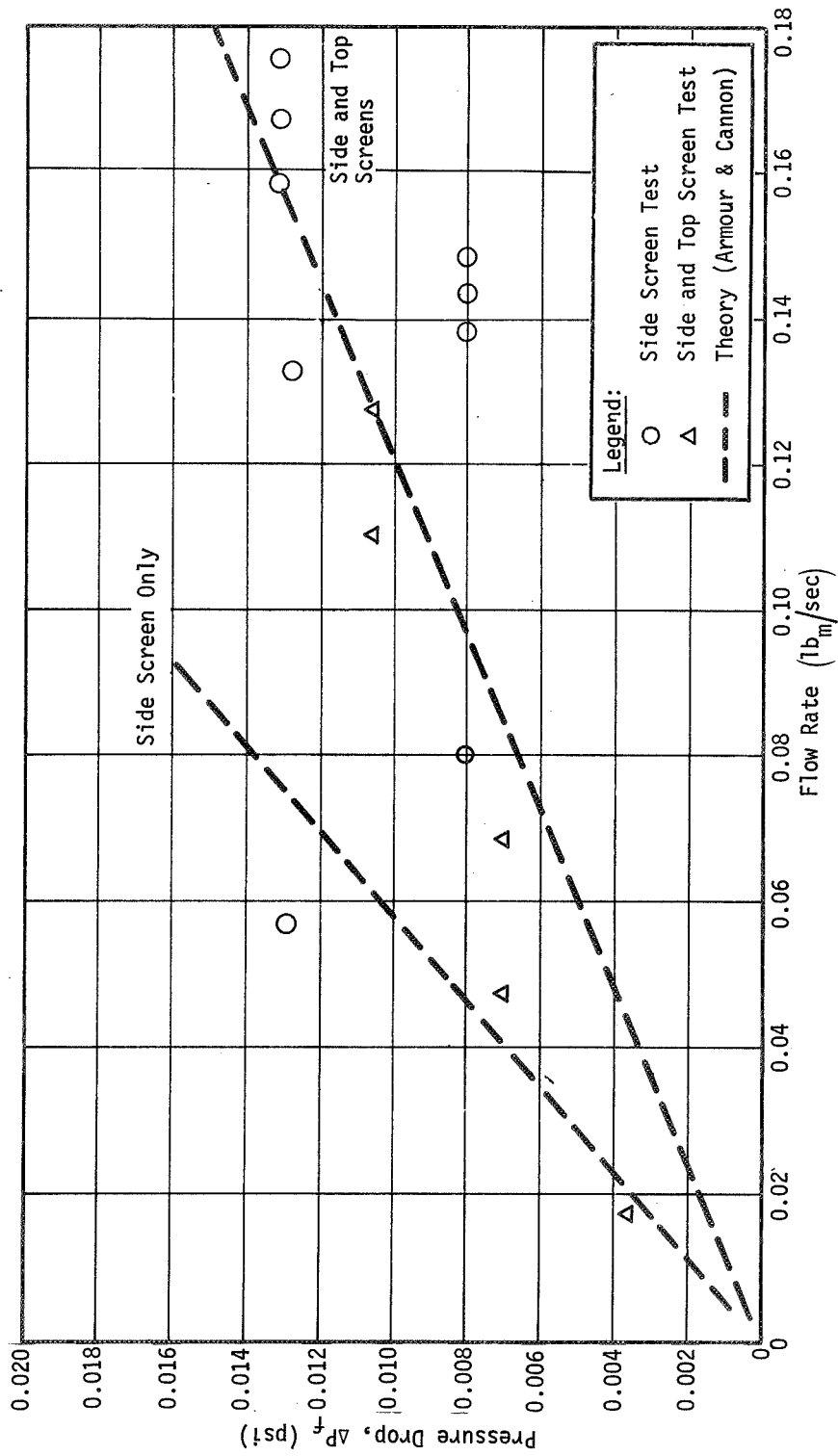


Figure A-11 Pressure Drop as a Function of Flow Rate for Device No. 3 (80x700 Mesh Screen)

is 0.1 psi (Fig. A-5) and provides a flow rate through the side screen of $0.12 \text{ lb}_m/\text{sec}$, Figure A-9. At this condition, the refill flow rate is $0.12 \text{ lb}_m/\text{sec}$ minus $0.05 \text{ lb}_m/\text{sec}$, or $0.07 \text{ lb}_m/\text{sec}$. As refill progresses, the rate will decrease linearly to zero at a bellows compression of 0.4-in. An average flow rate of $0.035 \text{ lb}_m/\text{sec}$ can then be used to determine the refill time required based on the bellows volume filled. In this example, the volume filled is 4.84 in.^3 (0.141 lb_m of methanol) and the refill time is 4.03 sec. As mentioned, refill is through the side screen only; therefore, complete settling is not required for refilling.

Working another example using $0.05 \text{ lb}_m/\text{sec}$ through the side screen and a 0.75-in. deflection of the bellows for Device No. 2 will tend to indicate the importance of the spring rate. The flow loss (Fig. A-10) is 0.046 psi, which corresponds to a bellows compression (Fig. A-6) of 0.1-in. The ΔP available for total flow through the screen at a bellows deflection of 0.75-in. is 0.349 psi, (Fig. A-6) which provides a flow rate of $0.383 \text{ lb}_m/\text{sec}$ (obtained by extrapolating the results presented in Fig. A-10). The initial refill rate for this device with the higher spring rate is $0.383 \text{ lb}_m/\text{sec}$ minus $0.05 \text{ lb}_m/\text{sec}$, or $0.333 \text{ lb}_m/\text{sec}$. Refill will stop when the bellows reaches the deflection which induces $0.05 \text{ lb}_m/\text{sec}$ of flow into the device, or 0.1-in. Using an average flow rate of $0.166 \text{ lb}_m/\text{sec}$, the refill volume is 9.16 in.^3 (between 0.75- and 0.10-in. deflection) and the refill time is 1.58 sec. Thus, the system with the higher spring rate is capable of refilling at a rate 4.75 times greater than the system with the lower spring rate (previous example).

A clearer picture of the capillary/bellows performance may be seen in Figure A-12. The curves shown are the result of cross-plotting the data presented in Figure A-10 with that from Figure A-6. The flow rate capability for the device (No. 2) is shown in Figure A-12 as a function of bellows deflection (the uppermost line for flow through both screens and the lower for flow through only the side screen). Referring to the previous example, point 1 represents flow out of the device for engine restart with no flow into the device. The path from 1 to 2 indicates compression of the bellows by tank pressurization to supply the engine with the $0.05 \text{ lb}_m/\text{sec}$ outflow. At a deflection of 0.75-in., settled liquid starts to cover the side screen, resulting in flow being induced

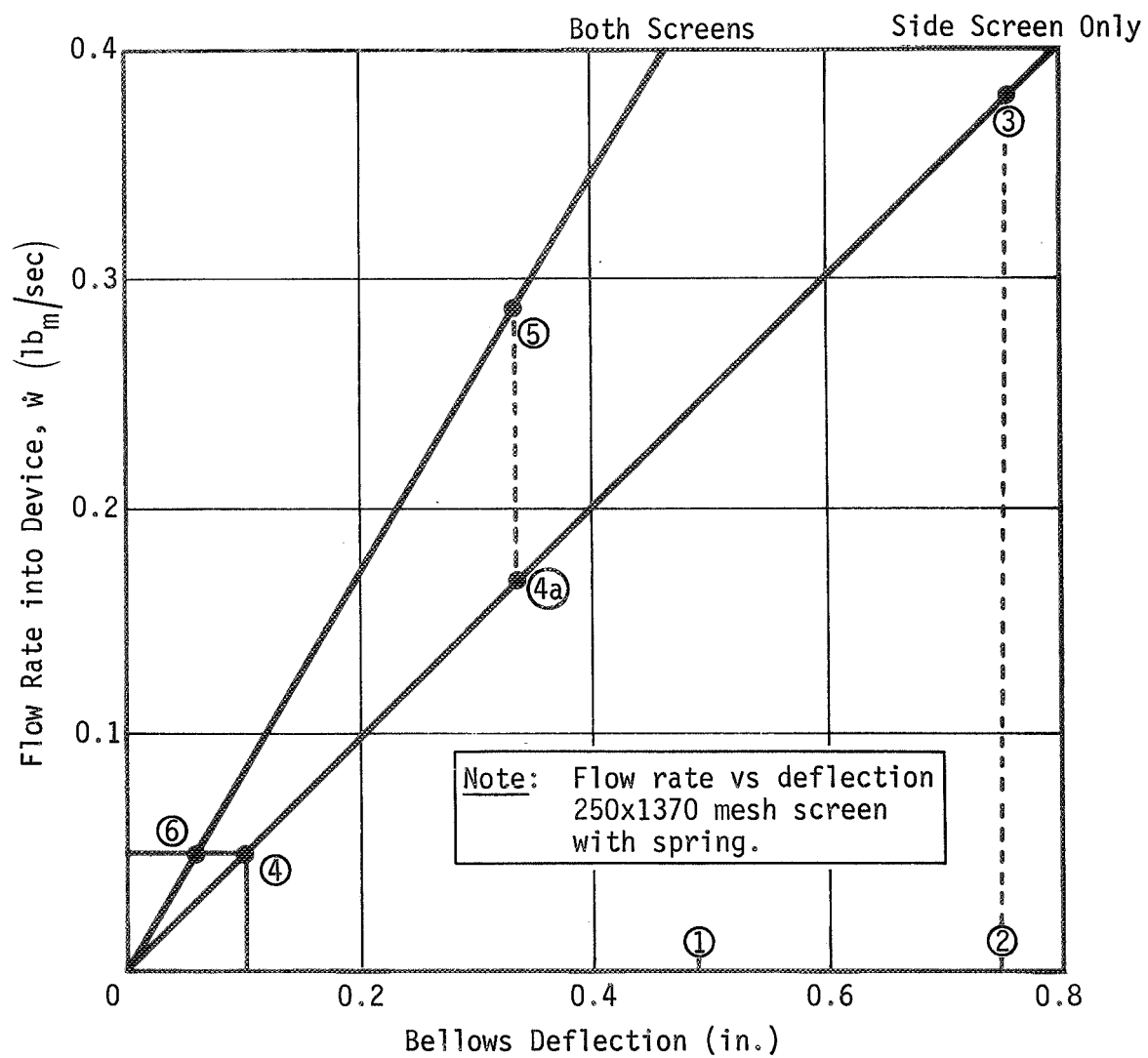


Figure A-12 Flow Rate into Device No. 2 as a Function of Bellows Deflection

into the device under the influence of the bellows expansion. Flow into the bellows increases to $0.383 \text{ lb}_m/\text{sec}$ (point 3). As the bellows expands, flow into the device decreases along the path from 3 to 4. If refilling continues without the top screen covered, point 4 will be reached at which point flow into the device through the side screen equals flow to the engine. No further movement of the bellows will occur unless outflow is terminated or the top screen is covered by liquid. If the top screen is not covered, the time required to move from 3 to 4 is 1.58 sec. If, however, prior to reaching point 4, liquid does cover the top screen (point 4a) the flow rate will increase to point 5 and then decrease along the upper-curve to point 6, the equilibrium condition. Refilling for this case requires less time and the device is filled to a greater level (less bellows deflection).

The results obtained from these rather limited and qualitative tests, tend to support the feasibility of the capillary/bellows concept as a propellant acquisition device. More quantitative data and vibration and slosh tests are required. Fabrication problems are not apparent since bellows and screen fabrication is the present state-of-the-art.

D. REFERENCES

- A-1. J. A. Salzman, et al.; *An Experimental Investigation of the Frequency and Viscous Damping of Liquids during Weightlessness*. NASA TN-D-4132, August 1967.
- A-2. Harris Research Laboratories: *Studies of Interfacial Surface Energies-Summary Report*. NASA CR-54175, December 1964.
- A-3. H. L. Paynter, et al.: *Experimental Investigation of Capillary Propellant Control Devices for Low-Gravity Environments. Vol II-Final Report*. NASA CR-110755, Martin Marietta Corporation, Denver, Colorado, June 1970.
- A-4. J. C. Armour and J. N. Cannon: "Fluid Flow through Woven Screens." *AIChE Journal*, Vol 14, No. 3, May 1968.